The University Of Sheffield.

The role of expansin in leaf development:

A molecular genetics and AFM approach

A thesis submitted by

HOE HAN GOH

For the degree of Doctor of Philosophy

Department of Animal and Plant Sciences

July 2011

Acknowledgements

I am very grateful for the invaluable support, guidance and advice throughout the research project and thesis preparation given by my supervisor Prof. Andrew Fleming. I am grateful for other guidance available from Prof. Mike Burrell.

Many thanks to Dr. Robert Malinowski and Dr. Anna Kasprzewska for helpful guidance on molecular works, Dr. Asuka Kuwabara for advice on histological works and microtechniques, Dr. Carmen Della-Forca and Dr. Martin-Timothy O'Donohue for advice on qRCR, Marion Bauch for general technical helps, Dr. Jen Sloan for protein works, Dr. Nic Mullin for AFM point measurements and data analysis, Dr. Lee Hunt and Dr. Caspar Chater for sharing the molecular reagents, motivations from Dr. Duncan Cameron (my undergraduate tutor), and not forgetting Dr. Alexis Peaucelle who is an enthusiastic scientist and a generous teacher who truly pioneered the use of AFM for studying plant tissue mechanics. Thanks to Bob Keen (lab manager) and Heather Walker for keeping the lab supplies flowing and Andy Kruppa (TAB Lab) for allowing the use of qPCR machine.

I would also like to acknowledge the hardworking project students: Rosie Hadfield who did all the cell counting and measurements, Gemma Mckenzie-Smith for her painstaking tracing of leaf images from sectorial induction experiment using the LeafProcessor and Katherina Bradfield for her help in hypocotyl measurements.

Thanks to all my friends and colleagues: Ross Carter, Phakpoom Phraprasert, Supatthra Narawatthana, XiaoJia Yin, Adam Hayes, Chloé Steel, Simon Wallace, Rachel George, Fawaz Al-Zahrani, Rodrigo Echegoyen Nava, Serina Akhtar, Phillipa Gullett, Stuart Smith and many more friends who I might have missed, for keeping my spirit up and sharing banters throughout my time doing the research. Not forgetting my fellow comrades at the Sheffield University Shodokan Aikido club.

I gratefully acknowledge the funding provided by the University of Sheffield studentship, supports given by National University of Malaysia and funding from the Malaysian Ministry of Education for previous undergraduate studies here. Finally, I would dedicate this thesis to my parents and family members who devoted their unwavering emotional support while I am conducting my further studies abroad.

Abstract

Leaf shape formation is a fascinating process involving the coordinated regulation of cell division and cell expansion, which ultimately relies on the control of cell wall expansion. Expansins comprise a large family of cell wall proteins which can non-enzymatically trigger the relaxation of the cell wall for expansion. They have been implicated in organ initiation, cell differentiation and organ growth. However, the exact mechanism of expansin action and functional role of different members of the expansin gene family is unclear.

Here, I focus on the largest subgroup of expansins (EXPA) to identify which genes are expressed during different stages of leaf development in Arabidopsis. This information was used to design an inducible artificial microRNA construct to target the knock-down of multiple expansin genes expressed during early leaf development. Through a series of experiments knocking down expansin gene expression at different stages of leaf development, I show that the suppression of expansin gene expression at later stages of leaf development is sufficient to repress leaf growth and alter leaf shape. This molecular genetic approach is combined with an atomic force microscopy (AFM) approach to investigate the role of cell wall mechanics in leaf growth. I describe the use of AFM for probing the leaf primordium mechanics and outline consideration for future work.

Contents

List of figures

Chapter 1

Chapter 2

Chapter 3

Chapter 4

Chapter 5

Chapter 6

List of tables

Chapter 2

Chapter 3

Chapter 4

List of abbreviations/ acronyms

ABA	Abscisic acid
ACC	1-aminocyclopropane-1-carboxylic-acid
AFM	Atomic force microscopy
amiRNA	Artificial microRNA
ANOVA	Analysis of variance
BL	Brassinolide
bp	Base pairs
BR	Brassinosteroid
CCD	Charge-coupled device
cDNA	Complementary DNA
CK	Cytokinin
cm	Centimetre
Col-0	Columbia-0
Ct	Threshold cycle
d.f.	Degrees of freedom
DAS	Day after sowing
Dex	Dexamethasone
DI	Deionised
DMSO	Dimethyl sulfoxide
DNA	Deoxyribonucleic acid
dNTP	2' Deoxynucleotide 5' triphosphate
dsRNA	Double-stranded RNA
EDTA	Ethylenediaminetetraacetic acid
EXLA	Alpha-expansin like
EXLB	Beta-expansin like
EXP	Expansin
EXPA	Alpha-expansin
EXPB	Beta-expansin
g	gram
GA	Gibberellic acid
GUS	β-Glucuronidase
IAA	Indole-3-acetic acid
kDa	Kilodalton
kg	Kilogram
kV	Kilovolt
L	Litre
LB	Luria broth
LCD	Liquid crystal display
M	Molar
MeJ	Methyl jasmonate
mg	Milligram
min	Minute
miRNA	MicroRNA
mL	Millilitre
mm	Millimetre

M-MLV RT	Moloney murine leukemia virus reverse transcriptase
mRNA	Messenger RNA
MS	Murashige and Skoog
msec	Millisecond
N	Newton
nM	Nanomolar
nN	Nanonewton
nt	Nucleotide
OD	Optical density
PCR	Polymerase chain reaction
pI	Isoelectric point
RNA	Ribonucleic acid
Rnase	Ribonuclease
RO	Reverse osmosis
rpm	Revolution per minute
RT	Room temperature
RT-PCR	Reverse transcription PCR
RT-qPCR	Real-time quantitative reverse transcription PCR
s	Second
SD	Standard deviation
SDS	Sodium dodecyl sulfate
SE	Standard error
SPM	Scanning probe microscopy
Ta	Annealing temperature
TAE	Tris acetate/ EDTA
T-DNA	Transferred DNA
Tm	Melting temperature
U	Unit
UHP	Ultra high purity
UV	Ultraviolet
V	Volt
v/v	Volume to volume
w/v	Weight to volume
WT	Wild type
X-GlcA	5-bromo-4-chloro-3-indoyl-β-D-glucuronide
ZEA	Zeatin
ΔΔCt	Comparative threshold cycle
µF	Microfaraday
µg	Microgram
µL	Microlitre
µm	Micrometre
µM	Micromolar

CHAPTER 1 General introduction

1.0 Introduction

The field of leaf morphogenesis encompasses not only a detailed mechanistic elucidation of leaf shape and size determination, but also involves an appreciation of the ultimate reasons for the diversity of leaf form. It spans all levels of biological complexity from biochemistry, cell biology, genetics, physiology, ecology, evolutionary developmental biology (evo-devo) to biophysics. The partitioning of leaf morphogenesis studies into these different aspects through a classical reductionist approach hinders a holistic interpretation as organ systems function coherently, with the whole being greater than the sum of the parts. This introduction will provide an overview of the different elements of leaf morphogenesis and attempt to generate an integrated view of the topic.

1.1 Significance of the study of leaf morphogenesis

Leaves are important due to their abundance and function in carbon fixation which sustains both natural and agricultural productivity. Plants have evolved leaves of diverse shapes and sizes (Bell, 1991). Even within the same plant two leaves can differ drastically, either for developmental (i.e. juvenile, vegetative and reproductive), seasonal (heterophylly) or functional reasons (e.g. submergence). This phenotypic diversity often reflects adaptive features to specific environmental conditions, related to the critical physiological and functional roles of leaves in water relations, respiration, photosynthesis and environmental sensing.

For example, ecological and evolutionary studies have implicated leaf marginal serrations and drip tips as adaptations and have been applied as biological proxies for ancient environmental conditions e.g. (Baker-Brosh and Peet, 1997; Burnham and Johnson, 2004; Peppe *et al.*, 2011). Consequently, investigations concerning the organisation of specialised cell types and the shapes of leaf are not only important to understand the fundamental principles of organ formation and for commercial improvement of crops and ornamental plants, but are also crucial for informing other research areas, such as emergent evo-devo and climate studies (Beerling and Fleming, 2007; Peppe *et al.*, 2011).

1.2 The central issue of morphogenetic studies

The complexity of the endogenous programme of leaf morphogenesis, coupled with the influence of genetic-environmental factors, poses a great challenge to understanding how leaf size and shape are determined. As organs are direct manifestations of cellular processes, studies have often focused at the cellular level on cell division, expansion and differentiation.

At the core of such endeavours lies a long-standing controversy between the polarised arguments on whether morphogenesis is a product of cell proliferation controlled at the whole-organ level (organismal theory) or is driven purely by cell division (cellular theory) (Hofmeister, 1867). The controversy arises since similar morphological structures develop on the basis of distinct types of histological organisation, with convergence of shape across taxa (e.g. green vs. red algae, Cactaceae vs. Euphorbiaceae), which implies fundamental morphogenetic mechanisms (Kaplan and Hagemann, 1991; Kaplan, 1992). Kaplan and Hagemann (1991) proposed that organismal regulation acts on 'subordinate' cells during morphogenesis and early histogenesis via apoplastic and symplastic continuities. In this view, cellular independence only occurs at the end of differentiation, as manifested by stomatal guard cells breaking plasmodesmatal continuity (Palevitz and Hepler, 1985), intrusive growth and cell separation to form intercellular spaces.

A *neo* cell theory proposed compartmentation and subdomain interactions that link development at cellular and organ levels by coordinating cell division and expansion (Tsukaya, 2003). This accounts for the intriguing compensatory phenomenon observed in cell division manipulation experiments (Hemerly *et al.*, 1995; Smith *et al.*, 1996) where integration of cell number and cell size often leads to the formation of leaves with near-normal macroscopic appearance despite disruption of cell division. Three independent mechanisms depending on the rate, duration and timing of cell expansion have been proposed to be responsible for the compensatory phenomena in leaves (Ferjani *et al.*, 2007). However, much work is still required to elucidate the pathways and mechanism of this compensatory system.

Returning to the controversy of organismal vs. cell-based theories on growth, why is there such a fuss? This is because the resolution of the issue will govern the direction of the field in developmental biology. As stated by Kaplan and Hagemann (1991)

"instead of focusing on the distribution of cell division, the plant biologist concern becomes how cell walls are made more pliable locally to result in the differential growth process seen in plant morphogenesis". The current trend of research towards bridging the two fields via better understanding of the molecular genetics and mechanics underlying leaf development, aided by computational approaches are described in the following sections.

1.3 Leaf morphogenesis – current state of knowledge

Despite developmental plasticity, leaves form in a predictable and modular manner: from the initiation of a leaf primordium, through ground-plan patterning and cell-type specification, to the eventual elaboration of leaf blade (Dengler and Tsukaya, 2001) (Figure 1.1).

Each phase of development with its inherent complexity has been extensively studied and reviewed at various levels such that an exhaustive and comprehensive treatment is beyond the scope of this thesis. Only a concise and directly relevant overview of each study area is given in the following sections, with emphasis on the limitations. This establishes a background for defining the scope of my study.

1.3.1 Morphogenesis at the molecular scale

Molecular genetics is the fastest growing area in the study of leaf morphogenesis. It is largely based on the mutational analyses of genes involved in patterning (Berna *et al.*, 1999), many of which have turned out to be homeotic regulators acting upstream in development, including the determination of founder cells, the establishment of polarity and the elaboration of the leaf lamina (Byrne, 2005; Kim and Cho, 2006; Kidner and Timmermans, 2007) (Figure 1.1). However, our understanding of the links to downstream mechanistic targets is still fragmented.

Despite the multi-gene influence on leaf traits, only a few have attempted the challenge of quantitative trait loci (QTL) mapping (Juenger *et al.*, 2005; Langlade *et al.*, 2005; Tisne *et al.*, 2008). These studies highlight epistatic interactions and the evolutionary modularity in leaf development, which accounts for many leaf shape mutants being pleiotropic in nature. Genome-wide transcriptomics and bioinformatic

analyses further support the phasing of morphogenesis, with heterochronic factors regulating the timing and duration of cellular processes (Beemster *et al.*, 2005; Efroni *et al.*, 2008).

Given that gene products cannot encode shape and size directly, the current challenge is to understand the spatiotemporal regulatory mechanisms through elucidating the pathways of the patterning and size-defining components (Tsukaya, 2003; Anastasiou and Lenhard, 2007; Barkoulas *et al.*, 2007; Krizek, 2008; Johnson and Lenhard, 2011).

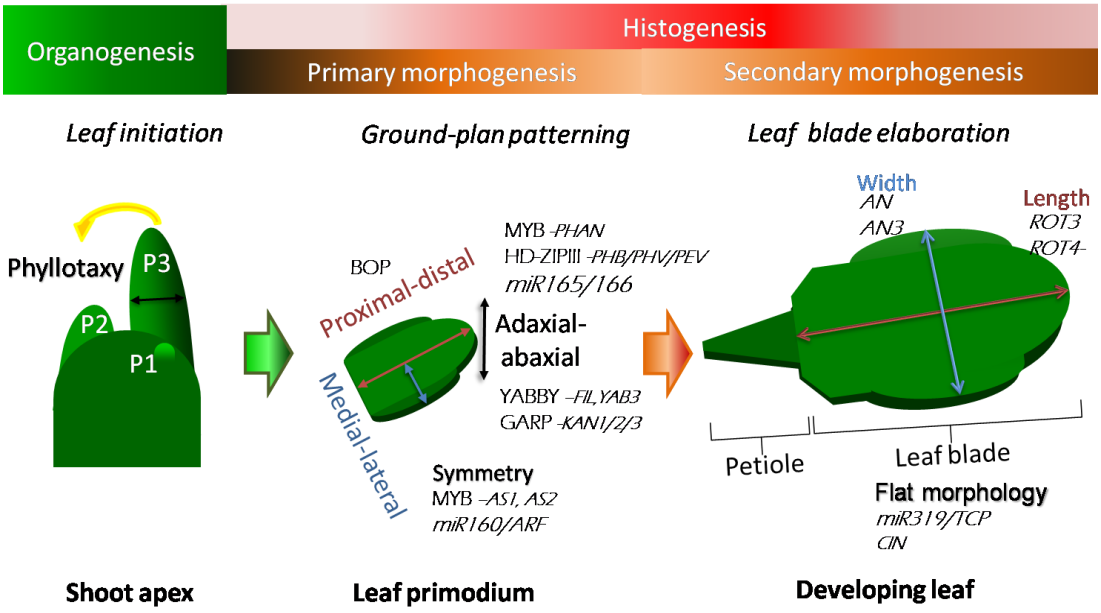

Figure 1.1. Leaf developmental processes in Arabidopsis with simple leaves and spiral phyllotaxy.

Three phases of leaf development: initiation through the specification of founder cells (organogenesis), primary morphogenesis (form generation) with the establishment of leaf polarities or ground-plan patterning and tissue specification (histogenesis – cell/tissue differentiation), and secondary morphogenesis of final leaf shaping through the elaboration of leaf blade. Leaf developmental stages can be represented by plastochron number with the newly initiated leaf bud denoted as Plastochron 1 (P1) and subsequently as P2 and P3 following the initiation of new leaves. Patterning is defined as a process that generates axes in the primary body plan, creates domains upon organ formation, and finally leads to differentiation into tissues and cell types (Cnops *et al.*, 2006). The adaxial-abaxial identity is determined early during leaf development in relation to the shoot apical meristem, and is required for dorsoventral flattening. The development along the proximal-distal axis is dominated by basipetal cessation of cell division at early stage whereas the processes resulting in duplicated mediolateral symmetry is not as apparent. Later stages of leaf development are largely cell expansion whereby different leaf shapes could be produced by allometric regulation. Genes (italic) with established roles in different aspects of leaf morphogenesis are listed with their functional categories/ families of transcription factor (non-italic). Refer to Kim & Cho (2006) for descriptions and references to the genes listed.

1.3.2 Morphogenesis at the cellular scale

Since leaves consist of cells, an examination of development at the cellular level is required. This includes the kinematic analysis of cell proliferation and histological analysis of cell number, size and shape e.g. Horiguchi *et al.* (2006). This can be carried out on the whole leaf or on selected regions of the leaf, sometimes aided by staining techniques and cell markers (Donnelly *et al.*, 1999; Bougourd *et al.*, 2000).

These studies have revealed that cessation of cell division generally occurs from leaf tip to base, with a limited contribution of marginal meristem activity towards leaf expansion and tissue differentiation. Different stages of development can be distinguished at the cellular level. For example, the initial meristematic stage is characterised by expansion accompanied by cell division, whereas development at later stages proceeds by cell expansion in the absence of division. How this is coordinated remains elusive despite considerable knowledge acquired on the regulation of cell cycle in growing leaves (Beemster *et al.*, 2005; Inzé and De Veylder, 2006).

1.3.3 Morphogenesis and hormones

Plant growth regulators (PGRs) include classic phytohormones (derivatives of aromatic amino acids, steroids and carotenoid compounds), short peptides, regulatory small RNAs, and certain metabolites (e.g. sucrose and trehalose), all of which are mobile signals (Palatnik *et al.*, 2003; Öpik and Rolfe, 2005). PGRs are pivotal in leaf morphogenesis, with direct or indirect roles in governing processes across subcellular, cellular and supracellular scales via crosstalk between different regulatory pathways and the transduction of environmental signals into developmental response (Gazzarrini and McCourt, 2003; Li *et al.*, 2007).

It is recognised that auxin plays a major role in patterning e.g. phyllotaxis and venation through long-distance polar transport, with effects on cell division, expansion and differentiation (Leyser, 2001; Benkova *et al.*, 2003; Berleth *et al.*, 2007). Changes in auxin distribution precede alterations of cell division and leaf morphology (Zgurski *et al.*, 2005). Notably, exogenous auxin can rescue auxin transport (*pin1*) mutants with aberrant leaf shape forming, depending on the concentrations and sites of auxin application (Reinhardt *et al.*, 2003). Auxin (long-

distance transported) crosstalk with other phytohormones (short-distance transported) confers combinatorial controls that culminate in tissue-specific effects (Teale *et al.*, 2008). For instance, differential concentrations of auxin, cytokinin and gibberellin have been implicated at the site of leaf primordium inception (Kepinski, 2006). Auxin homeostasis is also required for leaf flattening (Qin *et al.*, 2005). Meanwhile, the links between auxin-related factors and other master regulators of leaf polarity are coming to light (Pekker *et al.*, 2005).

Brassinosteroid (BR) is another important phytohormone with an emerging role in leaf morphogenesis. BR's interdependency with auxin influences both cell division and expansion (Altmann, 1998; Hu *et al.*, 2000; Nakaya *et al.*, 2002; Nemhauser *et al.*, 2004). BR is likely responsible for later stages of leaf morphogenesis as most BR-related mutants display a normal pattern of leaf expansion during the early phase of leaf development (<3 mm length) (Nakaya *et al.*, 2002). The final abnormal leaf shape is linked with reduced cell size and number. BR influences leaf-length more than leaf-width. This ties in to the involvement of the *ROTUNDIFOLIA3* gene product in BR biosynthesis with mutant plants having shorter, rounder leaves (Kim *et al.*, 2005). Recent studies confirm the direct relevance of brassinolide (BL) (the active molecular form of BR) in leaf morphogenesis. For example, the role of BL activity at the leaf margin is demonstrated by the rescue of the *dwf* mutant leaf shape by marginal cell-specific expression of *DWF4* which encodes an enzyme required for BL biosynthesis (Reinhardt *et al.*, 2007). Since only leaf shape but not size is restored, this study also implies independent regulation of leaf shape and size. Furthermore, the importance of a BR-mediated pathway specifically in the epidermis is shown by the reversal of *bri1* dwarfism by the expression of the *BRI1* (which encodes a brassinosteroid receptor) only in the epidermal layer (Savaldi-Goldstein *et al.*, 2007).

How BR-generated transcription factors relay their effect to the inner tissues without moving from the epidermis creates many questions on cell-cell communication, inter-layer coordination of cell proliferation, and the potential biophysical role of the growth process itself - reviewed in Savaldi-Goldstein and Chory (2008). The connections to the mechanical stimuli and mechanotransduction processes that restrict the leaf from being torn apart as it grows are also largely unexplored.

1.3.4 Biomechanics of leaf morphogenesis

Plant cell immobility and the structural and functional continuum imparted by cell walls allows the leaf to be considered as a coherent physical whole (Green, 1997) - reminiscent of the organismal theory (see above). To a certain extent, the physical growth processes of leaf tissue can be viewed to be a simple sum of the activity of the constituent cells, orchestrated by patterns of mobile signals. In this case, tissue-level physics with solid and fluid mechanics can be applied to growth process. Because plant cells are attached to their neighbours, their turgor force is transmitted to the least compliant (stiffest) walls in the tissue (Figure 1.2A) – leading to so called 'tissue tension' (Peters and Tomos, 1996). Furthermore, wall stresses in certain cell layers can arise from the turgor force of cells with walls of high compliance. Wall stresses lead to strain (deformation), which cumulatively could lead to organ shaping (Figure 1.2B) or even size control (Coutand *et al.*, 2009), as such supracellular wall stress might act as an organising force in plant morphogenesis (Szymanski and Cosgrove, 2009).

Looking at the subcellular level, the cytoskeletal architecture of actins and microtubules could receive mechanical cues (directly) as well as chemical signals (indirectly). In animals, mechanical signals have been shown to be transduced into changes in ion flux, molecular binding kinetics, signal transduction, gene transcription, cell fate switching and developmental patterning (Ingber, 2003a). Recently, matrix stiffness has shown to determine cell-cycle control by regulating cyclin D1-dependent RETINOBLASTOMA protein (RB) phosphorylation in animal cells (Klein *et al.*, 2009). This provides a direct link of physical force to a key cell cycle gene.

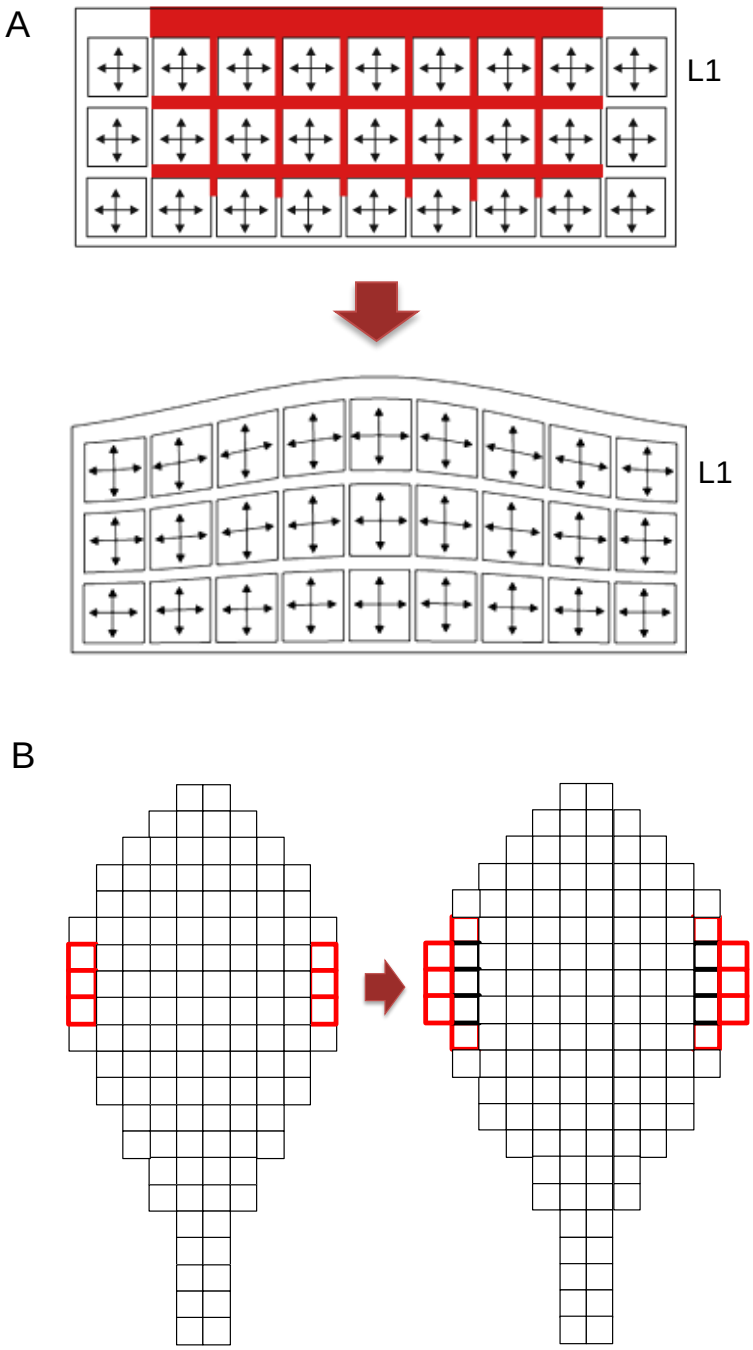

Figure 1.2. Conceptual models on how alterations in cell wall mechanical properties can lead to (A) local growth and subsequently (B) organ shaping. (A) Consider a group of cells across three tissues layers with all cells generating internal turgor pressure (crossed-arrows) which exert forces outwards equally in all directions. Normally, the cells on the outermost layer (epidermis, L1) sustain a greater tensile stress for lacking neighbours on one side. In a scenario when cell walls of a region of cells are altered to become more compliant (red colour), dissipation of wall stresses can happen locally. Consequently, the turgor force from other cells is transmitted to this region resulting in the outwards growth of the more compliant region until sufficient tensile stress is attained again in the outer cell walls to restrict growth. (B) At the organ-level, regional modulation of cell wall properties, which based on the same biophysical principle, can potentially lead to local outgrowth. Figure A is after Fleming (2006).

The cell wall-cytoskeleton-nucleus continuity means physical processes could play a more central role beyond simple promotion and inhibition of gene expression, allowing an interacting system of wall-cytoskeleton feedback (Dumais, 2007; Mirabet *et al.*, 2011). This might help determine the orientation of cell division and cell differentiation (Zajac and Discher, 2008). There might be a more direct role of geometrical specification by physical processes at the cellular and tissue level (Green, 1997). This possibility has been demonstrated with the induction of leaf initiation through local loosening of cell wall at the shoot apex (Fleming *et al.*, 1997) and the alteration of leaf shape (Pien *et al.*, 2001), which revived interest in the consideration of mechanical forces as biological regulators in plants. The overriding role of cell wall properties in governing organogenesis is also supported by experimental perturbation of the methyl-esterification status of cell wall pectins within the meristem, which dramatically alters the phyllotactic pattern, with inhibition of pectin de-methyl-esterification preventing primordia formation (Peaucelle *et al.*, 2008).

The idea that mechanics play a role in plant development is not new (c. thigmomorphogenesis), however compared to animal studies, only relatively recently has convincing evidence of mechanotransduction mechanisms become available. Thus, the experiments on expansins and pectins, and the role of mechanical signalling in developmental patterning have led to emerging interest in this area. The first molecular identification and characterisation of mechanosensitive ion channels in plant plasma membranes was recently reported (Haswell *et al.*, 2008), and Hamant *et al.* (2008) showed that tissue compression can trigger stress-induced changes in the orientation of cell division planes and cytoskeletal configuration. Furthermore, through the ablation of apical cells and theoretical computer model prediction of stress re-distribution, it has been shown that microtubules orient so as to resist physical stress. This implies that mechanical stress can contribute to morphogenesis not only as the driving force for cell expansion but also as a signalling factor, providing potentially long-range and effectively instantaneous coordination of cellular responses (Fleming, 2006; Dumais, 2009).

1.3.5 Morphogenesis at the ecophysiological scale

As indicated from the above discussion, there is no simple answer to understanding the mechanisms shaping leaves. In addition to the complications of the endogenous programme, the environment can alter many aspects of leaf growth. One approach to understand the problem is to try and tease apart the endogenous and the exogenous factors regulating morphogenesis.

Ecophysiological studies provide a framework to consider the selection pressures on the modularity and coordination of leaf shape which allow the optimal functioning of the leaf under varying physical parameters of light, water, gas and temperature. The availability of resources could link macroscopic growth with the level of molecular control (Walter and Schurr, 2005). The intuitive rationale is that the efficiency of leaf architecture relies on a balance between economic production of mechanical supporting tissue and an optimal leaf functioning for light interception, surface cooling, wind resistance, snow shedding, or shading of competitors.

Studies on the relationships between cellular processes and environmental conditions (light intensity, shading, day length, and water deficit) suggest an early determination of leaf size, and that whole-plant coordination of leaf expansion dynamics (rate and duration of cell expansion) is different between early and late stage of leaf morphogenesis (Cookson *et al.*, 2005; Cookson and Granier, 2006; Cookson *et al.*, 2006; Cookson *et al.*, 2007). Furthermore, the predominant control of leaf expansion switches from metabolics to hydraulics over the course of leaf development, which is consistent with an ontogeny which switches from a leaf being a sink to source of carbon assimilation during maturation (Pantin *et al.*, 2011). The significance of these observations and the exact regulatory mechanisms involved are yet to be clarified.

1.3.6 Modelling of leaf development

Mechanistic models of gene networks are useful to make sense of the links among various components in the system and to infer regulatory mechanisms (e.g. Coen *et al.*, 2004; Green *et al.*, 2010). The integration of the cellular framework with signalling pathways provides a spatial context for intercellular processes, allowing

the associated cellular processes to be investigated via manipulative experiments based on the predicted cellular responses (Jönsson and Krupinski, 2010). This reiterative inquiry linked with model refinement can also be instrumental for modelling correlative relationships, such as those revealed by ecophysiological studies which relate functional-architectural models of different leaf traits under different environments (e.g. Shipley *et al.*, 2006; Price and Enquist, 2007). The conceptual modelling of the rate and duration of leaf growth processes (e.g. Cookson *et al.*, 2005) is different compared to detailed mechanistic models based on the processes of cell division, cell expansion and tissue size control (e.g. Mizukami and Fischer, 2000; Beemster *et al.*, 2006). Combined modelling approaches could capture a greater level of whole-plant regulations which may be overlooked in less integrated studies (Tisne *et al.*, 2008; Granier and Tardieu, 2009).

On the other hand, descriptive modelling is visually more prominent. Computer simulations based on mathematical functions and physical theories can be created to simulate leaf growth (Wang *et al.*, 2004; Merks *et al.*, 2011) and to provide physical models of venation patterning (Runions *et al.*, 2005; Laguna *et al.*, 2008).

The challenge now is to formulate models that combine biophysical factors with empirical knowledge of the underlying molecular regulatory mechanisms of leaf growth patterns, and thus to describe molecular processes as integrated, hierarchical systems rather than isolated parts (Green, 1999). Recognising the many levels of plant modelling in which plants can be viewed as continuous mechanical entities, iterative branching systems, continuous chemical vessels, collections of cell or as collections of interacting network (Grieneisen and Scheres, 2009), it was concluded that the future of modelling relies on multilevel modelling and combined approaches (to test the same phenomena using different basic principles of modelling). For example, the study by Hamant *et al.* (2008) combined subcellular microtubule organisation, organ-level forces, cell polarity and auxin accumulation to study phyllotactic patterning and organ shape.

The following sections consist of further discussions on cell expansion and details of my approach to advance our understanding of different aspects of leaf morphogenesis.

1.4 The role of cell expansion in leaf morphogenesis

Cell expansion is a general term applied to the increase in cell volume. Cell division-dependent expansion and cell division-independent expansion are used to distinguish between meristematic growth and expansive growth. The latter usually refers to that of vacuolation and turgor-driven expansion, which happens much more rapidly than growth during cell division.

In the cell division zone during early leaf formation, cells grow and expand before mitosis and cytokinesis. Leaf cells continue to expand after cell division ceases, until their final volume is many fold that of their meristematic progenitors (Dale, 1988). Turgor-driven cell expansion is believed to contribute the most to mature leaf shape and surface area during the last stage of leaf morphogenesis (Van Volkenburgh, 1999). However, leaf allometry (length:width ratio) does not directly correlate with cell size, but to the cell number (Granier *et al.*, 2000; Cookson *et al.*, 2005). Cell shape bears little or no correlation to the overall leaf shape (Granier *et al.*, 2000). The most intriguing finding is that final leaf area is correlated to the maximum rate of absolute leaf expansion, but not to the duration of leaf expansion (Cookson *et al.*, 2005). This suggests that a specific mechanism is regulating cellular processes within a narrow developmental window during early leaf morphogenesis and is sufficient to determine the final leaf size.

Changes in tissue and organ morphology essentially involve the structural modification and reorganization of cell wall components, and/or the synthesis and deposition of new material into the existing wall. It is therefore imperative to consider the biochemical and physical factors that regulate wall modification and expansion.

1.5 The plant cell wall and cell expansion

The plant cell wall is a complex polysaccharide structure composed of a cellulose microfibril-hemicellulose network embedded in a secreted matrix of pectins and structural proteins, as shown in Figure 1.3A (Cosgrove, 2005). Cellulose microfibrils are highly ordered arrays of linear glucan chains synthesised at the plasma membrane. Hemicelluloses bind cellulose microfibrils together while pectins form

hydrophilic gels with calcium crossbridging. The mechanical and functional properties of cell walls depend on the nature of fibre composites and the extent of cross-linking.

Cell walls that are growing are less rigid and allow long-term irreversible stretching (yielding) or plastic extension to occur (Cosgrove, 1993). Wall expansion can occur even without wall synthesis, at least in the short term. Although growing cells continually synthesise new cell wall, it is believed to be secondarily coupled to wall loosening (Cosgrove, 1993). Wall loosening is the first step of cell expansion, requiring the rearrangement of load-bearing bonds to relieve wall stress and to allow polymer sliding as water is taken up secondarily. It should be noted that cell expansion is predominantly determined by wall-yielding characteristics rather than the regulation of turgor pressure (Cosgrove, 1993). In comparison, non-growing mature cells elastically (reversibly) swell during solute uptake via increasing turgor driven by osmosis.

A regulatory mechanism is crucial to allow the physical loosening of the immensely stressed cell walls while preserving the mechanical integrity required to counteract the immense internal turgor pressure of 10 to 100 MPa (Cosgrove, 1997). It is evidently possible to break various bonds in the wall without leading to prolonged wall expansion. For example, mechanical weakening of the cell wall with proteases which break down the structural protein network, leads to no significant extension in living plant cells or isolated walls (Cosgrove, 1987). There is as yet no direct evidence that cells can increase growth rate by synthesising or exporting more of any cell wall protein (Cosgrove, 2000a). Taken together, cell expansion is a coordinated process involving wall loosening specific to growth. A proposed key component of the wall-loosening process is the family of wall proteins termed expansins, discussed in the next section.

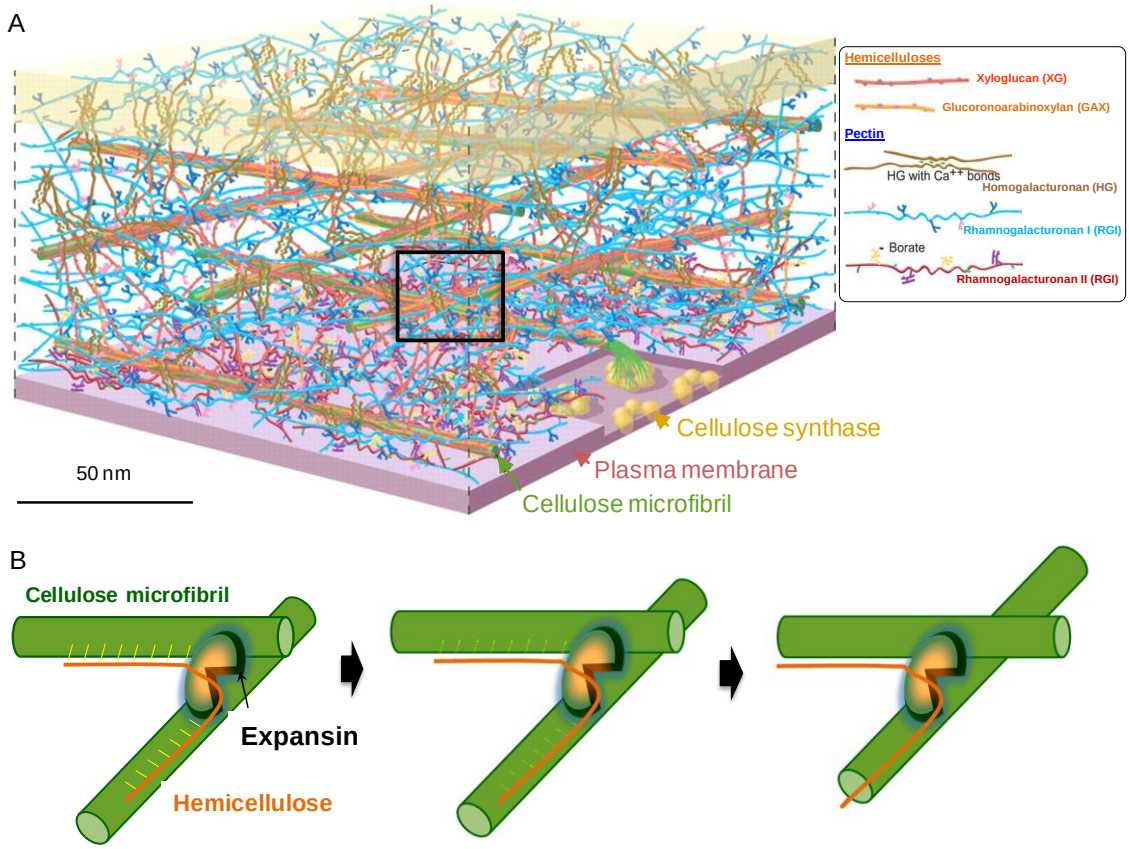

Figure 1.3. (A) A scale model of the Arabidopsis leaf cell wall modified from (Somerville *et al.*, 2004) to show the complex polysaccharide structure. Cellulose microfibrils, which are synthesised by cellulose synthase, are tethered together by various hemicelluloses and embedded in a pectin matrix. (B) A schematic diagram of expansin action in loosening plant cell wall by disrupting the hydrogen bonds (yellow lines) between the cellulose microfibrils and hemicelluloses, allowing the sliding of cellulose microfibrils against each other to release the stresses within the wall polymers (region as indicated by box in A).

1.6 Expansins and leaf morphogenesis

1.6.1 Characteristics of expansins

Expansins are cell wall proteins present in all land plants that can induce pH-dependent cell wall extension or "acid growth" with an optimal pH 4.5 (McQueen-Mason *et al.*, 1992). This results in a time-dependent irreversible extension of cell wall (creep) which can occur over a wide time range (<0.1 to >100 s) (Cosgrove, 2000b). Expansins bind tightly to the cell wall at the cellulose-hemicellulose junctions, and probably have limited mobility and turnover within the cell wall (Cosgrove *et al.*, 2002). The exact biochemical mechanism of action of expansin and the identity of its target site of action are as yet unclear. Cucumber expansin was showed to bind preferentially at the junction between cellulose and hemicellulose, with specificity for xyloglucan (Whitney *et al.*, 2000). It has been proposed that expansins directly induce wall extension by physically disrupting the hydrogen bonds between cellulose microfibrils and hemicelluloses as illustrated in Figure 1.3B (McQueen-Mason and Cosgrove, 1994)(McQueen-Mason and Cosgrove, 1995). This would be a unique mechanism in comparison to other classes of cell wall proteins as there is no known chemical modification or compositional change. In comparison, another cell wall protein, xyloglucan endotransglucosylase/hydrolases (XTHs), enzymatically break and reform glycosidic linkages within wall polymers in a longer timeframe (Rose *et al.*, 2002). Conversely, the fast and direct effect of expansin on the material properties of the cell wall, with no known role in signalling processes, renders it suited for biophysical studies (Fleming *et al.*, 1999). Further details on expansin will be described in Chapter 3.

1.6.2 Strategies for the functional study of expansins

Many isoforms of expansins that reflect the large multigene families which encodes this protein have been discovered (Lee *et al.*, 2001; Sampedro and Cosgrove, 2005).This reflects the widespread role of expansins in intrinsic growth events such as cell enlargement, fruit ripening, leaf abscission and floral organ development, as well as in response to environmental changes (Sharova, 2007). The fine regulation of expansin gene expression is likely to be facilitated by hormonal and environmental

signals through the hormonal regulatory elements found in the promoter regions of expansin genes (Lee *et al.*, 2001).

The functional study of expansins requires the quantification of their activity. It has been a problematic task because expansin is non-hydrolytic (Sampedro and Cosgrove, 2005). Researchers often do not go beyond the measurement of gene transcript abundance as an indication of expansin activity. Immunoblotting with commercial antibodies has been attempted to quantify expansin protein content. However, there are shortcomings with the specificity of antibodies to an undetermined subset of expansins (Rose *et al.*, 2000). To date, the most direct test of expansin activity is the extensometer assay. This is based on the ability of expansins to restore the acid creep of boiled cucumber hypocotyls or to enhance extensibility of artificial cellulose–xyloglucan composites (Whitney *et al.*, 2000; Chanliaud *et al.*, 2004). A major shortcoming is that such *in vitro* tests are usually made with a crude protein fraction of cell walls rather than with purified expansins and that the artificial or boiled wall may not actually mimic the situation in a living cell.

1.6.3 The role of expansin in leaf development

As mentioned, the first direct evidence on the potential biophysical role of expansin in morphogenesis is provided by the initiation of a leaf buttress at the tomato shoot apical meristem via expansin-mediated cell wall loosening (Fleming *et al.*, 1997). Leaf primordia are typically initiated in an orchestrated pattern (phyllotaxy, Figure 1.1), and expansin gene expression has been shown to be up-regulated at the site of future primordium emergence, preceding the primordium outgrowth (Fleming *et al.*, 1999). The local application of expansin-loaded microbeads at the sites of incipient leaf primordia can even reverse the natural phyllotaxy, resulting in out-of-sequence leaf emergence.

On the other hand, Pien and colleagues showed that local induction of expansin expression on a tobacco leaf flank during early stage development is sufficient to modify leaf shape, with bulging at the induction site (Pien *et al.*, 2001). This study suggests the existence of a cell-division-independent mechanism in controlling leaf morphogenesis, and close interaction between cell growth, division and

differentiation, as the programmed pattern of cell proliferation appeared to fill the available space within the organ. However, it was unclear how cell size and number were affected since a detailed histological analysis was lacking. Moreover, whether the local ectopic expression of expansin reflects an endogenous mechanism of leaf morphogenesis remains to be determined. For example, the endogenous expression of *AtEXPA10* was shown to be restricted to certain leaf parts including the base (petiole) and midrib and suppression of *AtEXPA10* expression in differentiating vascular tissue via an antisense approach led to dwarfed leaves with altered morphology (Cho and Cosgrove, 2000). Although it is unclear from these examples whether expansins are functioning specifically in morphogenesis or growth, the data support the concept that alterations in the biophysical parameters of leaf tissue can influence morphogenesis, as shown in animal tissue (Ingber, 2003b).

The significance of different tissue layers in the response observed to altered expansin activity is demonstrated by the different outcomes observed in the different approaches taken. For example, exogenous expansin failed to penetrate deep into all tissue layers, resulting in leaf-like but abnormal outgrowths (Fleming *et al.*, 1997). In comparison, formation of fully functional leaves can be induced by endogenous expansin expression in many cell layers (Fleming *et al.*, 1999). However, these abnormal outgrowths observed by epidermal application of expansin had trichomes and expressed a *Rubisco* gene typical of green leaves. This indicates a potential link of physical attributes (i.e. enhanced wall extensibility) to specific organ formation. This also implies that modulation of cell wall properties could bypass the sequential molecular cascade of genetic interactions that normally regulate development and directly affect growth. It is intuitive that chemical patterns (hormonal distribution and gene expression) are transduced via cell wall modification proteins into the physical pattern (altered distribution of physical stresses), but the reverse (a feedback system) whereby physical links into gene expression is less well explored. Relating chemical and physical processes in development will provide clues to resolve the missing link between genetic regulation and the actual process of morphogenesis. The aim of this thesis (detailed in the following section) was to use the expansin family of protein to explore the linkage of gene expression, cell wall mechanics and leaf morphogenesis.

1.7 Research outline

1.7.1 Aims

1. To test the hypothesis that the cell wall protein expansin is important for leaf morphogenesis through the functional analysis of expansins
2. To apply an atomic force microscopy (AFM) technique to the study of tissue mechanics during early leaf development

1.7.2 Objectives

1. To determine the expression pattern of expansin genes during leaf development in *Arabidopsis thaliana*
2. To use bioinformatic tools and literature mining to investigate expansin gene expression and its regulation
3. To generate inducible knock-down transgenic plants to test the role of expansins in leaf development
4. To develop an atomic force microscopy (AFM) technique for the *in vivo* study of tissue mechanical properties
5. To apply this technique to test the relationship between expansin gene expression and cell wall extensibility

1.7.3 Research questions

A. What is the role of expansins in leaf morphogenesis?
   - What is the spatiotemporal expression pattern of expansin genes?
   - How is the expression of expansin genes regulated?
   - How is leaf growth affected when expansin gene expression is altered during different developmental stages of leaf development?

B. What is the role of the plant cell wall in determining organ growth and form?
   - Can the manipulation of expansin gene expression affect leaf shape?
   - How is the growth pattern of the leaf primordium related to cell wall mechanics?

1.7.4 Hypotheses

1. The cell wall protein expansin plays an important role in growth during leaf development
2. The differential regulation of cell wall extensibility underpins leaf morphogenesis (Figure 1.2B)

1.7.5 Rationale

The study of the function of expansin is important for extending the common cause-and-effect paradigm relating gene activity to pattern and morphogenesis. There is strong evidence that the expression of expansin genes is influenced by phytohormones, especially auxin and brassinosteroids (Sanchez *et al.*, 2004), both of which have solid links to leaf morphogenesis (Li *et al.*, 2007; Sánchez-Rodríguez *et al.*, 2010). It would be interesting to know whether expansin regulation by these phytohormones confers any functional specificity in leaf development.

Many studies carried out on expansins are related to environmental conditions such as water deficit and submergence. For example, a tight association of specific expansins with maize leaf growth has been reported (Muller *et al.*, 2007), which is maintained between different genotypes and developmental stages, as well as under abiotic stress (water deficit). This suggests that expansins are an important part of the intrinsic leaf developmental programme, presumably by being endogenous regulators of cell wall softening.

On the other hand, there are still discrepancies in the correlation of expansin activity with growth (Cho and Kende, 1997c; Caderas *et al.*, 2000). For instance, it was found that there was low or no detectable expansin transcript and protein at the lower region of Festuca leaves with high elongation rate as compared to high expansin activity at the distal end with low elongation (Reidy *et al.*, 2001a).

Currently, there is surprisingly still no comprehensive published literature on the differential expression pattern and functional analysis of expansins during Arabidopsis leaf development. The exact biochemical mechanism of expansin action is not yet fully elucidated or the precise function of individual expansins (Cosgrove, 1999). The classical genetic approach of identifying and analysing single gene

knockouts has not provided significant functional results (Schipper *et al.*, 2002). This may reflect redundancy in the large gene family with overlapping expression patterns. Alternatively, different expansins may play unique developmental or tissue-specific roles but the phenotypes are subtle and required a more careful phenotypic analysis (Wu *et al.*, 2001; Sampedro and Cosgrove, 2005). This means that different expansins may be active in specific spatial and temporal domains, and the phenotype following gene inactivation could be overlooked. In addition, there is the possibility of post-translational regulation (Downes and Crowell, 1998) and cell wall 'desensitisation' (Rochange *et al.*, 2001) so that structural alterations are compensated for. Hence, there is a pressing need for more approaches to measure the effect *in vivo* of altered expansin gene expression, thus allowing confirmation of whether gene manipulation experiments do actually lead to a cell wall phenotype.

The quantification of tissue mechanical properties using AFM would provide the foundation for future studies in combining the molecular genetics and biomechanics of leaf development. This will enable hypothesis testing based on the manipulation of cell wall protein expression and the observed phenotypic and mechanic outcomes. In the long run, this could conceivably be the basis for the testing of biomechanical models based on the viscoelastic properties of the cell wall (Merks *et al.*, 2011). The long-term goal could then be achieving a convergence of molecular genetics and biophysics.

1.8 Thesis outline

This chapter has introduced the different aspects of research in the field of leaf morphogenesis, providing an overview, justifications and project outline for work reported in the subsequent chapters.

Chapter 2 describes the general materials and methods used throughout this study, as well as the more specialised technical details on the molecular works, experimentation and data analysis. Further method considerations for the atomic force microscopy (AFM) technique are provided in Chapter 5.

The main focus of Chapter 3 is on the expression pattern of the alpha-expansin gene family during Arabidopsis leaf development. A developmental staging system to minimise the inherent biological variation in leaf growth during sample harvest is described. Results obtained were compared to that available in the bioinformatic resources and literature, for discussion on the role of expansin.

Chapter 4 describes the incorporation of an artificial microRNA strategy with chemically-inducible gene expression system, to target the down-regulation of specific expansin genes identified to be expressed during early leaf development (Chapter 3). Different experiments performed to verify the functional role of expansin in leaf morphogenesis and organ expansion are reported.

Chapter 5 reports on a pioneering attempt to utilise an AFM approach for the characterisation of plant tissue mechanics during growth. The use of AFM to characterise the cell wall properties of tobacco and Arabidopsis leaf primordia is described with technical considerations and an outline of future work made.

Chapter 6 summarises the overall findings presented in this thesis for further discussion and put the current work into the context of leaf morphogenesis, as well as describing wider implications in the field.

CHAPTER 2 Materials and methods

2.1 Materials

2.1.1 General laboratory chemicals

General laboratory chemicals of analytical grade or equivalent were purchased from Sigma-Aldrich, Fisher, Duchefa Biochemie, Melford, or BDH. Enzymes and reagents were generally ordered from Bioline, Promega, Invitrogen, or Roche, whereas gel extraction and miniprep kits were from Qiagen.

Custom oligonucleotides were synthesised by Sigma Genosys. Automated DNA sequencing was performed by the Genetics Core Facility at the University of Sheffield (http://www.shef.ac.uk/medicine/research/corefacilities/genetics.html).

Water used for preparing growth media, buffers and solutions was either reverse osmosis (RO) or deionised ultra-high-purity (UHP) water from ELGA ion exchange system (Elga, Purelab), whereas nuclease-free water for molecular works involving DNA and RNA was from Ambion.

2.1.2 Plant materials

Seeds of wild-type *Arabidopsis thaliana* Columbia-0 (Col-0) were originally bought from NASC seed stock centre but had been propagated since then in the lab. Seeds of T3 pOpON::CsEXPA1 line 10/1 were generated by a previous postdoctoral research assistant (Dr. Robert Malinowski) in the lab and selfed for T4 generation.

2.2 Plant growth conditions

Standard methods of growing Arabidopsis on solid medium were followed (Weigel and Glazebrook, 2002). Seeds were surface-sterilised with 20% v/v bleach in 0.05% v/v Tween-20 for 10 min, rinsed 3x with autoclaved water, and stored for 5-7 days at 4^{o}C devoid of light. Stratified seeds were then sown onto square petri plates (12 x 12 cm, 6 x 6 seeds) containing 70 ml of growth medium with 0.5x MS salts (Sigma-Aldrich), 1% w/v sucrose, 0.8% w/v plant agar (Duchefa Biochemie). Where appropriate for selection of transformants and segregation analysis, antibiotics (50 µg/mL kanamycin for pOpON transformant plants) were included in the growth medium.

Plates were sealed with micropore tape (3M) and placed horizontally in a growth cabinet (Economic Delux, ECD01E Snijders Scientific b.v.) at 22^{o}C day/ 20^{o}C night under a 16-hour photoperiod at light intensity of 100 μmol m^{-2} s^{-1} photosynthetically active radiation supplied by white fluorescent tubes.

For the propagation and transformation of Arabidopsis plants, seedlings from the solid culture medium were transferred onto 16 cm^2 square pots containing M3 compost (Levingtons) containing 5% perlite at at 20^{o}C under a 16-hour photoperiod with irradiance of 100 μmol m^{-2} s^{-1}.

2.3 General nucleic acid techniques

2.3.1 Plant genomic DNA extraction

Genomic DNA was extracted using Shorty buffer (0.2 M Tris-HCl (pH 9.0), 0.4 M LiCl, 25 mM EDTA (pH 8.0), 1% SDS). Individual Arabidopsis leaves were placed in 1.5 mL microcentrifuge tubes, flash frozen with liquid nitrogen and then ground with plastic pestles. 500 μL of Shorty buffer was added and mixed by inversion. After centrifugation at 13000 rpm, 4^{o}C for 10 min, 350 μL of supernatant was transferred to fresh tubes containing 350 μL isopropanol, mixed by inversion and further centrifuged for 10 min. The supernatants were discarded and the pellets were washed with 80% ethanol before being air dried for 15 min at room temperature, and finally resuspended in 200 μL of TE buffer (10 mM Tris-HCL (pH 7.5), 1 mM EDTA).

2.3.2 Plant total RNA extraction

Total RNA was extracted by the guanidine thiocyanate method (Chomczynski and Sacchi, 1987) using TRIzol® Reagent (Invitrogen) according to the manufacturer guidelines. Briefly, the frozen samples (-80^{o}C) were ground using chilled, autoclaved plastic pestle in 1.5 mL microcentrifuge tubes. TRIzol (500 μL) was added with further grinding, followed by pelleting of the tissue residues prior to chloroform (100 μL) extraction and overnight isopropanol (300 μL) precipitation of RNA at -20^{o}C. Glycogen (10 μg) was used to assist RNA precipitation when extracting RNA from very small tissue quantity. After overnight precipitation, the RNA was pelleted by centrifugation at 13000 rpm, 4^{o}C for 20 min and washed with

ice-cold 80% ethanol before air drying at room temperature for around 5 min and resuspended in 15 µL of RNase-free water. The quality and quantity of RNA was checked using a NanoDrop ND-8000 UV-Vis spectrophotometer (Thermo Scientific). Equivalent amounts of RNA were used for cDNA synthesis, adjusted according to the band intensity from gel electrophoresis.

2.3.3 Reverse transcription/ cDNA synthesis

2-4 µg of total RNA, as standardised through gel electrophoresis and spectrophotometric measurement using NanoDrop 8000 (Thermo scientific), was cleaned using a DNA-free™ kit (Ambion), 1.5 µL 10x DNase buffer and 1 µL rDNase made up to 15 µL reaction with Rnase-free water, for 1 hour incubation at 42^{o}C using thermocycler. The enzyme was inactivated by 1 µL inactivation buffer with 30 min incubation at 37^{o}C. 10 µL of cleaned RNA was then used as template for the first-strand cDNA synthesis (25 µL reaction) using 200 units M-MLV reverse transcriptase Rnase H minus (Promega) with 5 µL of 5x RT buffer, 0.08 µg/µL oligo dT(18) and 5 µL 2.5 mM dNTP mix, incubated for 60 min at 42^{o}C.

For RT-PCR analysis of *EXPA*s during leaf development (Figure 3.6), 2 µg of total RNA extracted from pooled 97, 21 and 9 leaf primordia for D12, D14 and D16 samples respectively, and single leaves for D20, D24, D28 and D32 were used for cDNA syntheses. 35 to 70 dark-grown hypocotyls were pooled for RNA extraction for RT-PCR analysis of expansin expression in hypocotyl experiments.

2.3.4 Polymerase chain reaction (PCR)

Most PCR amplifications were carried out using BIOTAQ™ DNA polymerase (Bioline) in 25 µL reactions, typically as follows:

10x NH_4 buffer	2.5 µL
50 mM $MgCl_2$	1 µL
2.5 mM dNTP	1.5 µL
BioTaq DNA polymerase	0.2 µL (5u/µL)
10 µM Primer pairs	2 µL
RNase-free water	up to 25 µL

Primers for the RT-PCR analysis of *EXPA* transcripts (Figure 3.6) were designed using Primer-blast (http://www.ncbi.nlm.nih.gov/tools/primer-blast/) to: span across intron whenever possible to allow different-sized PCR products from cDNA and genomic DNA; have a melting temperature (Tm) of around 60^{o}C and 50% GC content; with product sizes around 400 base pairs (bp) (Table 2.1). Primer specificity was validated using Primer-Blast against genomic and reference mRNA sequences.

A Techne Touchgene Gradient Thermal Cycler (Krackeler Scientific Inc.) was used routinely with the following protocol:

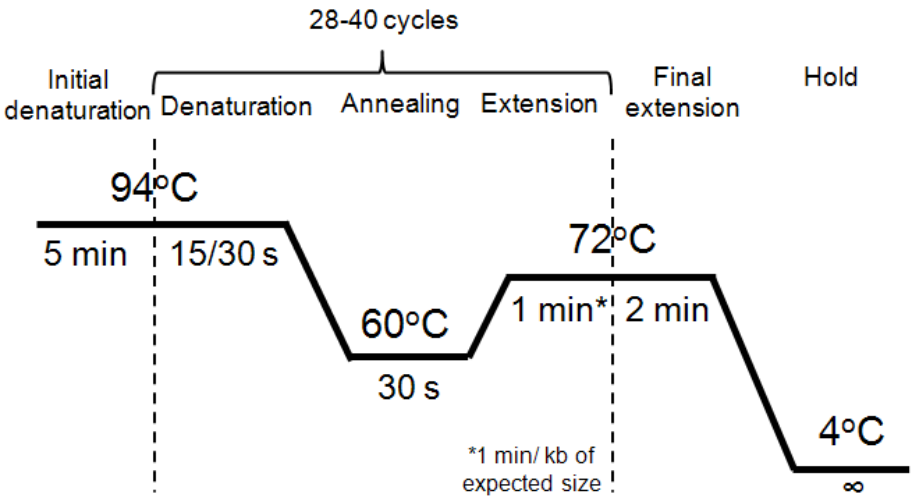

For RT-PCR analysis of *EXPA*s: Hot lid 105^{o}C 4 min, initial denaturation at 94^{o}C for 5 min, 35 cycles: 15 s at 94^{o}C, -1^{o}C s^{-1} to 60^{o}C, 30 s at 60^{o}C, 1^{o}C s^{-1} to 72^{o}C and 1 min at 72^{o}C, 1.8^{o}C s^{-1} back to 94^{o}C, with 1 min final extension 72^{o}C and final hold at 4^{o}C.

PP2A(A3) (At1g13320) was chosen as reference gene and internal control for PCR reactions, being reported as the most stably expressed gene across leaf development (Czechowski *et al.*, 2005) with expression level close to that of expansin genes in comparison to *RBCS* and 18S rRNA. Transcript analysis was independently repeated at least twice.

Table 2.1. Sequences of primer pairs used in α-expansin transcript RT-PCR analysis.

Gene	Accession no.	Sequence 5' → 3'	Length	Tm	GC%	PCR product size (bp)	
						cDNA	Genomic DNA
α-Expansins							
AtEXPA1	At1g69530	ACGTAGCTGCGCACCTGTGAA	21	66	57	428	598
		ACGCCTTACCGAACAACGCAG	21	67	57		
AtEXPA2	At5g05290	AAATTGTCCGCCTTCAAAAGTCT	23	62	39	430	528
		CTTTGCCTTAGCTAATGATAATGG	24	59	38		
AtEXPA3	At2g37640	GACTCGAAAGTTTTTGCCGGAG	22	64	50	432	1219
		TTTGCTCAGCCGAGTGACGAC	21	66	57		
AtEXPA4	At2g39700	GCTCGAAGGCGCTCTTGTTC	20	65	60	414	509
		TTGCGGTGATGAGGATCGAA	20	65	50		
AtEXPA5	At3g29030	ATACCGAAACTGCCCTCCGGT	21	61	57	445	856
		CATTGTGGTCACTGCCACTAAC	22	60	50		
AtEXPA6	At2g28950	GACTCTGAAGTTCTTTCCCATGA	23	60	43	434	1108
		ACTTTGCTCAGCCTAGTGACAAT	23	60	43		
AtEXPA7	At1g12560	ACGGAAATTAGCGGTGCTCTTG	22	65	50	436	520
		TTGGTACCAAGACTCCAACGCT	22	63	50		
AtEXPA8	At2g40610	GAACTGACCACCTTGGTAGGTT	22	59	50	430	921
		CCCTGGCCTCTCCAACGATAA	21	66	57		
AtEXPA9	At5g02260	GACGCGGAAGTTCTTGCCGG	20	69	65	439	1186
		TCCTAACTTTAATCAAGCTAGCGA	24	59	38		
AtEXPA10	At1g26770	CTTCTGCCCGCCAAATAACG	20	65	57	431	593
		GTCCACCGGCAAAAGTCTGG	20	65	55		
AtEXPA11	At1g20190	GACTCTGAAGTTCTTTCCCATGA	25	59	60	437	599
		ACTTTGCTCAGCCTAGTGACAAT	22	67	50		
AtEXPA12	At3g15370	ACGGAAATTAGCGGTGCTCTTG	23	61	44	442	927
		TTGGTACCAAGACTCCAACGCT	25	62	32		
AtEXPA13	At3g03220	GAACTGACCACCTTGGTAGGTT	21	63	52	358	878
		CCCTGGCCTCTCCAACGATAA	23	62	44		
AtEXPA14	At5g56320	GACGCGGAAGTTCTTGCCGG	21	65	57	437	516
		TCCTAACTTTAATCAAGCTAGCGA	21	71	57		
AtEXPA15	At2g03090	CGGCCGTCAATTCCGTTAAA	20	65	50	402	402
		AGGCGGGTGGTGAAATTCCT	20	65	55		
AtEXPA16	At3g55500	GTGGAAACGATGCTTCGGGA	20	66	55	435	682
		CTCCGGCCACGTTCGTAATC	20	65	60		
AtEXPA17	At4g01630	GAAGTTAACGTTGCTCTTGAAGC	23	60	44	435	435
		AACTTTGCTCAGGCAAGCGACA	22	67	50		
AtEXPA18	At1g62980	GCATGCGGTCAATGTTTCCA	20	65	50	447	628
		AGAGGTGAGCCGGAACGAGA	20	65	60		
AtEXPA20	At4g38210	AGGAGTGGAACTGCTTTCCTTG	22	62	50	435	435
		ATTCGGGACTCTCCTCCGATTA	22	63	50		
AtEXPA21	At5g39260	AAAGTTAGTCTTTCCATCAAAAGTC	25	57	32	424	424
		TTTATGTCCACCAGGATCCGCT	22	65	50		
AtEXPA22	At5g39270	AAAGTTAATCCTACCATCAAAAGTC	25	56	32	426	426
		AATTACAGCAAAACCACAGACCTT	24	60	38		
AtEXPA23	At5g39280	AAAGTTAATCTTTCCATCAAAAGTCT	26	57	27	425	425
		ATTACAGCAAAACCGAAGGCGTT	23	65	44		
AtEXPA24	At5g39310	AAAATTAACCTTTCCATCAAAACTCT	26	59	27	429	429
		GATTTTACCAAGCCCAATGACAAT	24	62	38		
AtEXPA25	At5g39300	AAAGTTAATCTTTCCATCAAAAGTCT	26	57	27	425	425
		ATTACTCCAAAACCGAAGGCGTT	23	64	44		
AtEXPA26	At5g39290	AAAAGTTAATCTTACCATCAAAAGTC	26	56	27	427	427
		AATTACAGCAAAACCACAGACCTT	24	60	38		
Controls							
AtRbCS	At5g38410	CTTCCTCTATGCTCTCCTCC	20	60	55	494	739
		GTTGTCGAATCCGATGATCC	20	64	50		
PP2A	At1g13320	ACGTGGCCAAAATGATGCAA	20	65	45	333	459
		CGCCCAACGAACAAATCACA	20	65	50		

2.3.5 Semi-quantitative reverse transcriptase-PCR (sq-RT-PCR)

Sq-RT-PCR for transcript expression analysis was performed in a similar manner as normal *Taq* PCR. However, the PCR cycle during the exponential phase was paused at defined intervals at the end of extension and aliquots (5 µL) were routinely taken at cycle 24, 28, 30 and 32. At the end of PCR, agarose gel electrophoresis was performed as described below with all of the aliquots loaded accordingly and visualised. The optical intensity of each band specific to each gene relative to the internal control was analysed using ImageJ (http://rsbweb.nih.gov/ij/) which provided a semi-quantitative measure of relative gene expression level based on three biological replicates.

Sq-RT-PCR analysis of pOpON::amiREXP (Figure 4.4) using RNA extracted from 12 DAS whole-rosette was performed using primers as in Table 2.1. Sq-RT-PCR analysis of staged-transfer induced (14-16 DAS) pOpON::CsEXPA1 whole-plants (4 µg) used forward primer-5'TTTGTCTTCACCTTCGCTGA3' and reverse primer-5' GCCTTGGCCATTGAGATAGT3' for *CsEXPA1* (Cucsa.143960.1), and used internal control *RBCS* and *PP2A* as in Table 2.1 (Figure 4.5). For sq-RT-PCR analysis of *EXPA8* (Table 2.1) expression in pOpON::CsEXPA1 hypocotyl (Figure 4.25), *ACTIN2* (At3g18780) was used as internal control: forward primer-5' TCAGCACATTCCAGCAGATG3' and reverse primer-5' TTAACATTGCAAAGAGTTTCAA3'.

2.3.6 Real-time quantitative PCR (RT-qPCR)

RT-qPCR experiments using SYBR® Green PCR master mix (Applied Biosystems) in 96-well optical reaction plates with optical adhesive covers (ABI PRISM™) were designed, performed and analysed using a StepOnePlus™ Real-Time PCR system with its accompanying StepOne Software (Applied Biosystems, version 2.2). Primers were designed using QuantPrime (http://www.quantprime.de/) and Primer-blast (http://www.ncbi.nlm.nih.gov/tools/primer-blast/) (Table 2.2).

Table 2.2. Sequences of primers used for RT-qPCR showing the results from standard graphs.

			Amplicon		Standard graph		
Gene	**Oligo**	**Sequence (5'→ 3')**	**Size (bp)**	**Tm**	**Slope**	**R^2**	**Efficiency**
AtEXPA1	qAtEXPA1FP	CTTACCGAAGAGTGCCGTGCGT	102	78	-2.95	0.99	118
	qAtEXPA1RP	CGGCTCCTCCGACGTTAGTG					
AtEXPA3	qAtEXPA3FP	CCCGTCTCCTATCGCAGGGTA	106	78	-2.92	0.99	120
	qAtEXPA3RP	CGCCGGCAACGTTAGTTACC					
AtEXPA5	qAtEXPA5ISFP	ATGGTACCCTCCCAACCACCA	109	77	-2.77	0.99	130
	qAtEXPA5ISRP	CGAGCTCCGAACCCTTCTATACATAAC					
AtEXPA8	qAtEXPA8FP	GAACTCATGGAGACGACGGA	89	84		Not determined	
	qAtEXPA8RP	AAGCTCCGCCCATGGTG					
AtEXPA10	A10OutFFP_ami	AACCCAACAACATAATTTCACATA	82	73	-2.95	0.98	126
	qAtEXPA10RP	TGTTAACAACTTGGGACTTGG					
AtEXPA13	qA13FP	CCGGTGCAGTATCGAAGGATCAAC	70	78		Not determined	
	qA13RP	TGCCTCCACCATCGACTGTAAAC					
AtEXPA15	qA15FP	GAGAATGTTCATGGGTAAGATGGG	77	76		Not determined	
	qA15RP	CATGAACAGAGCACACCATTGC					
CsEXPA1	qCsEXPA1FP	CCTCCTCTCCAACATTTCGAC	96	81		Not determined	
(Cucsa.143960.1)	qCsEXPA1RP	TGGTACCCTACGAAAGGAGAC					
UBC21	qAtUBC21FP	CTCTTAACTGCGACTCAGGGAATC	67	75	-3.49	1	93
(At5g25760)	qAtUBC21RP	TGTGCCATTGAATTGAACCCTCTC					
ACT2	qAtACT2RP	CTTCCGCTCTTTCTTTCCAAGCTC	76	75	-3.31	0.99	100
(At3g18780)	qAtACT2FP	ACCATTGTCACACACGATTGGTTG					

The PCR efficiencies of each primer pair (200-250 nM working concentrations) were determined from standard curve experiments (Figure 2.1, 2.2) using 1 µL of five 10-fold serial dilutions of cDNA from a starting concentration of 500 ng/µL (readings from NanoDrop 8000 (Thermo scientific)), 10 µL PCR master mix (2.0x) and nuclease-free water to a final reaction volume of 20 µL. The PCR programmes were performed as follows:

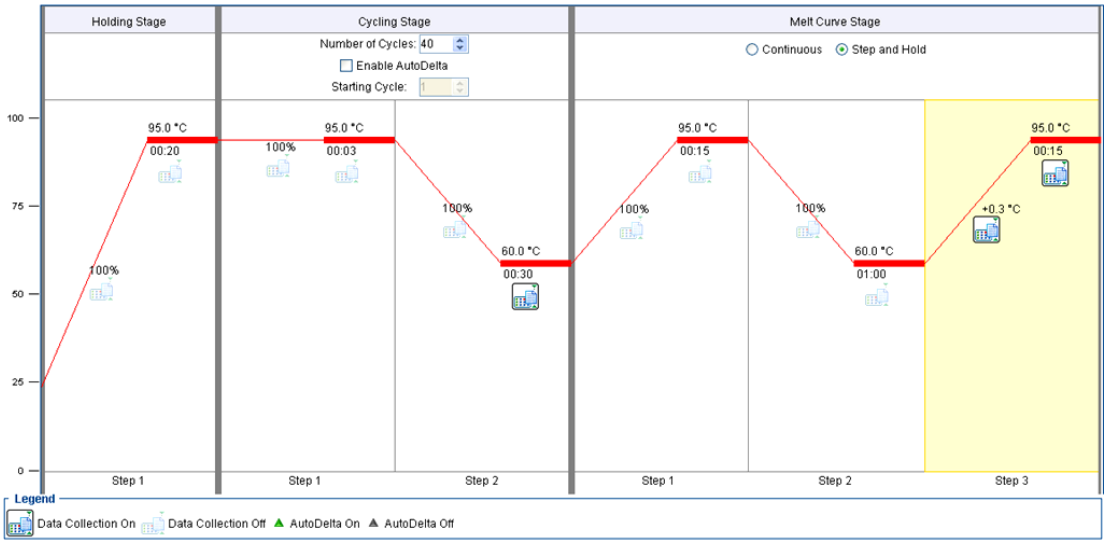

Any amplification which detected primer dimers from melt curve analysis was excluded from the data analysis. Respective PCR efficiency values (Table 2.2) were used when analysing the result from comparative C_T ($\Delta\Delta C_T$) experiments. A primer efficiency value of 100 was used whenever the exact efficiencies of primer pairs were not determined. In comparative C_T experiments for quantitative analysis of gene expression level, *UBC21* was chosen over *ACT2* as a reference gene, the gene showing more stable expression across all plant tissues and developmental stages (Czechowski *et al.*, 2005). The same cDNA samples as sq-RT-PCR were used in the $\Delta\Delta C_T$ experiments with equal dilutions.

2.3.7 Agarose gel electrophoresis

PCR products were mixed with 6x loading buffer (0.2% w/v bromophenol blue, 50% v/v glycerol) before routinely electrophoresed together with 5 μL Hyperladder I (Bioline) on 1% w/v 20-well 200 mL agarose gels (dissolved in 1x TAE buffer) containing ethidium bromide (0.5 μg/ mL) under 150 V for 1 hour. The DNA/ RNA was visualised using a BXT-20.M UV-transilluminator (Progen Scientific), and digital images taken by UVitech digital camera.

2.3.8 DNA gel extraction

DNA was recovered from agarose using the QIAquick Gel Extraction Kit (Qiagen) following the manufacturer's protocol at room temperature. Briefly, the band of DNA fragment was excised from the agarose gel using a clean scalpel blade under UV-transilluminator into pre-weighed microcentrifuge tube. 3 volumes of Buffer QG were added and incubated at 50^{o}C for 10 min with regular vortexing until all material was dissolved. The dissolved solution was then transferred to the QIAquick spin column, centrifuged at 13000 rpm for 1 min; flow-through discarded, the filter washed with 750 μL Buffer PE and centrifuged for 1 min. Centrifugation was repeated after discarding the flow-through. The column was then transferred to a fresh microcentrifuge tube, 30 μL of Buffer EB was added, left stand for 1 min, then the eluate collected after centrifugation at top speed for 1 min.

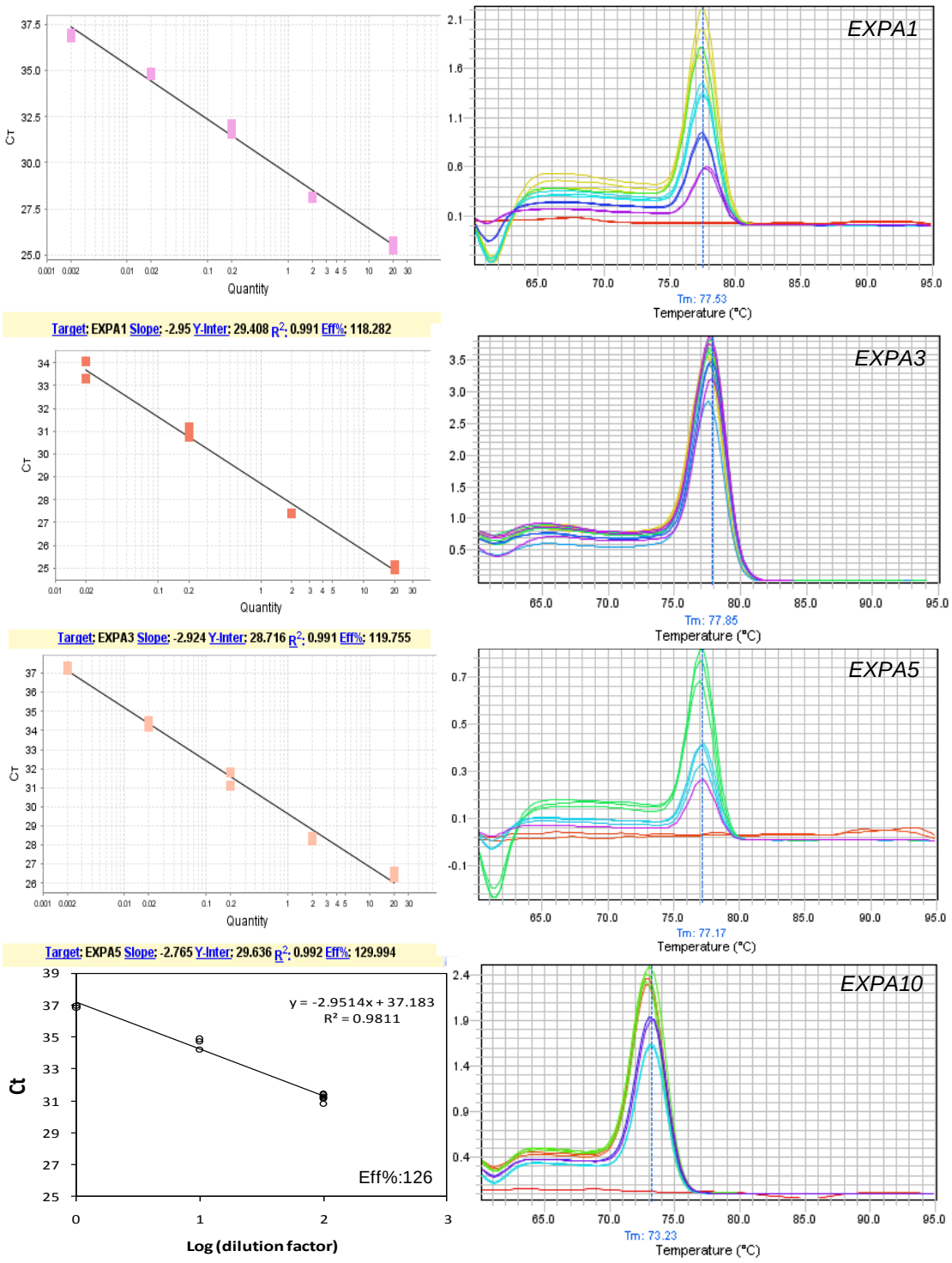

Figure 2.1. Standard curve and melt curve analysis of primer pairs of *EXPA1*, *EXPA3*, *EXPA5* and *EXPA10*, showing the primer efficiency (Eff%) and the melting temperature (Tm) of amplicon.

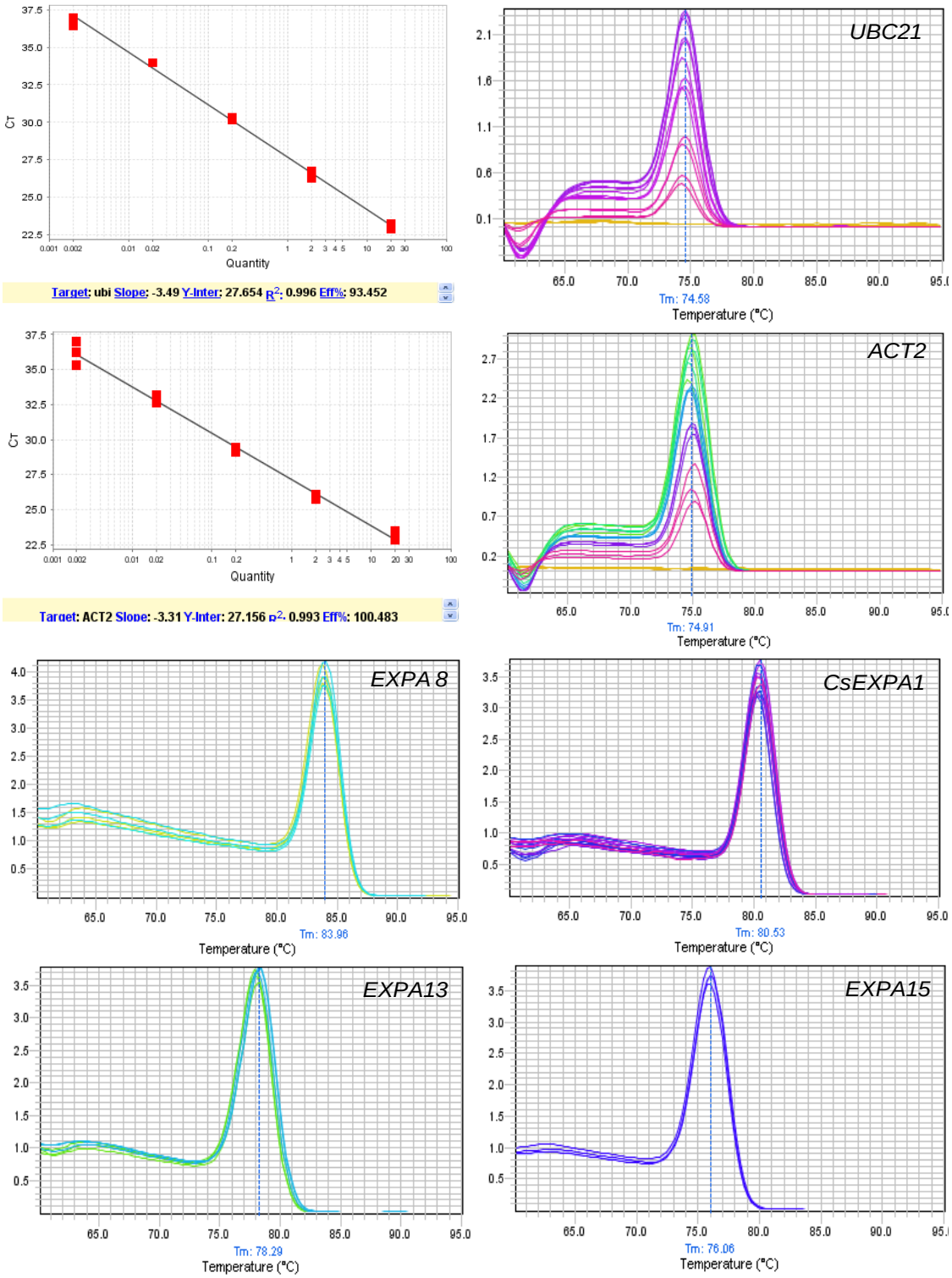

Figure 2.2. Standard curve and melt curve analysis of primer pairs of *UBC21* and *ACT2* showing the primer efficiency (Eff%) and the melting temperature (Tm) of amplicon. Only melt curve analysis is available for *EXPA8*, *EXPA13*, *EXPA15* and *CsEXPA1*showing the absence of primer dimers.

2.4 Cloning techniques

2.4.1 Generation of amiREXP construct

The amiRNA was designed using the Web MicroRNA Designer (WMD3, http://wmd3.weigelworld.org/cgi-bin/webapp.cgi) to target specific expansin genes (*EXPA10*, *EXPA1*, *EXPA5* and *EXPA3*) involved in leaf development (Figure 4.1B). Four primers (I to IV) were designed for overlapping PCR (site-directed mutagenesis) so that the miRNA and miRNA* sequences on the structural backbone of plant miRNA precursor sequence (miR319a) on pRS300 plasmid (courtesy of Prof. Detlef Weigel) are substituted by the desired 21 mer (Table 2.3).

Table 2.3. Primer sequences for amiRNA cloning. The capital letters in oligo I to IV correspond to the desired miRNA-miRNA* region.

Oligo name	5'→3' Sequence	Length (nt)
OligoA	CACCCAAGGCGATTAAGTTGGGTAAC	26
Oligo B	GCGGATAACAATTTCACACAGGAAACAG	28
Ami10,1,5,3_I	gaTCATTGTGCCGGAAGCACCACtctctctttgtattcc	40
Ami10,1,5,3_II	gaGTGGTGCTTCCGGCACAATGAtcaaagagaatcaatga	40
Ami10,1,5,3_III	gaGTAGTGCTTCCGGGACAATGTtcacaggtcgtgatatg	40
Ami10,1,5,3_IV	gaACATTGTCCCGGAAGCACTACtctacatatatattcct	40

OligoA primer (Table 2.3) was modified to included CACC at the 5' end (for additional 3' single-stranded overhang) to be TOPO®-cloning compatible for integration into pENTR™/D-TOPO® entry clone (Invitrogen) through directional TOPO® cloning. The overhang in the cloning vector (GTGG) invades the 5′ end of the PCR product, anneals to the added bases, and stabilizes the PCR product in the correct orientation.

The cloning protocol by Dr. Rebecca Schwab was followed (available online: http://wmd3.weigelworld.org/downloads/Cloning_of_artificial_microRNAs.doc):

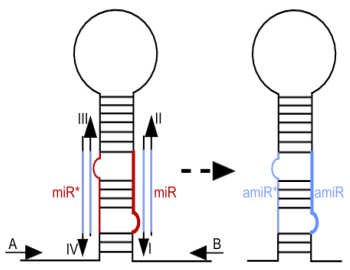

I: microRNA forward
II: microRNA reverse
III: microRNA* forward
IV: microRNA* reverse

Step	Forward oligo	Reverse oligo	Template	Product size (bp)
(a)	A	IV	pRS300	275
(b)	III	II	pRS300	176
(c)	I	B	pRS300	301
(d)	A	B	(a)+(b)+(c)	702

Oligonucleotides A and B are based on the template plasmid sequence (pRS300) which are located outside of the multiple cloning site. Primer I contains the amiRNA in sense orientation, primer II its reverse complement, primer III the amiRNA* sequence in sense and primer IV the amiRNA* sequence in antisense orientation. First round PCR of amiRNA step (a) to (c) were carried out using *Pfu* ultra high-fidelity DNA polymerase (Stratagene) on pRS300 plasmid as follows:

10x PCR buffer (with Mg^{2+})	5 µL
2.5 mM dNTPs	4 µL
10µM Forward primer	2 µL
10µM Reverse primer	2 µL
plasmid DNA (1:100)	2 µL
Pfu (2.5u/µL)	0.5 µL
RNase-free water	up to 50 µL

PCR programmes: hot lid 105^{o}C, initial denaturation at 95^{o}C for 2 min, 24 cycles of 95^{o}C 30 s, 55^{o}C 30 s, 72^{o}C 1 min and final extension 72^{o}C for 7 min.

The three resulting PCR products were ran on 2% agarose gel and purified according to section 2.3.8 and eluted in 20 µL RNase-free water, which then used for the final PCR step (d) as follows:

10x PCR buffer (with Mg^{2+})	5 µL
2.5 mM dNTPs	4 µL
10µM OligoA	2 µL
10µM OligoB	2 µL
PCR product (a)	0.5 µL
PCR product (b)	0.5 µL
PCR product (c)	0.5 µL
Pfu (2.5u/µL)	0.5 µL
RNase-free water	up to 50 µL

PCR programmes: hot lid 105^{o}C, initial denaturation at 95^{o}C for 2 min, 24 cycles of 95^{o}C 30 s, 55^{o}C 30 s, 72^{o}C 1 min 30 s and final extension 72^{o}C for 7 min. The fusion product of 702 bp (Figure 4.1D) was ran on 1% agarose gel and gel purified as above. The final eluent in 20 µL RNase-free water was used for a further pENTR™/D-TOPO® topoisomerase reaction.

2.4.2 pENTR™/D-TOPO® topoisomerase reaction

TOPO cloning was performed according to the manufacturer's protocol using 2 ng of PCR product, 1 µL of the provided salt solution and 1 µL of TOPO vector in a 6 µL reaction with RNase-free water, gently mixed and incubated at room temperature for 5 min before placed on ice. 2 µL of cloning reaction product was used for heat transformation of 100 µL of DH5α chemically competent *E. coli* (Bioline). Putative transformed colonies were bulked up by growth overnight (as per Section 2.4.4), minipreped (as per section 2.4.5) and the sequence checked.

2.4.3 LR clonase reaction

Inserts from pENTR/D-TOPO were recombined using LR clonase II (Invitrogen) into the Gateway®-compatible binary vector pOpON2.1 (Wielopolska *et al.*, 2005), with an entry vector and destination vector reaction ratio of 1:1 as follows:

Entry clone (50-150 ng)	1-7 µL
Destination vector (150 ng/µL)	1 µL
5x LR Clonase II enzyme mix	4 µL
TE buffer pH 8.0	up to 8 µL

This was mixed by flicking and incubated at 25°C in a water bath for 1 hour before the reaction was terminated by the addition of 2 µL proteinase K solution and incubation at 37°C for 10 min. 2 µL of LR cloning reaction product was used to transform competent *E. coli* cells as described in section 2.4.4.

2.4.4 Transformation of competent *Escherichia coli*

A 100 µL aliquot of competent *E. coli* cells (DH5α, Bioline α-Select Bronze Efficiency) was thawed on ice and 2 µL of cloning reaction product was added. The DNA and cell mixture was then incubated on ice for 30 min, before heat shock in a 42°C water bath for 30 seconds and then immediately placed on ice for 2 min. 900 µL of SOC medium (2% w/v tryptone, 0.5% w/v yeast extract, 0.4% w/v glucose, 10 mM NaCl, 2.5 mM KCl, 10 mM $MgCl_2$ & 10 mM Mg SO_4) was added and the mixture in a polypropylene tube was incubated at 37°C for 60 min with shaking at 200 rpm. 100 µL of the transformation mix was then plated on LB agar plates (1% w/v tryptone, 0.5% w/v yeast extract, 1% w/v NaCl, 0.5% w/v agar, adjusted to pH

7.5 with 5 N NaOH) supplemented with appropriate antibiotic (pENTR^{TM}/D-TOPO: 50 µg/mL kanamycin, pOpON2.1: 25 µg/mL spectinomycin) for selection and incubated at 37^{o}C overnight. Colony PCRs were carried out to verified the insertion using primer OligoA and M13 reverse primer-5'CAGGAAACAGCTATGACC3' which gave a product size of 875 bp. PCR-verified colonies were picked and bulked up through LB overnight culture (1% w/v tryptone, 0.5% w/v yeast extract, 1% w/v NaCl, adjusted to pH 7.5 with 5 N NaOH) supplemented with antibiotic, incubated at 37^{o}C with shaking at 200 rpm overnight.

2.4.5 Plasmid DNA preparation (miniprep)

Preparation of plasmid DNA was performed at room temperature using the QIAprep spin miniprep kit (Qiagen) following the manufacturer's protocol. An LB overnight culture was pelleted by centrifugation in a microcentrifuge tube at 13000 rpm for 1 min. The cells were resuspended in 250 µL of Buffer P1 by pipetting, followed by the addition of 250 µL Buffer P2 and mixed gently by inversion 4 to 6 times. 350 µL of Buffer N3 was added and the tube was immediately inverted gently 4 to 6 times. The lysate was centrifuged at 13000 rpm for 10 min and the supernatant was transferred to the QIAprep spin column, further centrifuged for 30 seconds. The flow-through was discarded and the column was washed with 750 µL of Buffer PE with centrifugation at 13000 rpm for 1 min. The centrifugation was repeated to remove any residual wash buffer after the flow-through was discarded. The column was transfer to a clean microcentrifuge tube, 40 µL of RNase-free water was added and left to stand for 2 min before centrifugation twice at 13000 rpm for 1 min. The isolated DNA was stored at -20^{o}C before further use.

2.5 Plant transformation with *Agrobacterium tumefaciens*

2.5.1 Transformation of *Agrobacterium* with plasmid DNA

50 µL of electrocompetent *Agrobacterium tumefaciens* cells of strain GV3101::pMP90RK were thawed on ice and 1 µL of miniprep DNA was added and transferred to a pre-chilled sterile electroporation cuvette (Eppendorf), subjected to 5 msec pulse of capacity 25 µF, 2.5 kV, 200 Ω on a Bio-rad Gene-Pulser. Immediately after electroporation, 500 µL of low salt LB medium (1% w/v tryptone, 0.5% w/v yeast extract, 0.5% w/v NaCl, adjusted to pH 7.0 with 5 N NaOH was added with

gentle mixing by pipetting into a fresh microcentrifuge tube on ice. This was incubated at 28°C with gentle shaking at 30 rpm for 4 hours before plating on LB agar plates containing 100 µg/mL rifamycin, 50 µg/mL gentamicin, 50 µg/mL kanamycin and 100 µg/mL spectinomycin. LB plates were incubated at 28°C for 3 to 4 days.

2.5.2 Preparation of *Agrobacterium* for floral dipping

An antibiotic-resistant colony of *Agrobacterium* from the LB plates (Section 2.5.1) was selected to inoculate 5 mL of low salt LB overnight culture containing the antibiotics (as section 2.5.1) at 28°C with shaking at 200 rpm. 800 µL of the overnight culture was stored as glycerol stocks with 200 µL of sterile 80% v/v glycerol at -80°C. The rest of the overnight culture was used to inoculate 200 mL of low salt LB containing antibiotics at 28°C with shaking at 200 rpm for 1-2 days until the optical density was approximately 0.8. The culture was divided evenly into six 50 mL-Falcon tubes and cells were harvested by centrifugation at 3500 rpm for 10 min. The cells were then resuspended in 0.5x MS pH 5.8 with 5% w/v sucrose and 0.05% v/v Silweet L-77, ready for floral dip plant transformation (Section 2.5.3).

2.5.3 Agrobacterium-mediated floral dip plant transformation

Arabidopsis thaliana plants (ecotype Col-0) grown in the compost (Levingston M3 compost) were transformed with *Agrobacterium tumefaciens* strain GV3101::pMP90RK harbouring the constructs by the floral dip method (Clough and Bent, 1998). The primary inflorescence stems were cut off to encourage the growth of secondary stems. After 5 to 10 days, the plants were transformed by the immersion of inflorescences in a suspension of *A. tumefaciens* solution (section 2.5.2) for 5 to 10 seconds with gentle agitation. Then, the plants were covered with a black plastic bag and kept in high humidity overnight. The floral dipping was repeated after one week on the newly bolted inflorescences. After that the plants were maintained as usual and well-watered until they set seed.

2.5.4 Screening of pOpON transformant plants

T1 seeds were collected, surface-sterilised and stratified as described in section 2.2. Seeds were sown on 0.5x MS medium containing 50 µg/mL kanamycin for selection and segregation analysis. PCR verification of the insertion using the genomic DNA

extracted according to section 2.3.1 was performed using oligonucleotides A and B (Table 2.3) based on a typical PCR programme (Section 2.3.4).

2.6 Treatments of pOpON transformant plants

2.6.1 Dexamethasone (Dex) induction test

For induction tests, the leaves or seedlings were harvested into 48-well plates containing either 10 μM Dexamethasone (Dex) prepared from 10 mM stock (Sigma-aldrich) in dimethyl sulfoxide (DMSO) through 1:1000 dilutions with water or 0.1% v/v DMSO (control).

For plate induction experiments, stratified seeds were sown at a density of 4 cm^2 per seed on 0.5x MS agar medium supplemented with various concentrations of dexamethasone made up using 10 mM stock in DMSO and using DMSO 0.1% v/v as 0 μM control.

For staged-transfer experiments, plants grown on 0.5x MS agar medium at density of 4 cm^2 per seed were categorised according to the number of the number of visible leaves (> 1 mm width) and the size of leaf 6. The modal category of plants with comparable developmental stages was chosen to be transferred to new small round petri dishes (5 cm diameter) containing 0.5x MS agar medium supplemented with DMSO 0.1% v/v (0 μM) or 10 μM dexamethasone.

For droplet induction experiments, inducer dexamethasone (10/20 μM) was prepared from 10 mM stock in DMSO and sterile Sephadex® G-100 beads (10-40 μm, Amersham Biosciences) to increase viscosity and aid the retention of inducer. Sephadex beads were rinsed three times in 1x phosphate buffer before made to final concentration of 50 mg/mL in autoclaved RO water. The mixture was left to stand overnight at 4^{o}C before applications using sterile pipette tips (0.1-10 μL).

2.6.2 Histochemical GUS assays

GUS assays were performed according to the standard protocols (Jefferson *et al.*, 1987) with modifications to increase the stringency of GUS activity localisation. The young seedlings were incubated in 90% acetone for 15–30 min on ice or vacuum infiltrated 2x 10 min to help penetration, and rinsed with sodium phosphate buffer

(pH 7.5) before the GUS staining buffer was added to the sample (100 mM sodium phosphate buffer NaH_2PO_4, pH 7.5, containing 0.5 mg/mL 5-bromo-4-chloro-3-indoyl-β-D-glucuronide (X-GlcA) prepared from frozen stock of 20 mg/mL X-GlcA (Apollo Scientific) dissolved in DMSO, 5 mM potassium ferricyanide $K_3Fe(CN)_6$, 5 mM potassium ferrocyanide $K_4Fe(CN)_6$, 0.1% w/v Triton X-100, 10 mM EDTA). The reaction was performed at 37°C in the dark for 24 hours.

2.7 Imaging techniques

2.7.1 Sample fixation, clearing and preparation

For histology studies, leaves were fixed in ethanol/acetic acid (7:1 v/v), then hydrated in 70% v/v aqueous ethanol were cleared using 50% v/v commercial bleach and rehydrated in 70% v/v aqueous ethanol.

2.7.2 Aniline blue staining

Aniline blue staining of septum walls of newly divided cells was employed to visualise the cell division events in young developing leaves which also revealed the orientation of cell division planes after the completion of mitotic division (Kakimoto and Shibaoka, 1992; Kuwabara and Nagata, 2006). The dissected shoots were fixed in a mixture of ethanol and acetic acid (7:1 v/v) and then rinsed in ethanol (95%). Subsequently, shoots were rinsed in 150 mM phosphate buffer (pH 9.0) for 30 min on ice before being immersed in 0.02% w/v aniline blue solution in 150 mM phosphate buffer (pH 9.0) for 14 days at 4^oC in dark. Observations were carried out with a fluorescence microscope (BX 51, Olympus) under UV excitation with a standard DAPI filter set, and fluorescence images were taken with the CCD camera. Under UV excitation, septum walls stained with aniline blue fluoresce yellowish green. Dividing epidermal cells were distinguished from stomatal mother cells by the spherical cell shape and distinct bright spots (likely to be chloroplasts).

2.7.3 Light microscopy

For histology studies, fixed leaves were mounted on slides with a drop of water and observed under Nomarski optics using a BX51 Olympus microscope fitted with a DP71 charge-coupled device (Olympus). Photomicrographs were taken under auto settings in tiff format using the accompanying Cell^B imaging software (Olympus).

Whole-seedling photographs were taken under a Leica stereomicroscope MZ FLIII with the accompanying SPOT^{TM} software (Diagnostic Instruments) or with a digital camera (Sony Cybershot DSC-H3).

2.7.4 Measurements of rosette, leaf and hypocotyl growth

For leaf growth analysis of Col-0 wild-type, all measurements were carried out digitally on photographs taken under a Leica stereomicroscope MZ FLIII with the accompanying SPOT^{TM} software (Diagnostic Instruments) or camera (Sony Cybershot DSC-H3).

For leaf shape analyses, fixed leaves as above were mounted on glass slides, unfolded whenever possible using a pair of blunt-end needles and flattened under cover slips. Photographs of arranged slides on white background (A4 white paper) with a standard 15 cm ruler for scaling were taken using digital camera (Sony Cybershot DSC-H3) with macros function and auto settings in jpeg format. The same applied for rosette and hypocotyl growth analyses, except without the sample mounting procedure, and dark background (black cardboard paper) for hypocotyl. Hypocotyl and root lengths were measured with a calibrated scale bar using ImageJ (http://rsbweb.nih.gov/ij/) by manual hand-tracing.

2.7.5 Plant growth analysis

Absolute expansion/ extension rate at time *j* (AER_j) over two time points (*j* ± 2 or 3 days) was determined using the following equation (Hunt, 1982):

$$AER_j = (m_j - m_{j-1})/ (t_j - t_{j-1}),$$

Where m is the measurement in area or length, t is time, and m_j and m_{j-1} are measurements at times t_j and t_{j-1}, the previous time point.

Relative expansion/ extension rate at time *j* (RER_j) over two time points (*j* ± 2 or 3 days) was determined using the following equation (Hunt, 1982):

$$RER_i = (m_j/m_{j-1})/ (t_j - t_{j-1})$$

Where m is the measurement in area or length, t is time, and m_j and m_{j-1} are measurements at times t_j and t_{j-1}, the previous time point.

2.7.6 Leaf image analysis

Acquired photographs of dissected leaves as described above were processed using Photoshop (Adobe® version CS3). A new blank layer of image was created for manual hand-tracing of leaf outlines using an LCD tablet (Wacom DTI-520) and to generate leaf silhouettes using the bucket tool. Measurements were then made using the wizard select and lasso deselect tools, to generate the data for the whole-leaf and lamina measurements respectively. Lamina width and length are the width and height of the bounding rectangle of the shape. Petiole length was calculated from the difference in height between the leaf and lamina measurement. For rosette area, a similar approach was taken by manually tracing the rosette outline, excluding the cauline leaves and separating the rosette with overlapping leaves to generate silhouettes of whole rosette for measurements.

2.7.7 Cell measurements

Cell area and dimensions were measured from Nomarski micrographs taken from the middle regions of leaf lamina (equidistant between midvein and margin) and petiole (equidistant from leaf base and petiole end) under 40x and 20x objective magnification respectively. Over 28 lamina palisade mesophyll cells were systematically sampled from the micrographs for measurements using ImageJ (http://rsbweb.nih.gov/ij/) by manual hand-tracing. For petiole, measurements were done on the third mesophyll cell file from either side of the petiole margin of the first sub-epidermal layer. The cell number and cell file were counted within the micrograph.

2.8 Statistical analysis

All statistical analyses were performed using Minitab® statistical software version 14.1. Datasets were examined for normal distribution; log-transformed for normal distribution or otherwise equivalent non-parametric tests were performed.

For the clustering of expression pattern in Chapter 3, an arbitrary number was given to each categorical level of expression and used as a basis for the clustering based on the similarity in the different levels of expression.

2.9 Atomic force microscopy

2.9.1 Plant materials

Tobacco *Nicotiana slyvestris* young primordia germinated on water-soaked sterile filter paper in round petri dishes (9 cm diameter) and incubated in the growth cabinet as for Arabidopsis (section 2.2).

2.9.2 Sample preparation

Dissected plant samples were embedded in 1% low-melting agarose (Melford Laboratories Ltd.) on microscope glass slides (Fisher Scientific).

2.9.3 AFM machine

Force maps were obtained using a NanoWizard I (JPK Instruments), which is a type I AFM with piezo-resistive element on the cantilever holder (Figure 2.3A), by using spherical colloidal probe (5 μm radius) made in house on beam-shaped silicon nitride cantilever of nominal spring constant 56 N/m (NANOSENSORS™ TL-NCH, Windsor Scientific). The force curves of point measurements were performed with Multimode® SPM with "J" scanner (Veeco Instruments), a type II AFM with piezo-resistive element on the sample stage (Figure 2.3B), by using standard oxide sharpened probes (20 to 40 nm radius) with triangular silicon nitride cantilever of nominal spring constant 0.58 N/m (SNL-10, Bruker). Both machines were equipped with a vibration isolation platform.

2.9.4 Software

Force maps were processed using the accompanying JPK Data Processing software (JPK Instruments). NanoScope®III software (v5.31R1) was used alongside Multimode® SPM (Veeco Instruments). The treatment of the experimental deflection vs. height curves from point measurements, their transformation into load vs. indentation depth curves, and their fit with theoretical relations was performed using PUNIAS (Protein Unfolding and Nano-Indentation Analysis Software, http://punias.voila.net/).

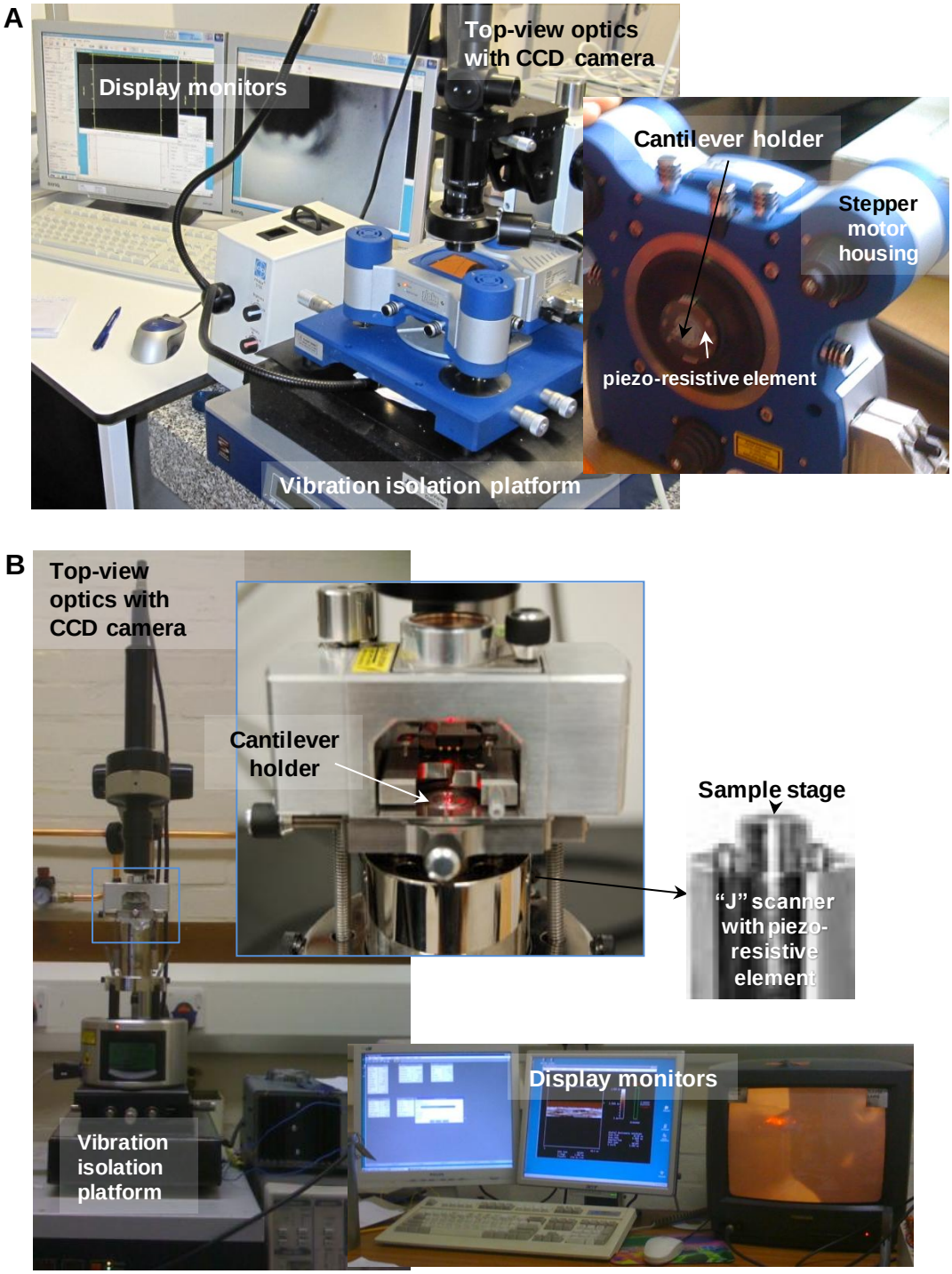

Figure 2.3. An overview of the atomic force microscopes used in current study: (A) JPK NanoWizard I, and (B) Veeco Multimode. Annotations highlight some of the similarities (top-view optics with CCD camera, display monitors and vibration isolation platform) and differences (location of piezo-resistive element and cantilever holder position) between the two machines.

CHAPTER 3 The expression of expansins during Arabidopsis leaf development

3.1 Introduction

Expansins comprise a large multigene superfamily of cell-wall loosening proteins. Based on phylogenetic sequence analyses (Sampedro and Cosgrove, 2005; Carey and Cosgrove, 2007), there are four families of evolutionary conserved expansins in all land plants which existed before the divergence of monocotyledons and dicotyledons (Figure 3.1).

EXPA or *α*-expansin is the first family identified from biochemical experiments, being the biggest and most diverse, followed by EXPB (β-expansin), and two smaller families of EXLA (EXPA-like) and EXLB (EXPB-like) proteins identified from genomic sequence analyses and with yet unknown physiological function (Sampedro *et al.*, 2006). All four families share a similar two-domain structure of cellulose binding domain and a cysteine-rich domain preceded by a signal peptide at the N-terminus presumably excised during processing in the endoplasmic reticulum (Cosgrove 2000). There are three highly conserved groups of amino acids, including six cysteines and four tryptophans (Figure 3.1). Cysteines can form disulfide bonds to stabilise the binding domain crucial in EXPA function (Yu *et al.*, 2011), while the conserved tryptophan residues resemble that of a cellulose binding domain. The few conserved charged residues may be particularly important for expansin function by mediating pH sensitivity as the protein's acidic optimum probably relies on carboxyl group protonation of these residues (Shcherban *et al.*, 1995).

In *Arabidopsis thaliana*, there are 38 genes classed as expansins, divided into 16 clades according to the monocot-eudicot phylogeny (Table 3.1, Figure 3.2). The Columbia ecotype of Arabidopsis contains two expansin pseudogenes: Ψ*AtEXPB6* has lost the promoter end and most of the first exon, whereas a 2-bp insertion frameshift results in a premature stop codon for Ψ*AtEXPA19*. However, these genes in the Landsberg *erecta* ecotype were found to be undisrupted and normally expressed (Sampedro *et al.*, 2005). Furthermore, recent genome annotation (TAIR9) proposed a gene model for *EXPB6* suggesting that it might not be a pseudogene.

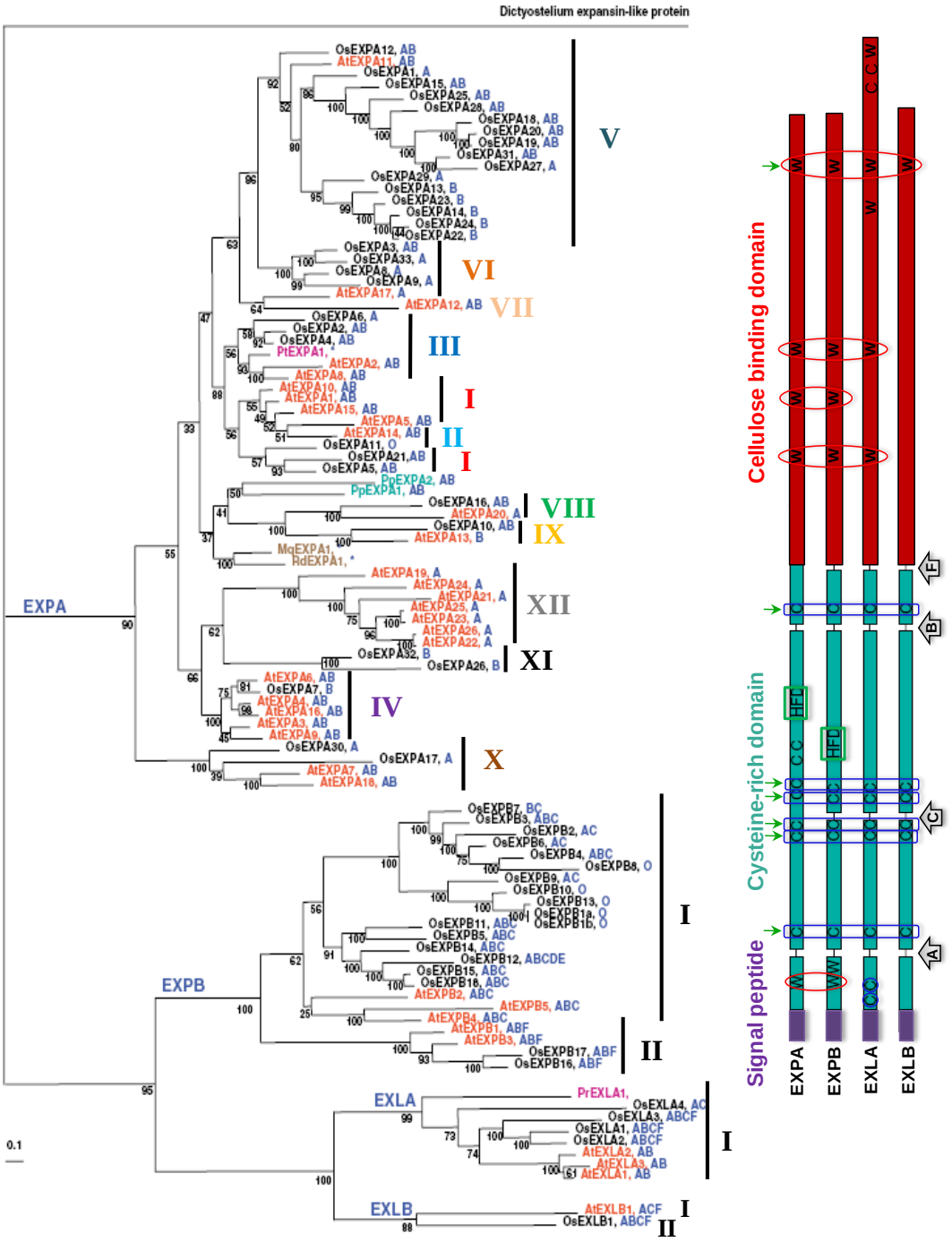

Figure 3.1. Phylogenetic tree of the expansin superfamily of Arabidopsis, rice, and selected other species adapted from (Choi *et al.*, 2006). Tree was created with the alignment of amino acid sequences of full-protein regions (including the signal peptide), using soil-dwelling amoeba *Dictyostelium* expansin-like protein sequence to root the tree. Genes of Arabidopsis are indicated in red, rice (*Oryza sativa*) in black, pines in purple, ferns in brown, and of *Physcomitrella* in green. The roman numerals represent the position-based monocot-eudicot expansin clade classification (Sampedro *et al.*, 2006). Intron types (A, B, C, D, E, F, O) are indicated next to each gene name in blue colour with reference to upward arrows on the schematic sequence structures for the four expansin families on the right (only A, B, C and F are shown) as modified from (Sampedro and Cosgrove, 2005). Positions of the highly conserved sequences, cysteines (C), histidine-phenylalanine-aspartate (HFD) motif, and tryptophans (W) are highlighted, with amino acid residues conserved in all families indicated by downward green arrows. Tree branch lengths are mean values proportional to the number of substitutions per site (bar = 0.1 substitutions/site).

Table 3.1. List of all expansin genes in *Arabidopsis thaliana* compiled from Arabidopsis.org (TAIR9) and UniProt database.

Expansin gene	AGI no.	UniProt accession	Monocot-eudicot Clade classification	Genomic seq. length (nt)	CDS length (nt)	cDNA (nt)	Protein length (a.a.)	Protein weight (kDa)	Isoelectric point
AtEXPA1	At1g69530.2	Q9C554	IA	1669	753	1315	250	26.5	9.09
AtEXPA2	At5g05290	Q38866	IIIA	1171	768	978	255	27.7	4.78
AtEXPA3	At2g37640	O80932	IVA	2149	789	1202	262	28.3	9.66
AtEXPA4	At2g39700	O48818	IVA	1753	774	1338	257	27.8	9.98
AtEXPA5	At3g29030	Q38864	IA	2051	768	1288	255	27.6	9.08
AtEXPA6	At2g28950	Q38865	IVA	2255	774	1386	257	27.8	10.03
AtEXPA7	At1g12560	Q9LN94	XA	1381	789	1033	262	28.8	9.38
AtEXPA8	At2g40610	O22874	IIIA	1695	762	1105	253	27.3	6.98
AtEXPA9	At5g02260	Q9LZ99	IVA	2089	777	1249	258	27.8	9.57
AtEXPA10	At1g26770	Q9LDR9	IA	1043	780	805	259	27.6	8.95
AtEXPA11	At1g20190	Q38864	VA	1329	759	1139	252	26.8	8.71
AtEXPA12	At3g15370	Q9LDJ3	VIIA	1506	759	931	252	27.6	10.44
AtEXPA13	At3g03220	Q9M9P0	IXA	1694	801	1174	266	29.0	8.14
AtEXPA14	At5g56320	Q9FMA0	IIA	1597	768	1203	266	27.7	9.99
AtEXPA15	At2g03090	O80622	IA	1790	762	1358	253	27.1	9.17
AtEXPA16	At3g55500	Q9M2S9	IVA	1352	783	1105	260	28.2	9.87
AtEXPA17	At4g01630	Q9ZSI1	VIA	875	768	768	255	27.7	9.94
AtEXPA18	At1g62980	Q9LQ07	XA	1435	774	1002	257	27.9	9.45
ψAtEXPA19	At3g29365	NA	XIIA	841		841			
AtEXPA20	At4g38210	Q9SZM1	VIIIA	1218	771	1142	256	27.9	8.41
AtEXPA21	At5g39260	Q9FL81	XIIA	1081	789	932	262	28.1	8.30
AtEXPA22	At5g39270	Q9FL80	XIIA	1033	792	792	263	29.0	8.84
AtEXPA23	At5g39280	Q9FL79	XIIA	994	780	780	259	28.4	7.24
AtEXPA24	At5g39310	Q9FL76	XIIA	1235	891	891	296	31.8	9.01
AtEXPA25	At5g39300	Q9FL77	XIIA	961	783	783	260	28.5	7.69
AtEXPA26	At5g39290	Q9FL78	XIIA	1038	792	792	263	29.0	8.69
			EXPA Average	**1432**	**780**	**1051**	**260**	**28.1**	**8.86**
AtEXPB1	At2g20750	Q9SKU2	IIB	1571	816	1141	271	29.1	9.57
AtEXPB2	At1g65680	Q9SHY6	IB	1134	822	822	273	29.1	8.24
AtEXPB3	At4g28250	Q9M0I2	IIB	2032	795	1327	259	28.4	8.85
AtEXPB4	At2g45110	Q9SHD1	IB	1839	780	956	259	27.2	7.19
AtEXPB5	At3g60570	Q9M203	IB	1217	759	759	252	27.3	9.74
ψAtEXPB6	At1g65681	NA	IB	1796	672	672	223	24.0	7.24
			EXPB Average	**1598**	**774**	**946**	**256**	**27.5**	**8.47**
AtEXLA1	At3g45970	Q9LZT4	ILA	1143	798	989	265	28.7	8.08
AtEXLA2	At4g38400	Q9SVE5	ILA	1298	798	1105	265	28.6	8.25
AtEXLA3	At3g45960	Q9LZT5	ILA	1145	792	973	263	28.6	9.22
			EXLA Average	**1195**	**796**	**1022**	**264**	**28.6**	**8.52**
AtEXLB1	At4g17030	O23547	ILB	1705	753	1093	250	27.9	7.11
AtEXLB2	At4g30380	NA	ND	509	372	372	123	13.3	8.37
AtEXLB3	At2g18660	NA	ND	999	393	779	130	14.5	9.50
			EXLB Average	**1071**	**506**	**748**	**168**	**18.6**	**8.33**
			Overall Average	**1411**	**758**	**1008**	**252**	**27.3**	**8.72**

***NA – Not available, ND – Not determined**
**** Colour intensities correlate to the values with darker colours corresponding to greater values**
***** There were two pseudogenes in Col-0 wild-type plant as indicated by Ψ (Sampedro *et al.*, 2005). However, these genes (GenBank accession no. AY843212 (*EXPA19)* & AY619565 (*EXPB6*)) are normally expressed in the Landsberg *erecta* ecotype. Furthermore, recent release of TAIR9 annotation indicates a gene model for *EXPB6* suggests it may not be a pseudogene in Columbia ecotype.**

EXPA and EXPB appear to act on different cell wall components but their native targets have not yet been well defined. Despite only ≈20% amino acid identity, EXPA and EXPB proteins are of similar size (≈28 kDa, Table 3.1), their sequences align well with one another, and they contain a number of conserved residues and characteristic motifs distributed throughout the length of the protein (see above).

Expansins often show tissue-specific expression patterns. This has been well-studied in both monocot and eudicot plant species, including deepwater rice (Cho and Kende, 1998; Lee and Kende, 2002), maize (Muller *et al.*, 2007), wheat (Lin *et al.*, 2005), forage grass (*Festuca pratensis*) (Reidy *et al.*, 2001a), tomato (Rose *et al.*, 1997; Caderas *et al.*, 2000; Chen *et al.*, 2001), and hybrid aspen (*Populus tremula* x *Populus tremuloides* Michx) (Gray-Mitsumune *et al.*, 2004). Despite the wealth of microarray experiments and thriving functional genomic studies in Arabidopsis, the expression pattern of expansins is still poorly characterised and the significance of this diverse expression pattern remains unclear. Expansins are amongst genes that show the greatest response breadth of gene expression, with *EXPA8* differentially expressed in 22 different experiments (Walther *et al.*, 2007).

Currently, only a handful of the 38 expansins genes in Arabidopsis are characterised in the literature. Genetic manipulation of *AtEXPA10* expression established its role in leaf growth, more specifically in the young growing petiole. Surprisingly *AtEXPA10* is expressed in the pedicel abscission region while Arabidopsis plants do not normally abscise (Cho and Cosgrove, 2000). On the other hand, *EXPA7* and *EXPA18* play a role in root hair initiation with their expression solely localised to root hair cell files (Cho and Cosgrove, 2002), whereas *EXPA17* has been implicated in lateral root formation, based on microarray experiments and RT-qPCR without further characterisation (Swarup *et al.*, 2008). In dicotyledons, focus has been given to the EXPA family as the literature so far points towards their role during vegetative phase, as compared to the EXPB family which was predominantly found to be expressed in the reproductive or generative phase of development. The converse is true for monocotyledons (Sharova, 2007).

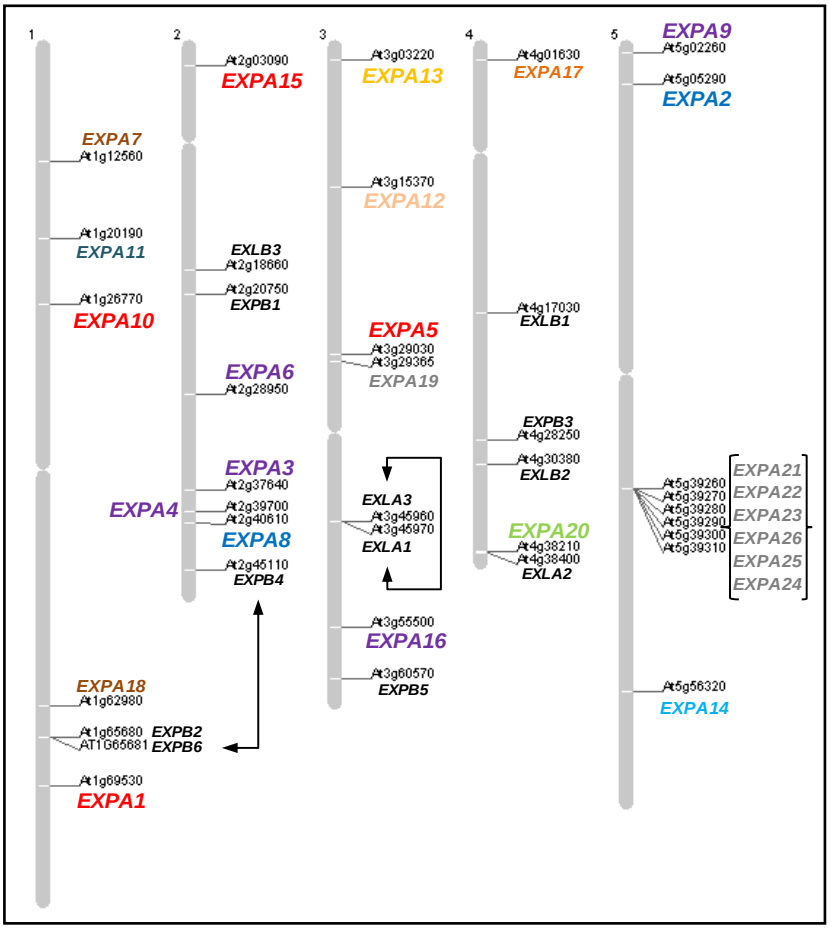

Figure 3.2. Physical map showing the genomic distribution of the Arabidopsis expansin genes. Numbers on top indicate the order of chromosome. AGI numbers and colour-coded gene names according to the position-based monocot-eudicot clade classification are shown to assist functional inference from position-based phylogeny history. Arrows and brackets indicate tandem gene duplication (after Sampedro and Cosgrove (2005)).

A few hypotheses have been proposed for the functional significance of these differential expression patterns (Cosgrove, 1998). First, the various expansin genes may be expressed in different growing organs or in different cell types to confer specific functions or physically act on different components of the complex wall. For example, EXPB was first identified in pollen as an allergen (Cosgrove *et al.*, 1997) and was subsequently found to function in loosening the grass cell wall. The much greater number of β-expansin genes in monocot rice then Arabidopsis, together with the specificity of maize expansin Zea m1 activity on grass walls, led to the proposal that β-expansins have evolved specialised functions (Cosgrove *et al.*, 1997; Wu *et al.*, 2001). This is in conjunction with the evolution of the grass cell wall, which has a distinctive set of matrix polysaccharides and structural proteins compared to other land plants (Carpita, 1996). Furthermore, the two expansins in cucumber possess different biochemical properties with respect to pH-dependence (McQueen-Mason and Cosgrove, 1995). Furthermore, even though the isoelectric point (pH when a protein has no net electrical charge) of expansins in Arabidopsis averages around pI 8.5, so that at pH 5.5 most expansins are positively charged (acidic state), there are

some extremes, ranging from pI 4.78 (EXPA2) to pI 10.55 (EXPA12) (Table 3.1). The significance of this difference remains unknown.

Secondly, different expansins could possibly control different cell wall regions which undergo various degrees and distinct directions of stretching – a property that is impossible to detect in conventional uniaxial expansin activity assays. This could permit localised transient relaxations of cell wall structure, tentatively allowing access to other modifiers of cell wall architecture. It has been shown that the mRNA transcripts localise in xylem cells of zinnia (Im *et al.*, 2000) and aspen (Gray-Mitsumune *et al.*, 2004), towards the apical or basipetal ends of growing cells, suggesting that there is a local secretion of expansins into the cell walls. Furthermore, the cell wall distribution of expansin protein was found to be localised according to the direction of growth in root (Zhang and Hasenstein, 2000). Nevertheless, expansin proteins can also be found diffusely throughout the cell wall and often around the intercellular spaces (Cosgrove *et al.*, 2002).

Another hypothesis is that different expansin isoforms could function in distinct physiological events involving wall modifications. Expansins have been shown to be involved in the growth of cucumber hypocotyls (McQueen-Mason, 1995), deepwater rice internodal extension (Cho and Kende, 1997a) and root elongation (Lee *et al.*, 2003). Apart from the prevalent function of expansins in cell elongation, they can also function in cell wall disassembly. For example, specific expansins play an active role in cell wall disassembly during fruit ripening (Rose *et al.*, 1997; Brummell *et al.*, 1999b; Harrison *et al.*, 2001; Hiwasa *et al.*, 2003; Yoo *et al.*, 2003; Sane *et al.*, 2005), potentially cell separation during leaf abscission (Cho and Cosgrove, 2000), lateral root formation (Greenwood *et al.*, 2006), or even air space formation. Furthermore, expansins also play role in tissue differentiation and morphogenesis such as root hair initiation (Cho and Cosgrove, 2002), meristematic organogenesis (Reinhardt *et al.*, 1998) and vascular tissue differentiation (Gray-Mitsumune *et al.*, 2004). The involvement of expansins in these varied processes could account for the multiplicity of regulation of expansin expression and activity in various tissues and at various stages of plant development.

A variation on this hypothesis is that two or more expansins may be expressed in the same cell but might be regulated by different stimuli, such as hormones, light, and environmental stresses (Shcherban *et al.*, 1995). Lastly, the expansin genes could just be redundantly expressed as functional insurance. However, no two expansin genes identified to date to have exactly the same spatial and temporal expression pattern, and there is no evidence that impaired expression of one gene enhances the expression of other expansin genes.

Consistent with the prevalence of expansin's involvement in growth processes, the reduction of expansin gene expression by antisense methods has been shown to inhibit growth (Brummell *et al.*, 1999a; Cho and Cosgrove, 2000; Choi *et al.*, 2003). However, there is not only a vague correlation between expansin expression patterns and growth rates, and also contradictory reports from various plant species (Caderas *et al.*, 2000; Reidy *et al.*, 2001a; Kam *et al.*, 2005; Muller *et al.*, 2007). A detailed study of expansin gene expression in fescue leaves revealed that these genes were expressed most strongly in the developing vascular bundles but the total level of gene transcription did not correlate with the growth rate in various regions of leaf extension zone (Reidy *et al.*, 2001a). The primary maize leaf resumed its growth at low water potential in the root zone, which correlated with an enhanced transcript level of expansin genes (Kam *et al.*, 2005; Sabirzhanova *et al.*, 2005). In gravi-stimulated rice shoots, the transcription level of *OsEXPA4* gene was three- to fivefold stronger in the rapidly growing abaxial half than in the adaxial half of the leaf sheath bases (Hu *et al.*, 2007). The fact that the expansin activity on growth might be confined to a specific phase of development (Sloan *et al.*, 2009) could account for the limited correlations sometimes observed. Nonetheless, understanding the expression pattern of expansins is essentially the first step towards interpreting the functional diversity and specificity for this family of cell-wall proteins, assuming that a specific protein is absent when no transcript of the gene is detected.

This chapter aims to identify the expansin gene family members involved in Arabidopsis leaf development, focusing on EXPAs due to their prevalent roles during vegetative growth in dicots. This will inform further studies (Chapter 4) to examine the functional and developmental specificity of expansins by targeted genetic manipulation of specific expansin genes.

3.2 Results

3.2.1 A developmental staging system of Arabidopsis *leaf growth*

In order to create a standard procedure to obtain reproducible results, a systematic staging system was applied for harvesting Arabidopsis Col-0 wild-type leaf tissue samples (Figure 3.3). On day 10 after sowing, seedlings were characterised under a stereomicroscope and categorised based on the number of visible leaves (width > 500 µm) and the smallest leaf size. Plants in the modal class were then transferred onto medium in new petri dishes and used as a starting population for analysis over the subsequent time period. In total, 288 and 358 seedlings were analysed in two independent studies, with only 41-45% of seedlings of equivalent developmental stages used for further studies, reflecting the great variations in growth under standard germination conditions (Massonnet *et al.*, 2010). Leaf 6 was chosen for this study because the fifth leaf onwards in Arabidopsis is regarded as a good representative of the rosette leaf, and there is large volume of studies on leaf expansion based on leaf 6 (Tsuge *et al.*, 1996; Cookson *et al.*, 2005; Cookson and Granier, 2006; Cookson *et al.*, 2007).

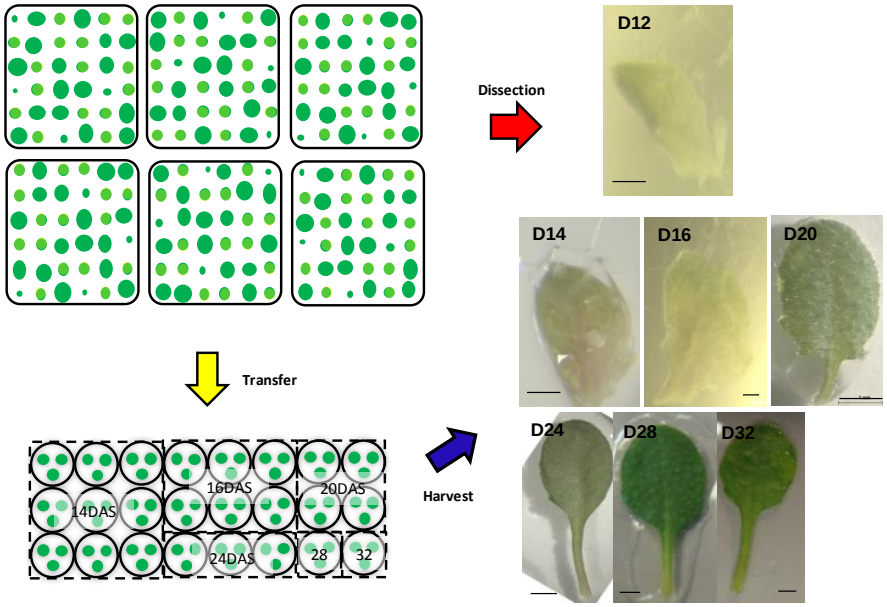

Figure 3.3. Staging system for leaf tissue sample harvest. 10-day-old seedlings were categorised according to the number of visible leaves and smallest leaf size, which then was tabulated to give the modal class. The transferred plants (from modal class) are then harvested on designated day after sowing (DAS). The categories close to the modal class were dissected for day 12 samples (leaf 6: 200-250 µm width). Scale bar: (D12) 50 µm, (D14, D16) 100 µm, (D20 - D32) 1 mm.

Destructive measurements of growth parameters during sample harvest showed that leaf development can be categorised into three approximate phases (Figure 3.4). This is consistent with the conventional leaf growth pattern of sigmoidal curves in Arabidopsis Col-0 wild type plants (Donnelly *et al.*, 1999; Granier *et al.*, 2002; Beemster *et al.*, 2005). In the experimental conditions applied here, the early stage of leaf 6 ranged from 10 DAS to 16 DAS, corresponding to a leaf width of 250 μm to 1100 μm. Aniline blue staining of newly formed cell plates in leaf samples on day 12, 14 and 16, showed that the cell division occurred throughout the leaf on day 12, in 90% of the leaf extending upwards from base on day 14, and in 75% of the leaf extending upwards from base on day 16 (Figure 3.5). This occurrence of cell division characterised the early stages of leaf 6 growth. This was followed by an expansion stage from 20 DAS to 28 DAS (2-7 mm in leaf width), and a mature stage after 32 DAS (>8 mm in leaf width) when growth rate declined to zero. The absolute extension rates of both length and width peaked at around 26 DAS, and this was reflected in the relative extension rates for leaf lamina measurements. Interestingly, this peak coincided with the complete cessation of cell division in the leaf blade as inferred from the data shown by Donnelly *et al.* (1999). The same growth pattern applied for the change in leaf area, except for a steep increase of area compared to a more gradual increase in length and width during the mid phase of leaf development.

The growth of the leaf blade width and length behaved differently during the expansion stage as indicated by the differences in the length:width ratios (lamina and leaf indices), with an otherwise relatively constant lamina index during other phases of leaf development (Figure 3.4A inset). During early leaf development the increase in lamina length and width was proportional but a burst of elongation along the lamina length during the mid-phase resulted in the increase of lamina index, which was followed by greater increase of lamina width with a consequential drop in lamina index. The leaf index was similar in trend except for a higher value at the end stage to due petiole growth.

Petiole growth lagged behind lamina growth with the extension of the petiole only observed from day 16 onwards. Leaf blade expansion was more consistent compared to the petiole elongation pattern, which varied across different plants even within the same plate. Consequently, the variation in total leaf length (lamina and petiole) was

much greater than for leaf width (Figure 3.4A). Furthermore, it is noteworthy that leaf blade width ceased to increase from 28 DAS while there were still signs of extension in petiole length after this time.

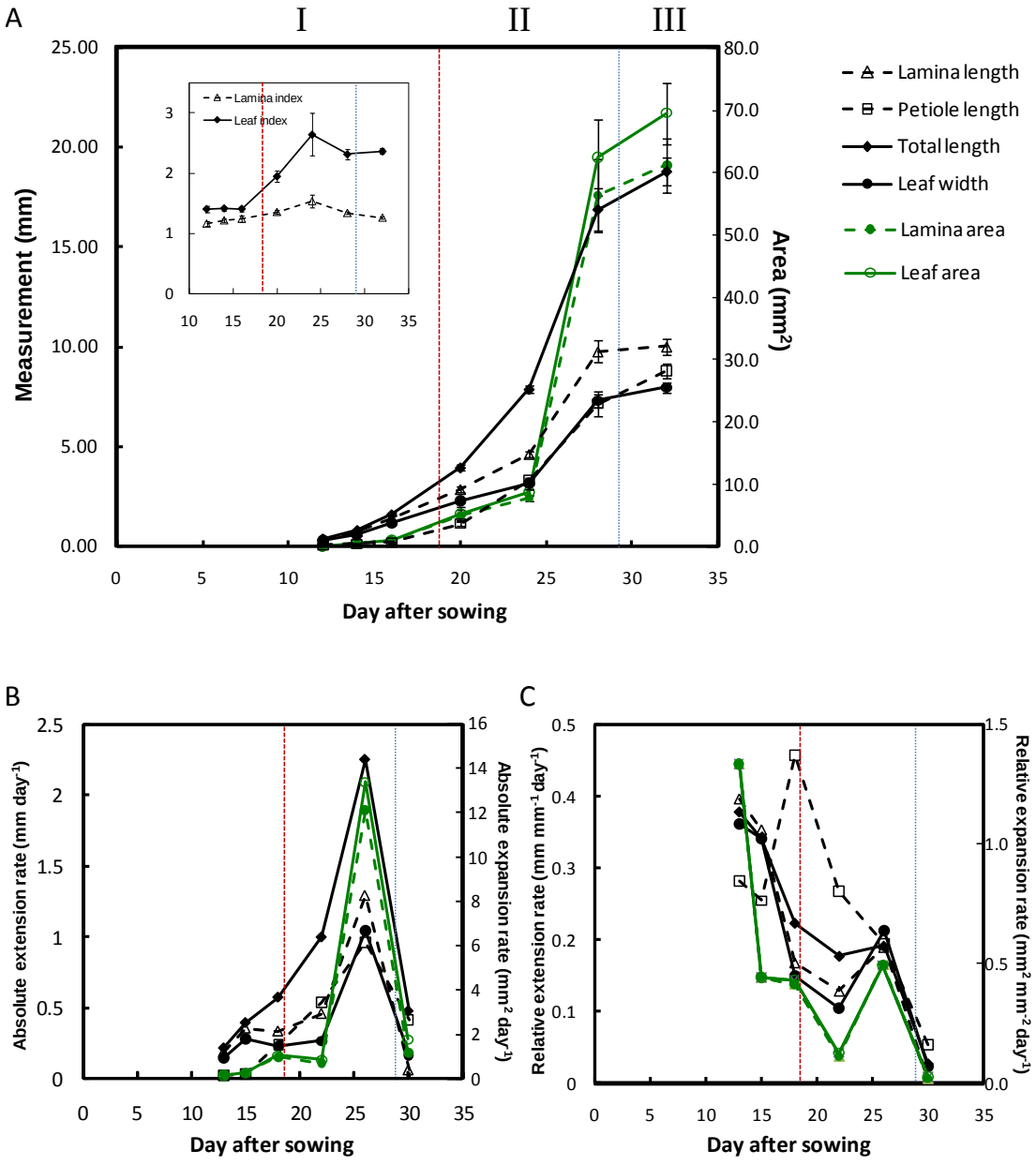

Figure 3.4. Time-course analysis of leaf growth on leaf 6 of Col-0 wild-type plants showing three phases of development (I – early stage, II - mid stage, and III - mature stage, as separated by the red and blue dashed lines). (A) Changes in leaf lamina length, petiole length, total (lamina and petiole) length, and leaf width over the course of 20 days. Vertical bars represent ± SE of the mean from 6-14 combined measurements from two independent studies. Inset shows the trend of changes in length: width ratio of lamina and whole-leaf over time. (B) Changes of absolute extension rates over time calculated from the averaged measurements. (C) Changes of relative extension rates over time calculated from the averaged measurements.

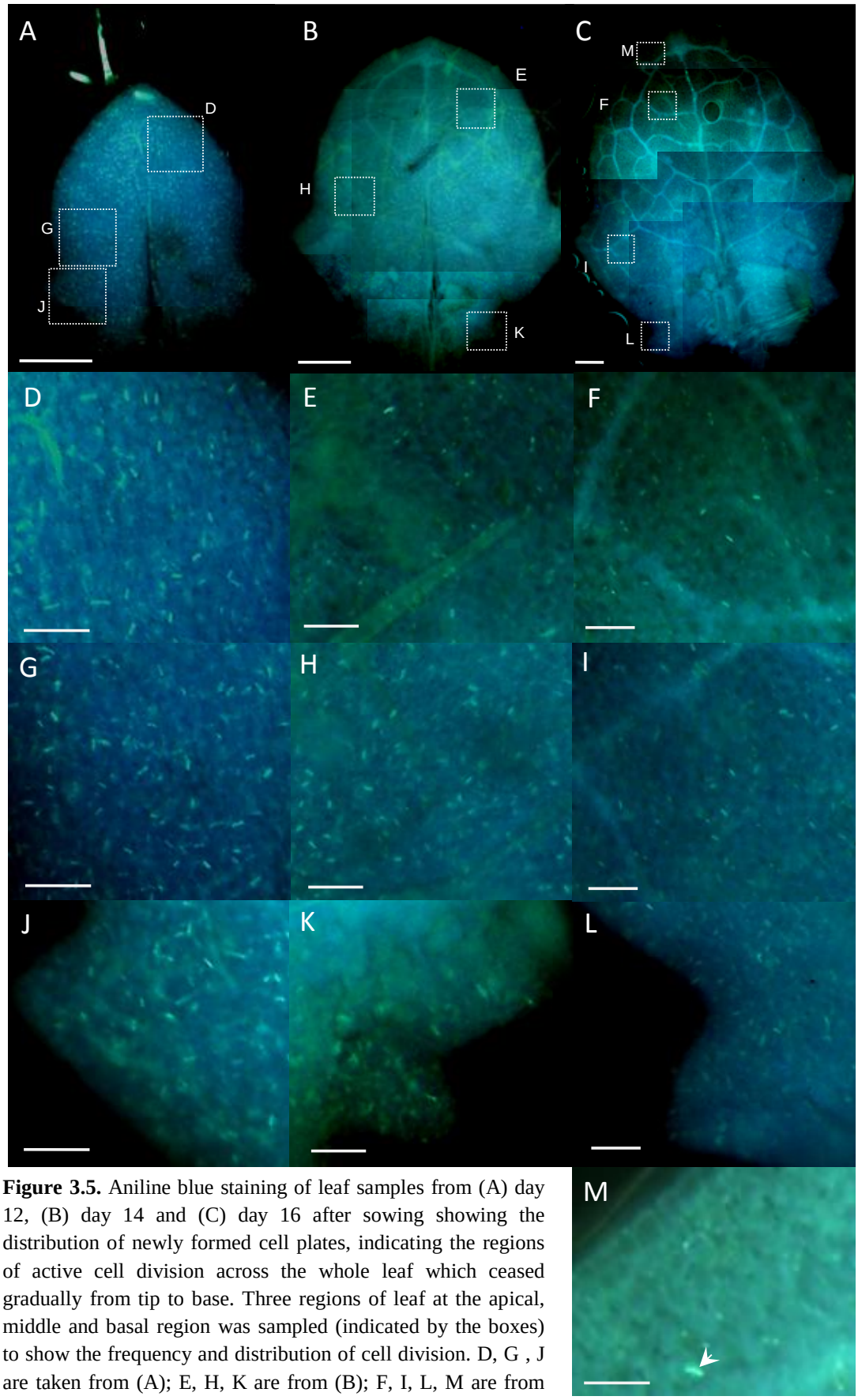

Figure 3.5. Aniline blue staining of leaf samples from (A) day 12, (B) day 14 and (C) day 16 after sowing showing the distribution of newly formed cell plates, indicating the regions of active cell division across the whole leaf which ceased gradually from tip to base. Three regions of leaf at the apical, middle and basal region was sampled (indicated by the boxes) to show the frequency and distribution of cell division. D, G , J are taken from (A); E, H, K are from (B); F, I, L, M are from (C). There is a more apparent reduction in cell division frequency between leaf apical ends (D-F) than the middle region (G-I) or basal ends of leaf (J-L). (m) Photograph showing fluorescence residues at the apical tip of a leaf on day 16 were largely due to remaining stomatal divisions (arrow head). Scale bars = 100 μm (A-C), 20 μm (D-M).

3.2.2 Molecular analysis of α-expansin gene transcripts reveals diverse expression patterns which correlate to different phases of leaf development

Having established a robust system for analysing the development of leaf 6, I performed a series of RT-PCR analyses using RNA extracted from dissected leaf 6 primordia at different stages of development. The aim was to provide an overview of which expansin transcripts are detectable at different stages of Arabidopsis leaf growth based on the developmentally equivalent leaves. This is different from previous investigations which used different leaf number (e.g. Table 3.3) or different position from the leaf base to represent different developmental stages (Reidy *et al.*, 2001a; Schmid *et al.*, 2005; Muller *et al.*, 2007).

RT-PCR of EXPA transcripts performed as described in section 2.3.3 showed a diverse pattern of α-expansin gene expression over the course of leaf 6 development (Figure 3.6). At the earliest stage of leaf development studied, 11 out of 25 EXPA genes were expressed, 4 of which were highly expressed (*EXPA5, EXPA6, EXPA10* & *EXPA15*). *EXPA3* and *EXPA4* were moderately expressed, whereas the rest (*EXPA1*, *EXPA2*, *EXPA13*, *EXPA16* & *EXPA20*) were just detectable, as indicated by the faint bands. A similar pattern was detected for leaf 6 on 14 DAS, except that one extra gene (*EXPA8*) was found to be lowly expressed, with reduced expression of *EXPA3* and *EXPA15*. Two additional α-expansin genes (*EXPA9* & *EXPA14*) were just detectable in leaves harvested from 16 DAS, while *EXPA1, EXPA4* & *EXPA13* showed a marked increase in expression. Total EXPA transcript level peaked on day 20 after sowing. *EXPA* expression levels in leaf sample from 20 to 28 DAS remained generally the same for *EXPA2, EXPA3, EXPA4, EXPA5, EXPA6, EXPA8, EXPA9, EXPA10,* and *EXPA11* (lowly expressed from 20-28 DAS). *EXPA1* was found to increase in expression while the reverse is true for *EXPA13* from 20 DAS to 24 DAS. *EXPA14* and *EXPA15* which were lowly expressed on 20 DAS ceased to be expressed thereafter. A greater intensity of *EXPA16* transcript was detected on 20 DAS as compared to 16 DAS which was sustained until 24 DAS, beyond on which it ceased to be detected. On 32 DAS, only 3 genes (*EXPA1, EXPA6* & *EXPA8*) remained highly expressed.

There was a sharp drop in the transcript levels of *EXPA3, EXPA4, EXPA5, EXPA10* and *EXPA13* from 28 DAS to 32 DAS, by which stage transcripts of only 9 out of 25

*EXPA*s were detectable. Transcripts of *EXPA7*, *EXPA12*, *EXPA17*, *EXPA18*, *EXPA21*, *EXPA22*, *EXPA23*, *EXPA24*, *EXPA25* and *EXPA26* were never detected over the course of leaf 6 development. *EXPA19*, which was reported as pseudogene in Col-0 ecotype (Sampedro and Cosgrove, 2005) was excluded from the expression study.

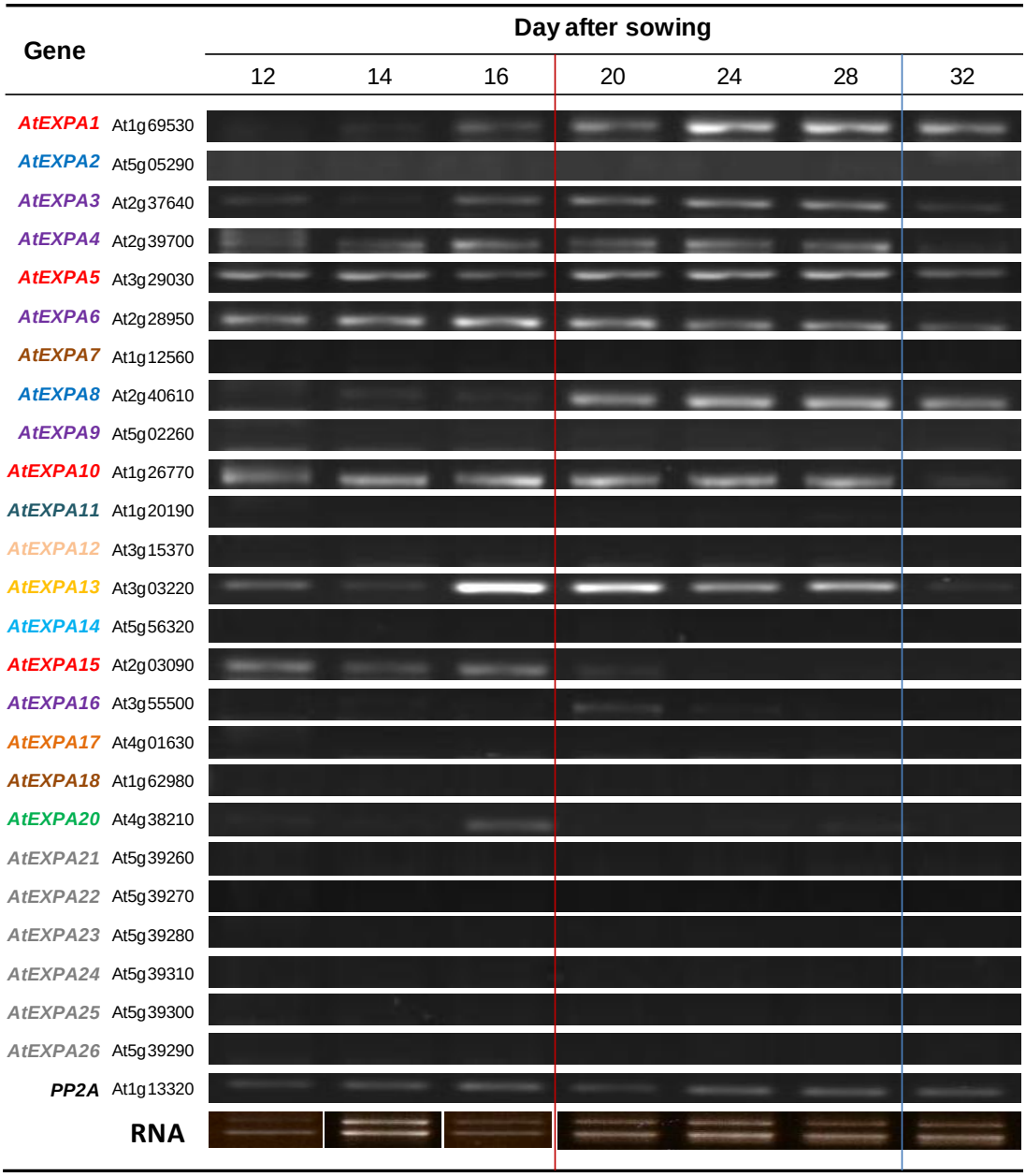

Figure 3.6. RT-PCR analysis of α-expansins transcripts during the course of leaf 6 development. 35 PCR cycles, repeated at least twice. The gene names are colour coded according to their respective group of monocot-eudicot clade classification as in Figure 3.1. *PP2A* was used as the internal control for PCR and the total RNA (2 μg) used for cDNA synthesis is shown. The red and blue lines correspond to Figure 3.4 in separating the sample into 3 developmental stages.

A summary of the *EXPA* transcript analysis is depicted in Figure 3.7 with the clustering of genes according to the similarity in overall expression pattern. This shows a pattern of *EXPA* expression that is consistent with the progression of leaf development with respect to the leaf growth analysis. There appears to be a distinct separation between the proliferative (12 -16 DAS) and expansion stage (20-28 DAS), whereas the distinction between the expansion stage and mature stage (32 DAS) is less distinct. Furthermore, the expression pattern on 12 DAS and 14 DAS is much more alike than that on 16 DAS, which is the stage when cessation of cell division at the leaf tip becomes clearly detectable (Figure 3.4). Intriguingly, the clustering also detects differences between the early and later phase of expansion stage, so that 24 DAS is more akin to 28 DAS than 20 DAS.

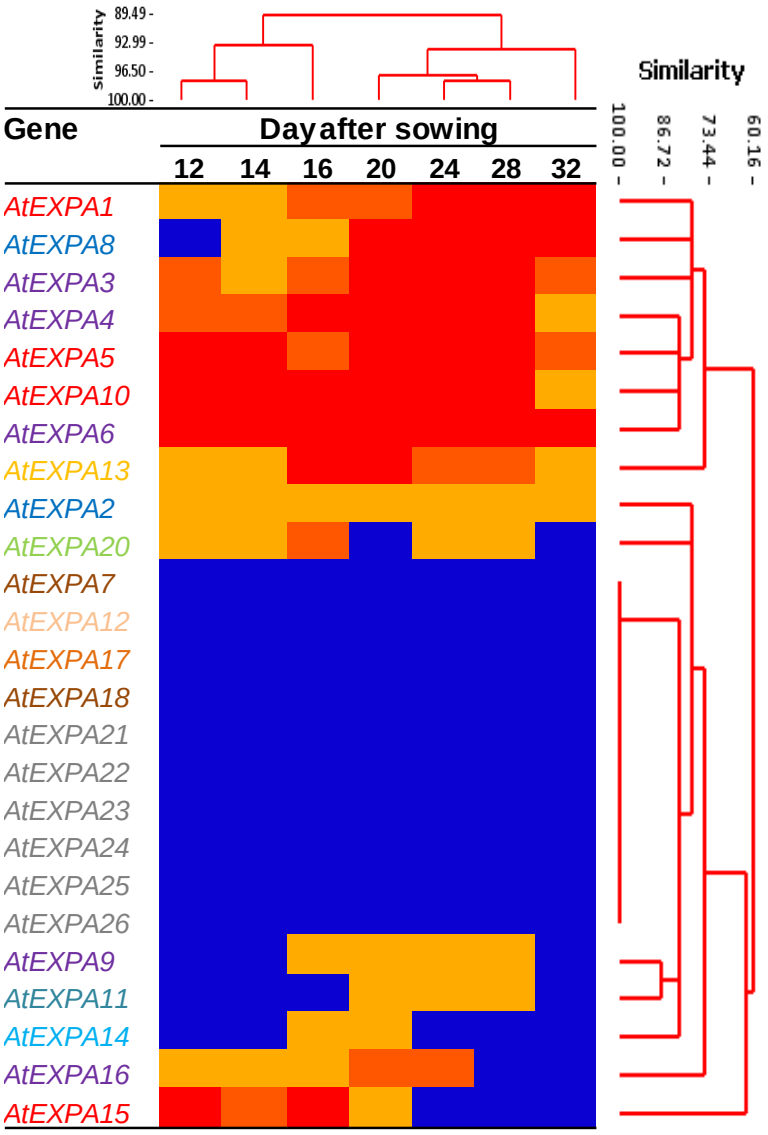

Figure 3.7. Summary of the transcript analysis of α-expansin expression during the course of leaf 6 development showing the relative expression level based on the internal control and relative RT-PCR band intensity (blue - not detected, yellow - low, orange - medium, red - high). The dendrograms were generated using the clustering function in Minitab based on similarity showing the grouping of leaf samples from different days and the differential expression of *EXPA* genes. The gene names are colour coded according to their respective group of monocot-eudicot clade classification as in Figure 3.1.

3.2.3 Literature and microarray data mining of expansin gene expression patterns

There is now an extensive database of plant gene expression data on microarray analysis and other approaches. Although these do not provide the spatial temporal resolution acquired in the experiment reported here, it was nevertheless useful to compare the experimental data from my study with those available in the databases. The following section describes a bioinformatic analysis of these data and provides an overview of the expansin gene expression and its regulation during leaf development. These results (together with the experimental data shown in the previous section) set the boundaries for the targeted manipulation of specific expansin genes described in Chapter 4.

Generally, the *EXPA* expression pattern in leaf development matched the results available in the literature (Cho and Cosgrove, 2000, 2002; Wieczorek *et al.*, 2006) and data from microarray experiments (Beemster *et al.*, 2005; Schmid *et al.*, 2005). The absence of *EXPA7* and *EXPA18* transcripts is consistent to their root-specificity while the decrease in *EXPA10* transcript level at the mature stage of leaf growth is consistent with its proposed role in the young developing leaf (Cho and Cosgrove, 2000, 2002).

A genome-wide expansin expression pattern across different tissue systems and developmental stages (Figure 3.8-9, Table 3.2), indicated that there is no expansin that is specifically expressed only during leaf development, in contrast to the root-specific expansins. This perhaps reflects the leaf as a prototypic organ system since the gene expression levels in this tissue were similar to that overall in the plant (Schmid *et al.* 2005). Frequently, the changes in expansin expression levels are more drastic during floral organ development than that during leaf development, perhaps reflecting the more elaborate organ components of the flower. Clade XII expansins appear to involve in the development of floral organs. The microarray data also suggest the involvement of some EXPB genes (*EXPB1* & *EXPB3*) in leaf development (Figure 3.8), which are not pursued in this thesis.

Table 3.2. Expression pattern of EXPA in different plant tissues as obtained from Genevestigator microarray data mining, except trichomes from (Jakoby *et al.*, 2008). Indivual expansin genes are color-coded according to the clade classification as Figure 3.1.

Tissue		Expressed expansin genes
Leaf		
	Trichomes	*A3 A6 A10 A13*
	Guard cells	*A1 A4 A16*
	Petiole	*A1 A5 A6 A11 A13*
Flower		
	Petals	*A1 A3 A5 A6 A8 A11*
	Pedicel	*A5 A6 A13*
	Mature pollen	*A4 A16 A21 A24*
	Stigma	*A5 A6 A10 A11*
	Carpel	*A6 A13*
Seed		
	Imbibed seed	*A1 A2 A3 A9 A10 A13 A15 A20 A23*
	Endosperm	*A2*
	Embryo	*A12 A20 A22 A23/25*
Root		
	Root cortex cell	*A11*
	Root phloem cell	*A13*
	Endodermis, cortex	*A9 A11 A12 A13*
	Stele	*A9 A13 A14 A15 A17*
	Root hair	*A7 A18 A17*
	Lateral root	*A7 A18*

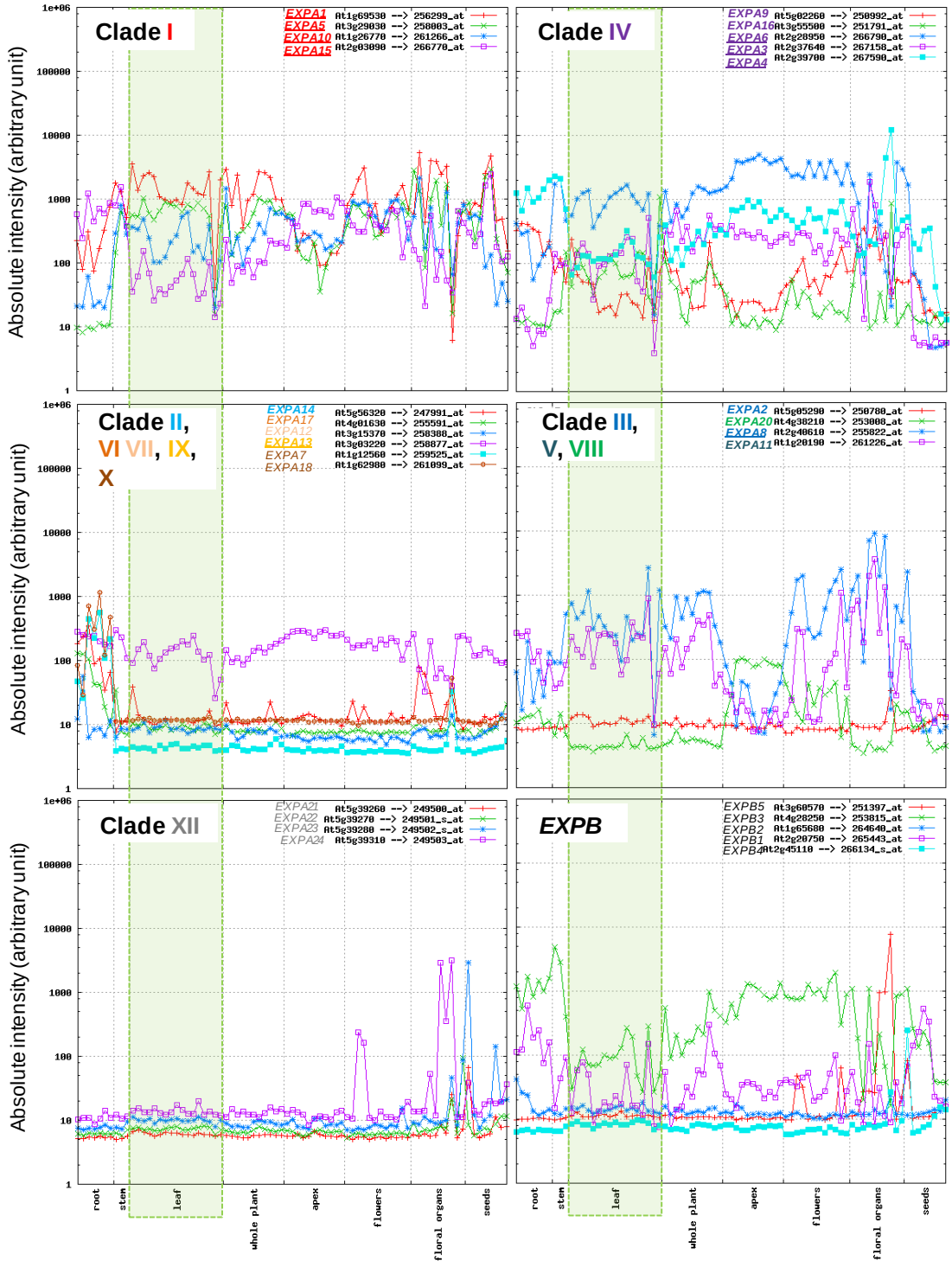

Figure 3.8. Microarray data of Arabidopsis expansin gene expression in different tissues across different developmental stages (Schmid *et al.*, 2005) compiled using AtGenExpress visualisation tool (http://jsp.weigelworld.org/expviz/expviz.jsp) according to colour-coded clade classification based on Figure 3.1. Highly expressed expansin genes from RT-PCR as shown in Figure 3.7 are underlined, whereas those with less abundant transcripts are bolded. Details on the tissues samples are shown in Table 3.3. Expression of expansin genes in leaf tissue samples is highlighted in green boxes. Data are based on the absolute intensity from microarray experiments.

Table 3.3. Details on the tissue samples of AtGenExpress developmental series taken from (http://www.weigelworld.org/resources/microarray/AtGenExpress/AtGE_dev_samples.pdf/). Leaf tissue samples with reference to Figure 3.8 are highlighted in green.

#	Sample ID	Experiment description	Genotype	Tissue	Age	Photoperiod	Substrate
1	ATGE_1	development baseline	Wt	cotyledons	7 days	continuous light	soil
2	ATGE_2	development baseline	Wt	hypocotyl	7 days	continuous light	soil
3	ATGE_3	development baseline	Wt	roots	7 days	continuous light	soil
4	ATGE_4	development baseline	Wt	shoot apex, vegetative + young leaves	7 days	continuous light	soil
5	ATGE_5	development baseline	Wt	leaves 1 + 2	7 days	continuous light	soil
6	ATGE_6	development baseline	Wt	shoot apex, vegetative	7 days	continuous light	soil
7	ATGE_7	development baseline	Wt	seedling, green parts	7 days	continuous light	soil
8	ATGE_8	development baseline	Wt	shoot apex, transition (before bolting)	14 days	continuous light	soil
9	ATGE_9	development baseline	Wt	roots	17 days	continuous light	soil
10	ATGE_10	development baseline	Wt	rosette leaf #4, 1 cm long	10 days	continuous light	soil
11	ATGE_11	development baseline	*gl1*-T	rosette leaf #4, 1 cm long	10 days	continuous light	soil
12	ATGE_12	development baseline	Wt	rosette leaf # 2	17 days	continuous light	soil
13	ATGE_13	development baseline	Wt	rosette leaf # 4	17 days	continuous light	soil
14	ATGE_14	development baseline	Wt	rosette leaf # 6	17 days	continuous light	soil
15	ATGE_15	development baseline	Wt	rosette leaf # 8	17 days	continuous light	soil
16	ATGE_16	development baseline	Wt	rosette leaf # 10	17 days	continuous light	soil
17	ATGE_17	development baseline	Wt	rosette leaf # 12	17 days	continuous light	soil
18	ATGE_18	development baseline	*gl1*-T	rosette leaf # 12	17 days	continuous light	soil
19	ATGE_19	development baseline	Wt	leaf 7, petiole	17 days	continuous light	soil
20	ATGE_20	development baseline	Wt	leaf 7, proximal half	17 days	continuous light	soil
21	ATGE_21	development baseline	Wt	leaf 7, distal half	17 days	continuous light	soil
22	ATGE_22	development baseline	Wt	developmental drift, entire rosette after transition to flowering, but before bolting	21 days	continuous light	soil
23	ATGE_23	development baseline	Wt	as above	22 days	continuous light	soil
24	ATGE_24	development baseline	Wt	as above	23 days	continuous light	soil
25	ATGE_25	development baseline	Wt	senescing leaves	35 days	continuous light	soil
26	ATGE_26	development baseline	Wt	cauline leaves	21+ days	continuous light	soil
27	ATGE_27	development baseline	Wt	stem, 2nd internode	21+ days	continuous light	soil
28	ATGE_28	development baseline	Wt	1st node	21+ days	continuous light	soil
29	ATGE_29	development baseline	Wt	shoot apex, inflorescence (after bolting)	21 days	continuous light	soil
30	ATGE_31	development baseline	Wt	flowers stage 9	21+ days	continuous light	soil
31	ATGE_32	development baseline	Wt	flowers stage 10/11	21+ days	continuous light	soil
32	ATGE_33	development baseline	Wt	flowers stage 12	21+ days	continuous light	soil
33	ATGE_34	development baseline	Wt	flowers stage 12, sepals	21+ days	continuous light	soil
34	ATGE_35	development baseline	Wt	flowers stage 12, petals	21+ days	continuous light	soil
35	ATGE_36	development baseline	Wt	flowers stage 12, stamens	21+ days	continuous light	soil
36	ATGE_37	development baseline	Wt	flowers stage 12, carpels	21+ days	continuous light	soil
37	ATGE_39	development baseline	Wt	flowers stage 15	21+ days	continuous light	soil
38	ATGE_40	development baseline	Wt	flowers stage 15, pedicels	21+ days	continuous light	soil
39	ATGE_41	development baseline	Wt	flowers stage 15, sepals	21+ days	continuous light	soil
40	ATGE_42	development baseline	Wt	flowers stage 15, petals	21+ days	continuous light	soil
41	ATGE_43	development baseline	Wt	flowers stage 15, stamen	21+ days	continuous light	soil
42	ATGE_45	development baseline	Wt	flowers stage 15, carpels	21+ days	continuous light	soil
43	ATGE_46	development baseline	*clv3-7*	shoot apex, inflorescence (after bolting)	21+ days	continuous light	soil
44	ATGE_47	development baseline	*lfy-12*	shoot apex, inflorescence (after bolting)	21+ days	continuous light	soil
45	ATGE_48	development baseline	*ap1-15*	shoot apex, inflorescence (after bolting)	21+ days	continuous light	soil
46	ATGE_49	development baseline	*ap2-6*	shoot apex, inflorescence (after bolting)	21+ days	continuous light	soil
47	ATGE_50	development baseline	*ap3-6*	shoot apex, inflorescence (after bolting)	21+ days	continuous light	soil
48	ATGE_51	development baseline	*ag-12*	shoot apex, inflorescence (after bolting)	21+ days	continuous light	soil
49	ATGE_52	development baseline	*ufo-1*	shoot apex, inflorescence (after bolting)	21+ days	continuous light	soil
50	ATGE_53	development baseline	*clv3-7*	flower stage 12; multi-carpel gynoeceum; enlarged meristem; increased organ number	21+ days	continuous light	soil
51	ATGE_54	development baseline	*lfy-12*	flower stage 12; shoot characteristics; most organs leaf-like	21+ days	continuous light	soil
52	ATGE_55	development baseline	*ap1-15*	flower stage 12; sepals replaced by leaf-like organs, petals mostly lacking, 2° flowers	21+ days	continuous light	soil
53	ATGE_56	development baseline	*ap2-6*	flower stage 12; no sepals or petals	21+ days	continuous light	soil
54	ATGE_57	development baseline	*ap3-6*	flower stage 12; no petals or stamens	21+ days	continuous light	soil
55	ATGE_58	development baseline	*ag-12*	flower stage 12; no stamens or carpels	21+ days	continuous light	soil
56	ATGE_59	development baseline	*ufo-1*	flower stage 12; filamentous organs in whorls two and three	21+ days	continuous light	soil
57	ATGE_73	pollen	Wt	mature pollen	6 wk	continuous light	soil
58	ATGE_76	seed & silique development	Wt	siliques, w/ seeds stage 3; mid globular to early heart embryos	8 wk	long day (16/8)	soil
59	ATGE_77	seed & silique development	Wt	siliques, w/ seeds stage 4; early to late heart embryos	8 wk	long day (16/8)	soil
60	ATGE_78	seed & silique development	Wt	siliques, w/ seeds stage 5; late heart to mid torpedo embryos	8 wk	long day (16/8)	soil
61	ATGE_79	seed & silique development	Wt	seeds, stage 6, w/o siliques; mid to late torpedo embryos	8 wk	long day (16/8)	soil
62	ATGE_81	seed & silique development	Wt	seeds, stage 7, w/o siliques; late torpedo to early walking-stick embryos	8 wk	long day (16/8)	soil
63	ATGE_82	seed & silique development	Wt	seeds, stage 8, w/o siliques; walking-stick to early curled cotyledons embryos	8 wk	long day (16/8)	soil
64	ATGE_83	seed & silique development	Wt	seeds, stage 9, w/o siliques; curled cotyledons to early green cotyledons embryos	8 wk	long day (16/8)	soil
65	ATGE_84	seed & silique development	Wt	seeds, stage 10, w/o siliques; green cotyledons embryos	8 wk	long day (16/8)	soil
66	ATGE_87	phase change	Wt	vegetative rosette	7 days	short day (10/14)	soil
67	ATGE_89	phase change	Wt	vegetative rosette	14 days	short day (10/14)	soil
68	ATGE_90	phase change	Wt	vegetative rosette	21 days	short day (10/14)	soil
69	ATGE_91	comparison with CAGE	Wt	leaf	15 days	long day (16/8)	1x MS agar
70	ATGE_92	comparison with CAGE	Wt	flower	28 days	long day (16/8)	soil
71	ATGE_93	comparison with CAGE	Wt	root	15 days	long day (16/8)	1x MS agar
72	ATGE_94	development on MS agar	Wt	root	8 days	continuous light	1x MS agar
73	ATGE_95	development on MS agar	Wt	root	8 days	continuous light	1x MS agar
74	ATGE_96	development on MS agar	Wt	seedling, green parts	8 days	continuous light	1x MS agar
75	ATGE_97	development on MS agar	Wt	seedling, green parts	8 days	continuous light	1x MS agar
76	ATGE_98	development on MS agar	Wt	root	21 days	continuous light	1x MS agar
77	ATGE_99	development on MS agar	Wt	root	21 days	continuous light	1x MS agar
78	ATGE_100	development on MS agar	Wt	seedling, green parts	21 days	continuous light	1x MS agar
79	ATGE_101	development on MS agar	Wt	seedling, green parts	21 days	continuous light	1x MS agar

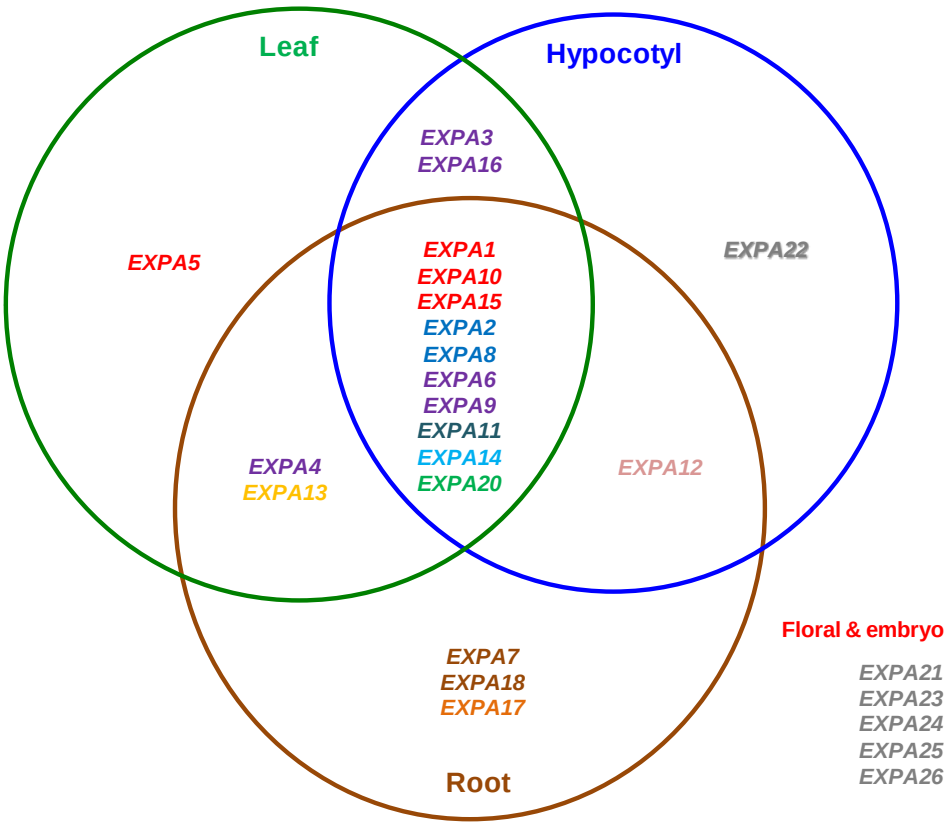

Figure 3.9. Expression pattern of *EXPA* family members in leaf, hypocotyl and root showing the abundance of overlapping expression. Data for hypocotyl tissue are from (Jamet *et al.*, 2009), root from (Wieczorek *et al.*, 2006), whereas that of leaf are compiled from current study. Floral organ and embryo are excluded from the Venn diagram for clarity due to highly overlapping expression (Table 3.2). The gene names are colour-coded according to their respective group of monocot-eudicot clade classification as in Figure 3.1.

The differential expression pattern of different *EXPA* genes is also consistent with the monocot-eudicot clade classification of expansins, so that similarly expressed expansin genes are often from the same clade (Figure 3.8). More than half of the *EXPA* genes (15 out of 26) were expressed during leaf morphogenesis (Figure 3.6). However, only 8 expansin transcripts in an ascending order: *EXPA6*, *EXPA5*, *EXPA10*, *EXPA4*, *EXPA3*, *EXPA1*, *EXPA8* and *EXPA13* can be considered to be abundant during leaf development. These genes dominate 4 clades, in which clade IV turned out to be the most abundantly expressed followed by clade I, clade III and clade IX. This is consistent with the emergent clustered expansin expression pattern obtained from *in silico* data mining of microarray data across various experiments and different tissues/ organs (Figure 3.10). This leads to the hypothesis that common regulators might be responsible for the differential regulation of expansin expression.

A more condensed summary on the hormonal regulation of expansin gene expression based on time-course hormone treatment experiments is depicted in Figure 3.11. This shows differential hormonal regulation on expansin genes from the same clade e.g. clade I expansin genes (*EXPA1*, *EXPA5*, *EXPA10* & *EXPA15*) show different effects of treatment by auxin and brassinosteroid. Furthermore, the clustering pattern of hormones based on their effects on the expression pattern of expansin genes is consistent with the general effects of respective hormones in promoting (CK/ZEA, GA) or restricting growth (ACC, ABA, MeJ) (Nemhauser *et al.*, 2006). Additionally, ethylene and cytokinins have been implicated in transverse cell expansion whereas auxin, gibberellin and brassinosteroids are often involved in longitudinal cell expansion (Nemhauser *et al.*, 2006). Inferring the functional specificity based on these observations and statistical clustering is not sufficient, due to the highly overlapping expression patterns of *EXPA*s in different tissues and the complicated effects of hormonal response. However, the patterns seem to suggest a cell-type specificity and therefore are consistent with the idea that expansins may be involved in specific cell or tissue differentiation rather than organ expansion *per se*.

Figure 3.10. Clustering of microarray data from AtGenExpress experiment series (Schmid *et al.*, 2005) using BAR Expression Browser (Toufighi *et al.* 2005) to identify common pattern of expansin expression. Details of sample and expression information are available online (http://www.weigelworld.org/resources/microarray/AtGenExpress/). Red-coloured boxes group the expansins detected in RT-PCR while brown boxes show the root-specific expansins.

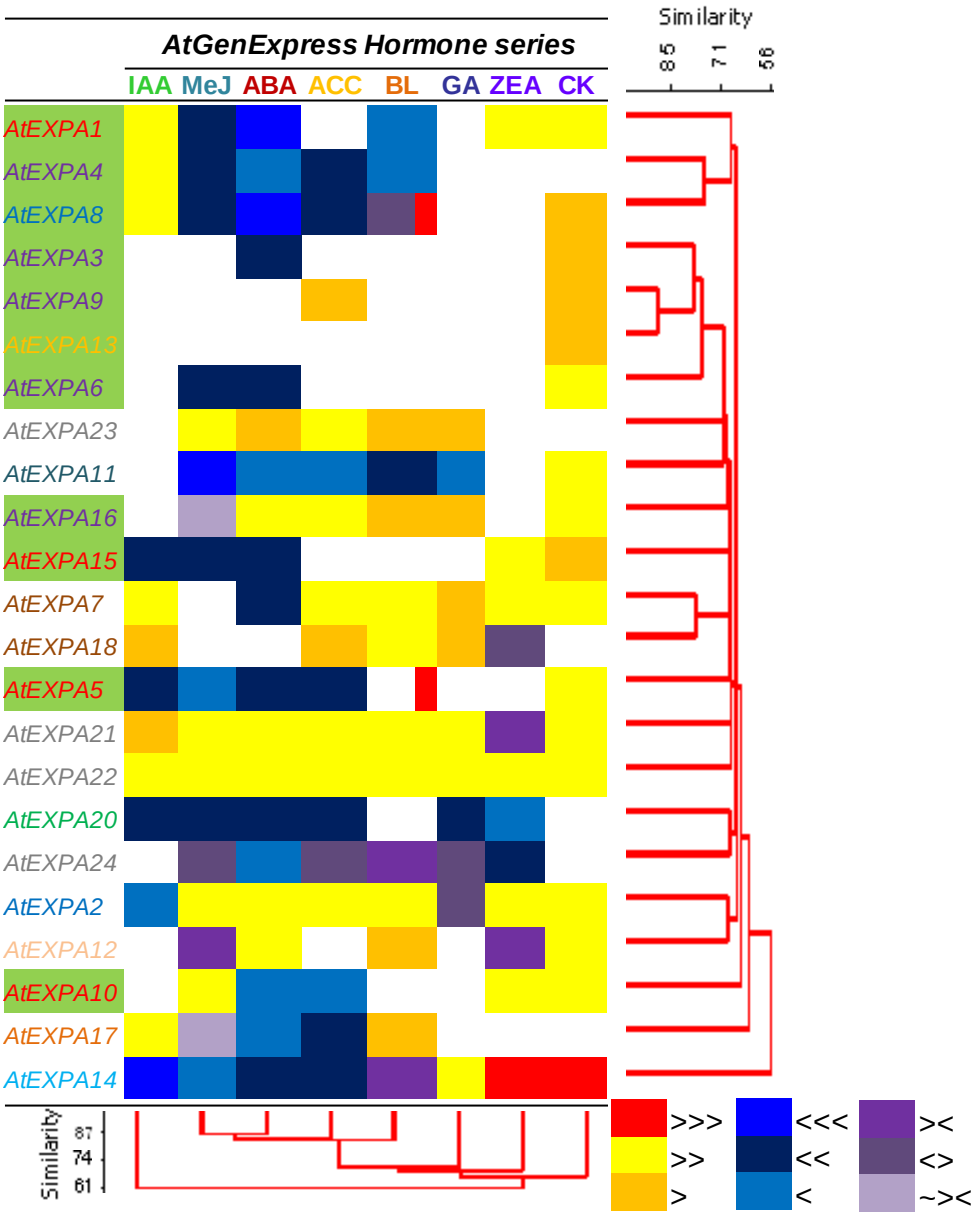

Figure 3.11. Summary of results from AtGenExpress hormone series time-course microarray experiments showing effects of different hormones on expansin expression. Expansin genes found to be expressed in the leaf are highlighted in green. Up-regulation is indicated by greater signs (>) and down-regulation lesser signs (<). The number of symbols is proportional to the intensity of up- or down-regulation. >< initial up-regulation followed by down-regulation, <> initially down-regulated then up-regulated, ~>< small up-regulation followed by great down-regulation. IAA, auxin; MeJ, methyl jasmonate; ABA, abscisic acid; ACC, 1-aminocyclopropane-1-carboxylic-acid (Ethylene); BL, brassinolide; GA, gibberellic acid; ZEA, zeatin; CK, cytokinin. Genes and hormones are clustered according to the similarity of expression patterns.

3.3 Discussion

3.3.1 Establishment of a standard staging system for Arabidopsis leaf growth

Arabidopsis leaf growth is highly variable even under a constant environment. This probably reflects weed ecology, as previously shown by its high natural variation, with over 100-fold variation in leaf 6 area on day 8 after initiation (Granier *et al.*, 2002). Hence, a leaf developmental staging system is essential if appropriate growth comparisons are to be performed, as will be seen later in Chapter 4.

In this chapter I have described such a system. This system allowed for RNA to be extracted from developmentally equivalent leaf samples for α-expansin transcript analysis. In order to reduce the study to a manageable size, my investigation focused only on leaf 6. Despite the artificial nature of growth on medium, leaf 6 undergoes the normal process of development (Figure 3.4), not only in the growth pattern but also reproduces the cessation pattern of cell division from leaf tip to base. This has been reported before (Donnelly *et al.*, 1999) and indicates a similarity in growth from cell-division dependent growth to vacuole-dominated growth. Furthermore, the growth analysis reported here is consistent with other earlier reports (Beemster *et al.*, 2005; Cookson *et al.*, 2005; Kuwabara *et al.*, 2011). The discussion on the growth analysis will be expanded on in Chapter 4, with the utilisation of same system for staged-transfer experiments.

3.3.2 The pattern of EXPA gene expression during Arabidopsis leaf development

Previous reports on the expansin gene expression pattern in the leaf are only available for monocot species such as rice, maize and fescue grass (Reidy *et al.*, 2001a; Lee and Kende, 2002; Muller *et al.*, 2007). Lee and Kende (2002) reported that the expression of seven *EXPA* genes is highest in the elongating region in deepwater rice leaf. Furthermore, there is a tight relationship linking the expression of three expansin genes to specific regions of maize leaf (Muller *et al.*, 2007). However, Reidy *et al.* (2001) concluded a limited correlation between expansin gene expression and leaf growth rate, compared to another cell wall gene family (xyloglucan endotransglucosylase/hydrolases) (Reidy *et al.*, 2001b). In these studies, different sections of monocot leaf (measured from leaf base) have been used to study the correlation of different expansin expression level with growth rate. This is because leaf growth in monocotyledonous consists of spatially and temporally

distinct four developmental phases (leaf zones) with elongation mainly occurring at the base of young leaf (Granier and Tardieu, 2009), analogous to that of root development (Scheres, 2007), with proliferative zone, elongation zone and maturation zone along the longitudinal axis. In comparison, the dicotyledonous leaf spans three developmental phases of proliferation, expansion and maturation, as described above, with no determinate leaf zone or temporally precise developmental phase. My investigation provides the first detailed study at the level of the individual defined dicot leaf throughout its developmental trajectory from an early stage when cell division is occurring throughout to the final mature leaf.

The results obtained here are consistent with the varied patterns of expansin gene expression, which change throughout leaf development, as reported previously in monocot plants (Reidy *et al.*, 2001a; Muller *et al.*, 2007), but less distinct. This perhaps reflects the spatially non-distinct nature of dicot leaf development, with intertwined cell division, cell expansion and cell differentiation within the same region. Hence, this would result in overlapping expression of most individual expansin genes during the course of dicot leaf development, compared to more distinct expression patterns when better defined monocot leaf regions undergoing different phases of development were studied. Despite the non-specific expression pattern of individual expansin genes, the overall concerted patterns of expression for the whole group of *EXPA* genes correlated with the progression of different leaf developmental stages (Figure 3.8).

Notably, a large number of expansin gene transcripts (11 genes) were detectable even at early stage of leaf development, in the absence of extensive turgor-driven cell expansion. This indicates that specific expansins may play role in the ontogeny of specific cell types rather than the overall organ expansion. Fundamentally, there are three major tissue types present in young leaf primordium i.e., dermal tissue, ground tissue and vascular tissue. The detected expansin gene may be required for the earliest cellular morphogenesis of specific cell types, such as trichomes, guard cells, xylem and phloem, which constitute the functional components of leaf architecture. This could explain the large number of expansin genes with overlapping expression in different organs if they share similar cell types. This is especially true

when considering the vascular system that develops throughout the plant and with more elaborate forms. Hence, there is no leaf-specific expansin gene.

However, there was a gradual increase in the expression of a number of *EXPA* genes expressed during specific leaf developmental stages, suggesting a role in specific elements of leaf differentiation. For example, *EXPA9*, *EXPA11* and *EXPA14* were expressed only from day 16 or day 20, within a small window of development and at relatively low levels (Figure 3.8). Day 16 is when the petiole became visible and suggests the involvement of these expansin genes, especially *EXPA11* which was previously detected in petiole (Table 3.2). The widespread expression pattern of *EXPA11* in petals, stigma, and root cortex cells suggest a generic role in ground tissue. For *EXPA14* which was detected only between day 16 and day 20 (Figure 3.7), its expression (amongst many other expansin genes) was found in stele (Table 3.2), which contains the vascular elements of the root. Furthermore, the expression of *EXPA14* is highly responsive to hormonal treatments (Figure 3.11). Interestingly, the expression of *EXPA9* is overlapping between that of *EXPA11* and *EXPA14* in root endodermis/cortex and stele (Table 3.2), which is also consistent with the expression pattern in leaf (Figure 3.7). How these observations are linked to the endogenous role of individual genes remains a mystery without data on gene localisation and functional analysis.

On the other hand, there was a correlation of overall *EXPA* transcript level and leaf growth. Considering the band intensities (Figure 3.6), the overall expression of *EXPA* genes was highest on day 24, prior to the maximum rate of extension/ expansion on day 26, and was maintained until day 28 before a drop in most of the expansin transcript levels. Expansin genes that are correlated with this pattern of growth include *EXPA1*, *EXPA3*, *EXPA4*, *EXPA5* and *EXPA8*. However, there is limitation to this speculation as the RT-PCR analysis carried out is not quantitative, and even with quantitative analysis there is a caveat that expression levels do not represent the actual expansin activity (Brummell *et al.*, 1999a; Caderas *et al.*, 2000; Rochange and McQueen-Mason, 2000). Furthermore, data from Sloan *et al.* (2009) suggest the presence of another (unknown) factor controlled in a developmental fashion which might potentiate endogenous expansin activity. Additionally, it has been shown that EXPB in soybean is highly regulated post-translationally such that

EXPB proteins are extensively modified by post-translational N-glycosylation and proteolysis (Downes *et al.* 2001). The measurement of expansin protein levels and activity are planned (see Chapter 4), but relating *EXPA* gene expression to function is not trivial. This is because cell wall modification is a complex and dynamic process such that a change in cell wall biochemistry or different functional conditions (pH, oxidative state) could act to override expansin activity (Darley *et al.*, 2001). Nonetheless, assuming no long distance transport of *EXPA* transcript or protein, then the absence of transcript indicates that a specific *EXPA* gene does not function in that tissue. Therefore, at a minimum, current RT-PCR analysis indicates that at least 11 expansin genes may play a role in early stage of leaf development, of which at least 5 genes are directly involved in leaf expansion.

Bearing the potential for gene redundancy even with this number of *EXPA* genes, it is surprising that the antisense of one gene (*EXPA10*) was sufficient to decrease leaf growth (Cho and Cosgrove, 2000). This could suggest that EXPA10 play major and irreplaceable role during leaf growth, or that the antisense might have affected the expression of other *EXPA* genes (unclear from earlier report without extensive molecular characterisation). Current expression analysis identified *EXPA* genes from predominantly four different clades that were highly expressed, of which genes from clade I (red, which includes *EXPA10*) and clade IV (purple) appeared to be the most promising as targets for studying their role in leaf growth. This leads to the next step in this project of utilising a novel amiRNA approach to down-regulate the expression of a specific group of related *EXPA* genes and observe the outcome on leaf growth and development, which will be described in the next chapter.

3.4 Summary

A system for the developmental staging of Arabidopsis leaves was established which facilitated the expression study of α-expansins. This system led to an expression profile of expansins during leaf morphogenesis which correlated to three different stages of development, albeit in a non-quantitative fashion. The same system will also be applied to studies aimed at the manipulation of expansin gene expression, described in the next chapter.

This study has demonstrated a specific overall pattern of *EXPA* expression during Arabidopsis leaf morphogenesis. Interpreting this expression data with the use of a position-based phylogeny tree of expansins from other species allowed a greater scope for the inference of expansin function and the generation of testable hypotheses on the regulation of expansins expression. For example, the tomato gene (*LeEXP2*) shown to be correlated with elongation growth (Caderas *et al.* 2000; Vogler *et al.* 2003) is in the same clade as *CsEXPA1* and *AtEXPA8* (Sampedro *et al.* 2006). The expression *EXPA8* is shown to correlate with the leaf expansion growth (Figure 3.7). The induction of exogenous gene such as *CsEXPA1* (Clade III) in Arabidopsis might affect the expression of related endogenous expansin genes such as *EXPA8*, or influence the normal developmental process governed by these endogenous genes, which will be explored in the next chapter.

Bioinformatic data mining of microarray allowed the comparison of the expression data obtained in this study with other analyses of expansins. In addition, it provided information on the potential role of expansins in tissue other than the leaf. For example, *EXPA12* and *EXPA17* share similar expression patterns to that of root-specific *EXPA7* and *EXPA18* (Figure 3.8), suggesting a similar root-specific function. Indeed, *EXPA17* was recently shown to be involved in lateral root formation (Swarup *et al.*, 2008). There seem to be a tendency to support the hypothesis for functional specificity of certain expansin genes in specific cell types. Differential expression response of genes from the same clade to different hormonal treatments suggests the requirement for differential regulation which might have functional/ physiological significance. However, it is difficult to disentangle tissue differentiation from growth without detailed functional analysis as it constitutes an inseparable part of a complex leaf development. Furthermore, the data gathered from the temporal studies of expansin gene expression will serve to inform further studies of endogenous gene expression through genetic manipulation (Chapter 4). Clade I expansin genes (*EXPA1, 5* &*10*) are chosen to be the targets for knock-down because of their abundance and widespread role across different plant species, as well as the established role of *EXPA10* in leaf growth (Cho and Cosgrove, 2000). The next chapter will describe the targeted inducible amiRNA strategy for studying the role of expansins in leaf development by knocking down the expansin identified in this chapter.

CHAPTER 4 Functional analysis of expansins in vegetative growth and organ morphogenesis

4.1 Introduction

Studying the pattern of when and where different expansin genes are expressed is informative. However, in order to validate any hypothesis of the functional role of expansin based on gene expression pattern, a more targeted approach has to be taken to directly manipulate the gene expression levels followed by observation of the resulting phenotype. In this Chapter, I will describe a series of experiments involving the inducible down-regulation of a group of expansin genes, with construct design derived from the Chapter 3 expression data.

Previous investigations on the role of expansins in leaf development have targeted the overexpression or suppression of specific expansin genes (Cho and Cosgrove, 2000; Pien *et al.*, 2001; Choi *et al.*, 2003; Sloan *et al.*, 2009). As outlined in Chapter 3, expansins are encoded by large multi-gene families, suggesting a great possibility of genetic redundancy which might obscure the functional analysis of individual gene members. Although a few successful investigations have been reported in which the expression of specific expansin genes has been repressed, leading to interpretable phenotypes (Cho and Cosgrove, 2000; Choi *et al.*, 2003), the characterisation of single gene mutants has generally not identified clear phenotypes (Cosgrove *et al.*, 2002; Li *et al.*, 2002; Schipper *et al.*, 2002).

It is noteworthy that the successful experiments mentioned have tended to use inducible or tissue-specific promoters to target repression of expansins, suggesting that temporal or spatial perturbation might be important for deciphering expansin gene function. Constitutive gene expression approaches have generally led to unstable and variable phenotypes (Cho and Cosgrove, 2000; Choi *et al.*, 2003). Additionally, these earlier results were generally reported when there was incomplete genomic information on both the full expansin gene sequences and the expression pattern within the plant. In Chapter 3, I have described a detailed expression analysis of all EXPA genes in Arabidopsis to fill in the gap on their expression pattern during the early stages of leaf development. The focus has been

mainly on leaf 6 as it is representative for the majority of other leaves, as seen in the growth analysis in Chapter 3. Leaf 6 is also a popular choice in other literature on Arabidopsis leaf growth (Cookson *et al.*, 2005; Cookson and Granier, 2006; Cookson *et al.*, 2006; Cookson *et al.*, 2007). This allows comparison of the results obtained here to those reported previously.

Previous successful repression of single expansin gene expression was mainly based on an antisense or hairpin RNA interference (hpRNAi) strategy (Brummell *et al.*, 1999a; Cho and Cosgrove, 2000; Choi *et al.*, 2003; Zenoni *et al.*, 2004). Here, I adopted a more recent artificial microRNA (amiRNA) approach, as reviewed in Ossowski *et al.* (2008), for targeted down-regulation of multiple expansin genes (Figure 4.1). The amiRNA approach is similar to the previous approaches in that it is based on the principles of double-stranded RNA (dsRNA) gene silencing with cleavage-mediated transcript degradation. It differs in the detailed mechanistic pathway, and the fact that amiRNA targets are easily predictable and thus can be optimised for high efficiency. This approach has been widely applied for highly specific post-transcriptional gene silencing since its introduction in Arabidopsis (Niu *et al.*, 2006; Schwab *et al.*, 2006) and has also been effective in rice, tobacco and tomato (Alvarez *et al.*, 2006; Warthmann *et al.*, 2008).The rapid uptake of this new technology for directed gene silencing is facilitated by the development of a user-friendly web-based platform, the Web MicroRNA designer (WMD at http://wmd3.weigelworld.org) which enables automated design of amiRNAs for genes of interest (Ossowski *et al.*, 2008). This tool offers computational incorporation of nucleotide mismatches that mimic the characteristics of an endogenous plant miRNA precursor sequence (miR319a) as the structural backbone, for the design of 21-base amiRNA candidates which complement imperfectly the target sequences by replacing the stem-loop forming duplex miRNA region (amiRNA*). Expression of amiRNA precursors in transgenic plants leads to an accumulation of mature amiRNAs processed by dsRNA binding proteins (HYL1, DCL1), which guide the RNA-induced silencing complex (RISC) to cleave target mRNAs, knocking down the expression levels of target genes (Figure 4.1A).

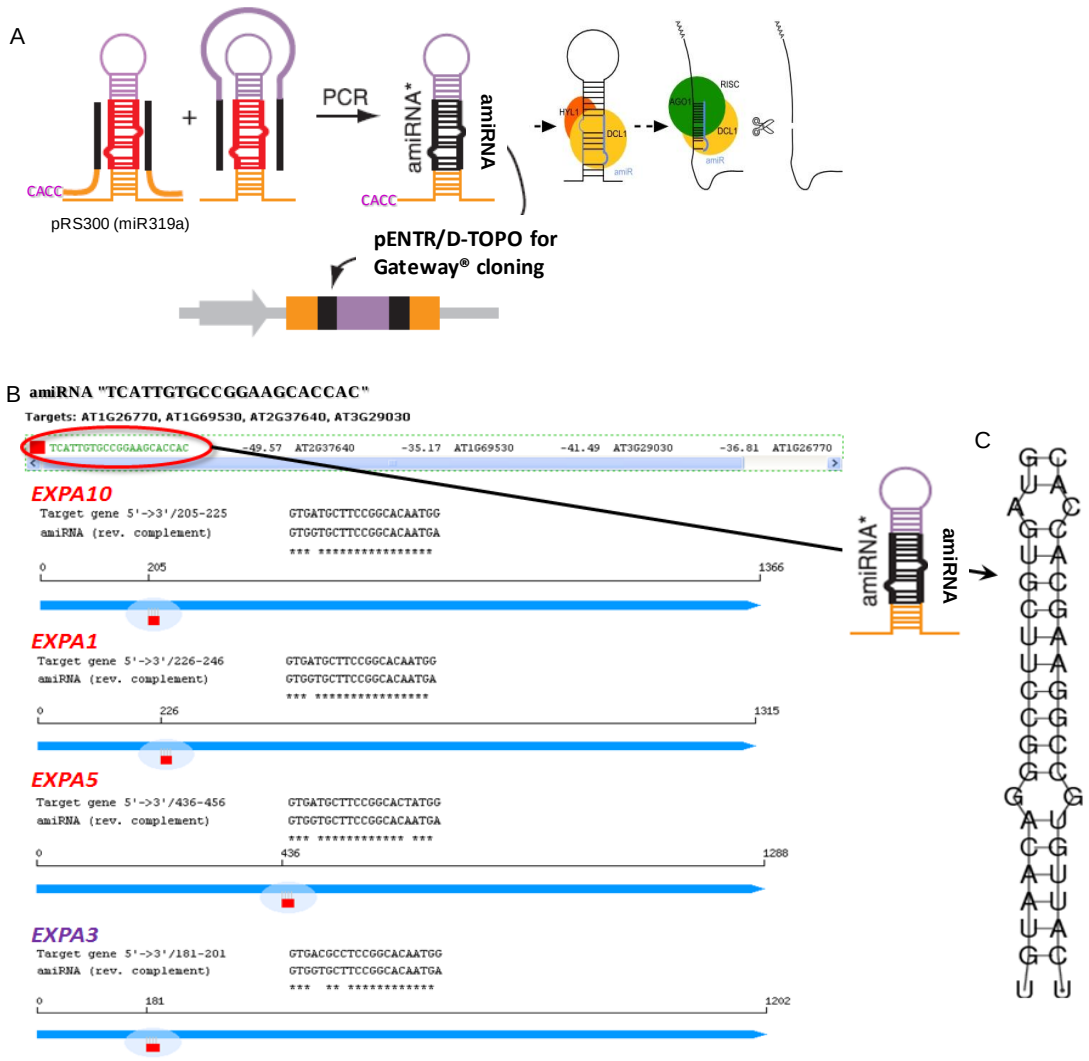

D **Sequence of amiR10,1,5,3:**

CACCCAAGGCGATTAAGTTGGGTAACGCCAGGGTTTTCCCAGTCACGACGTTGTAAAACGACGGCCAGTGAATTGTAATACGACTCACTATAGGGCGA
ATTGGGTACCGGGCCCCCCCTCGAGGTCGACGGTATCGATAAGCTTGATATCGAATTCCTGCAGCCCcaaacacacgctcggacgcatattacacatgttcatacactt
aatactcgctgtttgaattgatgtttt*aggaatatatatgt**aga*GTAGTGCTTCCGGGACAATGTtcacaggtcgtgatatgattcaattagcttcgactcattcatccaaatacgagt
**cgccaaaattcaaactagactcgttaaatgaatgaatgatgcggtagacaaattgga*tcattgattctctttga*TCATTGTGCCGGAAGCACCACtctctctttgtattccaatttcttgat
taatctttcctgcacaaaaacatgcttgatccactaagtgacatatatgctgccttcgtatatatagttctggtaaaattaacatttgggtttatctttatttaaggcatcgccatgGGGGGATCCAC
TAGTTCTAGAGCGGCCGCCACCGCGGTGGAGCTCCAGCTTTTGTTCCCTTTAGTGAGGGTTAATTTCGAGCTTGGCGTAATCATGGTCATAGCTGTTTCC
TGTGTGAAATTGTTATCCGC

T7 SP6 oligoA oligoB miRNA miRNA* cloning error

Figure 4.1. Artificial miRNA (amiR) approach for expansin gene silencing. (A) Schematic representation of amiRNA work flow adapted from Ossowski *et al.* (2008). First, the customised amiRNA was generated through overlapping PCR with modified primers (Section 2.4.1) for Gateway-compatible cloning (Section 2.4.2-3). This allows targeted transcript cleavage-mediated silencing. (B) Diagram showing the predicted target genes (colour-coded according to clade classification as described in Chapter 3) in a descending order of specificity according to hybridisation energy (kcal/mol) for the designed amiRNA sequence and (C) its predicted structure (Source: http://wmd3.weigelworld.org/cgi-bin/webapp.cgi). (D) Sequence of the designed amiREXPA for the down-regulation of *EXPA1,3,5,10* highlighting functional sites.

The dexamethasone–inducible pOpON system was chosen to inducibly overexpress the designed amiRNA construct (as described in Figure 4.2). The pOpON system is based on an improved version of glucocorticoid receptor-based, steroid-inducible system (Craft *et al.*, 2005; Moore *et al.*, 2006). A great advantage of the pOpON system is its enhanced bidirectional transcription upon induction which allows simultaneous transcription of the gene construct and an expression marker (*GUS*) at high levels with minimal amount of inducer dexamethasone (Dex) in a concentration-dependent manner. Furthermore, the system is compatible with Gateway-cloning system allowing a relatively convenient cloning procedure to incorporate amiRNAs (Karimi *et al.*, 2007).

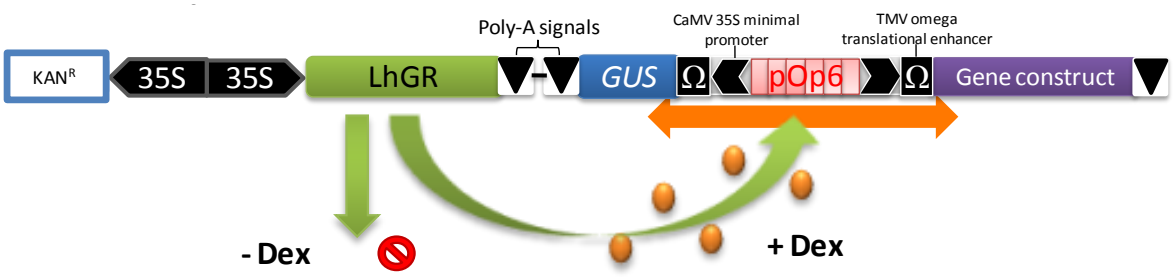

Figure 4.2. Schematic diagram of the pOpON^{Kan} two-component inducible system with kanamycin resistance selectable marker. The dexamethasone-inducible pOpON2.1 transactivating system contains two transcription units. The first unit employs a constitutive CaMV 35S promoter to express a Dex-responsive chimaeric transcription factor (LhGR). LhGR is an artificial fusion between a high-affinity DNA-binding mutant of *lac* repressor, transcription-activation domain-II of GAL4 from *Saccharomyces cerevisiae* and ligand-binding domain of a rat glucocorticoid receptor (GR LBD). The second unit consists of six copies of the multimerised *lac* operators (transcription factor-binding site pOp6) linked to a truncated 35S promoter, which forms the bidirectional promoter used to express the construct of interest and expression marker *β*-glucuronidase (*GUS*) gene. Each construct ends with poly-A signal that serves as transcription terminator. Circles representing dexamethasone (Dex) which binds and activates the constitutively expressed LhGR, in turn results in the transcription of both the gene construct and *GUS*.

My aim was to specifically down-regulate the target expansin genes (*EXPA1*, *EXPA3*, *EXPA5* and *EXPA10*) involved in leaf development with spatial and temporal control by incorporating the amiRNA approach with the pOpON system. This allowed me to address questions that remained unanswered from previous studies about the role of the many endogenous expansin genes expressed during leaf development. Are expansins involved in the differential leaf expansion along the transverse and longitudinal axes? Are expansins directly involved in leaf morphogenesis or are shape alterations an indirect consequence? Furthermore, there remain questions over the basic function of expansins in promoting growth. Thus, although some reports are consistent with expansin acting to promote growth via cell wall loosening, there are data indicating a contrary phenotype. For example, constitutive over-expression of *CsEXPA1*, a cucumber homolog of *LeEXP2* strongly expressed in the elongation zone of tomato hypocotyls under auxin stimulus, resulted in retarded growth of tomato plants and etiolated hypocotyls (Caderas *et al.*, 2000; Rochange *et al.*, 2001). These paradoxical observations will also be discussed in this chapter.

4.2 Results

4.2.1 Generation and molecular analysis of transgenic plants containing an inducible amiRNA construct for the specific down-regulation of selected expansin genes

The first aim of the experiments described in this chapter is to create transgenic lines via an inducible amiRNA approach, to down-regulate the expression of a number of expansin genes in a particular target tissue (Figure 4.1, 4.2). As described in Chapter 3, I chose the developing leaf of Arabidopsis as the organ of interest and, via a combined bioinformatic and experimental approach, identified a number of alpha-expansin genes (EXPAs) expressed during the early phase of leaf development. These include *EXPA10*, *EXPA5*, *EXPA3* and *EXPA1*, in which *EXPA10* has previously been functionally characterised to be involved in leaf growth (Cho and Cosgrove, 2000). These gene sequences were used to design an amiRNA construct to knock-down the expression of these target expansins (Figure 4.1B). This construct was then used to transform Arabidopsis (Col-0).

Six independent T1 pOpON::amiREXP transformants (constructs described in Figure 4.1D, 4.2) were obtained, selfed, and further characterised through segregation analyses (Table 4.1). Figure 4.3 shows the induction experiments to select for the most stable transformants with uniform growth. Homozygous T2 pOpON::amiREXP line 2-5 and line 3-22 which showed low background *GUS* expression and high *GUS* expression after Dex (10 µM) induction were chosen for further experiments. These lines are designated as pOpON::amiREXP (2-5) and pOpON::amiREXP (3-22) in the following experiments.

Molecular verification of amiR construct insertion in T2 transformants was performed through PCR of genomic DNA using transgene-specific primers (Figure 4.4A). The level of endogenous expansin gene transcripts after induction of the pOpON::amiREXP lines was tested using both sq-RT-PCR (Figure 4.4B) and RT-qPCR (Figure 4.4C). These results indicated that after whole plant induction with 10 µM Dex there was a significant ($p<0.05$) decrease in transcript levels for *EXPA1*, *EXPA10*, *EXPA5* and *EXPA3* within 2 days and up to 12 days relative to the control transcript (*UBC21*).

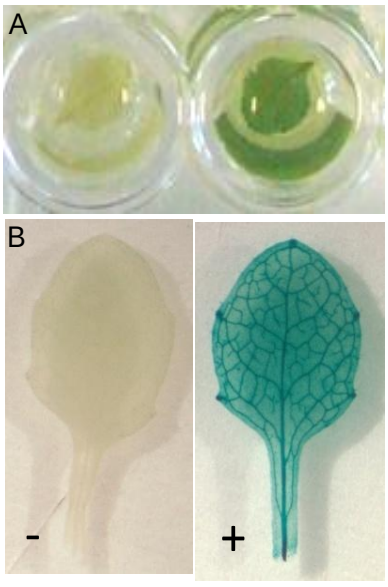

Figure 4.3. Induction tests for the characterisation and selection of T2 pOpON::amiREXP lines using (A) first leaf pairs (n = 24 per line) and (B) leaf 6 in solution with (+) or without (-) the inducer 10 µM dexamethasone overnight before GUS staining.

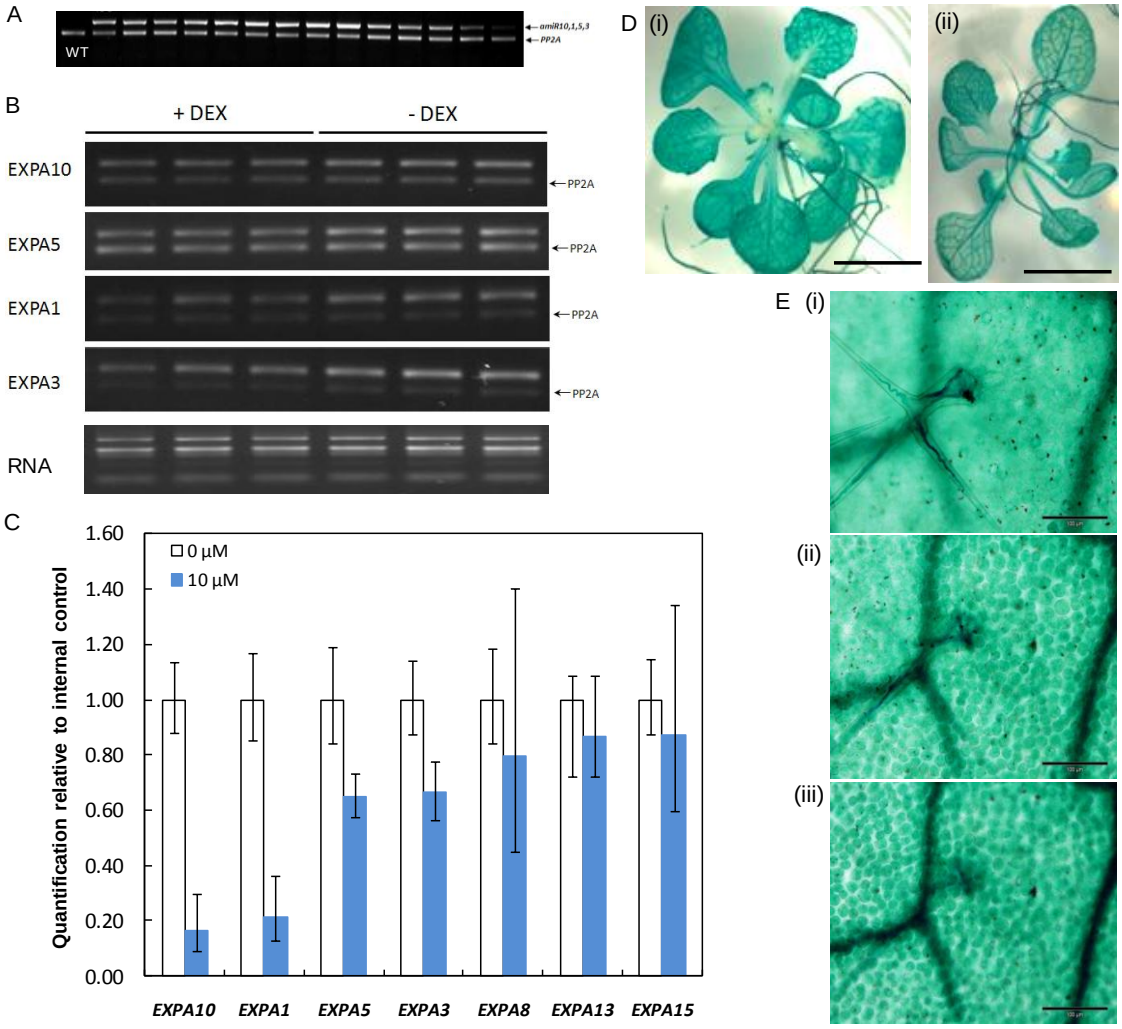

Figure 4.4. Characterisation of a number of independent pOpON::amiREXP (3) plants. (A) Molecular characterisation of *amiR10,1,5,3* insertion via PCR of genomic DNA from T2 transformants using Col-0 wild-type (WT) as negative control and *PP2A* as PCR control. (B) Semi-quantitative RT-PCR characterisation of amiR-targeted expansin gene transcript levels in three biological replicates of 12 DAS plant grown on half-strength MS agar medium supplemented with 10 µM dexamethasone (+DEX) or DMSO 0.1% (-DEX), showing bands at exponential phase of PCR cycles using *PP2A* as internal control. (C) RT-qPCR quantification of targeted (*EXPA10, 1, 5, 3*) and non-targeted (*EXPA8, 13, 15*) expansin transcript levels based on *UBC21* as reference gene. Values are means ± 1 SD from 2 biological replicates as per (B). (D) GUS staining of transformant grown on half-strength MS agar medium supplemented with 10 µM dexamethasone, harvested on 12 DAS, viewed from (i) top or (ii) bottom. (E) Gus staining showing induced expression across (i) epidermal, (ii) palisade, and (iii) vasculature layers. Scale bars = 5 mm (D), 100 µm (E).

Table 4.1. Segregation analysis of T2 (n > 61) and T3 (n > 15) generation of pOpON::amiREXP transformants for kanamycin-resistance (Kan^R).

T1 Line (T2)	% Kan^R	T2 Line (T3)	% Kan^R
1	93	1-3	100
		1-4	100
		1-12	100
		1-14	73
		1-15	100
		1-23	100
2	73	2-1	87
		2-2	100
		2-3	53
		2-4	67
		2-5	100
		2-6	80
		2-7	80
		2-13	100
		2-15	80
		2-17	100
		2-22	100
		2-23	73
3	95	3-1	100
		3-2	94
		3-4	100
		3-5	100
		3-7	100
		3-9	100
		3-13	100
		3-14	93
		3-15	100
		3-19	73
		3-21	80
		3-22	100
4	73	4-1	73
		4-2	60
		4-3	67
		4-4	80
		4-5	73
		4-6	60
		4-9	80
		4-10	73
		4-13	80
		4-14	80
		4-17	100
		4-18	87
		4-25	100
5	84	5-4	93
		5-19	80
6	89	6-9	100
		6-11	100
		6-13	87
		6-17	73

Non-target expansins for the amiREXP construct (*EXPA8*, *EXPA13* and *EXPA15*) did not show any significant decrease in transcript level, although in some cases the degree of signal variation was admittedly high (Figure 4.4C). Histochemical analysis of GUS expression in the induced pOpON::amiREXP plants indicated that GUS signal was present throughout the plant and in all layers of the leaves, although signal was less apparent in the shoot apex (Figure 4.4D-E).

As described in the materials and methods, a series of transgenic Arabidopsis (Col-0) lines containing a pOpON::CsEXPA1 construct had already been generated and partially characterised in the Fleming lab by Dr. Robert Malinowski. pOpON::CsEXPA1 contains a full-length cDNA of the first expansin isolated, cucumber (*Cucumis sativus*) expansin gene (*CsEXPA1*, 992 bp) with well-characterised *in vitro* and *in situ* cell wall-loosening function (McQueen-Mason *et al.*, 1992). These plants were incorporated in my analysis of the pOpON::amiREXP lines to investigate the counter-effect of expansin up-regulation as compared to expansin down-regulation.

Homozygosity of the pOpON::CsEXPA1 transformant line 10/1 was verified by 100% kanamycin-resistance in segregation analysis of T3 plants and molecular analysis performed. Semi-quantitative reverse transcription PCR (sq-RT-PCR) (Figure 4.5A) and RT-qPCR (Figure 4.5B) showed that the expression of *CsEXPA1* transcript was induced by the supply of Dex in a concentration-dependent manner. The translation of *CsEXPA1* into protein was verified by the detection of overexpressed expansin protein from Western blot (Figure 4.5C), carried out by Dr. Jen Sloan. Exploitation of the bidirectional promoter in the pOpON::CsEXPA1 construct allowed me to use GUS expression to confirm target gene inducibility and to characterise the pattern of GUS gene expression after the supply of Dex via the growth medium (Figure 4.5D). Expression was observed in all parts of the plant and in all cell layers (Figure 4.5E). There was a higher GUS signal apparent in the vascular system which may reflect the pathway of Dex movement through the plant and/ or may reflect the different histology of this tissue.

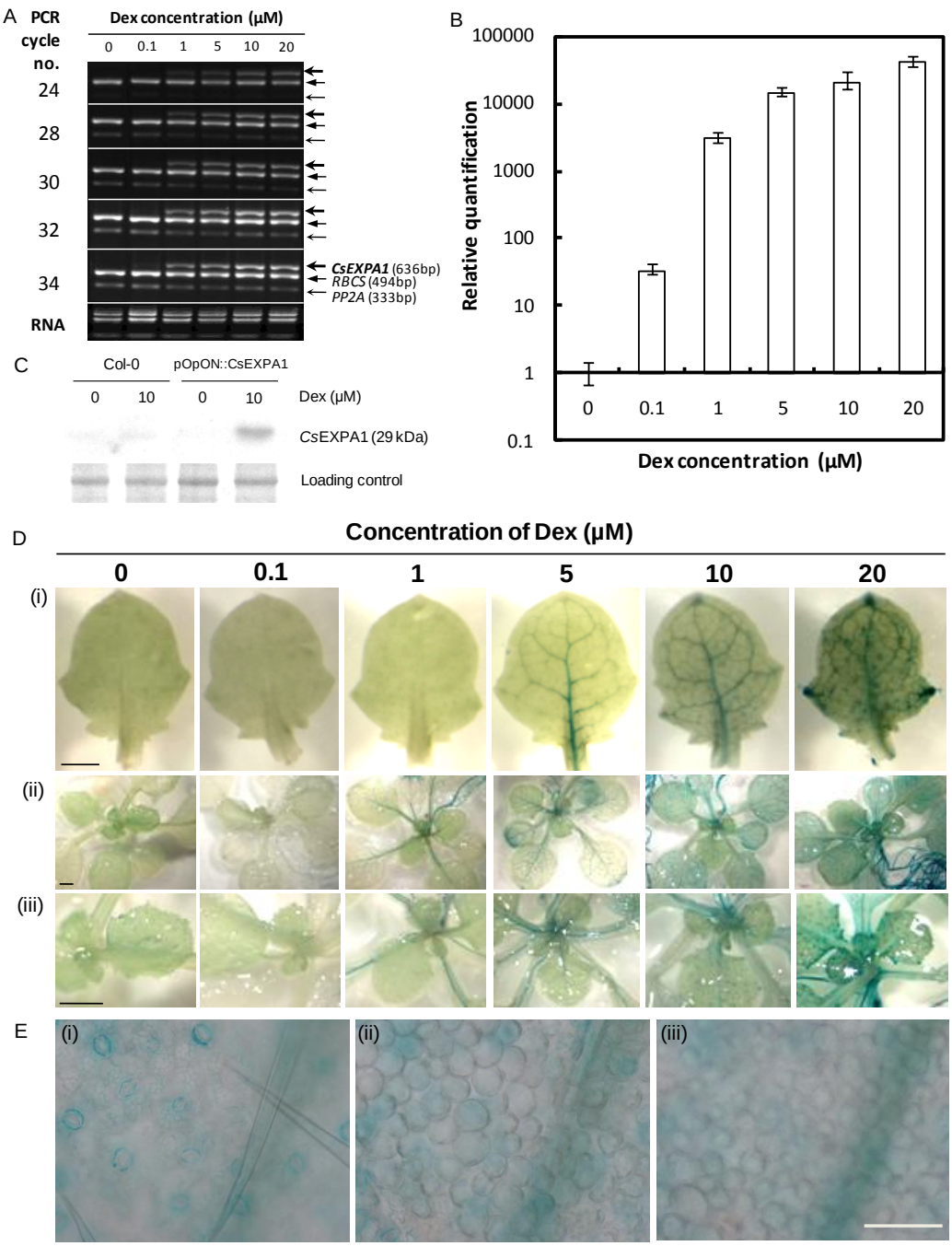

Figure 4.5. Characterisation of T3 homozygous pOpON::CsEXPA1 (10-1). (A) Semi-quantitative RT-PCR of *CsEXPA1* transcript abundance from staged-transfer induced plants at different Dex concentrations using *RBCS* and *PP2A* as internal controls. (B) Quantitative real-time PCR (RT-qPCR) analysis of *CsEXPA1* transcript abundance based on ΔΔCt using UBC21 as internal control and 0 µM as reference sample, plotted on a Log-scale. Error bars represent minimum and maximum range. (C) Western blotting of cell wall proteins (whole plant tissue) from 21 DAS plants grown with or without Dex. (D) GUS staining of induced (i) leaf 6 with different Dex concentrations harvested from (ii) seedlings transferred on 14 day after sowing (DAS) and after 24 hours induction (same as (A)). (iii) Magnified shoot apex of plants shown in (ii). (E) GUS staining showing induced expression across (i) epidermal, (ii) palisade, and (iii) vasculature layers of leaf 6 after10 µM induction. Scale bars = 1 mm (D), 50 µm (E).

4.2.2 Inducible suppression of expansin gene expression leads to growth repression

Following Dex induction the pOpON::amiREXP plants showed an overt and visible inhibition of growth relative to either mock-induced pOpON::amiREXP plants or Dex-treated Col-0 wild-type (WT) plants (Figure 4.6). Focussing on the phenotype of leaf 6, both lamina area and petiole length were significantly reduced ($p<0.05$) after Dex induction in the pOpON::amiREXP plants (Figure 4.7).

To further characterise this striking growth repression, I performed a series of growth analyses of induced pOpON::amiREXP plants using different Dex concentrations in which the inducer was supplied in the medium from germination

Figure 4.6. Comparison between Col-0 wild-type and pOpON::amiREXP (3) transformant plants grown on 0.5x MS agar medium supplemented with 10 µM Dex or DMSO 0.1% (0 µM) at 31 day after sowing (DAS). Ruler with mm scale in the middle.

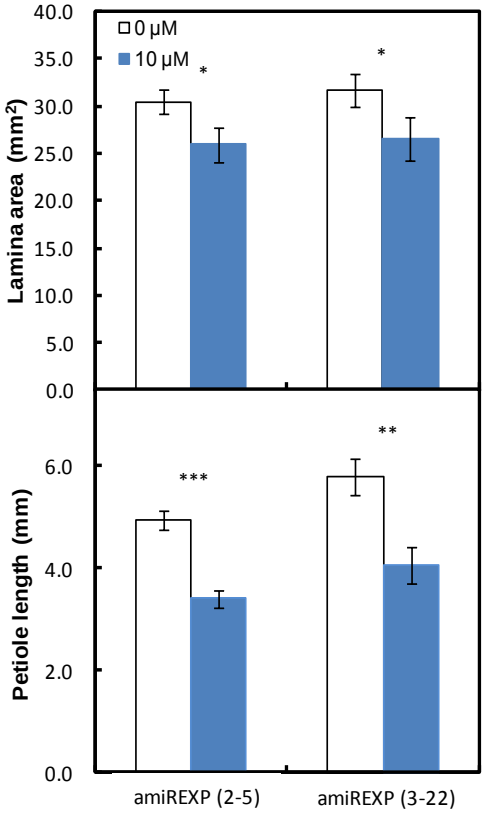

Figure 4.7. Comparison of leaf 6 parameters between induced (10 µM) and non-induced (0 µM) pOpON::amiREXP transformant plants 25 day after sowing. Values are means ± SE (n = 11-15). Two-sample t-tests, *p<0.05, **p<0.01, ***p<0.001.

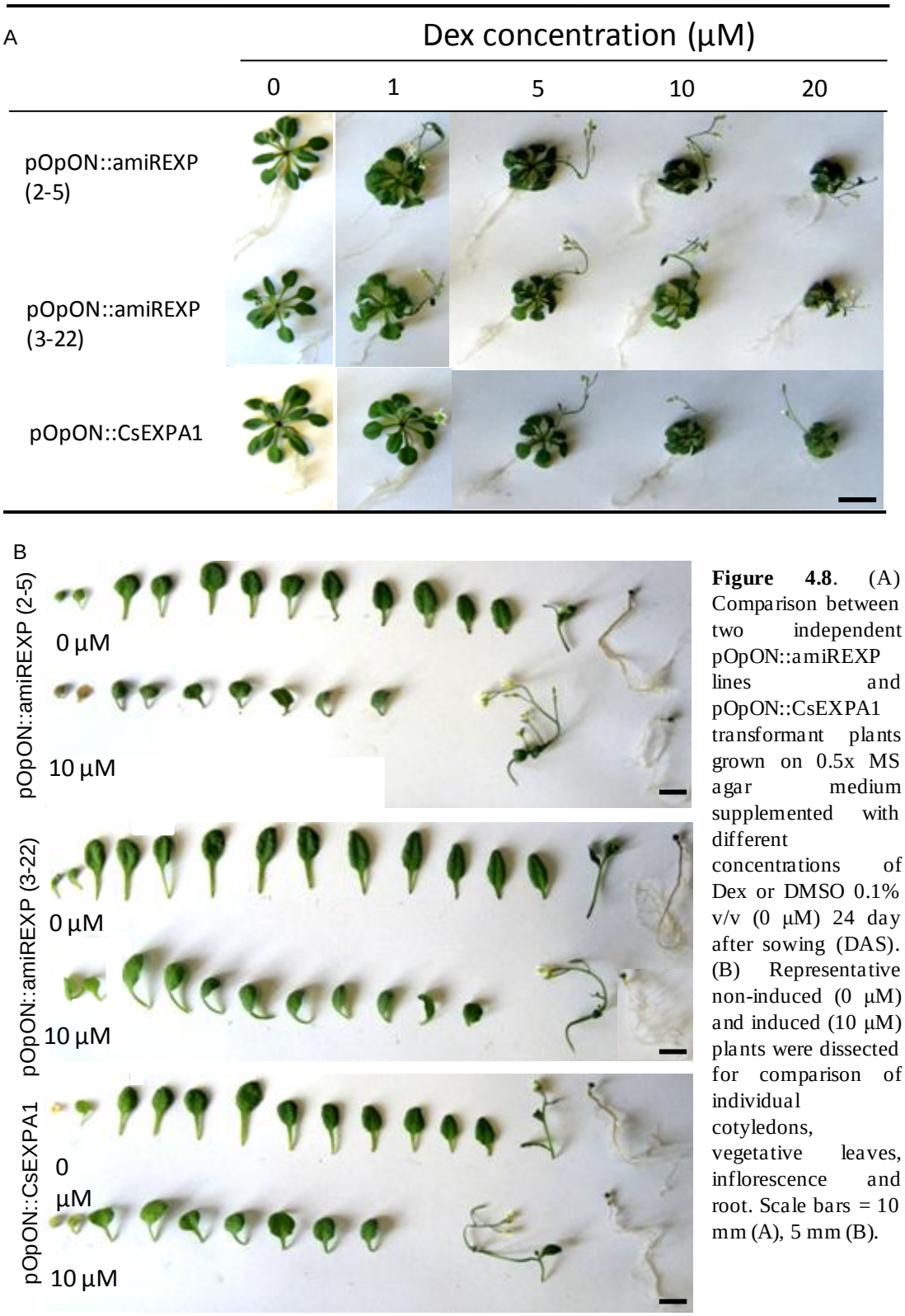

Figure 4.8. (A) Comparison between two independent pOpON::amiREXP lines and pOpON::CsEXPA1 transformant plants grown on 0.5x MS agar medium supplemented with different concentrations of Dex or DMSO 0.1% v/v (0 µM) 24 day after sowing (DAS). (B) Representative non-induced (0 µM) and induced (10 µM) plants were dissected for comparison of individual cotyledons, vegetative leaves, inflorescence and root. Scale bars = 10 mm (A), 5 mm (B).

onwards. In addition to the WT plants, I also included pOpON::CsEXPA1 lines in this analysis to compare the growth response to that observed after induction of expansin transcripts. An overview of typical plant phenotype at the end-point of these experiments is shown in Figure 4.8 and a more detailed time course of growth response from non-destructive measurements is shown in Figure 4.9-10.

As can be seen on Figure 4.8A, the induction of the pOpON::amiREXP plants with Dex at 1 µM already led to a visible phenotype at the level of the whole rosette. When individual leaves were dissected from these plants, it can be seen that all parts of the plant seemed to show a growth repression, especially from leaf 3 onwards showing downwards leaf curling (Figure 4.8B). Surprisingly, the induced pOpON::CsEXPA1 plants showed a very similar growth repression phenotype at high Dex concentrations.

A time course analysis of growth provided more insight into the dynamics of this growth repression. Considering first of all the rosette area (Figure 4.9), induction of the pOpON::amiREXP plants led to a significantly decreased final area ($p<0.001$) under all Dex concentrations. This decrease in rosette area first became significantly different from the control around 20 day after sowing (DAS). A very similar time course of growth repression was observed in the induced pOpON::CsEXPA1 plants at higher Dex concentrations (Figure 4.10). When the absolute areal growth rates of the rosettes were examined, it is apparent that although the growth rates were significantly decreased in the induced pOpON::amiREXP and pOpON::CsEXPA1, the pattern of growth rate was similar, i.e. started off with a low growth rate during early development and increased to a maximum around 15-18 DAS, before falling to lower values by 20-24 DAS. Thus, the induction of pOpON::amiREXP and pOpON::CsEXPA1 plants led to a depression in the absolute growth rate but the endogenous temporal pattern of growth was maintained. This is also apparent when the relative growth rates are considered. The pattern of change of relative growth rate is very similar for all plants and treatment although the values are generally lower in the induced pOpON::amiREXP and pOpON::CsEXPA1 plants.

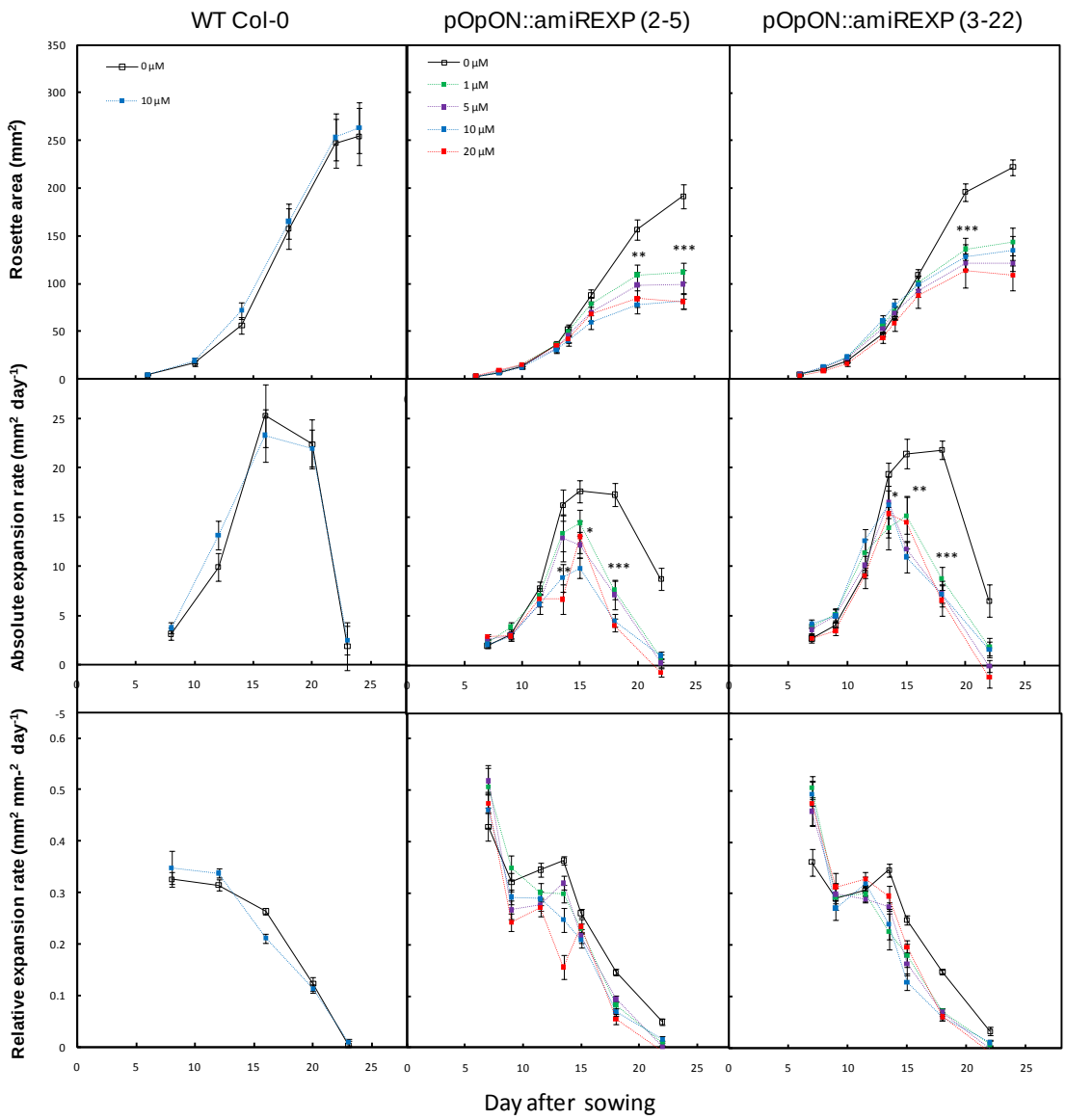

Figure 4.9. Comparison between Col-0 wild-type and pOpON::amiREXP (2-5) & (3-22) vegetative rosette growth dynamics under different concentrations of Dex. Rosette areas (coverage projections), absolute rosette area expansion rates, and relative rosette area expansion rates of 12 individual plants of each line, grown on half-strength MS agar medium supplemented with different concentrations of Dex or DMSO 0.1% v/v (0 µM), were measured from 6 to 24 day after sowing. Values are means ± SE (n = 12). One-way ANOVA, Tukey tests compared to 0 µM control *p<0.05, **p<0.01, ***p<0.001, asterisks were annotated only for the first instances when the difference become significant or when the significance level changes and left out subsequently for clarity.

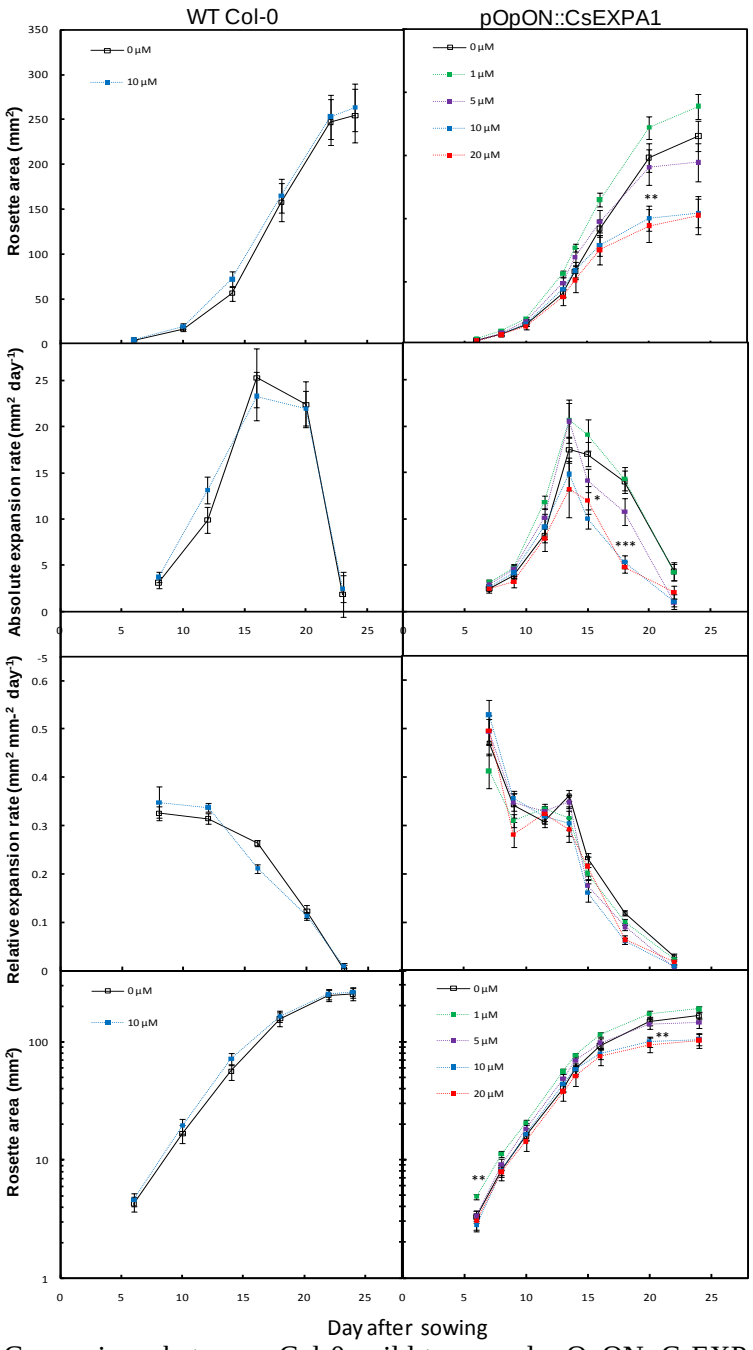

Figure 4.10. Comparison between Col-0 wild-type and pOpON::CsEXPA1 vegetative rosette growth dynamics under different concentrations of Dex. Rosette areas (coverage projections), absolute rosette area expansion rates, and relative rosette area expansion rates of 12 individual plants of each line, grown on half-strength MS agar medium supplemented with different concentrations of Dex or DMSO 0.1% (0 µM), were measured from 6 to 24 day after sowing. Values are means ± SE (n = 12). Rosette area is also plotted on a log Y-axis for clearer distinction of early rosette growth. One-way ANOVA, Tukey tests compared to 0 µM control *p<0.05, **p<0.01, ***p<0.001, asterisks were annotated only for the first instances when the difference become significant or when the significance level changes and left out subsequently for clarity.

Having characterised the influence of altered expansin expression on the whole-plant growth, I focused on the development of leaf 6 to investigate the effect at an individual leaf-level. Leaf 6 was harvested from plants germinated and grown on medium supplemented with various concentrations of Dex (Figure 4.11). There was a significant decrease in pOpON::amiREXP leaf lamina length, width and area relative to the mock-treated plants after induction with Dex at 5 µM or greater (Figure 4.11A). Similarly, there was a significant decrease in petiole length, although this phenotype was detectable at inducer concentrations as low as 1 µM (Figure 4.11B).

The morphometric (shape descriptor) alterations to the whole leaf, lamina and petiole were further examined using scale-independent circularity (4π area/ perimeter^2), such that a value of 1 equates to a perfect circular shape and decreases with more elongated or serrated shape. When the data were analysed using this derived parameter for circularity, it became clear that when considering the whole leaf (lamina + petiole) there was an increase in circularity after the induction of pOpON::amiREXP plants with Dex at concentrations of 1µM or greater (Figure 4.11C). An increased circularity indicates that the leaf shape has changed so that it is less elongated and more circular. The leaf silhouettes used for this analysis are shown in Figure 4.11D.

With respect to the pOpON::CsEXPA1 lines, induction with Dex did not lead to a significant decrease in lamina area (Figure 4.11A). After the induction with 1 µM Dex there was a slight, but significant ($p<0.05$) increase in lamina area, not observed at higher Dex concentrations. This increase in leaf area after induction with 1 µM Dex reflected an increase in both lamina length and width. However, although induction with 1 µM Dex also led to a significant increase in petiole length, inductions with higher concentrations of Dex led to a marked decrease in petiole length (Figure 4.11B). As a consequence of these differential outcomes of induction of the pOpON::CsEXPA1 lines, leaf circularity decreased significantly after induction with low Dex concentration and increased significantly following induction with higher Dex concentrations (Figure 4.11C).

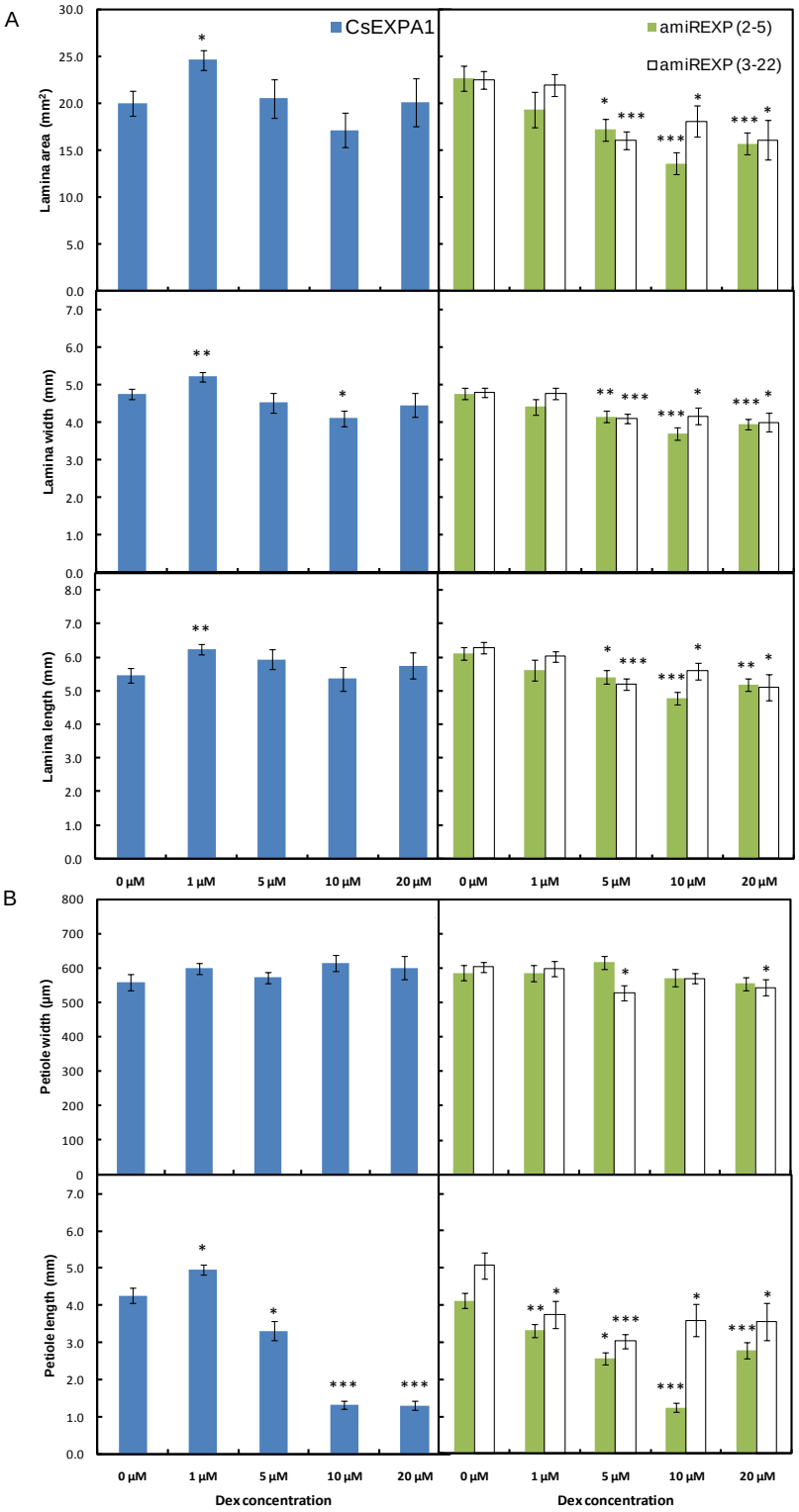

Figure 4.11. Legends on the following page.

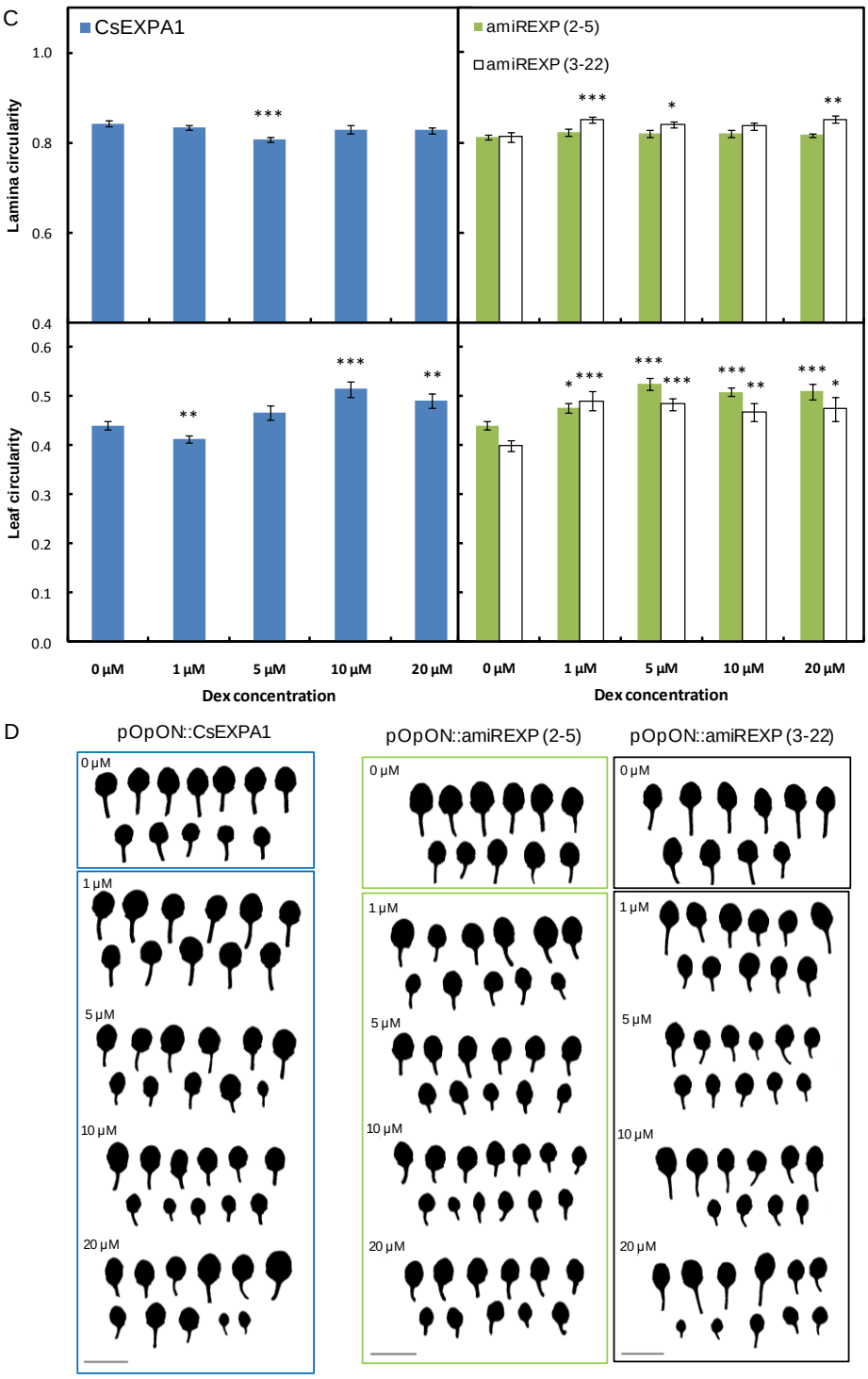

Figure 4.11. Comparison of leaf 6 (A) lamina and (B) petiole parameters of 27 DAS pOpON::CsEXPA1, pOpON::amiREXP (2-5) and (3-22) transformant plants grown on medium supplemented with different concentrations of Dex. (C) Morphometric comparison of leaf 6 lamina and leaf circularity with (D) their respective silhouettes. Values are means ± SE (n = 10-13). One-way ANOVA, Tukey tests compared to 0 µM control *p<0.05, **p<0.01, ***p<0.001.

The data described above indicate that altered expansin gene expression led to a change in leaf lamina and petiole growth. To investigate the cellular basis of these growth responses, I performed histological analysis based on the palisade mesophyll cells between induced and non-induced leaves (Table 4.2). Representative images of the pOpON::amiREXP leaves and petioles are shown in Figure 4.12 and 4.13. Considering the leaf tissue (4.12A and 4.13A), there was no obvious difference in cell size and cell number in the adaxial epidermis or in the mesophyll, despite a slight increase in mesophyll cell size (Table 4.2). Similarly, visual analysis of petiole tissue did not reveal any striking histological difference between control and 10 µM Dex-induced pOpON::amiREXP lines (4.12B and 4.13B), despite the significant decrease in petiole length and width (Figure 4.11B). This could partly explained by the reduced number of cell files in both palisade mesophyll and adaxial epidermal layers.

Analysis of the cellular phenotype of pOpON::CsEXPA1 leaf lamina tissue (Figure 4.14A) also did not indicate any massive change in cell size and shape, but a significant increase in cell size across the cell width was measured despite the significant decrease in overall petiole length after induction with 10 µM Dex (Figure 4.14B). However, this significant increase in petiole mesophyll cell size was accompanied by a significant decrease in the number of cell files in both the mesophyll and adaxial epidermal layers. Furthermore, the adaxial epidermal cell length was significantly reduced (Table 4.2).

Table 4.2. Histological analysis of the cell size and cell number at the middle region of mesophyll layer of leaf 6 lamina and petiole harvested on 27 DAS from transformant plants induced with different concentrations of Dex since sowing. At least 28 and 20 systematically sampled mesophyll cells were measured for lamina and petiole respectively. The values shown are mean ± SE, N = number of biological replicates. Bold and italicised numbers indicate statistical significance at $p<0.05$ in 2-sample t-tests using mean values (cell size) or Mann-Whitney U-tests (cell number/ cell file).

pOpON transformant lines	Dex concentration (μM)	Lamina mesophyll (n = 28, N = 6)						Petiole mesophyll (n = 20)				No. of cell file (N = 6)	
		Cell area (μm^2)	Cell width (μm)	Cell length (μm)	Transverse cell no.¥	Longitudinal cell no.¥	N	Cell area (μm^2)	Cell width (μm)	Cell length (μm)	Cell no. along cell file¤	Palisade mesophyll layer§	Adaxial epidermal layer§
pOpON::amiREXP (2-5)	0	532 ± 42	27 ± 1.0	26 ± 1.0	16 ± 0.8	14 ± 0.4	6	621 ± 57	25 ± 0.7	32 ± 2.0	19 ± 1.3	20 ± 0.6	25 ± 0.7
	10	672 ± 71	30 ± 1.3	30 ± 1.5	14 ± 0.8	13 ± 1.0	5	734 ± 70	29 ± 2.1	30 ± 2.1	18 ± 2.0	***17 ± 0.6***	***20 ± 0.6***
pOpON::amiREXP (3-22)	0	605 ± 24	28 ± 0.7	29 ± 0.7	17 ± 0.7	13 ± 0.5	4	620 ± 46	24 ± 1.0	33 ± 1.7	18 ± 0.8	19 ± 0.3	24 ± 0.5
	5	598 ± 19	29 ± 0.5	28 ± 0.5	16 ± 0.8	14 ± 0.5	5	654 ± 59	28 ± 1.4	30 ± 1.3	19 ± 1.3	***16 ± 0.3***	***21 ± 0.5***
pOpON::CsEXPA1	0	544 ± 32	27 ± 0.8	27 ± 0.8	19 ± 1.0	15 ± 0.7	5	666 ± 37	25 ± 1.1	35 ± 1.1	18 ± 1.0	20 ± 0.8	25 ± 0.6
	1	590 ± 36	27 ± 0.9	29 ± 1.0	19 ± 0.6	14 ± 0.3	6	669 ± 46	25 ± 1.0	34 ± 1.7	20 ± 0.8	19 ± 0.4	26 ± 0.5
	10	657 ± 54	30 ± 1.2	30 ± 1.4	17 ± 0.3	14 ± 0.6	5	***873 ± 31***	***31 ± 1.0***	36 ± 1.2	18 ± 0.8	***16 ± 0.6***	***22 ± 0.6***

¥ Cell number was counted within the area captured by the micrograph (268 μm x 356 μm)
¤ Cell number was counted along the leaf-length direction on the third cell file from the margin of petiole (536 μm length)
§ The number of cell file was counted from petiole within the area captured by the micrograph (536 μm x 712 μm)

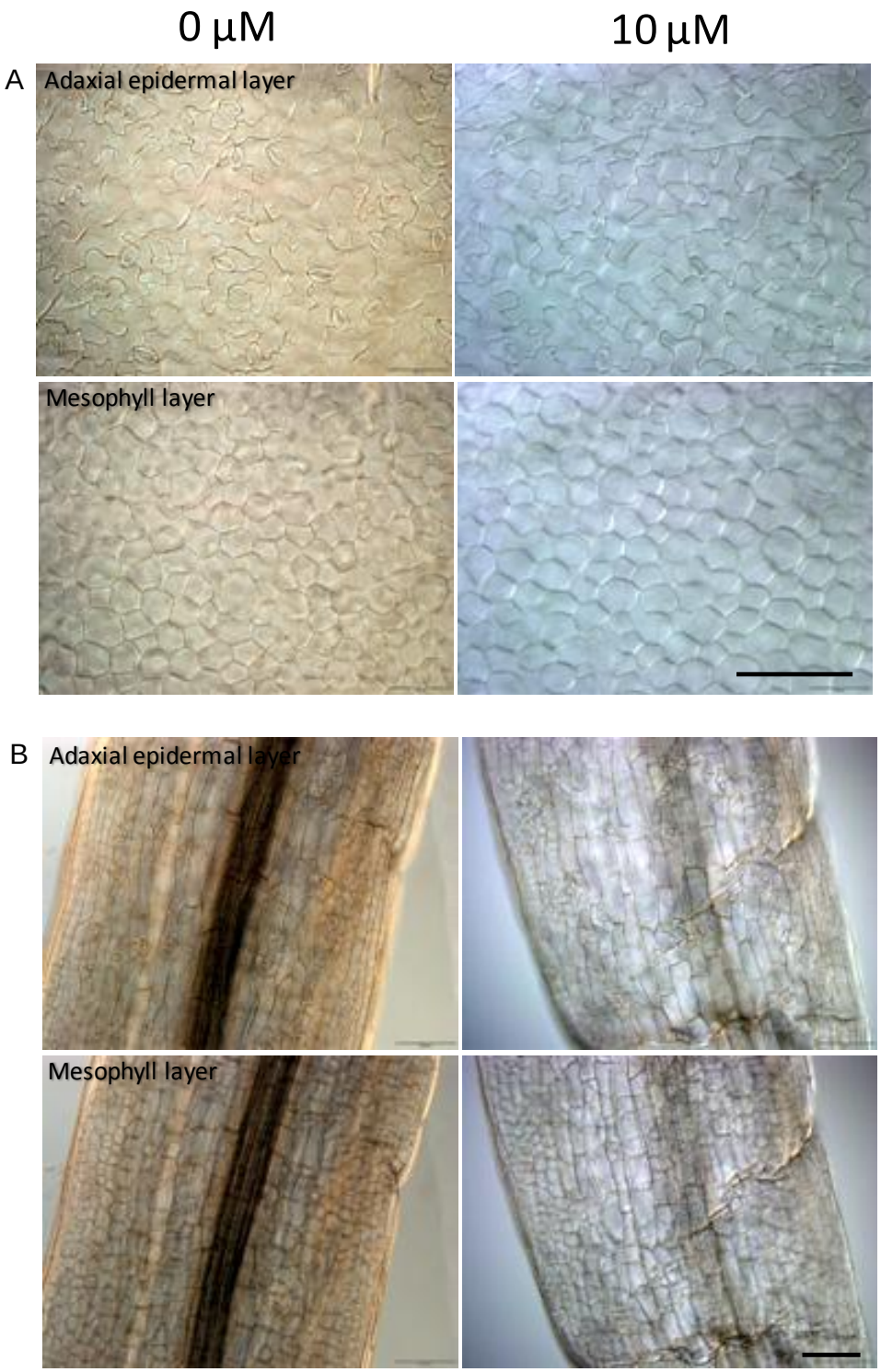

Figure 4.12. Cellular comparison of leaf 6 (A) middle lamina and (B) middle petiole showing representative images from pOpON::amiREXP (2-5) transformant plants grown on 0.5x MS agar medium supplemented with DMSO 0.1% v/v (0 µM) or 10 µM Dex. Scale bars = 100 µm.

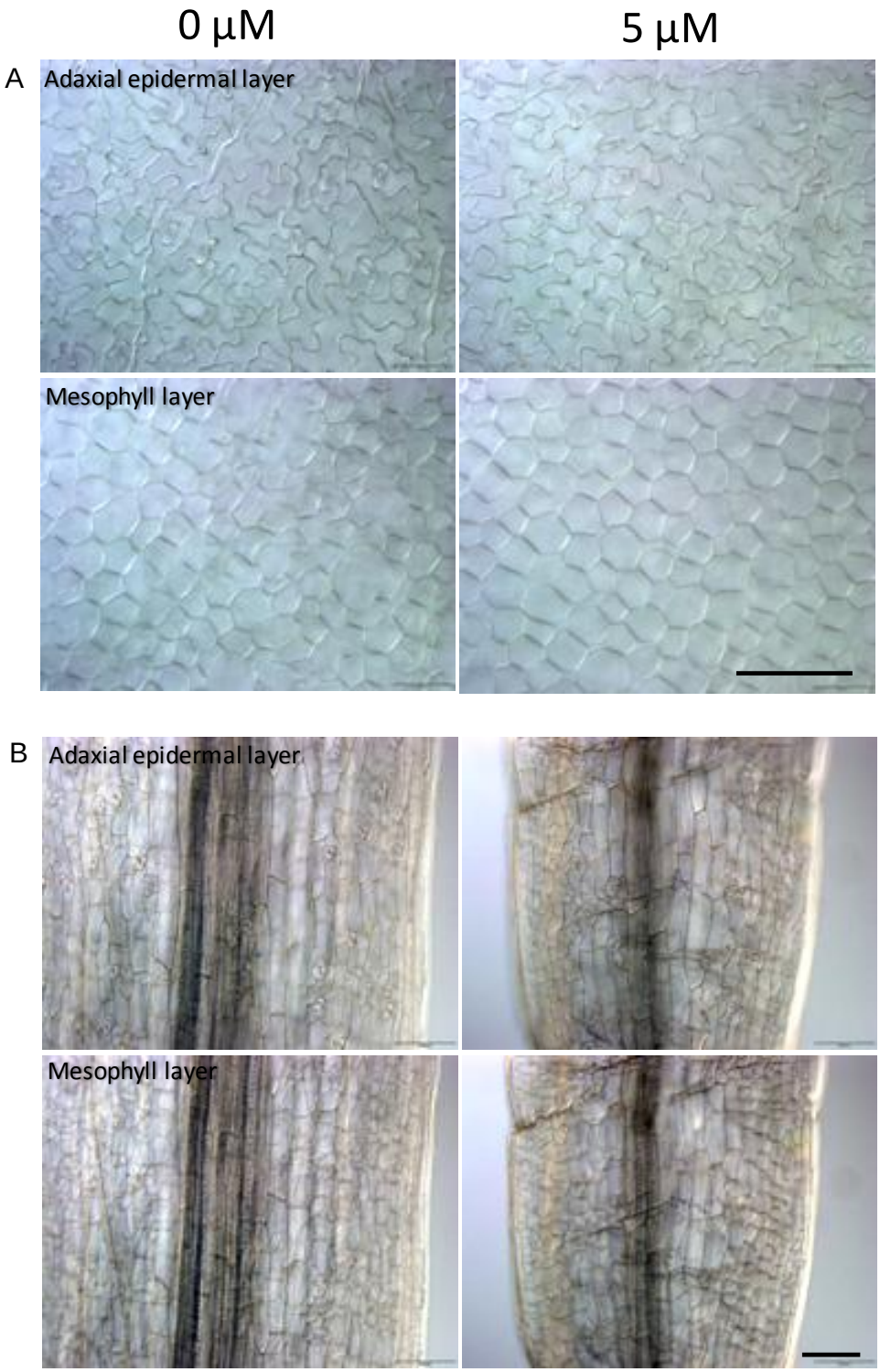

Figure 4.13. Cellular comparison of leaf 6 (A) middle lamina and (B) middle petiole showing representative images from pOpON::amiREXP (3-22) transformant plants grown on 0.5x MS agar medium supplemented with DMSO 0.1% v/v (0 µM) or 5 µM Dex. Scale bars = 100 µm.

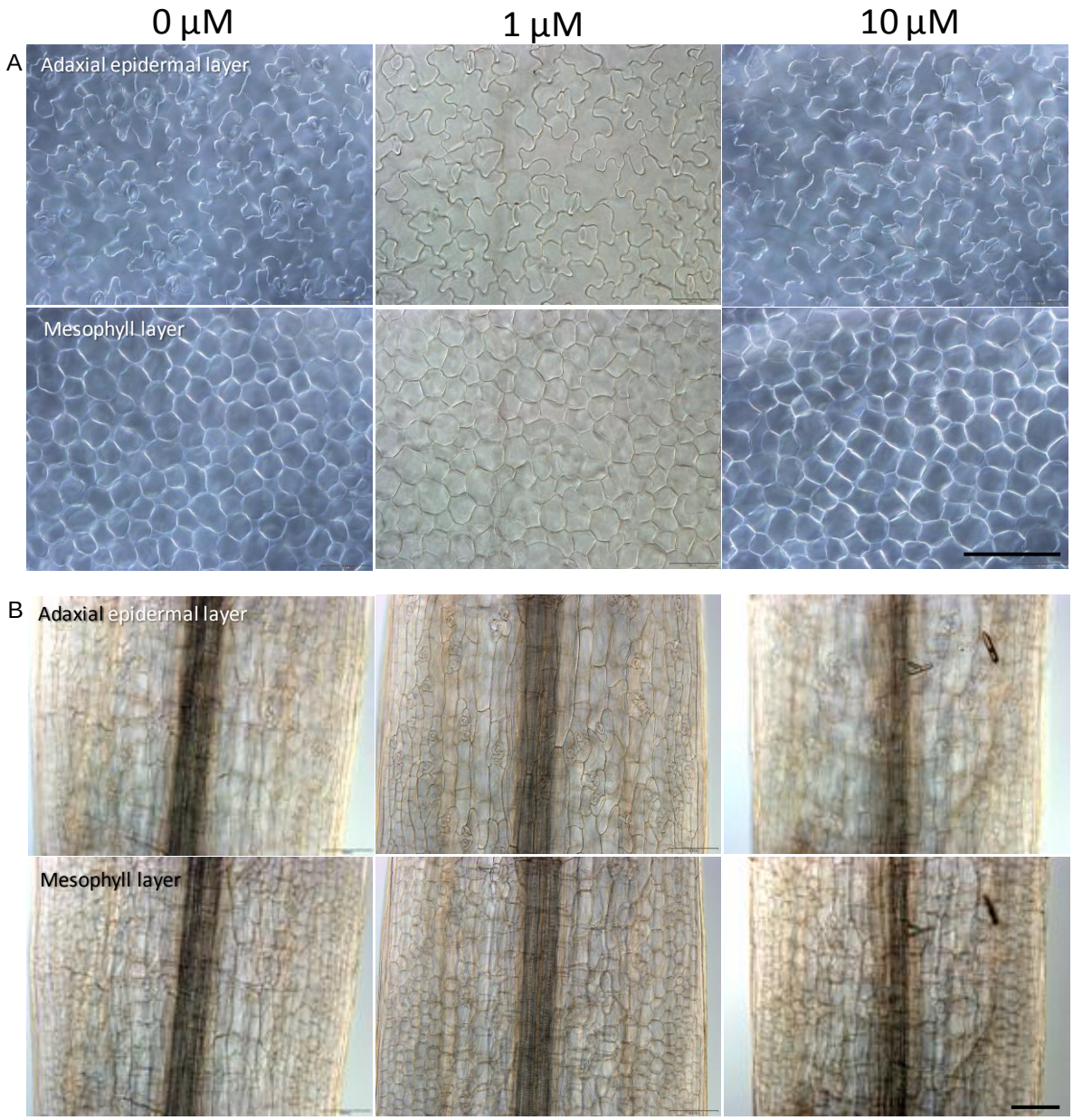

Figure 4.14. Cellular comparison of leaf 6 (A) middle lamina and (B) middle petiole showing representative images from pOpON::CsEXPA1 transformant plants grown on 0.5x MS agar medium supplemented with DMSO 0.1% v/v (0 µM), 1 µM or 10 µM Dex. Scale bars = 100 µm.

The growth dynamics of leaf 6 was studied by measuring leaf width over time to further investigate the response of leaf 6 to the altered expansin expression induced in the pOpON::amiREXP and pOpON::CsEXPA1 lines (Figure 4.15). As shown in Figure 4.15A, leaf width differed significantly in the induced pOpON::amiREXP lines relative to the control treated leaves only towards the end of leaf growth (22 DAS). When the leaf growth rate is considered (both absolute and relative), then both the induced and control pOpON::amiREXP lines show a similar pattern, the main difference being that the growth rates for the induced leaves are generally lower than that of the control. This difference is most marked over the latter part of the growth curve (18 DAS and later), again suggesting that the suppression of expansin gene activity influences leaf growth mainly over the later phase of development.

When the time course of petiole extension is considered (Figure 4.15B), a similar pattern emerges for the pOpON::amiREXP lines, i.e. the decrease in length and extension rate occurs predominantly towards the end of extension period. However, it is noticeable that during the early phase of petiole extension (around 15 DAS), the length and extension rate of the induced pOpON::amiREXP lines was greater than the controls. Similar growth dynamics were also shown by the induced pOpON::CsEXPA1 plants with decreased growth occurred mainly over the latter period of development and there was an early phase when the induced tissue had a tendency towards a higher rate of extension (Figure 4.15B).

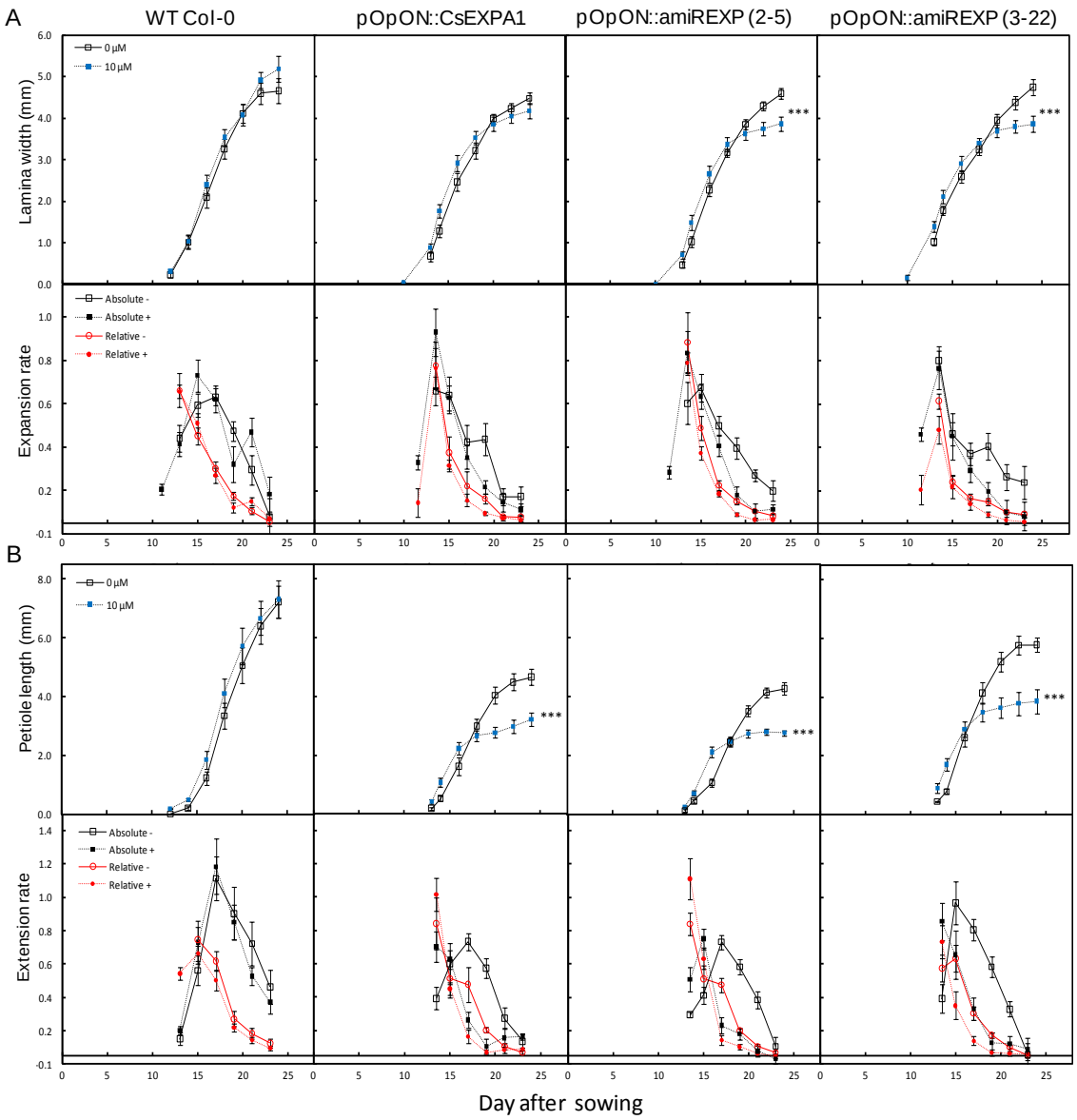

Figure 4.15. Comparison of (A) the expansion of leaf 6 lamina width and (B) the extension of leaf 6 petiole length over time of Col-0 wild-type, pOpON::CsEXPA1, pOpON::amiREXP (2-5) and pOpON::amiREXP (3-22) transformant plants grown on 0.5x MS agar medium supplemented with DMSO 0.1% v/v (0 µM / -) or 10 µM Dex (10 µM / +). The unit for absolute expansion/ extension rate is mm day^{-1}, and the unit for relative expansion/ extension rate is mm mm^{-1} day^{-1}. Values are means ± SE (n = 12). Two-sample t-tests, ***p<0.001.

The experiments described above involved the supply of the Dex inducer throughout the growth period from germination onwards. Apart from the repressive effects on rosette and leaf growth, the number of vegetative leaves and the time to flowering were also affected. Figure 4.16 shows that there is a significant reduction in the number of vegetative leaves and advanced time to flowering with shortened duration between floral transition to bolting in pOpON::amiREXP plants at concentrations as low as 1 μM Dex. A similar response was observed in pOpON::CsEXPA1 plants but mainly when induced at 5 μM Dex or greater (Figure 4.16). Interestingly, the time when there was significant difference in leaf number (16 DAS) coincided with the peak of rosette expansion (Figure 4.9-10). The results suggested that there might be a differential response to altered expansin expression depending on the developmental phase of the responding leaf, and at the whole-plant level. This raises the question on whether the repressive effect on leaf expansion might be indirectly due to the advanced time to flowering, as it has been shown previously to affect leaf growth (Cookson *et al.*, 2007).

To address this question and further investigate the possibility of developmental-phase dependent effects, I performed a series of experiments in which plants were germinated under non-inductive conditions and then transferred to inductive conditions at particular time points in development.

I first focussed on the pOpON::amiREXP lines and on the possibility that suppression of expansin gene expression during the latter part of leaf development might be sufficient to induce a decrease in leaf growth. Plants were germinated and grown under non-inducing conditions until 14 DAS (approximately the mid-point of growth of leaf 6), then transferred to either Dex-containing or control medium. Plants were then left for a further 10 days before analysis (Figure 4.17-18). Considering first the measurements on lamina length, width and area, no immediate trend was obvious, although one line did show a consistent decrease in lamina length (Figure 4.17A). Petiole length appeared to be more dramatically affected by induction, with the younger leaves (leaf 7 and 8) showing a significant repression of growth in both lines (Figure 4.17-18).

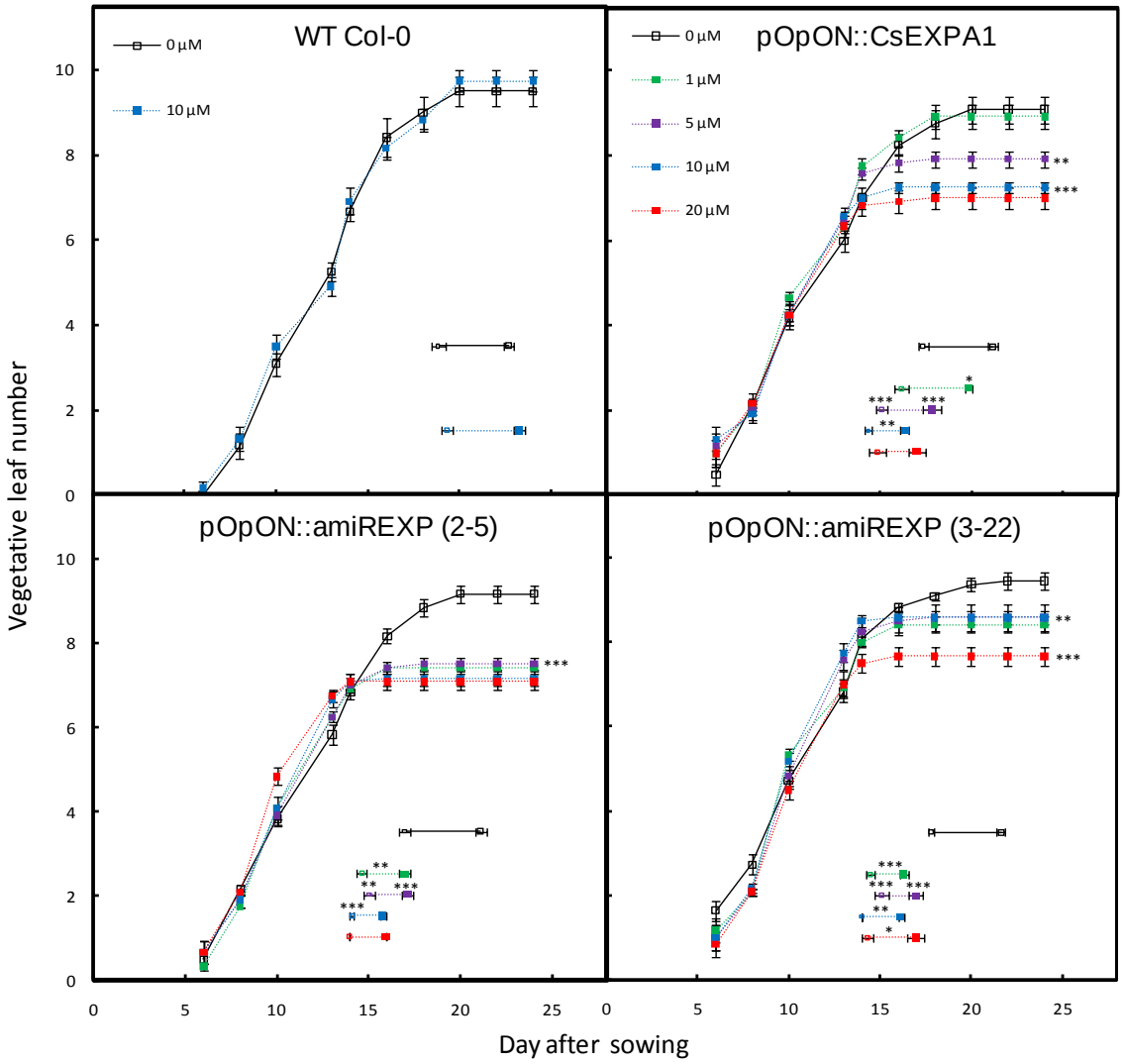

Figure 4.16. Changes of vegetative leaf number over time (6 to 24 day after sowing) of Col-0 wild-type, pOpON::CsEXPA1, pOpON::amiREXP (2-5) and (3-22) plants under different Dex concentrations. Number of visible leaves (> 1 mm width) from 12 individual plants of each line (mean ± SE), grown on half-strength MS agar medium supplemented with different concentrations of Dex or DMSO 0.1% (0 µM), were counted. Lower right corner showing the day when inflorescence bud becomes visible on shoot apex (smaller open symbol), the day of bolting (larger closed symbol) and the duration between inflorescence transition and bolting (connecting horizontal line). Mann-Whitney tests or One-way ANOVA, Tukey tests compared to 0 µM control *p<0.05, **p<0.01, ***p<0.001, asterisks were annotated only for the first instances when the difference become significant or when the significance level changes and left out subsequently for clarity.

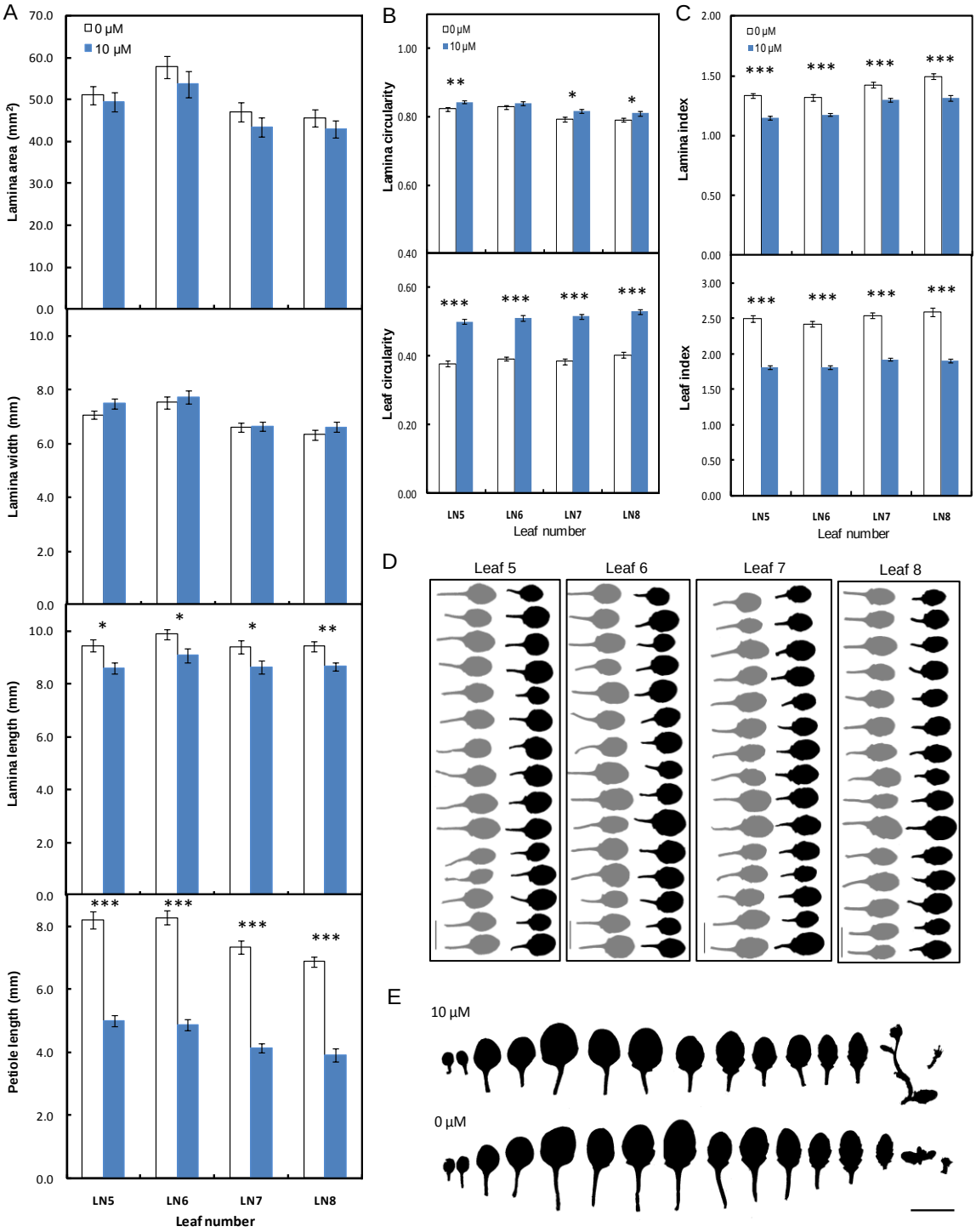

Figure 4.17. Staged-transfer induction of pOpON::amiREXP (2-5) transformant plants. (A) Comparison of leaf 5 to leaf 8 of induced (10 µM) and non-induced (0 µM) plants transferred on 14 DAS and harvested at 24 DAS. Morphometric comparison of leaf 5 to leaf 8 of induced and non-induced plants based on circularity (B) or length:width ratio (C). Values are means ± SE (n = 15). Two-sample t-tests, *p<0.05, **p<0.01, ***p<0.001. (D) Light-(0 µM) and dark-shaded (10 µM) silhouettes of analysed leaves. (E) Silhouettes of representative dissected induced (10 µM) and non-induced (0 µM) plants. Scale bars = 10 mm.

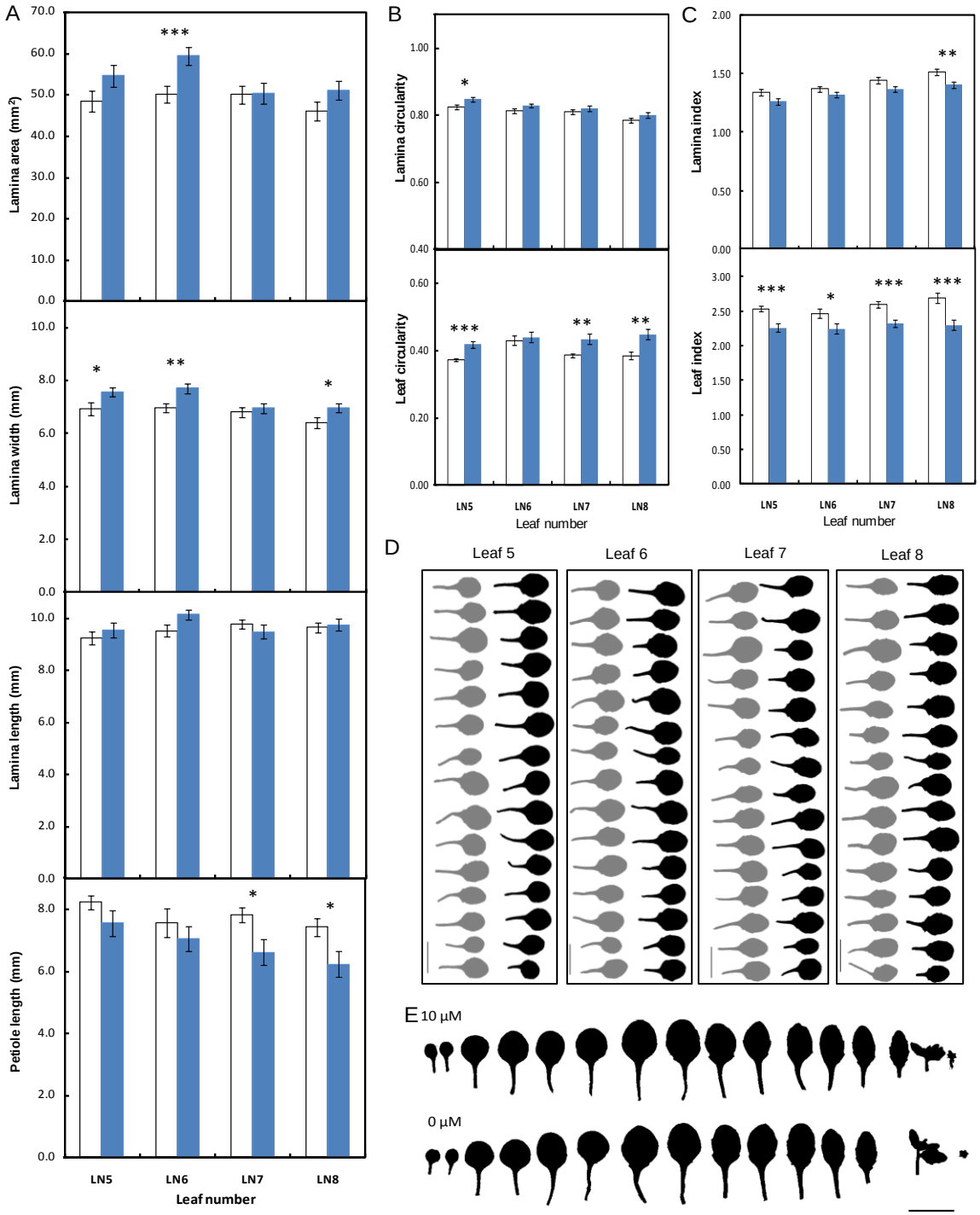

Figure 4.18. Staged-transfer induction of pOpON::amiREXP (3-22) transformant plants. (A) Comparison of leaf 5 to leaf 8 of induced (10 µM) and non-induced (0 µM) plants transferred on 14 DAS and harvested at 24 DAS. Morphometric comparison of leaf 5 to leaf 8 of induced and non-induced plants based on circularity (B) or length:width ratio (C). Values are means ± SE (n = 15). Two-sample t-tests, *p<0.05, **p<0.01, ***p<0.001. (D) Light-(0 µM) and dark-shaded (10 µM) silhouettes of analysed leaves. (E) Silhouettes of representative dissected induced (10 µM) and non-induced (0 µM) plants. Scale bars = 10 mm.

When leaf circularity was calculated, a more consistent picture emerged, with almost all leaves showing an increased circularity after induction of pOpON::amiREXP from 14 DAS to 24 DAS (Figure 4.17B, 4.18B). The same applied for the leaf index (leaf length:width ratio). The exposure of the younger leaves (leaf 7 and 8) to the inducer would have encompassed a broader phase of development, even before their initiation. However, for the older leaves examined in this experiment (leaf 5 and 6), Dex induction would have been restricted to the later phase of leaf development, yet a growth repression and shape change response was still observed. Thus the data indicate that repression of expansin gene expression during the later stage of leaf growth is sufficient to alter leaf shape.

With respect to the pOpON::CsEXPA1 plants a more detailed transfer experiment was performed in which, following germination under non-inducing conditions, plants were transferred at particular time points to inducing or control medium and leaf measurements taken after a further 48h. These data indicate that with respect to lamina width, length and area, as well as petiole length, a significant repression of growth was only observed in the plants transferred at 22 DAS (red box in Figure 4.19A). Representative leaves are shown in Figure 4.19B. When the absolute and relative width extension rates are plotted against time, it can be seen that transfer at 22 DAS spanned across a second peak of growth rate (Figure 4.19C).

In a further experiment, pOpON::CsEXPA1 plants were grown under non-inducing conditions and transferred to induction medium at different time points and left to grow until analysis on 24 DAS. Transfer on 11 DAS corresponds to the earliest stages of leaf 6 development whereas transfer on 18 DAS was after the peak of growth (Figure 4.15). Despite a greater tendency for decreased leaf growth, there was no consistent shift in leaf lamina parameters when transferred earlier (Figure 4.20). However, the effects on petiole length of different leaf number were intriguing. Petioles of all leaf number were reduced when transferred on 11 DAS, while only the petioles of leaf 5 and 6 were reduced on 18 DAS transfer. This suggests a gradient of effect on petiole length depending on the extent of petiole elongation. These data suggest that there is a phase during later leaf growth which is sensitive to the alteration in expansin gene expression.

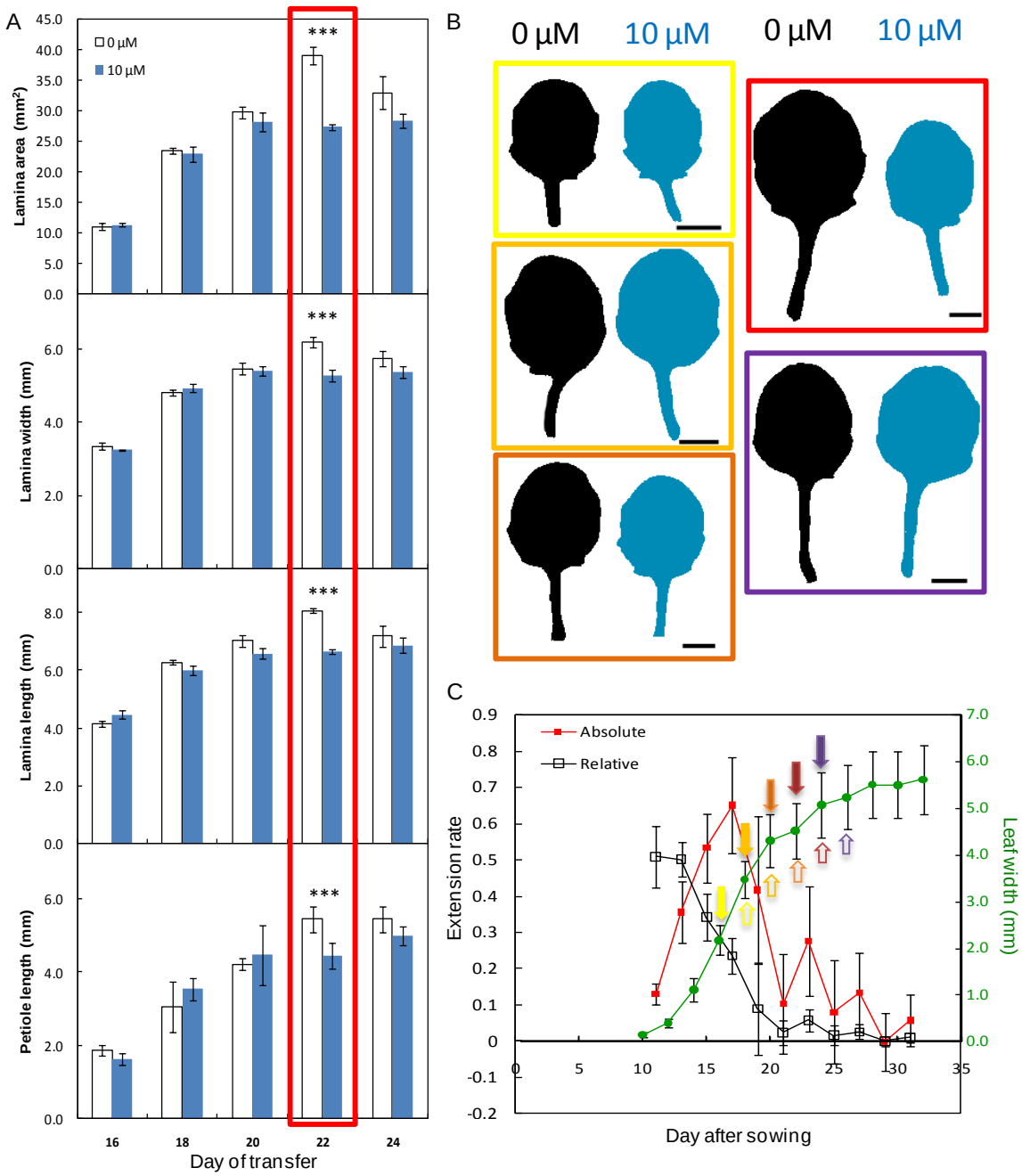

Figure 4.19. T3 pOpON::CsEXPA1 staged-transfer induction. (A) Comparison of leaf 6 harvested from plants transferred to 0.5x MS agar medium supplemented with DMSO 0.1% (0 µM) or 10 µM Dex for 48 hours on different days after sowing. Mean values ± SE (n = 3). Two-sample t-tests, ***p<0.001. (B) Silhouettes of induced and non-induced leaf 6. Border colours correspond to the open arrows in C. (C) Growth analysis of T3 pOpON *CsEXPA1* leaf 6. Green line indicates the change in the leaf width over time, red line represents the absolute growth rate (mm^{-1} day^{-1}), and black line for the relative growth rate (mm mm^{-1} day^{-1}). Values are mean ± SD (n = 42 of 10-11 plants from 4 independent plates measured non-destructively under stereomicroscope from 10 to 32 DAS). Colour-coded solid and open arrows, indicate the day of transfer and harvest respectively. Scale bars = 2 mm.

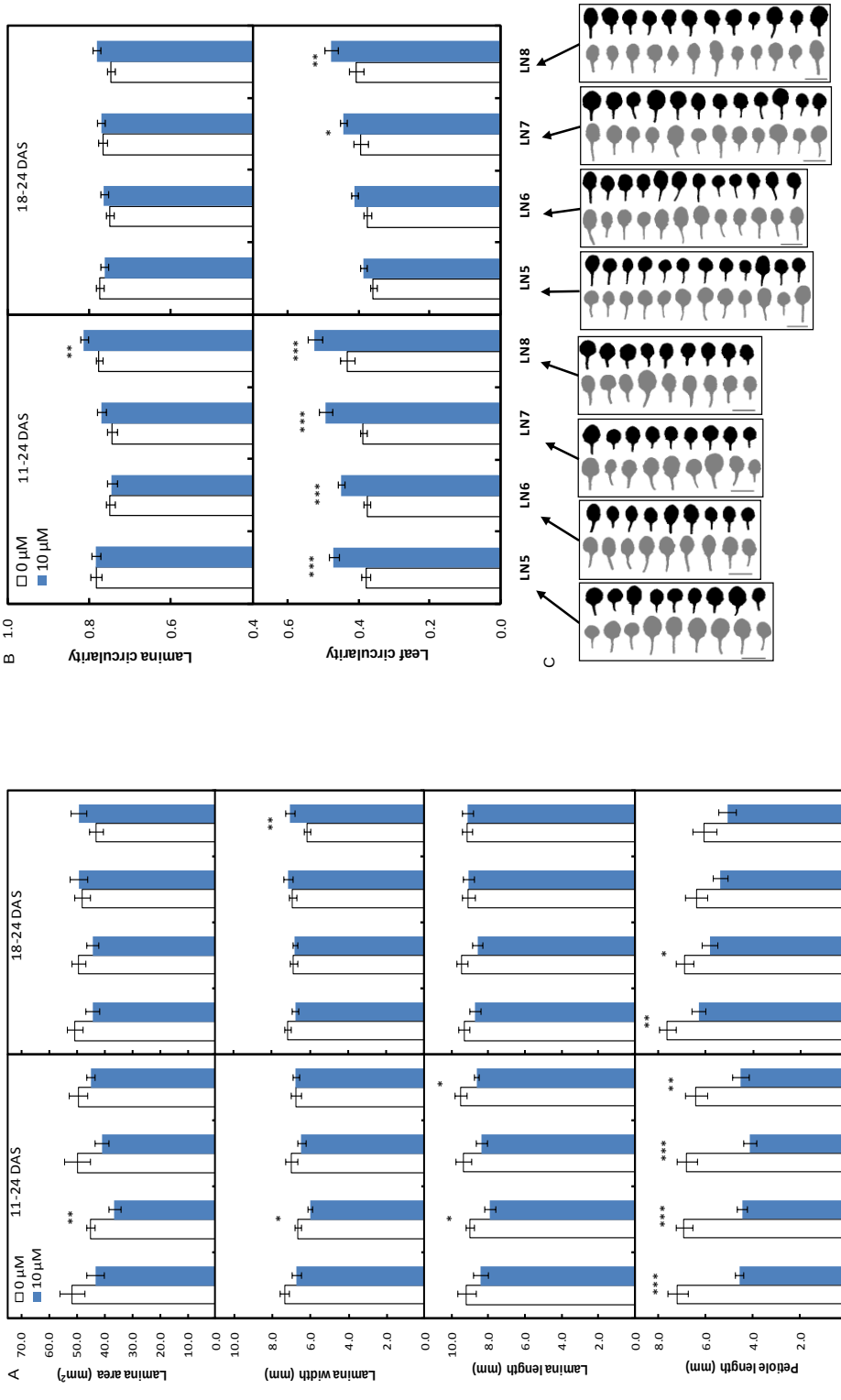

Figure 4.20. Staged-transfer induction of pOpON::CsEXPA1. (A) Comparison of leaf parameters from plants of equivalent developmental stages which were transferred onto 0.5x MS agar medium supplemented with DMSO 0.1% v/v (0 µM) or 10 µM Dex on 11 DAS (n = 9) or 18 DAS (n = 12) and harvested at 24 DAS. Values are means ± SE. Two-sample t-tests, *p<0.05, **p<0.01, ***p<0.001. (B) Morphometric comparison of leaves as per A. (C) Light-(0 µM) and dark-shaded (10 µM) silhouettes of respective leaf number were indicated by the arrows.

4.2.3 Localised manipulation of expansin gene expression

In the experiments described above the Dex inducer was supplied in a temporally controlled fashion through the medium so that all parts of the plant were induced (Figure 4.4-5). To explore the possibility of using the pOpON system to provide some degree of spatial control on gene induction, I performed a series of experiments in which the inducer was loaded into Sephadex bead (G100), which were then applied to the surface of developing leaves. The aim was to investigate whether such localised inducer application was sufficient to lead to localised induction of the constructs in the pOpON::amiREXP and pOpON::CsEXPA1 plants.

In the first experiment I used the first pair of true leaves as the target for localised gene induction to investigate the effects of manipulating expansin expression level at different phases of leaf development (Figure 4.21). First leaf pairs are easiest to access and generally grow in symmetry making them ideal for pairwise comparison. 20 μM Dex droplets were applied to one of the leaf pair on day 6, day 8 or day 12 after sowing, corresponding to the proliferative, expansive and maturing stage of first leaf development, and allowed to grow to maturation on 20 DAS before analysis. GUS histochemistry indicated that this approach allowed restriction of gene expression to the target leaf (Figure 4.21B). Analysis of lamina width, length and area, as well as petiole length indicated no significant difference in these parameters between the induced and non-induced leaves for either the WT control or pOpON::CsEXPA1 plants (Figure 4.21A). For the pOpON::amiREXP lines there was a significant decrease ($p<0.05$) in final leaf area of the induced leaf relative to the non-induced only when the induction was performed on day 8 (Figure 4.21A). With respect to petiole length, decrease in length was recorded only in one of the pOpON::amiREXP lines on day 8 induction.

Following from the first leaf-pair experiments which indicated a period of plant or leaf sensitivity towards the manipulation of expansin levels, shoot apex induction experiments were performed, in which droplets of 20 μM Dex were applied onto shoot apices at 12 DAS, resulting in the induction of leaves at various stages of development (Figure 4.22). During the 8 days from treatment to harvest, 4 to 5 leaves would have been initiated in addition to the 5 or 6 leaves which were present on day 12 (Figure 4.16). Hence, leaf numbers represent the different developmental

stages of exposure to changes in expansin levels. On 12 DAS leaf 1 and 2 were maturing while leaf 3 to 5 were growing towards maturation, leaf 6 was just emerging and leaf 7 was undergoing under initiation. The results appeared to support a developmental phase-dependent effect of expansin on leaf growth such that significant differences in lamina areas were confined to leaf 6 and 7, whereas petiole lengths of leaf 3 to 6 or 7 were reduced (Figure 4.22A). There was no effect on leaf 8, perhaps due its early stage in development in terms of lamina expansion and petiole growth. Furthermore, it appeared that lamina length was more affected in pOpON::amiREXP than pOpON::CsEXPA1 transformant plants.

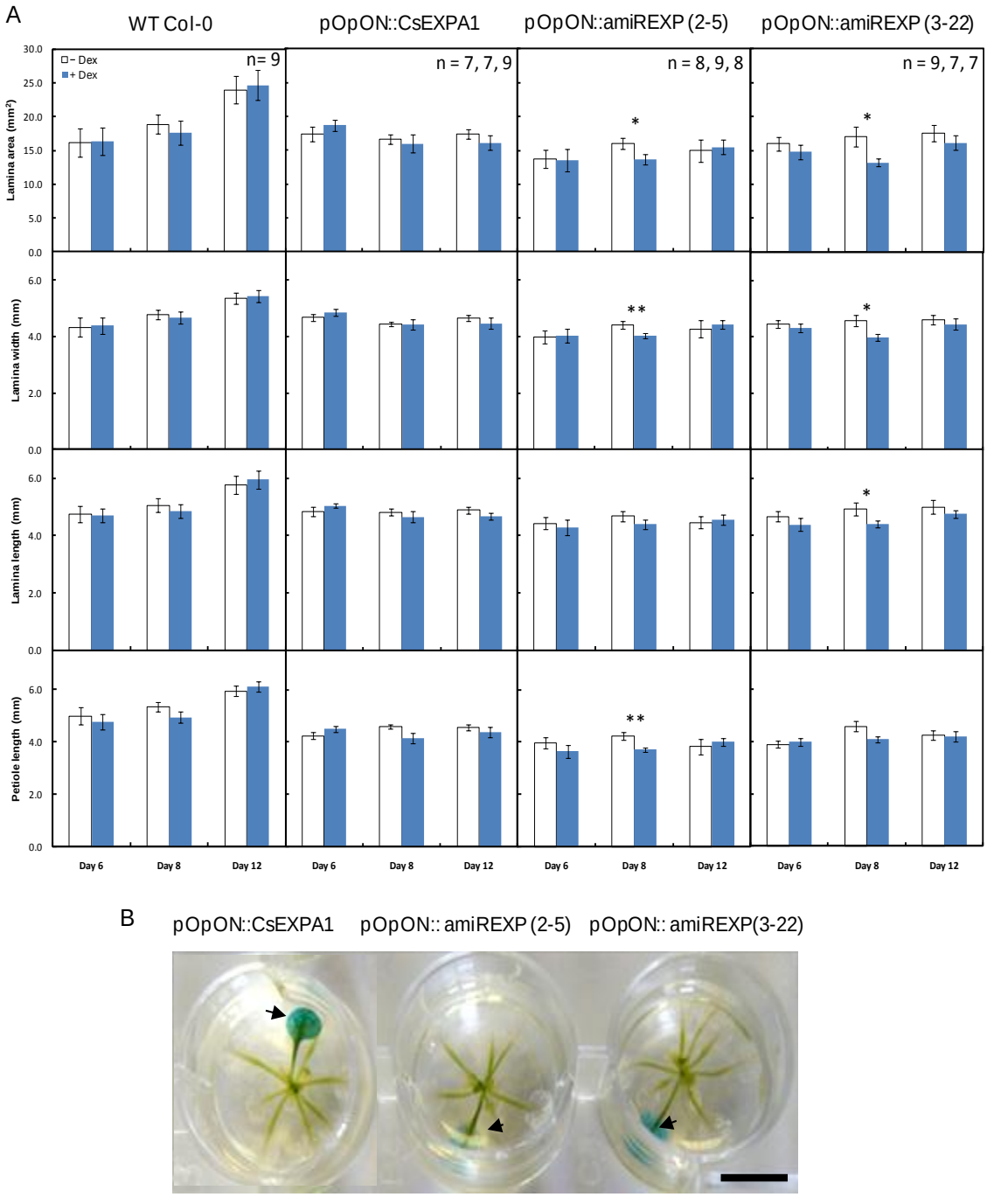

Figure 4.21. First leaf-pair induction experiments. Pairwise comparison of induced [+Dex] and non-induced [-Dex] first leaf pair harvested from Col-0 wild-type, pOpON::CsEXPA1, pOpON::amiREXP (2-5) and pOpON::amiREXP (3-22) plants on 20 DAS. Treatments were given at three time points: 6, 8 and 12 day after sowing. Values are means ± SE (n as indicated at top right corners). Paired t-tests, *p<0.05, **p<0.01. (B) GUS staining showing stringent induction to one of the first leaf pair as intended. Scale bars = 10 mm.

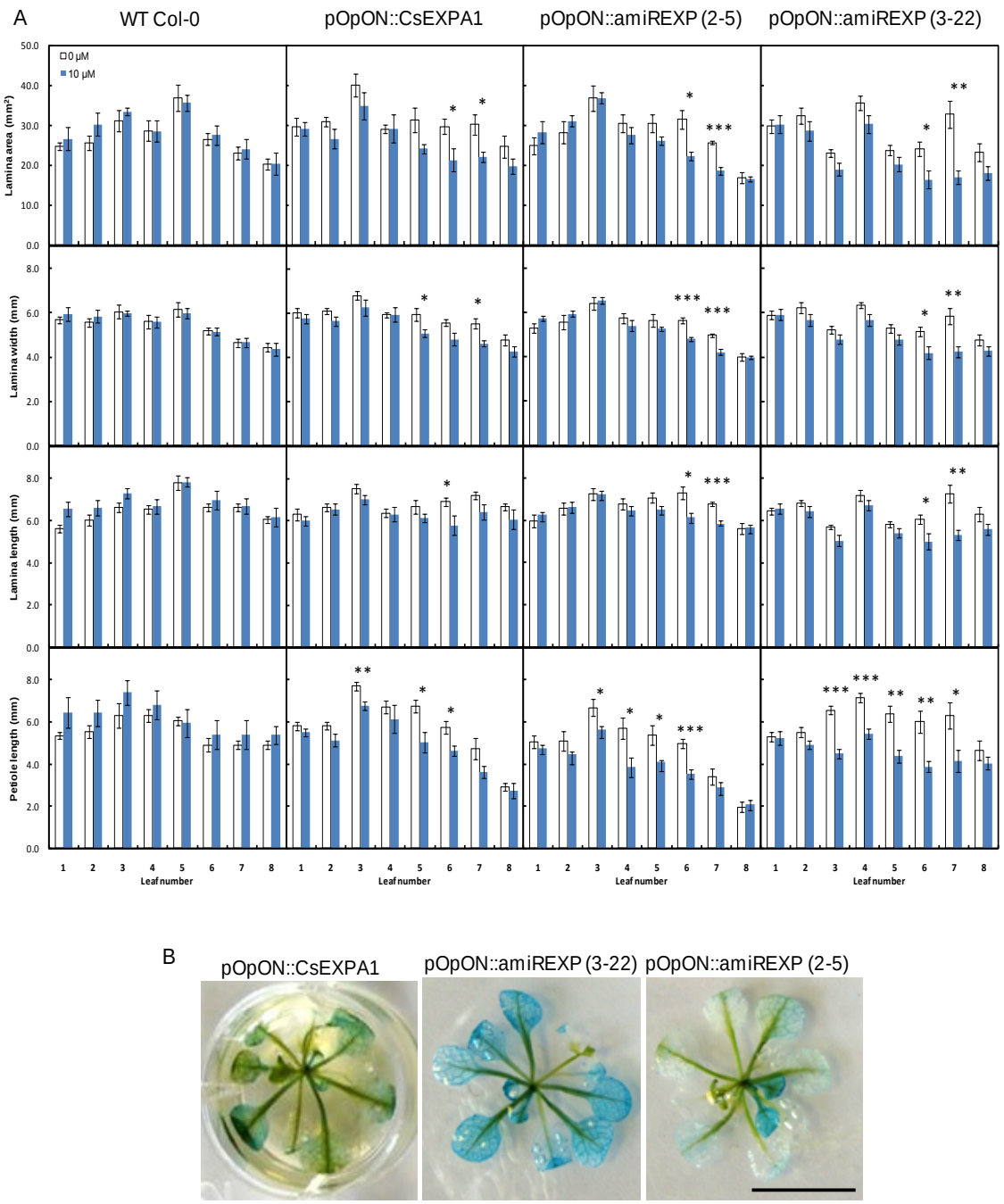

Figure 4.22. Shoot apex induction experiments. (A) Comparison between induced (10 µM) and non-induced (0 µM) individual leaves dissected from Col-0 wild-type, pOpON::CsEXPA1, pOpON::amiREXP (2-5) and pOpON::amiREXP (3-22) plants 8 days after treatment (12 to 20 DAS). Induced leaf samples were validated by GUS staining. Values are means ± SE (n = 5-7) (B) Representative GUS stained and partially bleached plants. Scale bars = 10 mm.

To confirm the results from whole-plant transfer induction of pOpON::amiREXP plants in which suppression of expansin gene expression during a later phase of leaf development was sufficient to lead to a decrease in leaf growth, I performed localised leaf 6 induction. Figure 4.23A shows that localised expression was enough to repress leaf growth relative to mock-treated leaves on both 14 and 16 DAS. Furthermore, the data indicate that lamina width was only sensitive to expansin suppression on 14 DAS as compared to lamina length. Conversely, petiole length was more sensitive when induced at later stages. However, these differences were only statistically significant in one of the pOpON::amiREXP lines consistent with previous results (Figure 4.17-18). Histochemical analysis of GUS expression confirmed that this localised induction of the pOpON::amiREXP leaves did lead to restriction of gene expression to the targeted leaf (Figure 4.23B).

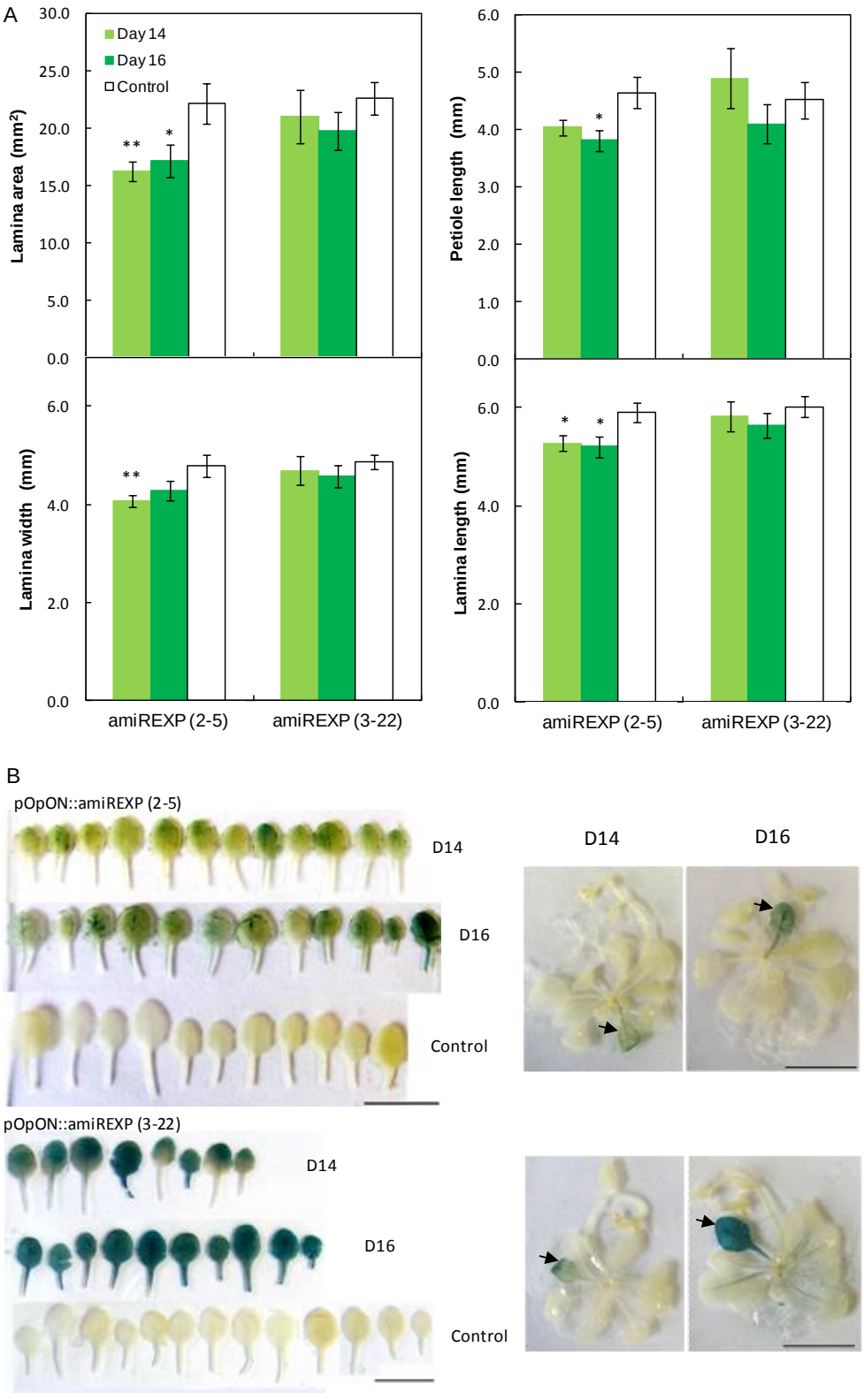

Figure 4.23. Legend overleaf.

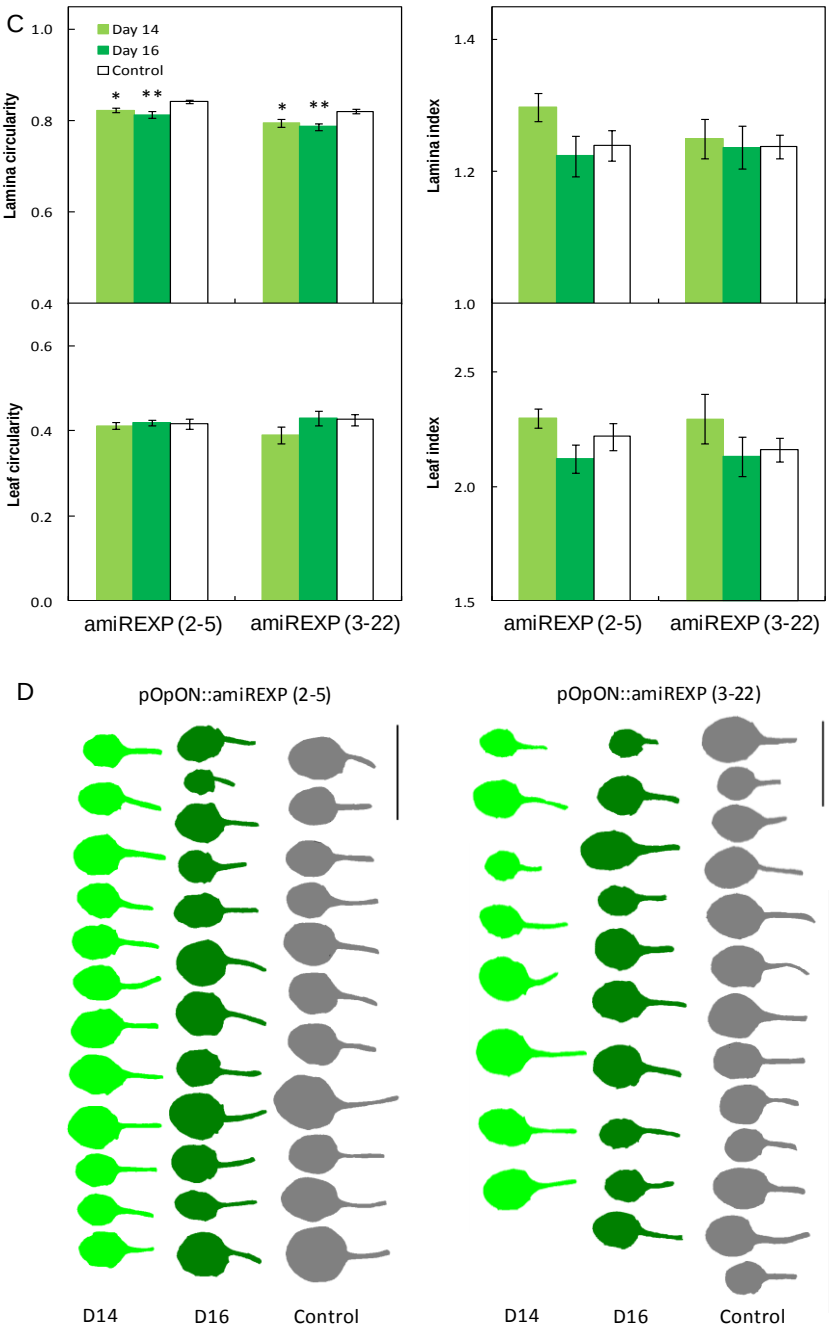

Figure 4.23. Leaf 6 induction of pOpON::amiREXP transformant plants. (A) Comparison of leaf parameters of induced and non-induced leaf 6. Droplets (2-5 µL) of 20 µM Dex or DMSO 0.1% v/v (control) were applied onto the leaf blades at 14 or 16 DAS. Leaves were harvested on 24 DAS. Values are means ± SE (n = 8-15). One-way ANOVA, Tukey tests compared to control *p<0.05, **p<0.01, ***p<0.001. (B) GUS staining of treated plants and dissected leaf 6. Arrows pointing at induced leaf 6 from day 14 and day 16 induction. (C) Morphometric comparison of induced and non-induced leaf 6, as per A. (D) Analysed leaf silhouettes. Scale bar = 10 mm.

To investigate whether the spatial resolution of gene induction could be increased, I performed a series of experiments in which the Dex-loaded Sephadex was manipulated onto different regions of the surface of leaves at different stages of development. Due to time restrictions, this series of experiments was only performed on the pOpON::CsEXPA1 plants. The results are shown in Figure 4.24. Different portions of the leaves were induced (as indicated) and GUS histochemistry performed 48h and 96h later. The data indicate that localised GUS induction could be achieved in a wide range of leaves and in a number of different positions on the leaf with high efficiencies, but proved to be more difficult with younger leaves due to the smaller area. The leaves from the experiment described in Figure 4.24 were analysed for leaf shape using the LeafProcessor tool (Backhaus *et al.*, 2010). This allows comparison of different leaf sectors to explore potential differences in different parameters such as sectorial area. Analysis of the sectorial areas resulting from local induction of the pOpON::CsEXPA1 construct did not reveal any significant differences between induced and non-induced sectors (Table 4.3, Table 4.4).

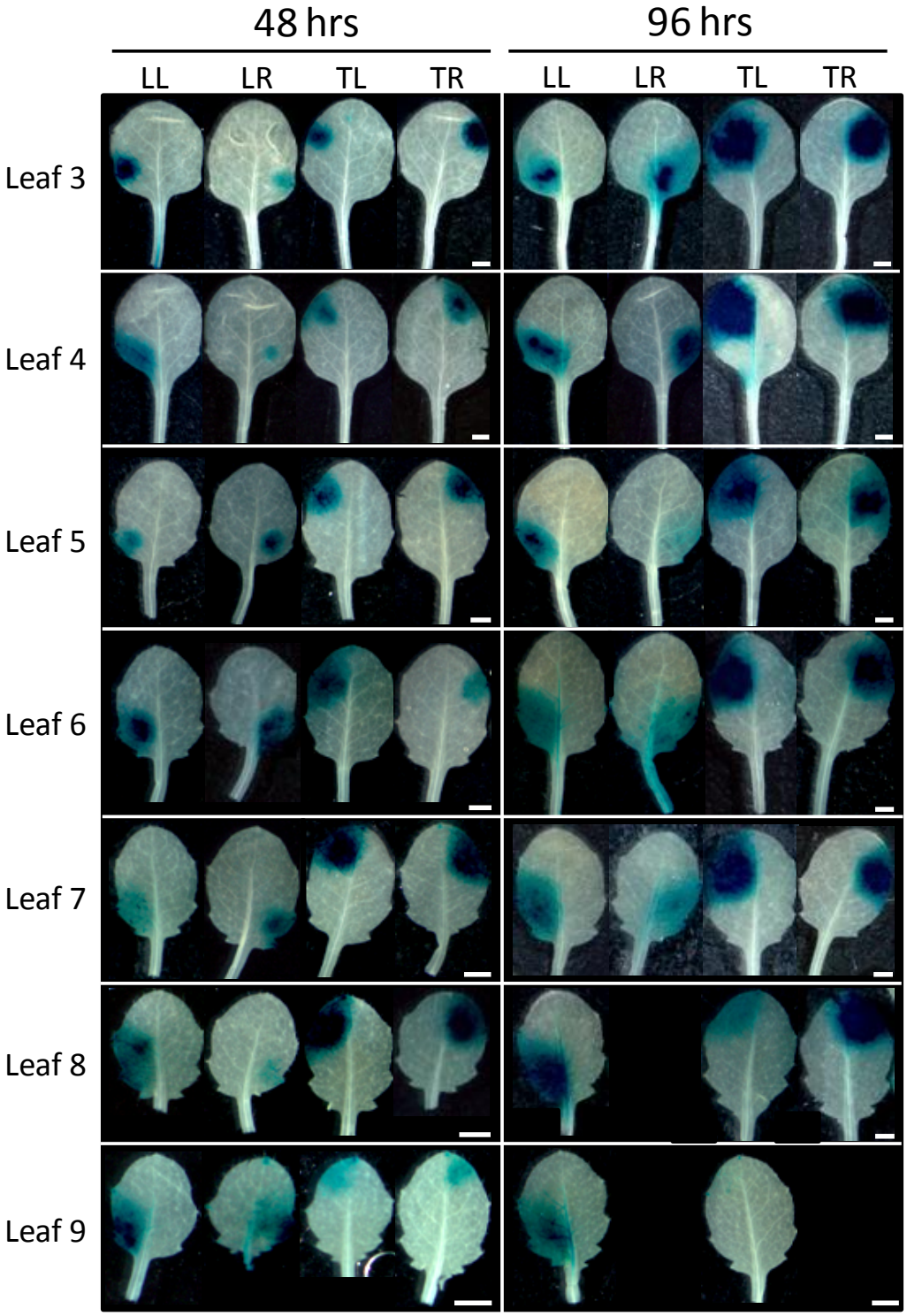

Figure 4.24. Sectorial induction experiment on pOpON::CsEXPA1 transformant leaves. Lower left (LL), lower right (LR), top left (TL) or top right (TR) corner of leaf blade on day 18 after sowing and harvested after 48 or 96 hours of treatment. Plants were subjected to GUS staining before dissected and pooled into same leaf stage (leaf number) for imaging and analysis. Representative images were shown. Scale bars = 1 mm.

Table 4.3. Leaf area analysis of sectorial induction experiment using LeafProcessor. One-way ANOVA test for normally distributed data, non-parametric Kruskal-Wallis test otherwise. *d.f.* = degrees of freedom, LL, lower left; LR, lower right; TL, top left; TR, top right.

Leaf number	Duration of induction (hours)	Leaf sectors that differ	Kruskal-Wallis *p*-value	One-way ANOVA *p*-value	*d.f.*
L3	48	-	-	0.514	41
	96	-	-	0.306	43
L4	48	LL-TR	0.012	-	48
	96	-	-	0.119	47
L5	48	TL-LR; TR-LR	0.004	-	52
	96	-	-	0.312	33
L6	48	-	-	0.071	49
	96	-	-	0.885	28
L7	48	-	0.518	-	36
	96	-	-	0.144	13
L8	48	-	-	0.729	34
	96	-	-	0.853	7
L9	48	All		0.003	13
	96	All	-	0.286	2

Table 4.4. Comparison between areas of the induced and non-induced leaf sectors. NS = no significant difference at $p<0.05$. Numbers represent the degrees of freedom (*d.f.*).

Duration of induction	Induced leaf sector	Leaf number						
		L3	**L4**	**L5**	**L6**	**L7**	**L8**	**L9**
48 hours	Lower left (LL)	NS	NS	NS	NS	NS	NS	NS
		43	39	59	55	31	11	11
	Lower right (LR)	NS	NS	NS	NS	NS	NS	
		31	51	43	47	10	23	
	Top left (TL)	NS	NS	NS	NS	NS	NS	NS
		55	54	47	63	55	47	27
	Top right (TR)	NS	NS	NS	NS	NS	NS	NS
		35	47	59	30	45	55	11
96 hours	Lower left (LL)	NS	NS	NS	NS	NS		NS
		47	43	43	47	7		7
	Lower right (LR)	NS	NS	NS	NS			
		47	55	35	11			
	Top left (TL)	NS	NS	NS	NS	NS	NS	
		39	55	35	35	19	23	
	Top right (TR)	NS	NS	NS	NS	NS		
		39	35	19	18	23		

4.2.4 Effect of altered expansin gene expression on hypocotyl extension

Although the focus of this project is to investigate the role of expansins in leaf growth, studies on the growth of pOpON transformant hypocotyls were carried out to examine the effect of manipulated expansin expression level on organ expansion. Hypocotyls have provided the model system for expansin since its first discovery (McQueen-Mason *et al.*, 1992) and can be used for activity assays on cell elongation (Cosgrove, 1993; Shcherban *et al.*, 1995) due to growth being solely due to cell expansion (Gendreau *et al.*, 1997). The manipulation of expansin gene expression led to repression in hypocotyl extension in pOpON::CsEXPA1 seedlings germinated in the dark on Dex-containing medium (Figure 4.25C). RT-PCR analysis of these seedlings confirmed that the *CsEXPA1* transcript was detectable only in the induced seedlings (Figure 4.25A) and that induction did not trigger down-regulation of its homolog counterpart in Arabidopsis (*EXPA8*) (Figure 4.25B). Histochemical analysis confirmed that GUS reporter gene expression was only detectable in the induced seedlings and was present throughout the hypocotyl (Figure 4.25C).

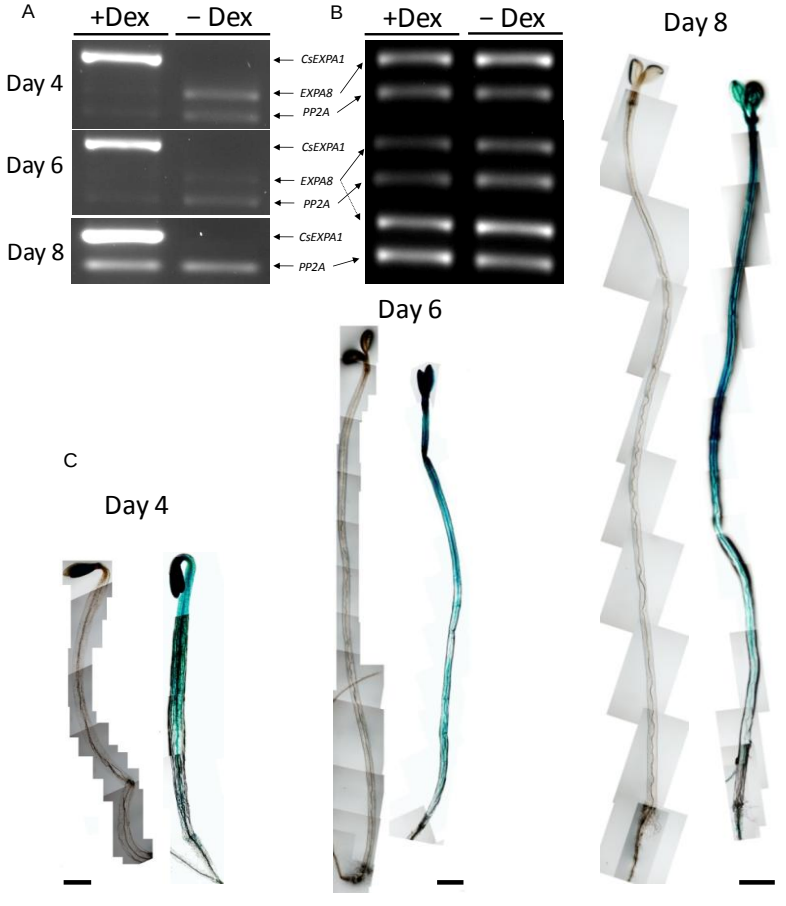

Figure 4.25. (A) Molecular validation of *CsEXPA1* expression in pOpON::CsEXPA1 hypocotyls grown on 0.5x MS agar medium supplemented with 10 µM dexamethasone (+Dex) or DMSO 0.1% v/v control (- Dex) for 4, 6, or 8 days. (B) Semi-quantitative PCR analysis of *AtEXPA8* (*CsEXPA1* homolog) using sample as per A and *PP2A* as internal control, showing bands during the exponential cycle phase. (C) GUS staining of non-induced and induced hypocotyls as per A. Scale bars = 1 mm

A time course analysis of hypocotyl and root growth in the pOpON::CsEXPA1 plants germinated in the dark and sacrificed for analysis at various time points confirmed that hypocotyl length was significantly decreased in the induced plants (Figure 4.26). Conversely, hypocotyl width was increased and this was significant at $p<0.05$. Final root length showed a tendency to decrease in the induced seedlings, although the inherent variation in root length meant that this difference was not statistically significant relative to the control seedlings (Figure 4.26). Again, GUS histochemistry confirmed that reporter gene expression was only detectable in the induced seedlings and seemed to be present in all tissues (Figure 4.26B). A similar time course analysis of pOpON::amiREXP lines indicated that suppression of expansin gene expression led to a significant decrease in hypocotyl length and that induction led to the accumulation of GUS reporter gene signal only in the induced seedlings (Figure 4.27).

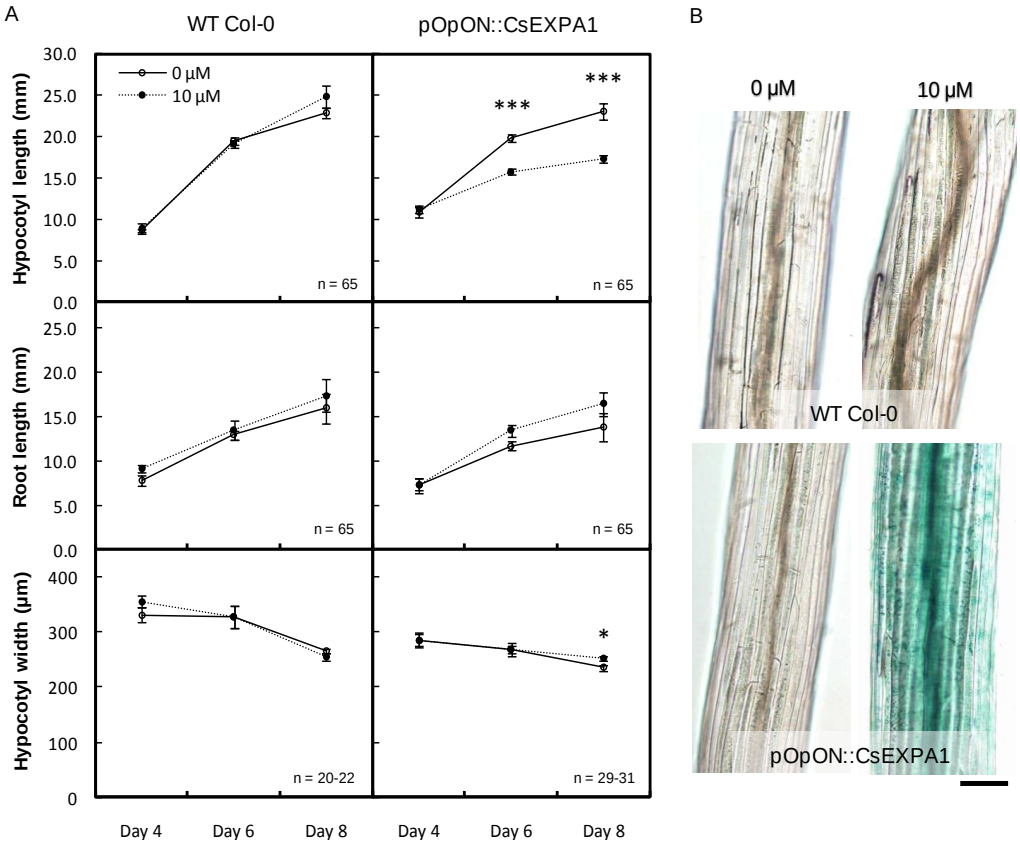

Figure 4.26. Time-course study of hypocotyl and root growth of Col-0 wild-type and pOpON::CsEXPA1 transformant seedlings in the dark. (A) Comparison between hypocotyl and root length of seedlings grown on 0.5x MS agar medium supplemented with 10 µM dexamethasone or DMSO 0.1% (0 µM). Values are means ± SE (n as indicated). Two-sample t-tests, *$p<0.05$, ***$p<0.001$. Hypocotyl widths were measured from micrographs at mid-point region between cotyledons and root (n = 3 to 9 for day 4 and day 6). (B) Representative middle regions of hypocotyl after GUS staining. Scale bar = 100 µm.

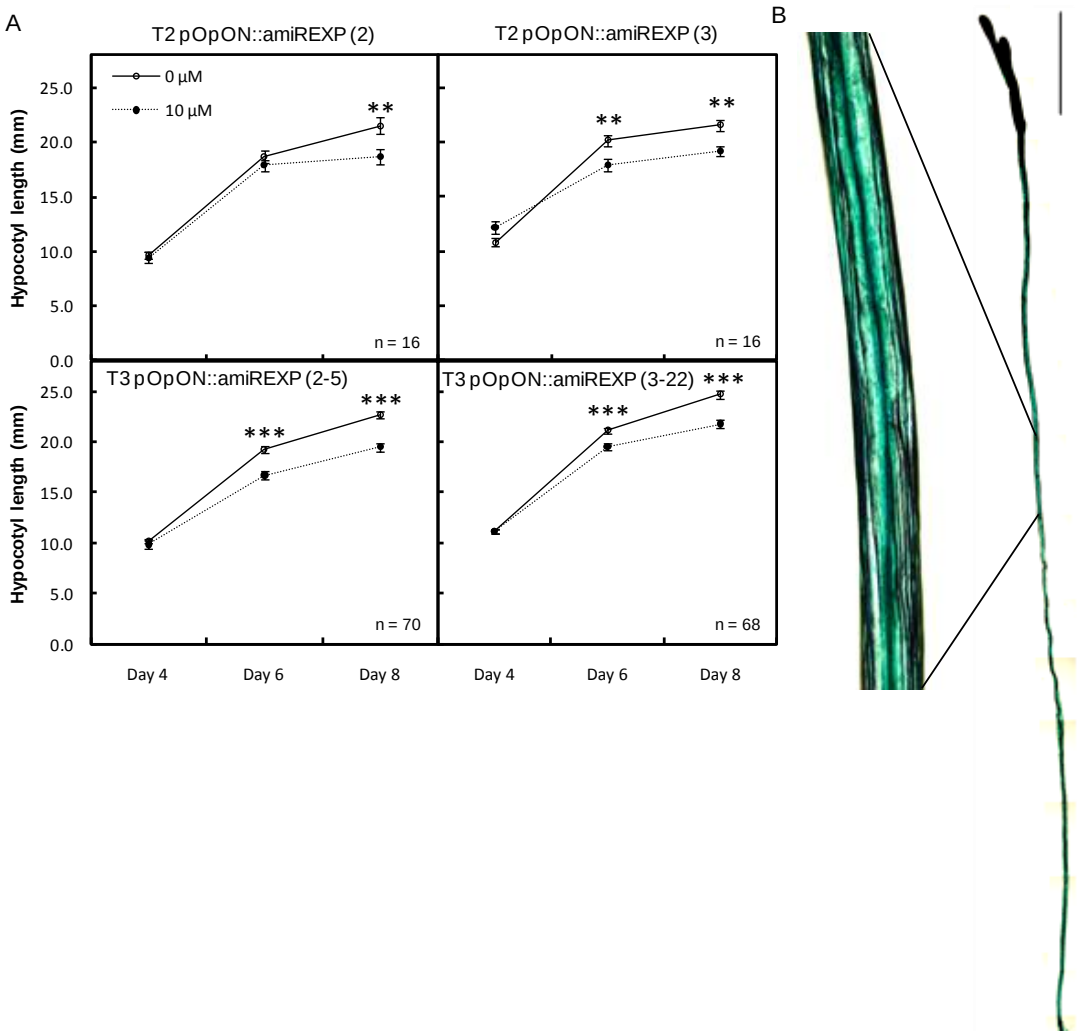

Figure 4.27. Time-course study of hypocotyl growth of T2 and T3 pOpON::amiREXP transformant line 2 and line 3 seedlings in the dark. (a) Comparison between hypocotyl length of seedlings grown on 0.5x MS agar medium supplemented with 10 µM dexamethasone or DMSO 0.1% (0 µM) at a density of 70 seeds per plate over 3 rows. Photographs were taken under dim green light on day 4 and day 6. Values are means ± SE. Two-sample t-tests, *p<0.5, **p<0.01, ***p<0.001. (B) Representative middle region of pOpON::amiREXP (3) hypocotyl after GUS staining. Scale bar = 2 mm.

4.3 Discussion

In this Chapter I have described a series of experiments in which an approach was taken to inducibly alter the expression of a group of expansin genes during leaf development and the outcome on leaf growth observed. The results indicate that amiRNA can be used to down-regulate the expression of a group of expansin genes and that this leads to a repression of leaf growth. In addition, my analysis suggests that there is a differential response to this manipulation depending on the tissue and stage of development.

4.3.1 Approaches to repressing expansin gene expression

I explored the use of an inducible amiRNA system to down regulate expansin gene expression. The amiRNA approach has been previously used to down-regulate *Auxin Response Factors2, 3,* and *4* using an Arabidopsis-based synthetic miR-ARF in Arabidopsis, tomato and tobacco, resulting in dramatic transformation of abaxial leaf tissue into adaxial ones in all three species (Alvarez *et al.*, 2006). This suggests it is a means to tackling the problem that genetic redundancy poses for the functional analysis of gene families even across diverse species. However, there must be a limit to the number of genes that can be targeted by an amiRNA.

In this study, I chose a number of expansin genes which are closely related in sequence and which (based on RT-PCR data) represent the predominant expansin genes expressed during leaf development. The molecular analysis of the pOpON::amiREXP lines indicated that the system can be used to down-regulate the expression of four target expansin genes. An obvious question is whether this leads to subsequent down-regulation of the level of proteins encoded by these genes. Expansin proteins are relatively stable and the antibodies available generally do not discriminate between different expansin gene products (Rose *et al.*, 2000). Moreover, there are data indicating that the relationship between expansin mRNA level and protein is often complicated, such that high transcript levels do not necessitate high expansin protein levels (Brummell *et al.*, 1999a; Rochange and McQueen-Mason, 2000).

At present I have no Western blot data indicating that the induction of the amiREXP construct led to a lower level of the relevant expansin proteins or activity and this is clearly a priority for future research (work on-going with Dr Jen Sloan). Nevertheless, our phenotypic analysis showed that growth suppression was observed following the induction of the pOpON::amiREXP lines, indicating that the manipulation of the endogenous expansin transcript levels had an effect on plant growth. Taken together, the data support the idea that inducible amiRNA is a valid and useful approach to down-regulate the expression of a group of target expansin genes, although protein and activity data would fully substantiate this claim. The inducible system provided a powerful means to regulate the temporal and (to some extent) the spatial repression of these target genes (as discussed in the next section).

4.3.2 The use of an inducible system to regulate gene expression

Previous functional studies of expansin utilised a herbicide safener-inducible gene expression system (De Veylder *et al.*, 1997) which could result in growth retardation with prolonged exposure to the herbicide safener (Choi *et al.*, 2003), whereas the tetracycline repressor based, tetracycline-inactivatable system (Gatz *et al.*, 1992) employed in Sloan *et al.* (2009) required repeated treatments due to the short half-life of the inducer, which can also be detrimental to plant growth when in excess.

The pOpON system as described above (Craft *et al.*, 2005) has been widely used to regulate the expression of target genes in other developmental studies of Arabidopsis (Heisler *et al.*, 2010; Shkolnik-Inbar and Bar-Zvi, 2010; Blanvillain *et al.*, 2011). This system has also been successfully employed in our lab to study the role of cell division to leaf growth (Kuwabara *et al.*, 2011; Malinowski *et al.*, 2011). Dexamethasone (Dex) is an animal steroidal compound which is required in a small amount and normally does not affect plant development. With the exception of the Gal4-based GVG system (Aoyama and Chua, 1997; Kang *et al.*, 1999; Amirsadeghi *et al.*, 2007), there is no report of a glucocorticoid receptor-based, steroid-inducible system adversely influencing endogenous gene expression. Furthermore, the current study has demonstrated the versatility of pOpON system in allowing flexible ways of local or global induction, which also shows that it is a powerful tool to limit the

manipulation of gene expression to particular phases of plant growth and development.

4.3.3 Repression of expansin gene expression leads to decreased leaf growth and altered leaf shape

There are two previous reports of decreased expansin gene expression leading to decreased leaf growth in Arabidopsis (Cho and Cosgrove, 2000) and in rice (Choi *et al.*, 2003). Cho and Cosgrove (2000) used a gene-specific promoter to target repression of a single expansin (*EXPA10*) in the petiole, mid-rib and abscission zone, whereas Choi *et al.* (2003) used a herbicide safener-inducible gene expression system. The results presented here add to this body of work by showing a decreased leaf growth phenotype through repressing the expression of a group of expansin genes in an inducible fashion during plant development.

The current study was designed so that I could investigate the functional role of expansins in leaf shaping separate from leaf growth. Hence, comparisons were often performed using absolute parameters such as area, length and width, alongside the relative parameters of circularity and length:width ratio. In all of the experiments carried out on pOpON::amiREXP transformant plants (including plate induction, staged-transfer induction, shoot apex induction or individual leaf induction experiments) which suppressed expansin transcript levels, leaf growth was repressed and consistently resulted in alterations of leaf shape as calculated by the morphometric parameters. The circularity measurement has been shown to be the most effective parameter for distinguishing different leaf shapes, mainly due to the small value of within-sample variations (Backhaus *et al.*, 2010). This was also the case here, so that changes in the lamina circularity were found to be significant when the linear measurements did not indicate any major change (Figure 4.11, 4.23).

Increases in leaf circularity were mainly due to the decreased petiole length after induction. This suggests greater petiole sensitivity towards changes in the levels of expansin expression than the leaf blade. This is phenotypically apparent by the formation of more compact rosettes with shorter leaves (Figure 4.8). The effect of expansin suppression on petiole elongation perhaps reflects its linear nature of

growth compared to the two-dimensional expansion of the leaf blade. Changes in linear expansion are more readily detectable. Furthermore, the inherent greater sensitivity of the petiole to growth repression suggests a major role of the target expansins in longitudinal growth. This is consistent to the observation that two of the amiRNA targets, *EXPA10* and *EXPA5* are predominantly expressed in the leaf petiole (Cho and Cosgrove, 2000; Son *et al.*, 2010).

The involvement of expansins in petiole elongation is not clear. It has been shown that the petiole exhibits complex hyponastic growth upon auxin acidification in response to shading which involves a multitude of other hormonal regulations (Cox *et al.*, 2004; Millenaar *et al.*, 2009). However, the extractable expansin activity and susceptibility of petioles to expansin extracts are similar in control and shade-treated plants (Sasidharan *et al.*, 2010). On the other hand, *EXPA* has been shown to be upregulated during the submergence of flood-tolerant *Rumex palustris* preceding petiole elongation (Vreeburg *et al.*, 2005). Despite the uncertain environmental regulation of petiole growth, the results presented here suggest an expansin function in endogenous petiole growth, which abolishes the hyponastic response when absent (personal observation).

In addition, the shoot apex droplet induction experiments indicated a longer period when expansin gene expression can effect petiole growth than for the leaf lamina. When induction was performed on day 12 after sowing, significant effects were largely confined to the lamina of leaf 6 and 7, but to the petioles of leaf 3 to 7 (Figure 4.22). This is consistent with a longer and more plastic phase of petiole elongation, but a shorter and more restricted period of lamina development when expansin can influence this process. Furthermore, petiole elongation generally happens later during leaf development.

The phenotype of induced pOpON::amiREXP plants after plate induction only become clearly visible during the later stages of rosette development, which is consistent to that reported previously (Cho and Cosgrove, 2000), suggesting a phase-dependent function for expansin during leaf development. This idea has been tested on tobacco leaves inducibly overexpressing a heterologous expansin protein which showed that the effects of expansin upregulation on leaf area were prominent only during the expansion phase of leaf development (Sloan *et al.*, 2009). The results

from the first leaf-pair induction experiments (Figure 4.21) support this hypothesis. Repression of endogenous expansin gene expression caused significant decreased leaf growth only when induced during the mid-phase of first leaf development.

To investigate this further, a staged-transfer experiments were carried out (Figure 4.17-18). This showed that the repression of expansin expression during later phases of leaf development was sufficient to repress leaf growth in one of the transformant lines. In both lines the leaf shapes were similarly altered, with overall shorter and more compact leaves (Figure 4.17D, 4.18D). Localised leaf 6 induction further confirm the observation that lamina expansion is sensitive to the manipulation of expansin expression during the mid-phase of leaf development and also suggests a phase-dependent differential sensitivity of lamina width and length extension to altered expansin gene expression (Figure 4.23). Furthermore, these further experiments did not affect the number of vegetative leaves (results not shown), as was the case in plate induction (Figure 4.16). This supports the idea that expansin has a direct influence on leaf growth rather than an indirect effect via advancing flowering time (Cookson *et al.*, 2007).

Micrographs taken across the middle regions of lamina and petiole showed that there was no massive decrease in cell size when expansin gene expression was suppressed (Figure 4.12-13). A previous study showed decreased cell length in the petiole when *EXPA10* was suppressed (Cho and Cosgrove, 2000). Other studies using an antisense approach also showed a decrease in cell length of rice mesocotyls (Choi *et al.*, 2003) and significant reduced size in the epidermal cells of petunia petal limbs following the suppression of expansin expression (Zenoni *et al.*, 2004). However, the results presented in Table 4.2 appeared to be inconsistent with findings in the literature. Despite repressed leaf growth and reduced petiole length which was consistent to that of reported, there were no significant changes in the mesophyll cell size when expansins were down-regulated, but the number of petiole cell files was reduced. If the lamina mesophyll cell density remained unchanged, a reduced lamina area suggests a decrease in total cell number. Hence, this suggests that expansin down-regulation after sowing may have affected the process of cell proliferation or differentiation. Notably the vasculature of the induced petiole was strikingly narrower than that of non-induced plants (Figure 4.13). This suggests that suppressed

expansin expression might affect other aspects of leaf growth such as the development of vascular tissue, which might have been overlooked previously. Alternatively, small changes in cell size might be sufficient for the observed decreased leaf growth and might not be statistically significant due to the variation between leaf samples. Overall, the data gathered here support the idea that appropriate endogenous expansin gene expression is required for leaf growth.

4.3.4 The conundrum of growth repression from expansin overexpression

One would expect an increase in growth when expansin is overexpressed. However, this was found only to be true when expansin expression was induced at 1 μM Dex (Figure 4.10-11), despite no significant changes in cell size (Table 4.2). Surprising results were obtained from pOpON::CsEXPA1 transformant plants induced with higher concentrations of Dex, with repressed growth in rosettes, leaves and hypocotyls being observed (Figure 4.10-11, 15, 19, 26). The adaxial epidermal cell length of petiole was significantly reduced. Furthermore, there was a significant increase in petiole mesophyll cell size especially across the cell width when the growth of the petiole was repressed. A similar observation has been reported on decreased hypocotyl length with increased diameter in tomato plants overexpressing *CsEXPA1*, and similarly at a cellular level for epidermal and cortical cells, with decreased cell length but increased transverse cell circumference (Rochange *et al.*, 2001). Constitutive overexpression of expansin in transgenic plants often resulted in variable phenotypes (Cho and Cosgrove, 2000; Choi *et al.*, 2003; Wang *et al.*, 2011), which motivated these investigators to exploit tissue-specific expression or inducible systems for further studies, as discussed above (Cho and Cosgrove, 2000; Choi *et al.*, 2003). This indicates the importance of spatial control of expansin gene expression and leads on to the question on how expansin overexpression can disrupt growth.

The overexpression of an expansin involved in tomato fruit softening resulted in reduced fruit size and slightly smaller leaves, while the suppressor lines showed no noticeable difference (Brummell *et al.*, 1999a). This led the authors to propose that a specific expansin is only required at a small amount for its functioning during fruit softening. When present in excess, the authors suggested that degradation of hemicelluloses led to the observed phenotype perhaps by exposing previously

inaccessible cell wall components to degradative enzymes (Rose *et al.*, 1997; Brummell *et al.*, 1999a). This is consistent with the proposed mechanism of expansin functioning in physically disrupting the hydrogen bonds between the cellulose microfibrils and hemicelluloses (Figure 1.3B) that tether the whole load-bearing structure together(McQueen-Mason and Cosgrove, 1994; McQueen-Mason and Cosgrove, 1995). Physical separation of microfibrils has shown to be required for cell wall extension (Marga *et al.*, 2005), but this separation might make the structure open to modifications by many enzymes (Cosgrove, 1999, 2005).

These observations led to the proposal of a dose-dependent effect of expansin, such that growth is promoted at moderate level but inhibited when in excess. This view is supported by the dose-dependent effect of bacterial cellulose-binding domains (CBDs) on pollen tube and root elongation (Shpigel *et al.*, 1998). It should be noted that expansin is the main family of plant proteins with CBD (Shoseyov *et al.*, 2006). Expansin enhances elongation at low concentrations but inhibits growth when in excess, maybe via steric hindrance of cellulose fibril access by other cell wall proteins that modulate expansion. For example, auxin-induced growth or cellulose microfibril assembly can be disrupted by dyes or antibodies specific to certain cell wall components or enzymes (Hoson and Nevins, 1989; Haigler, 1991; Inouhe and Nevins, 1991).

On the other hand, bacterial cellulose synthesis and polymerisation appears to be accelerated in the presence of CBD and dye, which behave as cellulose-intercalating agents for the enhanced incorporation of cellulose (Benziman *et al.*, 1980; Shpigel *et al.*, 1998). This is consistent with the increased amount of cellulose in plants over-expressing expansin (Wang *et al.*, 2011) and the decreased cellulose in plants with decreased expansin expression (Zenoni *et al.*, 2004). Expansin might act to prepare the cell wall for cellulose deposition by separating the cell wall matrix for the incorporation of new wall materials during expansion. Hence, an excess of expansin might disrupt early cell wall modification, resulting in a reduced susceptibility to the necessary modifications during later stage of cell wall extension, perhaps due to feedback mechanisms involving other cell wall proteins or components.

A dose-dependent effect is consistent with the observations in Rochange *et al.* (2001) that the growth of hypocotyl was normal at lower expansin levels and only affected

in tomato transformant over-expressing *CsEXPA1* at high level. This was also observed here with shorter and thicker hypocotyls of Arabidopsis pOpON::CsEXPA1 transformant plants induced only at high Dex concentrations (Figure 4.26). Although the growth of the hypocotyl only involves cell expansion (Gendreau *et al.*, 1997), the regulation on the deposition of wall materials and their modifications can be dynamic for changes in cell wall thickness (Refrégier *et al.*, 2004; Derbyshire *et al.*, 2007). It is widely accepted that the orientation of cellulose microfibrils is important for determining the direction of growth (Baskin, 2005). An excess amount of expansin might disrupt the directional structuring in the cellulose-hemicellulose architecture, resulting in more isotropic cell growth and hence a retarded hypocotyl elongation and increased cell width. More detailed biochemical studies are required to test these various hypotheses.

4.4 Summary

In this chapter, I have described the characterisation of a molecular tool based on a chemically-inducible gene expression system which allowed me to down-regulate the expression of a group of targeted expansin genes (*EXPA10*, *EXPA1*, *EXPA5*, and *EXPA3*) identified to be expressed during early leaf development. The use of an artificial miRNA approach provided the flexibility in spatial and temporal control over target gene expression. A series of induction experiments were carried out which confirm the involvement of these endogenous expansin genes in normal leaf growth. In particular, suppression during later phases of development was sufficient to repress leaf growth and alter leaf shape. Furthermore, the study of an inducible expansin-overexpressor line suggested that leaf and hypocotyl growth may be sensitive to the amount of expansin present, with retarded growth when the expansin gene was highly expressed.

CHAPTER 5 The application of atomic force microscopy (AFM) to the *in planta* characterisation of tissue mechanical properties

5.1 Introduction

Plant development is robust in that the organ size and shape is species-specific and consistent despite plants being situated in a highly variable environment. At the same time, the precise geometry of organs (such as leaves) is highly adaptable to the environment. For example, although leaves generally develop into a flattened form to optimise light interception for photosynthesis, the shape and size of a leaf from any individual plant reflects a number of environmental parameters that the plant has been exposed to. Thus, the growth processes which lead to this form must, on the one hand, be sufficiently robust to cope with the variations in growth conditions yet, at the same time, allow integration of environmental signals to provide an appropriate growth response.

Leaf morphogenesis begins with the formation of a buttress on a shoot apical meristem and ends with the development of a fully expanded blade with petiole (Figure 1.1). Although this process clearly requires co-ordinated cell division, expansion and cell differentiation, a large body of evidence indicates that control of plant growth involves regulation of cell wall structure and function (see Chapter 1). In previous chapters, I have provided evidence for the role of expansins in leaf development. These data, in conjunction with a number of other studies, support the hypothesis that cell wall proteins, such as expansins, regulate the mechanical properties of the cell wall and, thus, set the limits for growth. However, although the mechanism by which these proteins actually influence cell wall mechanics is still largely speculative. This reflects to some extent our limited information on plant cell wall mechanics, particularly as it relates to the *in vivo* situation. This gap in our understanding itself reflects technical limitations. Thus, although a number of approaches to measuring cell wall structure and function have been taken (discussed below), these all have limitations in either a reliance on the analysis of processed

(dead) material and/or measurement of material at a resolution far lower than that at which morphogenesis occurs.

The physical properties of cell walls are closely linked to cell growth/ functioning and have been studied for a long time e.g. (Heyn, 1933; Nilsson *et al.*, 1958; Cleland, 1971; Wu and Sharpe, 1979; Sellen, 1980; Taiz, 1984; Carpita and Gibeaut, 1993), and recently reviewed in (Burgert, 2006). These properties not only include the purely physical composite nature of the cell wall (Jarvis and McCann, 2000), but also the mechanical behaviour that arises from growth processes which may be lost when studied in isolation (Thompson, 2008). Cell wall mechanics (particularly extensibility) have commonly been studied *in vitro* with excised tissue sample subjected to a constant stress or constant strain, and the changes in tissue extension or stress decay over time measured This is respectively known as creep test and relaxation test (Cosgrove, 1993). The slope on a stress-strain curve, which represents the relationship between stress (the applied load) and strain (deformation), define the mechanical properties of a material. In terms of standard engineering material parameter, this is denoted as the elastic or Young's modulus, which reflects the intrinsic material properties.

Such approaches have been extensively implemented in the study of cell wall proteins, such as expansins. The activity of expansins in the extension of cell walls was shown by *in vitro* extensometer assays (as mentioned in Section 1.6.2) with the use of heat-killed plant tissues, such as hypocotyl (McQueen-Mason *et al.*, 1992), coleoptiles (Choi *et al.*, 2003), internodes (Cho and Kende, 1997b) and leaf strips (Keller and Cosgrove, 1995). However, *in vitro* extensometer assay is limited by the fact that measurements are made on multicellular tissues with different cell types, which may differ in cell wall properties.

Furthermore, the mechanics of the plant cell wall cannot be simply defined by a single value of elastic modulus as it exhibits unique rheological properties. The cell wall in living and growing plant tissue is dynamic and allows concurrent deposition of wall material and irreversible expansion provided that the turgor pressure surpasses a certain threshold (Thompson, 2005). Thus, although *in vitro* approaches can clearly provide important basic information on the cell wall, there will always be the possibility that the data captured do not truly reflect cell wall behaviour in living

plant cells. To circumvent this limitation, attempts using both turgor pressure probes micro-penetration (glass probe fitted with sensitive load- and deflection-transducers) and micromanipulative compression techniques have been taken (Hiller *et al.*, 1996; Tomos and Leigh, 1999; Blewett *et al.*, 2000; Wang *et al.*, 2006). For example, the ability of expansins to increase the cell wall elasticity in living single suspension-cultured tomato cells has been demonstrated through micromanipulative compression (Wang *et al.*, 2008). Consistent to this report, the overexpression of expansin in guard cells was shown to decrease the volumetric elastic modulus via cell pressure probe on epidermal peels (Zhang *et al.*, 2011b).

Nonetheless, these techniques suffer from the limitation of obtaining single-cell measurements. Most morphogenic events involve the action of many cells, thus relating measurements on single cells to the parameters of a region of tissue is problematic. Microindentation is a more promising approach and has been used to relate local mechanical properties of the cell wall with tip growth in pollen tubes (Zerzour *et al.*, 2009). However, this technique lacks the sensitivity required to separate the relative contribution of the cell wall properties and turgor pressure in response to the applied force at tissue-level. Furthermore, results from tissue indentations are dependent on tissue geometry which is not always trivial to obtain (Geitmann and Ortega, 2009).

Since its invention in 1986 (Binnig *et al.*, 1986), atomic force microscopy (AFM) has been widely applied for the imaging of biological samples in their natural aqueous environment at high resolution, from the nanometer to micron range The basis of AFM is shown in Figure 5.1. A soft cantilevered beam that has a sharp tip at its end is brought in contact with the surface of the sample. The force between the tip and the sample causes the cantilever to deflect in accordance with Hooke's Law. The degree of deflection is measured by the laser reflected off the back of the cantilever beam onto an array of position-sensitive photodetectors. The angular deflection of the cantilever at any given point on the sample is given by the differences between the laser reflections received by the individual photodetectors. This allows the AFM to construct a topographic image of the sample surface non-destructively with continuous contact of the tip with the sample (contact imaging mode). To avoid damaging the sample surface, the tip is maintained at a constant

angular deflection through a feedback mechanism which adjusts the distance between the tip and the surface to keep a constant applied force, via controller on the piezo-elements which move in all three axes relative to the tip. The Z-movement (height) maintains the force at the right level, while the X- and Y- movements allow the tip to raster-scan over the sample. The topographical image of the scanned area is the resulting map of the tip's relative distance from the surface at different X-Y values of the scan.

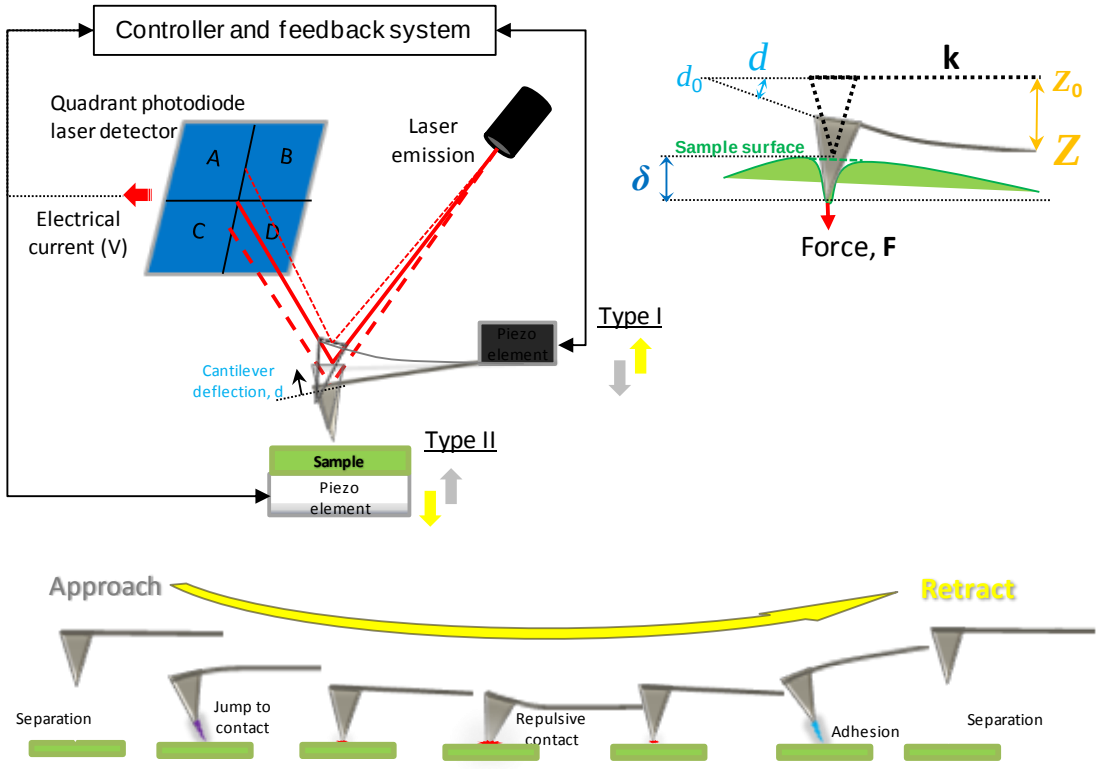

Figure 5.1. Mechanism of atomic force microscopy. Atomic Force Microscopy (AFM) is a type of scanning probe microscopy (SPM) typically applied to high-resolution nanoscale measurement. It consists of a microscale cantilever with a sharp tip at its end that is used to probe the sample surface. Either the cantilever (Type I) or the sample stage (Type II) is fabricated with piezo-resistive elements that act as a strain gauge. To measure, the AFM tip is extended towards (grey block arrows) and retracted (yellow block arrows) from the specimen surface while the static deflection of the cantilever, *d*, is monitored as the differential laser deflection onto the photodiode laser detector, which is split into 4 quadrants to detect vertical and lateral forces (transduced as electrical current), alongside the piezoelectric displacement, *z*. When the tip is brought into proximity of a sample surface, different forces, F between the tip and the sample lead to a deflection of the cantilever according to Hooke's law, F = k*d*, where k is the cantilever spring constant.

Imaging of mechanical properties with the AFM is possible by taking force curves for quantitative analysis (Burnham and Colton, 1989), as illustrated in Figure 5.2. Since the cantilever spring constant is known, the stiffness of the sample can be calculated from the gradient of the curve. This is done by measuring the gradient of the contact region of the force curve at a specific loading force and treating the cantilever and the sample as two linear springs in series, essentially "sharing" the loading force. During force mapping (Baselt and Baldeschwieler, 1994), force curves are taken while the tip is raster scanned laterally across the sample (Figure 5.3). In this respect, AFM approach is similar to microindentation in that both techniques exert a constant force resulting in sample indentation. However, AFM has much greater sensitivity capable of exerting far lower forces (nN) to a very local area using a micro-/nanometric probe (“tip”) attached to a spring-like cantilever, with the advantage of simultaneously imaging the measured surface. This demonstrates a tremendous value for studying important lateral variation of anisotropic cell wall properties, including the surface topography, elasticity and even the physicochemical properties.

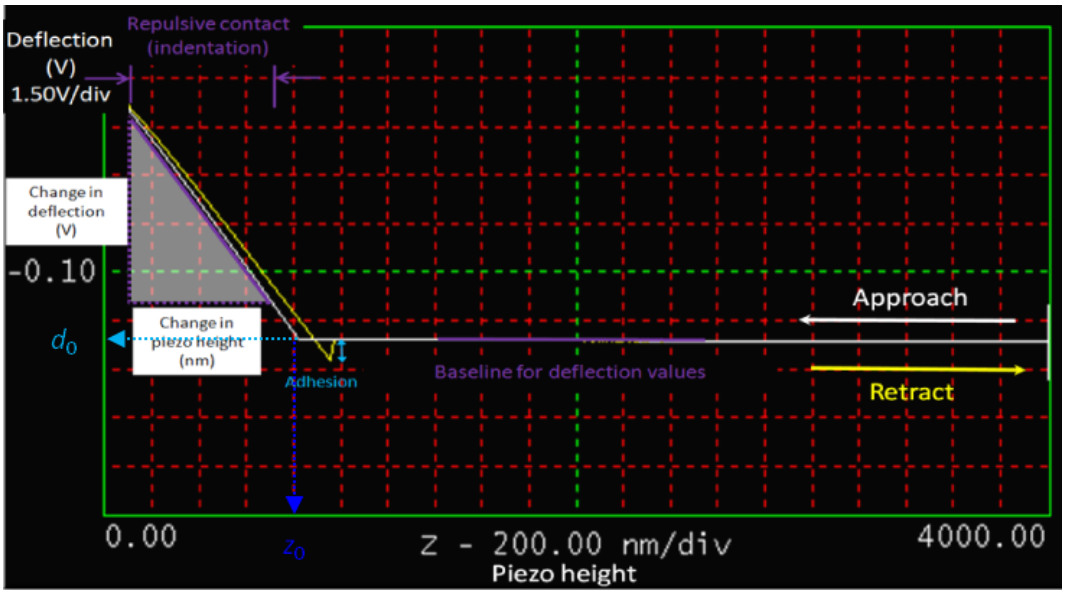

Figure 5.2. An example of annotated force curve generated on a surface with infinitely stiff surface relative to the cantilever stiffness. On a stiff sample the force curve basically shows two regions: (1) the off-contact, where the tip is not touching the sample and thus the deflection stays constant (to the right in the trace) and (2) the in-contact, where the cantilever is deflected proportional to the sample height, resulting in a slope (to the left). The slope is used to calibrate the optical lever sensitivity of the position-sensitive photodiode to convert the voltage (V) measured into cantilever vertical deflection.

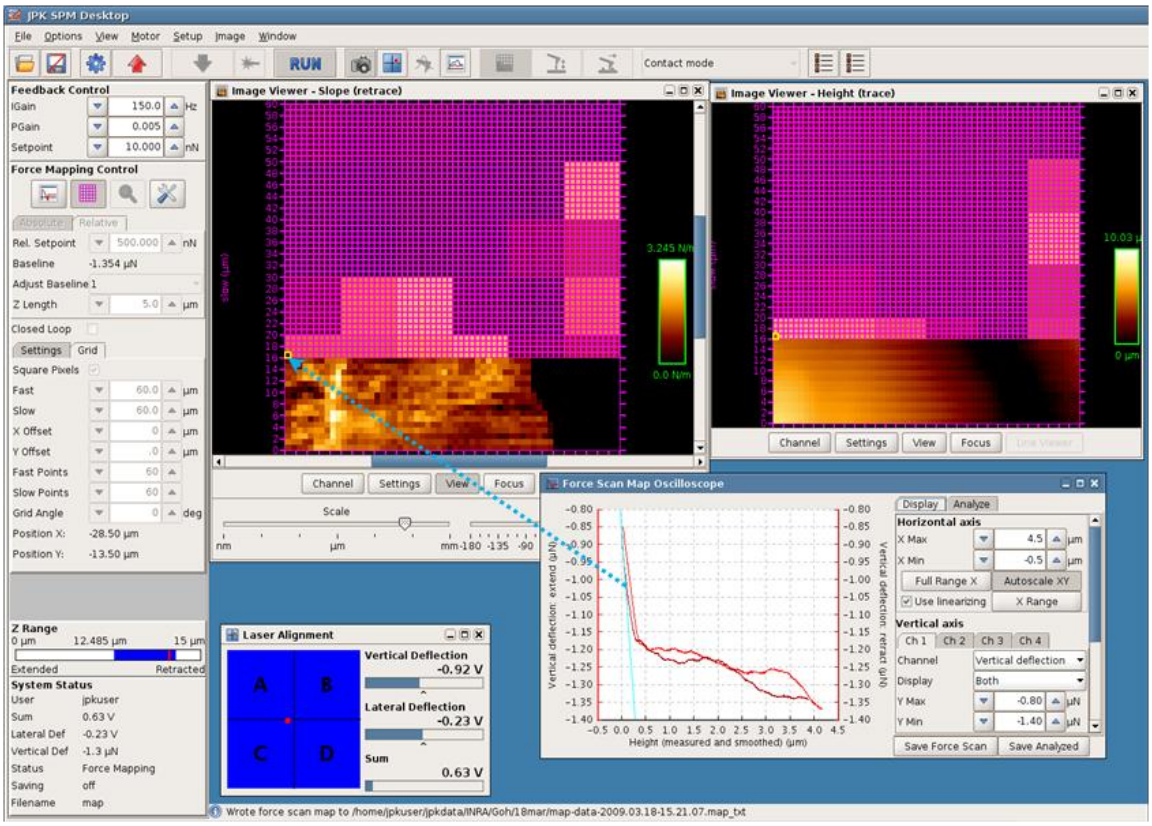

Figure 5.3. A screenshot of the control panel during force mapping. Two types of information can be obtained during force mapping: topographical image and force map. Force curve is taken while the tip is raster scanned laterally (fast) across the sample and slowly along the Y-axis. The slope is directly translated from force measurement into relative map of stiffness (N/m) as indicated by the arrow, while the topographic height map of the scanned surface is reconstructed simultaneously based on the point of contact and piezo movement. Hence, the topographical image is a reconstruction from the compensatory motions of the stage needed to maintain constant loading force and the force map is the representation of the sample resistance to deformation as the sample is vertically indented by the tip to a fixed extent.

The application of AFM has been widespread in mechanical studies of bacterial, yeast and mammalian cells (Radmacher *et al.*, 1996; Radmacher, 2002; Alonso and Goldmann, 2003; Touhami *et al.*, 2003; Scheuring and Dufrêne, 2010; Turner *et al.*, 2010). In plants, its application has so far been largely limited to surface imaging (Wiśniewska *et al.*, 2003) and the imaging of cell wall components, such as the cellulose microfibrils (Van Der Wel *et al.*, 1996; Morris *et al.*, 1997; Marga *et al.*, 2005; Harris *et al.*, 2010). Recently AFM has been employed for the measurement of the elastic moduli of isolated walls from the stalks of cotton, rice, soybean and wheat (Wu *et al.*, 2010), as well as dehydrated secondary wall of wood cells (Gindl *et al.*, 2004). These studies have all used isolated (dead) material. However, with the advancement of instrumentation, there is a growing interest to apply AFM for *in vivo* cell wall mechanical studies (Siobhan *et al.*, 2011). Very recently, AFM has been successfully applied to the study of local variation in wall stiffness studies on dissected shoot apical meristem (SAM) (Milani *et al.*, 2011). Milani *et al.* (2011) reported that the dividing tip of the SAM is much stiffer than the differentiating flank of the meristem through very local quantification of outer wall mechanical properties. Despite these advances, there has (to date) been no report on the use of AFM to analyse the mechanical properties of intact, living plant tissue. In particular, AFM has not yet been exploited as a tool to investigate the role of gene products proposed to play a role in the control of cell wall structure/function.

To take full advantage of AFM and reduce artefacts from sample handling, an approach with minimal sample preparation is ideal. Below, I describe my pioneering attempt to apply AFM to the study of mechanical properties of intact young growing leaf primordia, in order to understand the mechanical changes underlying leaf morphogenesis. The focus of the results and discussions will be mainly based on the biological implications rather than the details on the technical aspects of the techniques. Essential technical details are provided in the methods section and discussed where appropriate.

5.2 Method considerations

5.2.1 Instrumentation

Two different types of probe cantilevers were used in this study (Figure 5.4). Force maps were obtained using a NanoWizard I (JPK Instruments), which is a type I AFM, by using self-fabricated spherical colloidal probe (5 μm radius) on beam-shaped silicon nitride cantilever of nominal spring constant 56 N/m (NANOSENSORS™ TL-NCH, Windsor Scientific). The force curves of point measurements were performed with Multimode® SPM (Veeco Instruments), a type II AFM, by using standard oxide sharpened probes (20 to 40 nm radius) with triangular silicon nitride cantilever of nominal spring constant 0.58 N/m (SNL-10, Bruker). It is necessary to have a cantilever soft enough to be deflected by small forces (low force constant) and has a high enough resonance frequency (i.e. short cantilever) to not be susceptible to vibrational instabilities.

All measurements were carried out in contact mode. The optical lever sensitivity of the cantilever was calibrated on microscope glass slides (ThermoFisher scientific) under reverse osmosis water, where spring constants were derived from thermal tuning (Cleveland *et al.*, 1993; D'Costa and Hoh, 1995).

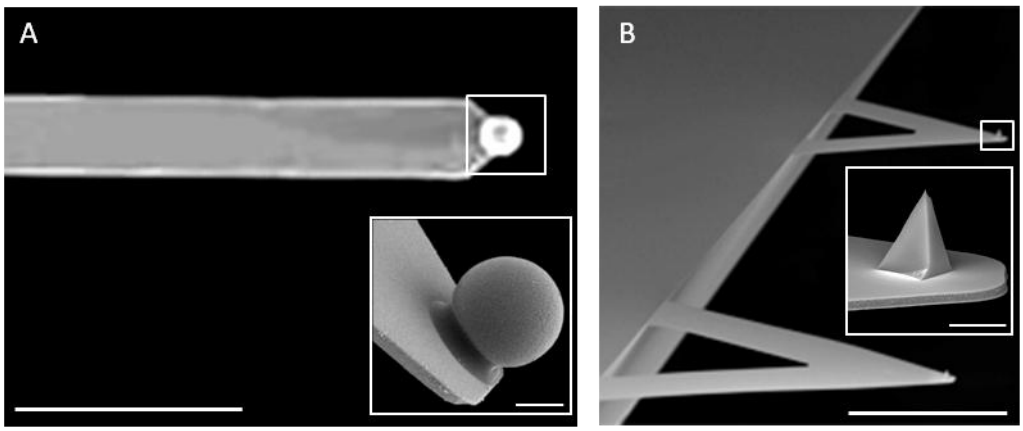

Figure 5.4. Two types of probe cantilever used. (A) Representative picture of a self-fabricated spherical colloidal probe (5 μm radius) on a beam-shaped cantilever using two-component glue. (B) Pyramidal-shaped tip with 2-12 nm radius on a v-shaped cantilever. Insets showing magnified image of the boxed area. Scale bars = 100 μm; 5 μm (insets). Pictures taken from the manufacturer's website.

5.2.2 Force map analysis

To investigate the mechanical properties of leaf primordium at various locations, force-volume images consisting of arrays of 50 x 50 force curves (described below) were recorded in parallel with topographic images. For each force curve, the sample vertical displacement, *z*, was controlled to obtain the same maximum vertical deflection, *d*, and thus the same maximum applied force. Force map reflects qualitatively that the sample mechanical properties were generated by taking a slice of the force-volume at a given sample height in the contact region of the curves (Heinz and Hoh, 1999).

An important consideration is the geometry of the surface measured. An ideal force measurement should be normal to the surface to ensure only vertical deflection of the cantilever is accounted for. A sloping surface can easily result in artefacts of measurement due to the unwanted effects of lateral deflection from the cantilever, especially true when a cantilever of high sensitivity is used or when a greater loading force is applied (Radmacher, 2002). Therefore, the topographic height map is very important for sound interpretation of the force map. Experimentally, this artefact can be checked by analysing scans from different orientations and comparing the measurements at the same point. Essentially, the force measurements should be independent of the topography.

5.2.3 Force curve analysis

In a typical AFM force measurement, a force curve is obtained by monitoring the changes in piezo height, *z*, in relation to the cantilever deflection, *d* (Figure 5.1). In the case of soft samples, the measurable deflection can be smaller than the movement of the sample due to sample indentation. The indentation depth, δ, of tip into sample surface is equal to the difference between the cantilever deflection measured on a hard surface and on a soft surface. This is calculated from the normalised baseline value when the tip is off-contact i.e. deflection offset (Figure 5.2). The deflection of the cantilever is proportional to the loading force which can be computed based on the known cantilever spring constant, k. Hence loading force versus indentation (F *vs.* δ) curves can be derived from force curves. The slope of F *vs.* δ curve can be considered to be a qualitative stiffness measurement which reveals different mechanical properties of the scanned surface (Labernadie *et al.*, 2010).

5.2.4 Quantitative analysis of force curves

Quantitative analysis can be very difficult as it requires a good description of the tip-sample interaction and knowing the different forces acting on the cantilever (Piétrement and Troyon, 2000). This is especially true when using a very sharp tip with a very sensitive cantilever of low spring constant as they are subjected to greater interference from tip-sample interactions (Figure 5.1). This needs to be accounted for when considering the model to describe the *F vs.* δ curve.

Nevertheless, a proximate elastic modulus of the sample, *E*, can be obtained by fitting the nonlinear *F vs.* δ curve to a model based on simple tip and sample indentation geometry. The Hertz model (Hertz, 1882; Sneddon, 1965), which assumes frictionless flat contact surface, linear elasticity, small strain, isotropic and homogenous material, predicts in the case of an infinitely stiff tip resembling a cylindrical cone and a soft, flat sample the following relation between indentation and loading force: $F = \frac{2E}{\pi(1-\nu^2)} \tan(\alpha)\,\delta^2$, where F is the loading force, E is the Young's modulus, ν is the Poisson ratio (typically 0.5 for incompressible biological material), α is the opening angle of the cone which is 45^o in our case (value given by the manufacturer Bruker), and δ is the indentation depth. This quasi-quadratic relation is observed for the majority of *F vs.* δ curves.

In the case of force curves, rearrangement of equation to substitute for $F = k(d - d_0)$ and $\delta = (z - z_0)$ gives:

$$d = \frac{2E}{k\pi(1-\nu^2)} \tan(\alpha)\,(z - z_0)^2 + d_0$$

, where k is the cantilever spring constant, and d_0 is the deflection offset which can be easily determined by calculating the mean deflection at the very beginning of the force curves (typically the first 200 nm) when the cantilever is off sample surface (Radmacher, 2002). z_0 is defined as the height where the cantilever deflection begins to level off from the horizontal line, d_0 (Figure 5.2). Determining z_0, the offset of the sample height, is straightforward with force curves on stiff substrate or samples which show a sharp kink in the deflection at the point of contact (Figure 5.5 A, B), but is less definitive with force curves on soft samples (Figure 5.5 C, D). In the case of forces curves showing hysteresis (Figure 5.6), the extending trace of the force curve was chosen to represent the stiffness measurement and modulus.

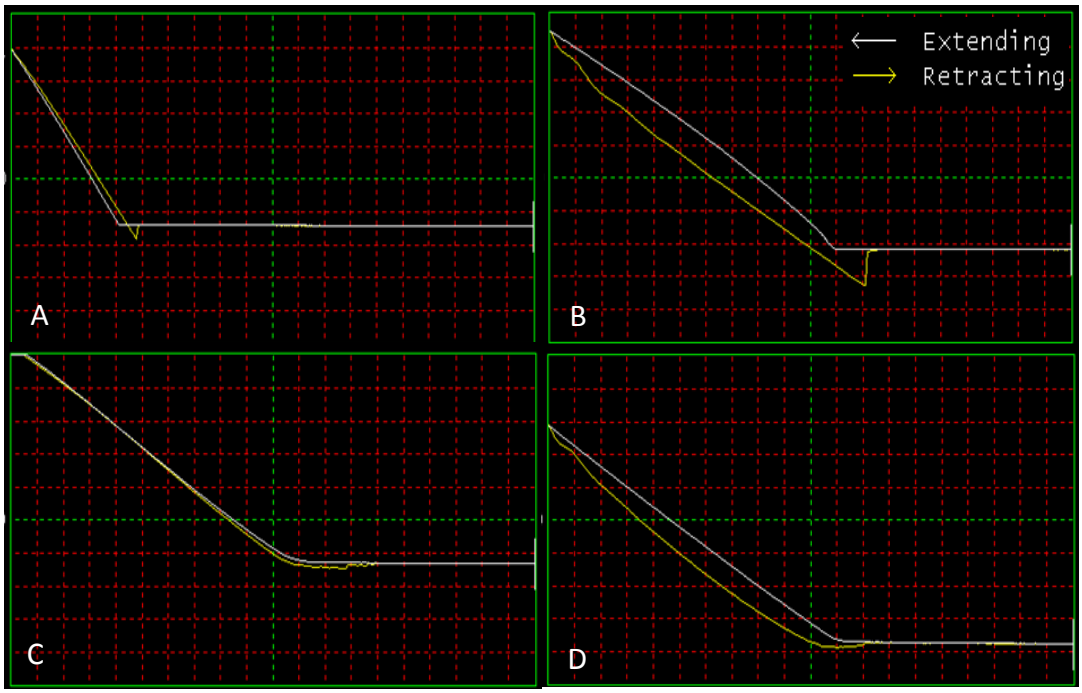

Figure 5.5. Types of force curves obtained from leaf primordial point measurements showing different features which reflect the mechanical properties of plant cell wall. (A) Curve obtained on a hard surface. (B) Curve showing initial stiff surface, get softer with increasing load potentially due to plastic deformation or relaxation process. The kink in the retracting trace is due to adhesive force. (C) Surface which is soft initially and then stiffen with increasing load showing little hysteresis. (D) Similar to C but with large hysteresis. Curves with well-defined interface (A, B) indicate a sharp change in deflection, whereas curves with poorly defined interface (C, D) suggest a more pliable initial interaction.

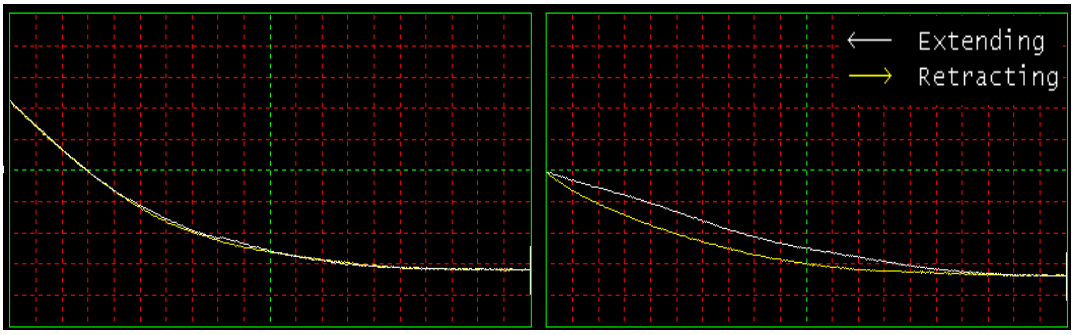

Figure 5.6. Hysteresis of force curves. (A) Curve taken on stiffer area of the sample showed little difference between approaching (white) and retracting (yellow). (B) Curve taken on softer area showed significant hysteresis, indicating that the point of indentation is not returning to its original height after indentation within the timescale of single measurement (< 1 sec). This may indicate the viscous behaviour of plant cell wall.

As the Hertz model assumes a homogeneous and infinitely large sample it can be appropriate only as long as the indentation is smaller than the thickness of the sample. Hence, the extent of indentation depends on the question one is asking. In the case of studying very local cell wall properties, indentation should not exceed the cell wall thickness, modelled to be 250 nm in SAM (Milani *et al.*, 2011). If the range of the force curve used for analysis is chosen such that the cell wall is substantially compressed, the values of the elastic modulus would be erroneous as it would also involve the underlying turgor pressure. If the question is on cellular mechanic properties, indentation should not surpass the depth that would involve the neighbouring cells. In this study, force mapping was performed with less than 1 μm indentation to study tissue properties, with stiffness fitted using a 150 nm range of the force gradient. For local point measurements to study cell wall properties, the indentation is less than 400 nm with contact stiffness values taken from force gradient within a narrow range of 40 nm. Nevertheless, it should be noted that the relative measurements of stiffness remained comparable between the fully turgid and semi-plasmolysed tissue immersed in mannitol solution (results from empirical works not shown). Therefore, the contribution of turgor pressure was considered to be negligible for relative comparison of tissue stiffness within the same force map.

On the other hand, Hertzian models do not take into account tip-surface adhesion (Johnson *et al.*, 1971). Since most adhesion forces were always small or negligible in this study, and any force curves that showed large adhesion were excluded from the analysis. This is evidenced by the fact that 78% of 1400 force curves reported here from point measurements can be fitted with an $R^2 > 0.96$, and 60% with $R^2 > 0.99$.

5.3 Results

5.3.1 Force maps reveal heterogeneity in cellular and tissue mechanical properties

To study the mechanical changes during early leaf morphogenesis, I performed AFM force mapping as described above on young tobacco seedlings, more specifically on intact leaf primordia (300-400 μm), with the cotyledons and more mature young leaves carefully removed for access. The whole seedling including the root was embedded sideways on a glass microscope slide with the infiltration of low-melting agarose, exposing only the area for scanning (Figure 5.7A). The sample was always kept under water. The leaf margin is an area of great interest because it forms the boundary between the upper and lower surfaces of the lamina, and is believed to play an important role in the control of leaf shape (Reinhardt *et al.*, 2007; Malinowski *et al.*, 2011). Hence, the initial study was focused on the marginal area of leaf primordium, which also has the advantage of being relatively easy to access.

Figure 5.7C shows the stiffness measurements across two independent leaf primordia margins obtained from 2500 force curves over a total scan time of 20 minutes each. These are presented as force maps together with the topographic height maps (Figure 5.7B) automatically reconstructed from the force scans. Force scanning every 2 μm i.e. 50 x 50 pixels strikingly reveals cellular resolution. Outlines of individual cells are clearly visible as stiffer anticlinal walls. The stiffness measurements within single cells appeared to be non-homogenous with increasing compliancy toward the centre. At larger scale, there is no indication that the height of the sample surface influenced the force measurement, with little correlation between topography (Figure 5.7B) and force maps (Figure 5.7C), i.e., the differential stiffness measure is not simply due to topography. Furthermore, the samples are prepared in opposite orientations but show similar results. In both cases the adaxial side facing towards the shoot apical meristem is about two-fold stiffer than the abaxial side. Additionally, the boundary between the two sides of the leaf (abaxial and adaxial) appeared to be much stiffer than other regions.

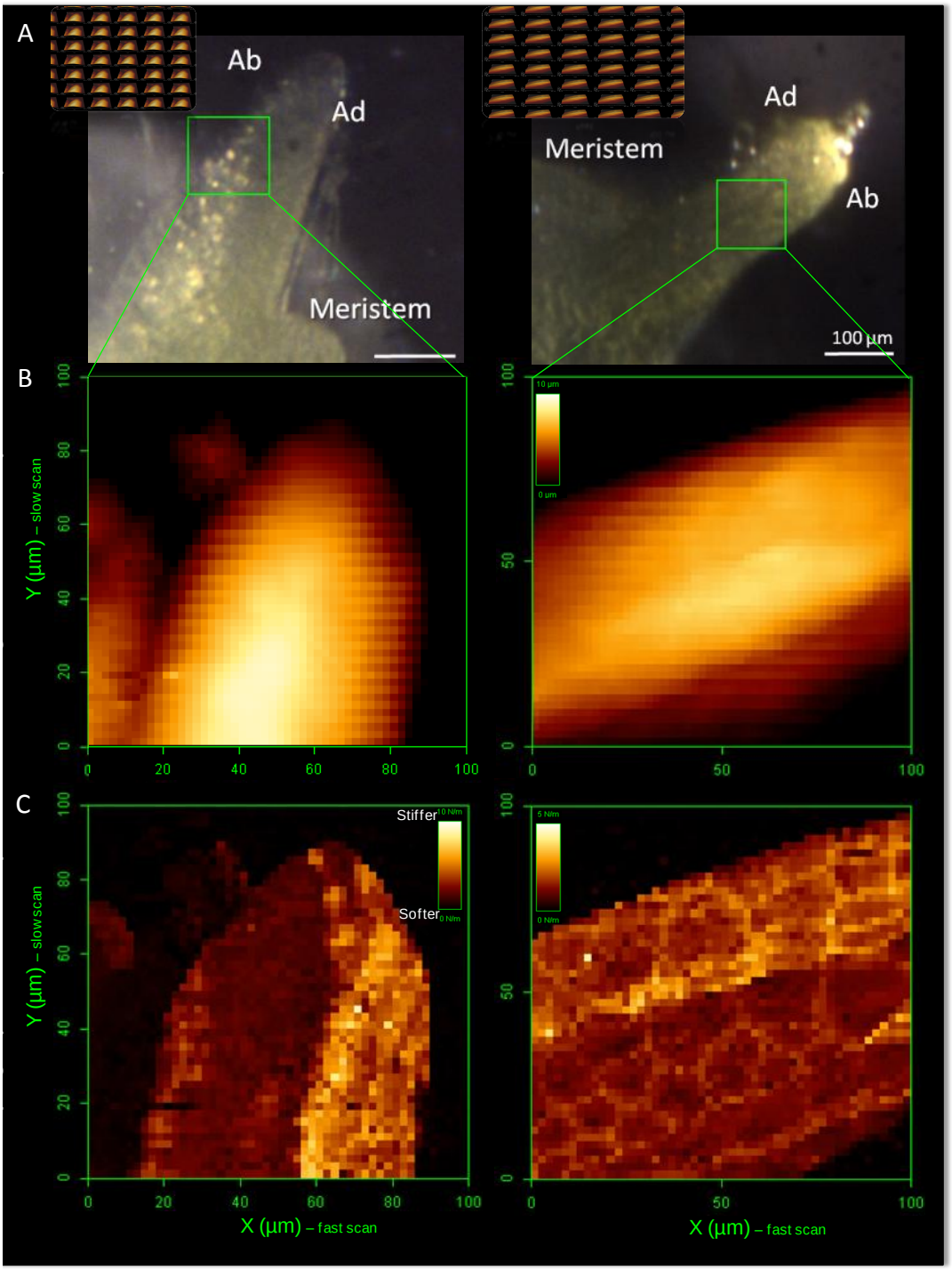

Figure 5.7. Force maps taken across two independent samples of tobacco leaf primordia showing the distinct tissue stiffness with the adaxial (ad) side being stiffer then the abaxial (ab) side. (A) The region scanned. Areas of force measurement are indicated by the green boxes. Insets show the three dimensional height mapping of the primordial surfaces. (B) Topographic height map of the scanned surface. (C) The stiffness measurements on a relative scale. Scale bars = 100 µm.

5.3.2 Independent point measurements corroborate force map results

To validate these observations through an independent platform, I performed more detailed force scans using a different AFM machine with much greater sensitivity and less indentation. During automated force mapping, only one force curve was taken at each point of measurement. For a more precise approach, manual forces curves were taken repeatedly at each sampling point to check the reproducibility of force curves. This was carried out systematically down the length and across the tobacco primordium (Figure 5.8). There appeared to be a stiffer region near the tip of the leaf primordium (20-30 μm from the tip) followed by a softer region, then a stiffer region towards the base of the primordium (Figure 5.8A). Measurements taken across the primordium from the adaxial to the abaxial side revealed a pattern in which the adaxial tissue became gradually stiffer towards the margin of the leaf, followed by a precipitous fall in stiffness on the abaxial side, but which recovered in regions closer to the abaxial edge (Figure 5.8B). Individual measurements were robust with low variance of measurements taken from any one spot on the leaf.

At first glance, there was no clear pattern of stiffness emerged from the point measurements. One possibility is that this may be due to the probe hitting different parts of the cell during point measurements. As our initial scanning measurements indicated, there is heterogeneity in stiffness within single cells and our point measurements were not restricted to any particular position within a leaf. To check this idea, transects were made across the force maps at different regions and orientations to simulate possible scenarios of point measurements (Figure 5.9). Indeed, the stiffness profiles were as similarly variable as the results from point measurements, albeit both were carried out under using different parameters. When going down the length of leaf primordium, the most likely scenario would be that point measurements were sampled along the boundary between the two sides (Figure 5.9A). Within the two sides, the stiffness profiles were less variable but there was a large fluctuation at the boundary region consistent with that seen with point measurements (Figure 5.9B). This demonstrates the great value of force mapping for the interpretation of tissue mechanical properties.

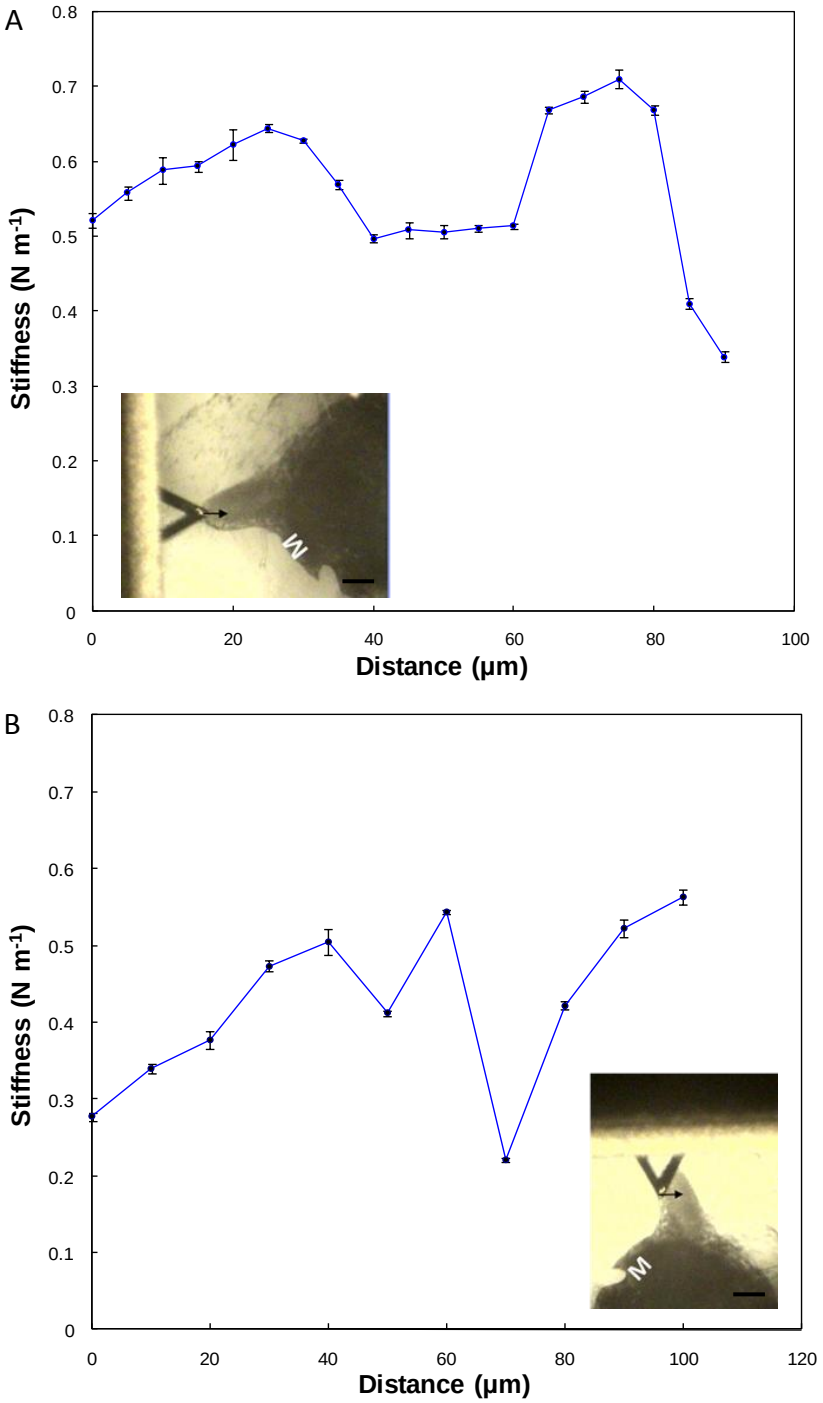

Figure 5.8. Point measurements (A) down along the margin of a tobacco leaf primordium towards the meristem (M), and (B) across the tobacco leaf primordium from adaxial to abaxial side. Arrows showing the direction of sampling. Values are means ± SD from 10 repeated measurements. Scale bars = 100 μm.

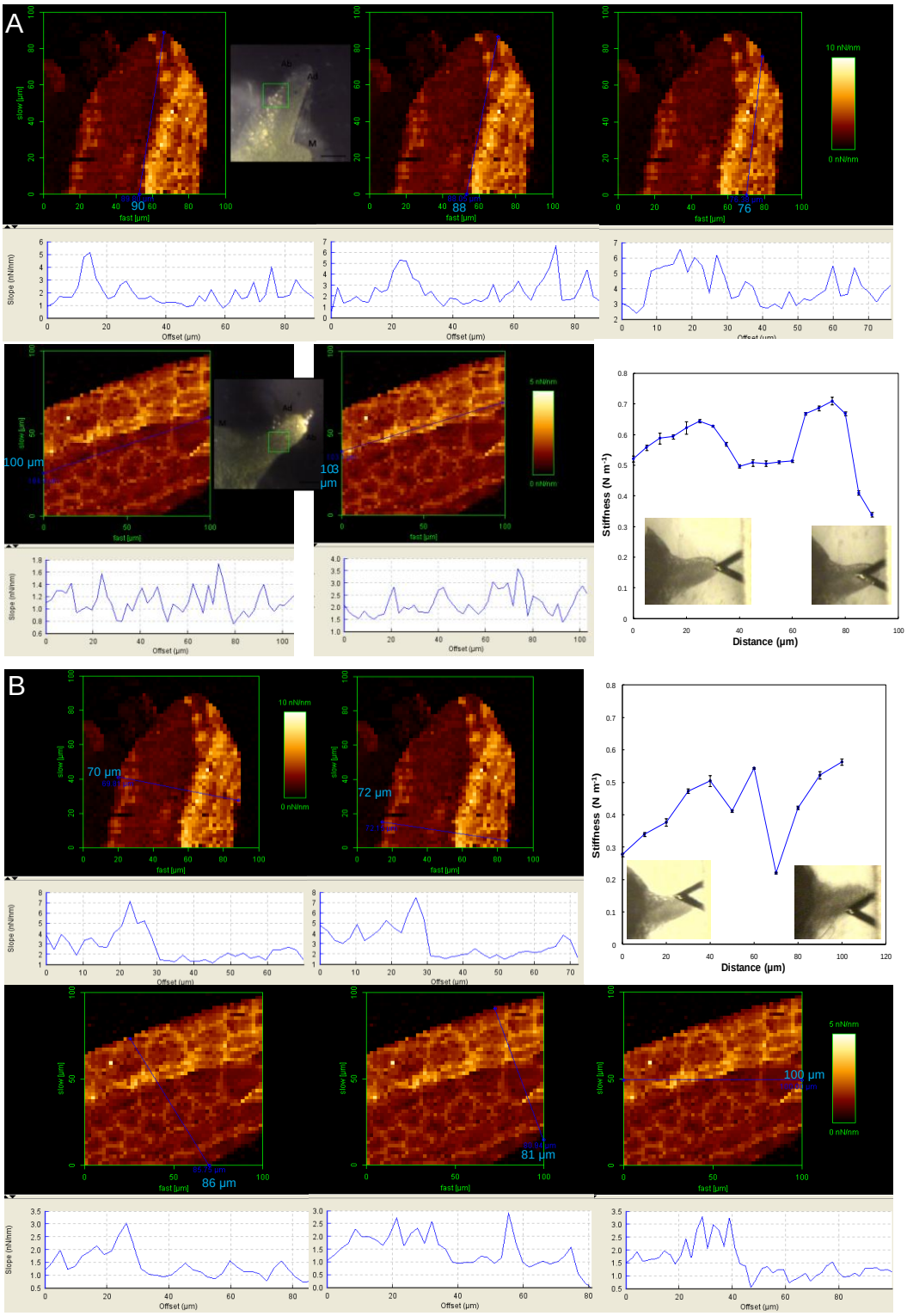

Figure 5.9. Comparison of stiffness measurements extracted from transects of independent force maps and point measurements (A) along, and (B) across the tobacco leaf primordia. The transects across the force map in different orientations with respect to the direction of point measurements are indicated as blue lines with distance in µm shown at the end of transect. The profiles of the stiffness measurements across different transects are depicted in the graphs under the force maps. Insets of point measurement graph show the picture of the start and end points of measurement.

To investigate the applicability of force mapping as a proxy for cell wall mechanical properties, force maps taken along the margin of a tobacco leaf primordium were pieced together using the same relative scale, and fitted with Hertz's model to yield a map of elastic modulus for quantitative comparison (Figure 5.10). Understandably, this allows only a crude comparison to be made as force maps suffer from imprecision in quantification due to many uncertainties underlying the model fitting, as well as greater indentations beyond the cell wall thickness (as discussed in method considerations). This is clear as many of the force curves cannot be fitted and result in black pixels on the map of Young's modulus (Figure 5.10E). Nevertheless, this map was useful to show the direct correlation between stiffness and elastic modulus. Furthermore, one can see the that with the force mapping approach the tip and base of the leaf are distinctly stiffer than the region just below the tip (Fig. 5.10E), which is reminiscent of the longitudinal pattern of stiffness obtained from the point measurements (Figure 5.8A).

Figure 5.11 shows the comparison between the Young's modulus from point measurements and sampling of force map. Young's modulus values of 0.24±0.04 (n = 26), 0.25±0.06 (n = 21), and 0.18±0.03 (n = 16) were obtained along the adaxial, middle and abaxial side respectively (Figure 5.11A, B). The rather large standard errors on the obtained average values reflect variability of the point measurements along the surface of the same side as well as variability associated within single cells. Although the differences in adaxial and abaxial values were not statistically significant, they were comparable to that obtained by use of force maps (Figure 5.11C). The margin boundary between the stiffer adaxial and softer abaxial sides appeared to be stiffer by up to 1 MPa. On average, the adaxial side has a higher value of Young's modulus and a higher variation in stiffness than the abaxial side (Figure 5.11D, E).

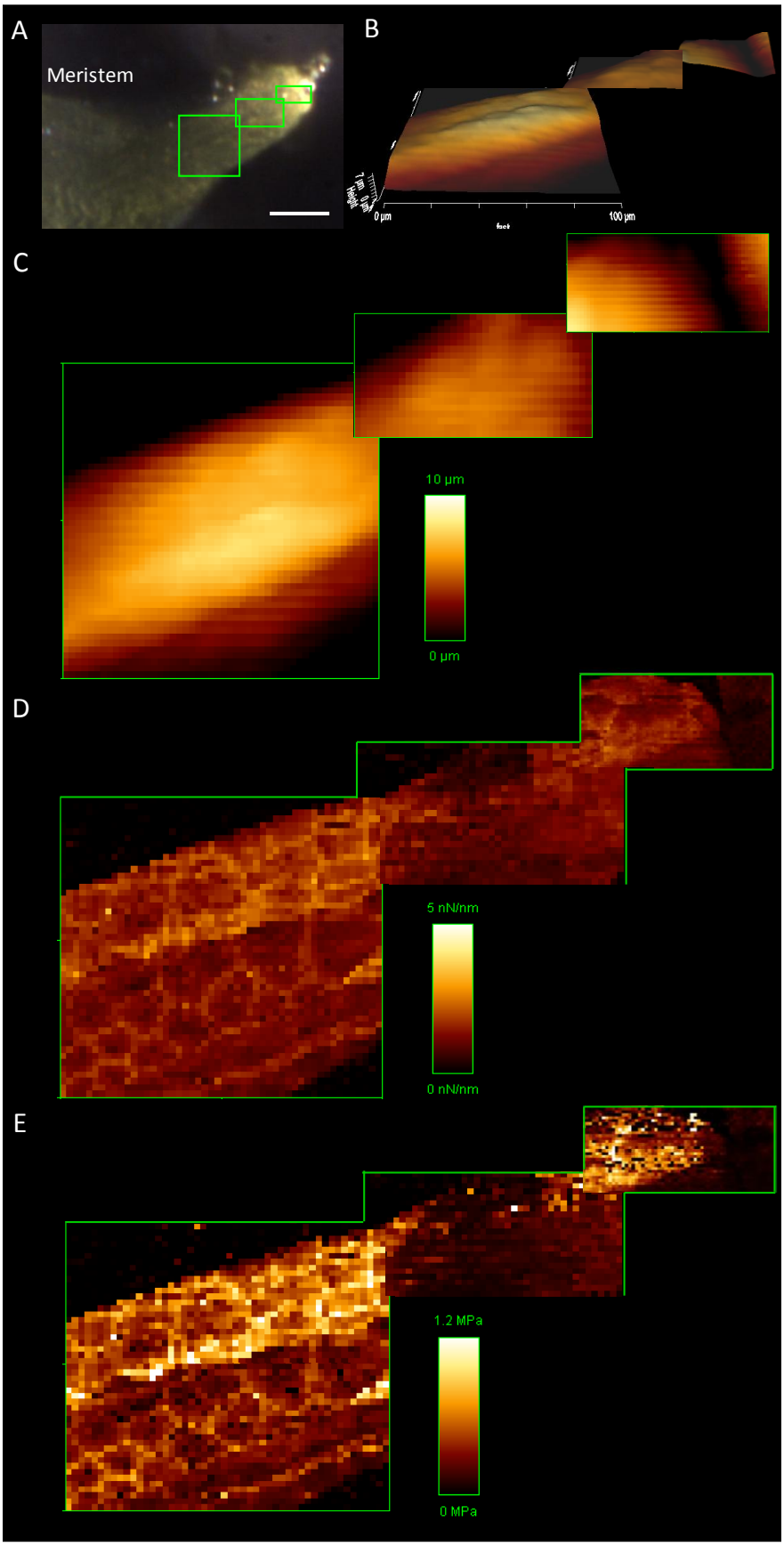

Figure 5.10. Force maps taken along the margin of tobacco leaf primordium. (A) The regions scanned (green boxes). Topographic height map of the scanned surface in (B) three dimension and (C) two dimension. (D) the stiffness measurements on a relative scale. (E) Map of Young's modulus after force curve fitting with Hertz's model. Scale bar = 100 µm.

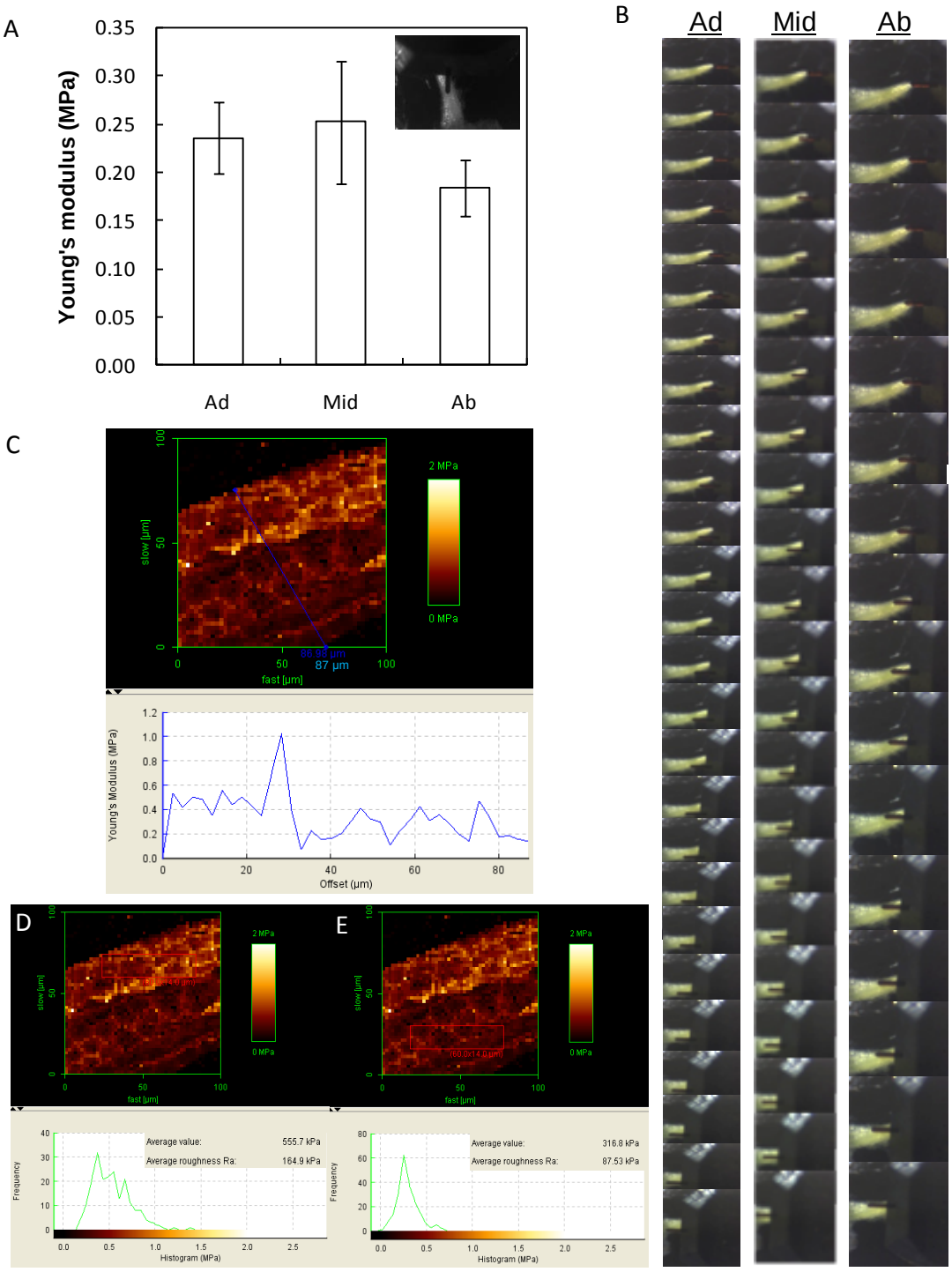

Figure 5.11. Comparison between force maps and point measurements on the margin of tobacco leaf primordia. (A) Young's modulus calculated from individual force curves fitted with Hertz's model obtained from point measurement along adaxial (Ad), middle (Mid) and abaxial (Ab) region of leaf primordium. Values are means ± SE (n = 17-27). (B) Sequential images of the location measured. (C) Transect across the Hertz's model- fitted force map of leaf primordium indicated as blue lines with distance in µm shown at the end of transect. The profile of the Young's modulus across the transects are depicted in the graph under the force map. Young's modulus map sampling on the adaxial (D) or abaxial (E) surface showing the histograms under the map with the sampled area indicated by red boxes.

5.3.3 Mechanical properties of Arabidopsis *leaf primordia*

The data described above indicated that tobacco leaf primordia show distinct variation in mechanical properties. To investigate whether this was the case in other plants, I decided to carry out detailed point measurements using Arabidopsis leaf primordia. A wealth of genetic material is available for this model plant (including the lines described earlier in this thesis with respect to altered expansin gene expression). Thus, if a robust pattern of mechanical properties can be established for this material, it would open the door to a large number of investigations linking gene function with tissue mechanics and morphogenesis. At the same time, the relatively small size of Arabidopsis leaves and their accessibility raises challenges for this type of analysis.

Figure 5.12 shows the results of an experiment in which point measurements were taken with AFM across the abaxial surface of a young leaf primordium (width ≈ 300 μm). Due to the constraints on access, the point measurements could not be taken in a simple orthogonal pattern mirroring the leaf lateral/longitudinal axis. Rather, the X-axis measurements extend inwards from a point on the leaf edge slightly off centre from the true leaf tip in a direction which cuts across the longitudinal axis of the leaf (black line in 5.12A). The Y-axis measurements are orthogonal to the X-axis and thus traverse across the abaxial surface, crossing the true longitudinal axis (black dotted line in 5.12). The point measurements are shown in a colour-coded fashion in Fig. 5.12B. The black dotted line in Fig. 5.12B indicates the approximate orientation of the leaf longitudinal axis (midvein), with the leaf tip towards the (0, 0) co-ordinate. The results indicate a complicated pattern across the abaxial surface. The tip of the leaf again seems to represent an area of relative stiffness (high Young's modulus) with a region just behind the tip showing a relatively low stiffness (indicated by both the X-axis (red) measurements and the Y-axis (green) measurements). This similarity in value obtained by orthogonal measurements again suggests that this relatively soft region behind the leaf tip is not an artefact of topography but reflects a real difference in tissue mechanical properties. Further back along the longitudinal axis towards the base of the leaf there is a region of stiffer tissue (towards co-ordinates (100, 100) of the lateral "yellow" measurements. Variation in tissue stiffness is also observed other regions across the leaf surface,

although the density of point measurements taken makes it difficult to draw a true stiffness map across the entire abaxial surface.

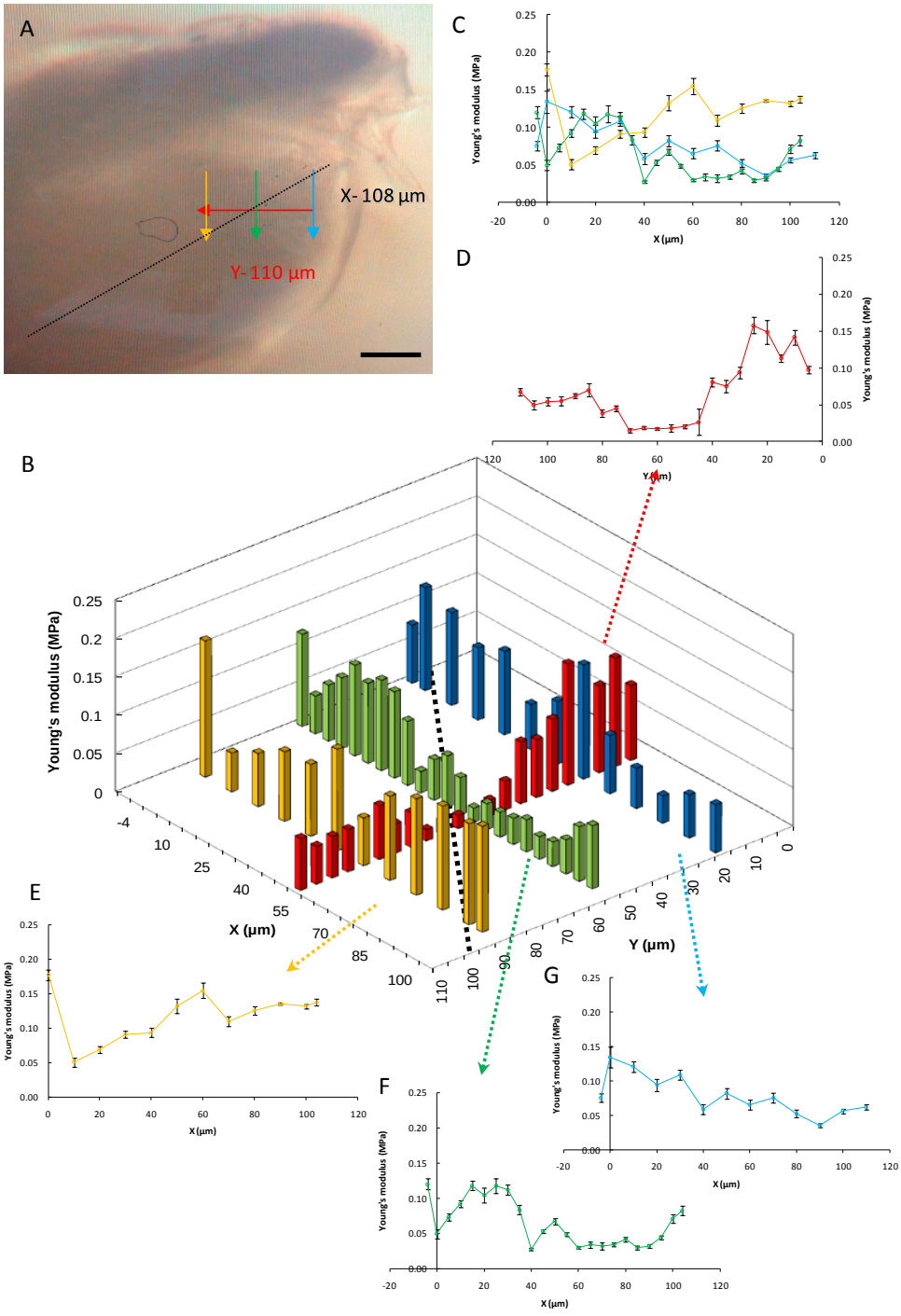

Figure 5.12. Point measurements of the abaxial surface of an Arabidopsis leaf primordium. (A) Photo of the measured area of the leaf primordium showing the proximate transects of the systematic point sampling for force scan. Values indicate the distance of the transects along the X-axis and Y-axis. Black dotted line indicates the leaf midvein. (B) Quantitative measurement of the cell wall elastic modulus plotted according to the colour-coded transects in the direction of the solid arrows and dashed line as per (A). (C) Measurements along the Y-axis. (D) Measurements along the X-axis and respective plots (E, F, G) for clarity. All values are means ± SD (n > 10). Scale bar = 100 µm.

Figure 5.13 shows the results of a series of point measurements taken along the margin of an older leaf primordium (length ≈ 500 μm). In this case, due to the orientation of the sample the X-axis measurements provide a reasonably good reflection of the longitudinal axis along the leaf margin, whereas the Y-axis measurements provide a good reflection of changes in stiffness in an orthogonal direction. Along the longitudinal axis ("red" measurements in Fig. 5.13B) there is again a pattern in which there is a region behind the leaf tip in which tissue stiffness is relatively low. Across the orthogonal Y-axis the differences in measurements are not so apparent. However, in all cases the individual measurements at a point show low variation and, moreover, at the crossover points of the measurements taken in the X and Y orientation the measurements show a good level of consistency, indicating that any differences observed are unlikely to represent artefacts related to topography.

Finally, it is noticeable that the absolute quantification of Young's moduli all lie within the range of 0.1 to 1.6 MPa and were very comparable to those obtained using the force mapping approach. This is despite the fact that the measurements were taken from different leaf samples and using two different platforms of AFM with different sensitivities. This consistency using two different methodologies increases the confidence in the values obtained.

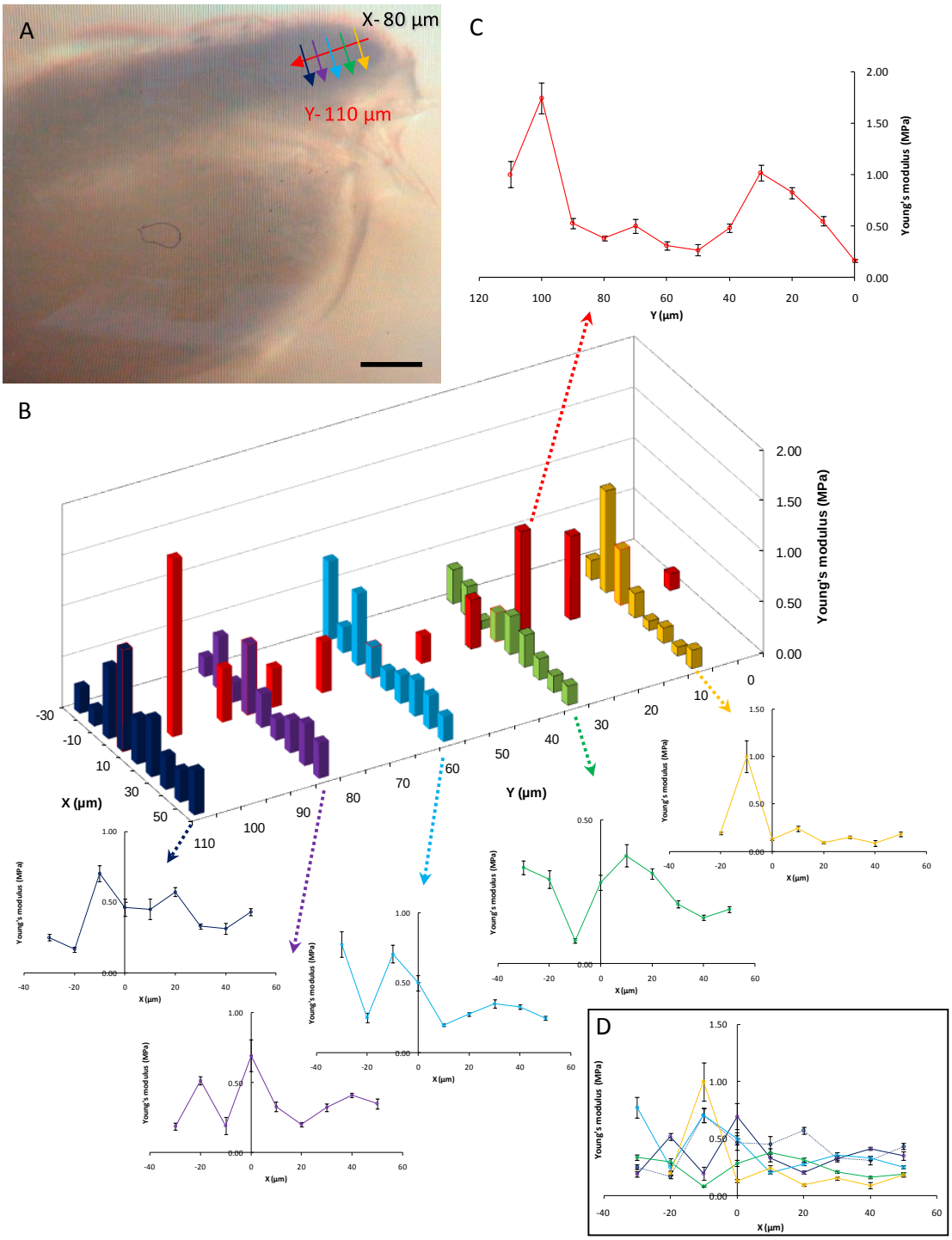

Figure 5.13. Point measurements of the side of an Arabidopsis leaf primordium. (A) Photo of the measured area of the leaf primordium showing the proximate transects of the systematic point sampling for force scan. Values indicate the distance of the transects along the X-axis and Y-axis. (B) Quantitative measurement of the cell wall elastic modulus plotted according to the colour-coded transects in the direction of the solid arrows as per (A). (C) Measurements along the Y-axis. (D) Measurements along the X-axis and respective plots are indicated by the dashed arrows for clarity. All values are means ± SD (n > 10). Scale bar = 100 µm.

5.4 Discussion

In the results reported above, I have demonstrated the utility of AFM as a method to identify and characterise differential tissue mechanical properties in young, intact, living leaf primordia of tobacco and Arabidopsis. Below I discuss some aspects of AFM and lessons to be taken into consideration for future research if AFM is to be established as a standard technique for studying tissue mechanics during morphogenesis.

5.4.1 Applicability of AFM for the characterisation of in vivo plant tissue mechanical properties

The application of a technique in a novel context requires a number of points to be taken into consideration to ensure appropriate interpretation of the data. In the context of AFM measurements of living plant tissue the first and most important point is to understand and define exactly what is being measured. AFM developed for the measurement of uniform planar solids. In contrast, the plant cell wall is a highly complex compound material which shows a combination of elastic and viscous properties. Moreover, biological surfaces are generally non-planar except for very small areas. Thirdly, in living tissue an internally generated turgor pressure acts on the cell wall, potentially confounding measurements aimed at discovering mechanical properties of the cell wall. At the same time, the biologically relevant properties of the cell wall may depend on the material being under tension, so that removal of turgor pressure may itself confound the measurement of biologically relevant properties. Clearly, any data obtained from living plant tissue with AFM must be interpreted by taking these facts into consideration.

For any new measurement system it is very useful to compare the data obtained from the new system with those by other more established classical methods. As mentioned, AFM is fundamentally similar to other well-established approaches in the study of cell wall mechanical properties such as extensometer or Instron (named after the manufacturer), which is based on the stress and stain relationship (Cosgrove, 1993). The big difference lies on the scale and sensitivity. Nevertheless, the force curves obtained reflect a great extent the viscoelastic properties of the plant cell wall (Figure 5.5). The hysteresis in the force curves (Figure 5.6) is akin to that of

obtained during loading and unloading cycle of Instron measurements, which suggests a plastic deformation. Recent reported values using Instron approach include the young internodes of poplar (3.7 MPa) (Park *et al.*, 2004) and winding liana (8-10 MPa) (Köhler *et al.*, 2000), 1-4 MPa for maize mesocotyls (Schopfer *et al.*, 2001) and 21-28 MPa for Arabidopsis hypocotyls (Ryden *et al.*, 2003). However, comparison is not straightforward as these tests were performed differently to AFM by applying uniaxial tensile stress to a clamped tissue. A value of 2 GPa was reported for single suspension-cultured tomato cell measurement, in which the entire cell was subjected to mechanical stress by micromanipulative compression (Wang *et al.*, 2008). Recent model predicted the mechanical properties of a primary plant cell wall to range from 41-405 MPa and 0.7-42 MPa respectively, along and transverse to the direction of cellulose microfibrils (Kha *et al.*, 2010). In general, the values obtained here with AFM approach (0.1-2 MPa) are considered to be at the lower range of the scale, which may reflect the very young stage of tissue with intensive cell expansion. It may also indicate differences in the technical aspects of AFM to other methods with respect to the scale of measurements.

To explore different scales of measurement, I applied two distinct approaches of AFM to investigate the same organ, young developing leaf primordia, of two plant species. The spherical colloidal tip for force mapping interacts with much greater area in contact as compared to the sharp pyramidal tip for spot measurements (Figure 5.4). Hence, the forces measured from both approaches were accounted for by very different indentation depths (1 μm vs. 400 nm), which reflect the different extent of cell wall area measured. Despite differences in the machines, probe types and tissue samples, comparable values of elastic modulus to that of literature (as discussed above) can be obtained. Furthermore, these values agree closely to values below 10 MPa reported by Milani *et al.* (2002) on the shoot apical meristem (SAM), with over 75% measurements from the flank of SAM below 2 MPa. This is surprising because the authors chose a more defined approach, with much less indentation (~ 150 nm) in the quantification of local cell wall properties, yet the quantitative values are comparable to that reported here. This suggests that the contribution of turgor pressure to the measurements made in current study may not be as prominent as I have anticipated. If this is to be the case, I can exclude the possibility of profound cell–cell mechanical interactions and intercellular water flows. Furthermore, the

scenario that it might involve cells sliding relative to one another is unlikely because of the very small force applied (< 50 nN).

Nevertheless, the AFM approach is not without its shortfalls. There is no doubt about the sensitivity of AFM for extremely small-scale measurements as suggested by its name and purpose of invention for nano-range imaging. In this respect, high sensitivity of AFM may be a double-edged sword when this technique is applied to tissue-level measurements. To obtain a precise quantitative value on a sample surface, the scope of measurement becomes constrained to a very local area. This is due to high sensitivity of the cantilever to lateral forces imparted by surface geometry as the tip orientation is not normal (90^o angle) to the point of contact (Section 5.2.4). To circumvent this issue, previous investigators took measurements only over a very small area (Milani *et al.*, 2011), similar to that of point measurement approach reported here. However, this still require force curve filtering and assumptions on the simple models e.g. Hertzian model used for curve fitting (Dintwa *et al.*, 2008) as described in Section 5.2.4. Moreover, the measurements obtained can be very varied due to the heterogeneity of cell wall properties even at subcellular level (Figure 5.7). This confined previous investigators, who acknowledged this inherent variability, to target only specific middle region of cells (Milani *et al.*, 2011). However, this required surface imaging due to a limitation in optical visualisation. Hence, this greatly limits the throughput of data acquisition to only 13 excised shoot apical meristems with about 300 force curves taken from each location of interest (Milani *et al.*, 2011).

Point measurements, albeit suffice to detect a certain pattern (Figure 5.11A), would require a great number of force curves within locations of interest to show statistical significance. Furthermore, this approach essentially missed out many features at supra-cellular level, which are of great interest in the field of morphodynamics to observe changes in tissue mechanics over time. A good agreement of quantitative values at the points of cross-over during orthogonal transect sampling of point measurements (Figure 5.12-13) suggests that the influence of tissue geometry may not be profound (Dintwa *et al.*, 2008). In this respect, I have demonstrated a great advantage of taking force maps (Figure 5.9-10), which pose a trade-off between scale and precision at current stage of technique development. At present, the

stiffness values calculated are the force required to deflect the surface by a given distance at the point of contact - this includes contributions from all the possible deflection mechanisms (deflecting the cell wall elastically at the site of contact, large scale bowing of the surface, plastic deformation of the wax layer, etc.). Some calculations and perhaps modelling would be required in order to separate the contributions from different mechanisms to obtain true values of cell wall elasticity. Nevertheless, the success of force maps in capturing the supra-cellular as well as subcellular heterogeneities in elasticity reflect its tremendous value for qualitative studies. Furthermore, the ability of AFM to reconstruct the topographic data during force mapping could be utilised to tease apart the relative contribution of lateral forces from surface geometry. A calibration curve approach has been proposed to correct for large deformations (Dintwa *et al.*, 2008). Hopefully, with this optimisation this technique can be developed for standard quantification in the future.

Lastly, concerning the tissue sample viability, my approach with minimal preparation to ensure intact root and shoot (except dissected mature leaves) allowed the measurement on leaf primordium to be taken over long time range. Low-melting agarose was chosen to embed the sample, by infiltrating the surrounding of the seedling on glass slide, worked well in keeping the sample steady and hydrated. Undoubtedly, to acquire real time data on growth processes *in vivo* is of great challenge and sample preparation is of primary consideration to ensure true representation rather than artefacts of sample handling. This possible artefact is excluded by good agreements of different measurements taken at the same position but at different time points over 30 minutes apart (Figure 5.12, 5.13), as well as between two leaf primordia on the same shoot with over 3 hours apart (Figure 5.12 vs. 5.13). Furthermore, this approach of sample preparation may allow time-course experiment to follow changes in cell wall properties with growth. Overall, the results presented here which agree well with that of reported in the literature increase the confidence for data interpretation.

5.4.2 The biological significance of differential stiffness between leaf primordial surfaces

Despite the potential confounding effect of turgor, force maps obtained in this study suggest distinct mechanical characteristics between the upper and lower surfaces of young tobacco leaf primordia. The adaxial-abaxial leaf polarity is genetically determined during early leaf development (Bowman *et al.*, 2002). Leaf dorsoventrality is essential for the blade outgrowth and the flattened architecture of leaf. This is clear from the radialised rod-shaped 'leaf' with the absence of lamina in leaf polarity mutant tobacco and Arabidopsis plants (McHale and Marcotrigiano, 1998; Siegfried *et al.*, 1999; Kerstetter *et al.*, 2001; Iwakawa *et al.*, 2002; McHale and Koning, 2004). The genetic pathways controlling the leaf polarity has been extensively studied (Barkoulas *et al.*, 2007; Kidner and Timmermans, 2007). To my knowledge, there is no report on the link of these genetic networks to differential mechanical properties of the resultant tissues. It would be interesting to study whether there is a functional basis to this difference by performing AFM force mapping on some of the leaf polarity mutant plants.

Meanwhile, one can speculate the functional significance for the mechanically distinctness of the two leaf sides. Leaves are not flat at inception and primordia grow upwards to partially cover the shoot apical meristem before growing outwards into a more flattened form (as described in Chapter 1, Figure 1.1). To generate this upward curling, the abaxial leaf side must grow faster than the adaxial side. The results presented here suggest this differential growth may arise by differential cell wall properties. Thus, if the force for growth (the result of combined metabolic and turgor processes which underpin growth) were the same in both the presumptive adaxial and abaxial sides of a leaf, a relatively stiffer cell wall matrix on the adaxial side would automatically result in a higher growth rate on the abaxial side relative to the adaxial side. This would ensure that the young primordium curved inwards over the apical meristem. According to this hypothesis, key downstream effectors of the identified ab/adaxial factors (Figure 1.1) (Eshed *et al.*, 2001) would be effectors of cell wall structure/architecture. Data mining of microarray data obtained from such mutants would allow a first test of this hypothesis. It would also be very interesting to investigate whether the differential stiffness measured in wild type primordial is altered in the various extant ab/adaxial mutants.

On the other hand, it is possible that the differential tissue mechanical properties observed arise from growth processes themselves rather than being regulated *per se*, resulting in a chicken-and-egg dilemma. Again, investigation of leaf ad/abaxial mutants would help resolve this issue. A number of authors have proposed that the outermost tissue layer (L1) is believed to control growth (Marcotrigiano, 2001; Anastasiou and Lenhard, 2007; Savaldi-Goldstein *et al.*, 2007; Savaldi-Goldstein and Chory, 2008) and, especially, that the leaf margin might play an important role in leaf morphogenesis (Reinhardt *et al.*, 2007). The results reported here seem to indicate that the marginal cells are relatively stiffer than the surrounding cells (Figure 5.11), perhaps to counteract the greater tensile stress between the two surface layers with distinct mechanical properties (Figure 5.7). Further studies characterising leaf polarity mutant plants using the AFM approach will help clarify this and much of the interesting questions arising from my current work.

5.4.3 Future implications for the application of AFM

Although there is still much work to be done to formalise the protocols for the application of AFM to living plant tissue and to relate the underlying cell wall biophysics and osmotic turgor in relation to the measurements made, my work provides a starting point for applying the AFM technique to the study of plant tissue mechanics during organ morphogenesis. AFM is also potentially of great value for detailed studies on the dynamics of cell wall behaviours at subcellular resolutions, to understand the pliancy changes in cell wall during single cell division or cell expansion within a tissue context. By changing the probe dwell time and frequency of the cantilever movements, AFM technique could be developed to study single-cell extensibility at high resolution by recording changes over short-term time scale.

Currently, there is a growing interest for studies on cellular growth processes, with a focus on the modelling of cell wall biomechanical responses to tensile stress generated by turgor pressure, to bridge the gap between genetics and biophysics (Geitmann and Ortega, 2009; Boudaoud, 2010; Geitmann, 2010; Hamant and Traas, 2010; Uyttewaal *et al.*, 2010; Mirabet *et al.*, 2011). These mathematical models require quantitative data on relevant biophysical parameters, geometry and cellular structure. In this respect, I have demonstrated the possibility of using AFM to provide data for such models, providing quantitative information on cell wall

mechanics and surface topography. More empirical studies are required to establish a standard protocol for larger scale tissue mechanic studies but meanwhile one could already perform studies on more defined, local cellular structures, for example the guard cells and pavement cells in the developing leaf epidermis. Other areas of interest would be investigations on root hair initiation, gravitropic root bending, as well as hypocotyl elongation. These systems have the advantages of relative ease of access for analysis and a wealth of genetic tools for testing specific hypotheses. Other more challenging projects include the morphogenesis of floral organs on young inflorescence meristem, and the formation of leaf serrations or hydathodes. All of these topics suffer from a major gap in our understanding of how the patterns of transcription factors and signalling components are actually transduced into altered form. Advances in AFM technology provide a key to unravelling this problem. In particular, when combined with better fluorescence optics, computational approaches and molecular genetics, the way is open to the development of a new field of mechanomorphodynamics.

5.5 Summary

This chapter reports on my attempts to develop a method for the *in vivo* analysis of plant cell wall properties at a resolution appropriate for the study of plant morphogenesis. I have described my pioneering approaches in using AFM for the studies of leaf primordial tissue mechanics *in planta*. I have demonstrated that the finer scale and greater sensitivity of AFM technique, has allowed the identification of differential tissue mechanical properties previously overlooked by the more limited *in vitro* studies. The different features of the force curves obtained reflect the viscoelastic nature of plant cell wall. By using AFM of different platforms and comparing results obtained from different plant species, the measurements appear to show reproducible trends between leaves, independent of the timing of analysis and the analysis methods. This indicates a marked difference in cell wall mechanical properties across the dorsoventral axis of young leaf primordia with a more compliant abaxial side, whereas the gradients of different cell wall properties across the mediolateral axis of the abaxial surface were more complicated. Additionally, I have also discussed the different considerations to be made when applying the AFM approach for the quantification of cell wall properties. Simple Hertzian mechanics (Section 5.2.4) may be inadequate to describe the geometry and forces involved in the indentation of leaf primordia cells. This is unsurprising as we know that the leaf structure is far from homogenous and isotropic at the length scales involved in the measurement. However, a crude proximate approach did produce comparable results with other studies and future optimisation with calibration curves could resolve this issue. Overall, AFM has been shown to be a promising approach for *in vivo* study of plant organ mechanics. Ultimately, this technique will then be used to analyse the outcome of altered expansin activity on plant tissue *in vivo*.

CHAPTER 6 General discussion

In this chapter, I bring together the findings from previous chapters to discuss the principle conclusions, the position of current research project in the field, further implications and future work to address the unresolved questions. To begin, I will first outline the principle findings from current work:

6.1 Summary of principle conclusions

- Despite varied expression patterns of individual expansin genes, the overall expression pattern of *EXPA* genes in Arabidopsis Col-0 wild-type leaf development correlates with the progression of different developmental stages.
- Across different stages of Arabidopsis leaf development, expansin transcripts are most abundant during the mid-phase of leaf development with the greatest number of detected *EXPA* transcripts just before the peak of maximum expansion and an abrupt change in a major leaf morphometric parameter (length:width ratios).
- RT-PCR analysis and microarray data mining indicate that there is no leaf-specific expansin gene expression, whereas some expansin genes are expressed specifically in the root (*EXPA7, 17, 18*, and possibly *EXPA12* &*14*) or floral organs (*EXPA21, 22* & *23*).
- The expansins found to be expressed during Arabidopsis leaf development are largely dominated by the members of clade I (*EXPA1, 5, 10* & *15*) and clade IV (*EXPA3, 4, 6, 9* & *16*). Not all of these genes are grouped together in the clustering of microarray data from AtGenExpress experiment series based on different tissue samples, suggesting a cell-type rather than tissue-specific function of diverse expansin genes. Furthermore, expansin genes from the same clade do not group together in the clustering of microarray data from the AtGenExpress hormone experiment series, indicating

functional specificity may be conferred by differential hormonal regulation of expansin genes of the same clade.

- Targeted down-regulation of expansin gene expression during leaf development (*EXPA1, 3, 5* & *10*) resulted in repressed leaf growth, which confirms the role of expansins in leaf growth.
- Targeted over-expression of *CsEXPA1* promoted leaf growth at low level, but repressed growth when expressed at high level despite a significant increase in petiole mesophyll cell size. This suggests suggesting a dose-dependent effect of expansin on growth.
- The effects of manipulating expansin gene expression (both down-regulation and over-expression) are more pronounced in the petiole than the lamina, suggesting a more complex regulation of lamina growth than petiole elongation.
- The manipulation of expansin gene expression (both down-regulation and over-expression) at defined stages of leaf development showed that the alteration of expansin expression level during the mid-phase is sufficient to repress lamina growth, whereas petiole elongation is still sensitive to expansin expression level at a later phase of leaf development.
- Leaf shape is shown to be altered when expansin gene expression is manipulated (both down-regulation and over-expression), as indicated by morphometric analysis (circularity and length:width ratio), sometimes even without any drastic change in leaf growth (length, width and area).
- The effect of repressed growth in the leaf (both down-regulation and over-expression) was also observed in the hypocotyl, similar to observed reduced petiole elongation.
- An attempt to use atomic force microscopy (AFM) technique to study cell wall mechanics *in planta* raises the possibility of studying the effect of altered expansin gene expression *in vivo*.
- The force maps taken from the margin of tobacco leaf primordia show distinct mechanical properties between the adaxial and abaxial surfaces, with the latter being more compliant and the boundary between the two sides being much stiffer.

- Attempts using AFM point measurements to quantify the cell wall properties at different locations on the Arabidopsis leaf primordium were confounded by high heterogeneity in subcellular cell wall mechanics. However, the results obtained showed a consistent pattern of a regionally more compliant area on the abaxial surface between the margin and midvein, not far behind the leaf tip.
- The quantification values (elastic moduli) obtained are reproducible between two plant species and between different approaches of measurement over time on different platforms, as well as comparable to those reported in the literature. This increases confidence in the data. Further optimisation of the AFM technique is required to widen its application for the study of plant tissue mechanics *in vivo*.

6.2 The functional role of alpha-expansins in Arabidopsis leaf development

Previous investigations on the expression pattern of expansins in leaf development showed inconsistency in the correlation between expansin gene expression and the pattern of growth (Caderas *et al.*, 2000; Reidy *et al.*, 2001a), as described in Chapter 3. This may be due to the varied patterns of individual expansin gene expression, as seen in Figure 3.7. Not every expansin gene's expression is correlated with the progression of leaf development, which may indicate that if some of the expansin genes are involved in specialised functions. This is supported by the observed pleiotropic phenotypes in most studies involving expansin manipulation (Cho and Cosgrove, 2000; Rochange and McQueen-Mason, 2000; Choi *et al.*, 2003; Zhao *et al.*, 2006; Wang *et al.*, 2011). Many different tissue and cell types are created during leaf development, including the vascular bundles (xylem, phloem and cambium etc.), jigsaw puzzle-shaped pavement cells, kidney-shaped guard cells and branched trichomes, which conceivably have different requirements for cell wall modification during differentiation. Furthermore, different growth patterns of distinct cell types may be required in different tissue layers. For example, the spongy mesophyll layer not only requires cell expansion but also a coordinated separation of cell walls between neighbouring cells to create airspaces (Dale, 1988; Jarvis *et al.*, 2003). In addition, the growth between different regions of a leaf surface may differ such that

leaf tip does not grow as much as the middle region of leaf blade, and the cell wall of leaf margin may require different cell wall properties to counteract the tensile stress that arises from growth of the internal surfaces. This suggests a need for tight local regulation of expansion at the cellular and tissue level during leaf development, which might be reflected in a tight but complex regulation of expression of the genes controlling cell wall architecture, such as expansins. Indeed, it was reported that the expression of three expansin genes was tightly linked to the progression of maize leaf development regardless of different environmental factors (Muller *et al.*, 2007).

Here, I speculate on the expansin function based on the results obtained from current work (Chapter 3) and gene expression pattern reported in the literature. The specific role of EXPA7 and EXPA18 (clade X) in lateral root initiation and root hair formation has been verified in the literature (Cho and Cosgrove, 2002), which is consistent with no transcript being detected in leaf. Based on a common expression pattern, the gene products of *EXPA17* (clade VI), *EXPA12* (clade VII) and *EXPA14* (clade II) may also be involved in root development. Indeed, EXPA17 has recently shown to be involved in lateral root emergence (Swarup *et al.*, 2008). The expression of *EXPA12* was found in endodermis/ cortex cells, whereas *EXPA14* is expressed in the stele, is highly regulated by most phytohormones and was found at a low level during the mid-phase of leaf development. Expression of expansin genes from clade XII (*EXPA19, 21-26*, the largest clade in Arabidopsis) was not detected during leaf development and appeared to be specialised for the development of floral organs specifically in dicot plants as this clade is lost in monocot plants (Sampedro *et al.*, 2006). The expression of *EXPA11* (the only member of clade V) was detected in most organs, notably the root cortex cell and was found at a low level from the mid to late phase of leaf development. Little is reported on clade V genes, which has greatly expanded in the monocot rice (16 members, the largest clade) (Sampedro *et al.*, 2006), but one can infer its role to be essential and widespread. Similarly, *EXPA13* (the only member of clade IX) was found to be highly expressed in most organs, uniquely found in phloem cells and its expression peaks during the mid-phase of leaf development.

Clade IV (*EXPA3, 4, 6, 9* & *16*) is the biggest clade of expansins expressed during leaf development, with *EXPA3, 4* & *6* found throughout all stages, *EXPA9* expressed during mid-phase, whereas *EXPA16* transcripts were detected during the early phase,

increased during mid-phase and were undetectable during the later stage of leaf development. Based on the reported functions of clade IV homologs in tomato (*LeEXPA1, 4, 9* & *18*), members of this clade are functionally diverse in dicot plants (compared to monocot rice which has only 1 member). Transcripts of *LeEXPA4* were found in tomato fruit and *LeEXPA1* was shown to be involved in fruit softening (Rose *et al.*, 1997; Rose *et al.*, 2000). *LeEXPA18* transcripts are abundant in the emerging leaf primordia (serving as a molecular marker of leaf initiation) and correlates with meristematic activity in the apex, leaf primordia, and developing flowers, whereas *LeEXPA9* transcripts are distributed evenly in submeristematic tissues (Reinhardt *et al.*, 1998). This is relevant to the possible meristematic function of *EXPA3* with its expression in the shoot apical meristem and up-regulation specifically within the nematode-induced syncytium (Wieczorek *et al.*, 2006).

On the other hand, a clade IV expansin homolog in Chinese fir (*ClEXPA2*) is associated with secondary growth and its overexpression resulted in ubiquitous thickening of the xylem cell wall due to ectopic secondary wall deposition (Wang *et al.*, 2011). Conversely, *ClEXPA1* (Clade III) is preferentially expressed in the cambium region and its overexpression resulted in increased tobacco stem diameter (Wang *et al.*, 2011). Other homologs of clade III expansins include tomato *LeEXPA2* whose expression coincides primarily with expansion in leaves, stems and flowers (Reinhardt *et al.*, 1998), cucumber CsEXPA1 which functions in hypocotyl elongation (McQueen-Mason *et al.*, 1992), and rice OsEXPA4 which is involved in internode elongation (Cho and Kende, 1997b). This suggests clade III expansins (*EXPA2* & *8*) function in expansion growth, which is consistent with the increasing expression of *EXPA8* throughout the course of leaf development, although *EXPA2* was found to be only lowly expressed. However, this inference of function may not be valid as the tomato *LeEXPA2* transcript abundance was found to be negatively correlated with hypocotyl growth, i.e., less abundant in dark-grown hypocotyls which grow 6 times faster than light-grown hypocotyls (Caderas *et al.*, 2000).

Lastly, members of clade I expansins (*EXPA1, 5, 10* & *15*) were all detected during leaf development with rather varied patterns. *EXPA15* was only expressed until early mid-phase. Increasing *EXPA1* expression from early to late phase is consistent with its reported function in mature guard cells (Zhang *et al.*, 2011b). *EXPA5* and *EXPA10* are similarly highly expressed throughout leaf development, except that

EXPA10 expression level drops off at the mature leaf stage. This is consistent with their similar expression pattern as visualised by GUS histochemical staining of promoter::GUS transgenic lines, with expression at the base of emerging first true leaves, in young but not old leaves, and in petioles (Cho and Cosgrove, 2000; Son *et al.*, 2010). However, *EXPA5* expression was restricted to the lower region of the expanding leaf margin and flower receptacles, while the expression of *EXPA10* extended toward the whole midrib of the third leaf onwards (with a progressive restriction to the petiole vasculature as the leaf matures) and in growing trichomes. Furthermore, EXPA10 is the only expansin demonstrated to be involved in Arabidopsis leaf growth (Cho and Cosgrove, 2000), whereas *EXPA5* was shown to be uniquely expressed in above-ground organs and appeared to be specifically repressed in the root (Park *et al.*, 2010). The expansins from this clade were chosen as targets for gene knock-down to study the role of expansins in leaf morphogenesis, which will be further discussed in the following section.

6.3 The mechanism of Arabidopsis leaf morphogenesis

As described in Chapter 1, the development of the planar leaf form requires a complex integration of many tissue types arising from different cellular processes: cell division, cell expansion and cell differentiation (Poethig and Sussex, 1985; Dale, 1988; Pyke *et al.*, 1991). Therefore, the shape and size of a leaf can be viewed as an emergent property of complex interactions between tissues and regional differences in the growth behaviour of cellular domains. Based on the results obtained from my study and current understandings of leaf development, a simple two-dimensional mechanistic growth model of Arabidopsis leaf morphogenesis is depicted in Figure 6.1. This model incorporates the general pattern of basipetal cessation of cell division (Donnelly *et al.*, 1999) and the progression through cell expansion and cell differentiation in relation to the general observed growth/ expansion rates at different stages of leaf development.

This model highlights that changes during early and late phases are driven by different cellular processes: cell division vs. cell expansion. Early leaf morphogenesis is dominated by cell division/differentiation processes, which provide the building blocks for growth and allows the generation of functional

features along the leaf margin, e.g., serrations, through regional growth (Bilsborough *et al.*, 2011) or even localised repression of growth (Malinowski *et al.*, 2011). This is shown by the drastic changes in the shape outline of Arabidopsis during the early stage of leaf development which smoothen out at later stages (Figure 6.1).

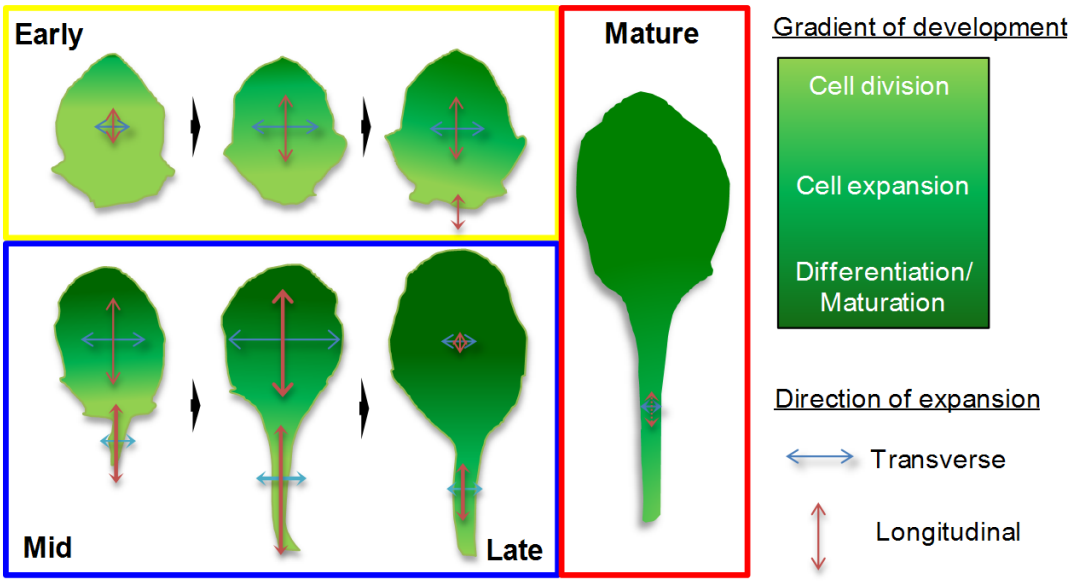

Figure 6.1. A model of Arabidopsis leaf morphogenesis across different developmental phases (progression indicated by block arrows), based on the patterns of cell division, cell expansion and cell differentiation (represented by the green colour gradient). During leaf development, cell division followed by cell expansion with intermittent cell differentiation, ceases first in the distal portion of lamina and continues longest at the base. The length and thickness of the arrows represent the relative magnitude of extension rate along the width and length of the lamina or petiole, with longer and thicker arrows mean greater values (see Chapter 3). Initial growth is driven by cell division-dependent processes resulting in almost isotropic transverse and longitudinal growth. During the mid-stage when cell proliferation transition to cell expansion, there is a rapid growth with greater magnitude in the longitudinal axis driven by vacuole-dominated cell enlargement, followed by a sudden cessation of growth. Dashed arrow indicates the plasticity of growth upon environmental stimuli (e.g. light).

Essentially, the blueprint for the leaf shape has been laid down during this proliferative phase (Sinha, 1999). Interestingly, cells exiting the proliferative state grow the fastest and show the strongest increase in cellular DNA content (ploidy level) via endoreduplication (Kheibarshekan *et al.*, 2011). Consequently, faster growth of the smaller pavement cells surrounding the guard cells relative to the larger pavement cells may cause the uneven topography and the elevated guard cells (Kheibarshekan *et al.*, 2011). The characteristic jigsaw shape of pavement cells is also established during this proliferation-to-expansion transition (Kheibarshekan *et al.*, 2011). Furthermore, time course observations of developing pavement cells reveal an initial wave of lobe initiation, followed by an extended phase of isotropic cell expansion which ends abruptly with no growth beyond maturity (Zhang *et al.*, 2011a). To a great extent, this cellular growth pattern mirrors that of whole-leaf growth (Figure 6.1).

Therefore, the balance between cell proliferation and cell expansion is considered key to overall leaf morphogenesis. It is thought that the outcome of cell division on morphogenesis is dependent on the anatomical or developmental context which underlies its mechanistic relationship with growth; as such there may also be an indirect link of cell division to growth rate via altered tissue differentiation (Fleming, 2002). This is supported by the observed altered leaf shape in experiments involving the manipulation of genes involved in the cell cycle (De Veylder *et al.*, 2001; Wyrzykowska *et al.*, 2002; Dewitte *et al.*, 2003; Kuwabara *et al.*, 2011; Malinowski *et al.*, 2011). In comparison, there are far fewer studies specific to the role of cell expansion in leaf morphogenesis (Pien *et al.*, 2001; Sloan *et al.*, 2009), perhaps limited by the lack of known genes which directly control cell expansion compared to the relatively abundant regulators of the cell cycle. This thesis adds to this body of studies on the role of cell expansion in leaf development. Below, I discuss further the different aspects of leaf morphogenesis with respect to cell expansion in relation to the results obtained from the current study.

Despite the limited correlation between cell size and final leaf size (compared to cell number) (Cookson *et al.*, 2005), the process of cell expansion dominates the larger part of leaf development, as seen from the multi-fold increase in leaf size. Furthermore, it has been shown that the manipulation of cell division pattern did not result in leaf blade area changes until a relatively late stage, despite earlier changes

in cell size (Kuwabara *et al.*, 2011). This suggests a control mechanism involved in the regulation of final leaf size during later stages of leaf development. In this study, I have demonstrated that the manipulation of expansin expression at this later stage of development is sufficient to repress leaf growth and alter leaf shape, suggesting that the regulation of cell wall proteins during cell-division independent expansion can determine leaf growth.

On the other hand, a regional regulation of cell wall properties may be determinant for the differences in the growth rate depicted in Figure 6.1. Differential growth rates between adjacent regions have been proposed to be essential for morphogenesis (Fleming, 2002). For example, leaf epinasty is a consequence of faster growth in the top part of leaf surface (adaxial) relative to the bottom part of surface (abaxial), as shown by the auxin-mediated curving of interveinal leaf strips, excised from growing tobacco leaves (Keller and Van Volkenburgh, 1997). Conversely, leaf hyponasty is a consequence of opposite differential growth between the two surfaces, resulting in upward leaf movement or even upright leaf curling, which is also an auxin-mediated response in cell expansion (Lippincott and Lippincott, 1971). These observations support the role of differential cell expansion in leaf development.

My attempts to apply AFM to the study of leaf tissue mechanics support the idea of differential cell wall properties underpinning differential cell expansion. I could detect supra-cellular differences in cell wall stiffness across the upper and lower surfaces of leaf primordia, with the latter being more compliant (Figure 5.7). Furthermore, the marginal cells appeared to be much stiffer than the surrounding cells. This may be crucial for withstanding a greater tensile stress along the boundary of the two surfaces which have different mechanical properties. This juxtaposition of cells possessing adaxial and abaxial identities appears to be essential for lamina outgrowth (Waites *et al.*, 1998). On the other hand, the softer regions near the middle part of the abaxial surface (Figure 5.9-10, 5.12-13) may correlate with faster growth in the middle region of the leaf, which translates into the observed wider dimension of the mid-leaf.

The observed outcomes on growth mentioned above involve the coordinated growth across different tissue layers. This is manifested as resultant growth (observed leaf shape) from the specified cellular and supracellular mechanics (cell wall properties)

required to achieve equilibrium in tissue mechanics (tensile stress) as described in Figure 1.2 (Chapter 1). Within a single tissue layer, especially the epidermis which sustains much greater tensile stress than other tissue layers, the tension can be more difficult to convert into movement to dissipate the stress. It has been proposed that the characteristic jigsaw puzzle-shaped pavement cells are a consequence of differential stresses arising from differential relative cell expansion rates (Kheibarshekan *et al.*, 2011). The speculation is that these differential stresses are transduced into the realignment of cortical microtubules parallel to the maximal stress directions, as shown by Hamant *et al.* (2008), which precedes the emergence of lobes leading to interdigitations with neighbouring cells, presumably to counteract the cell-cell tension (Panteris and Galatis, 2005; Kotzer and Wasteneys, 2006). Curiously, while the majority of pavement cells undergo interdigitation with adjacent cells, those overlying the midvein remain unlobed and resemble the uniaxial cells of elongation organs e.g. hypocotyl (Kotzer and Wasteneys, 2006). This may reflect the stress pattern of leaf growth mechanics, such that the uniaxial tension along the midrib greatly surpasses the lateral tensile stress. To demonstrate the underlying causal relationship between the cell wall mechanics and the resultant growth will require an *in vivo* technique, in which the AFM has shown to be a promising approach. Alternatively, this may indicate a role of the midrib in driving longitudinal leaf growth. This is relevant as the repressed leaf growth observed here following down-regulation of *EXPA1*, *EXPA3*, *EXPA5* and *EXPA10* may be a consequence of developmental disruption in the leaf vasculature (Figure 4.13B).

The role of the midrib in leaf growth is linked to the tight relationship between development of the vascular system and leaf patterning. This link is suggested by unsuccessful attempts so far to identify mutants with abnormal vein pattern and relatively normal leaf shape and size (Candela *et al.*, 1999). In Arabidopsis, leaf venation patterning is an early, progressive, and hierarchical process whereby vascular cells undergo faster cell division than other cell types (Candela *et al.*, 1999). It is possible that a common morphogenetic mechanism controls both venation and whole-leaf growth, i.e. vein patterning is a consequence of leaf growth (Mitchison, 1981). Furthermore, despite the outgrowth of a flat lamina being abolished in the tobacco *lam-1* mutant plant, a rod-shaped lateral organ with normal length is observed (McHale and Marcotrigiano, 1998). This shows that the vascular system

and blade outgrowth can be regulated independently, with an intrinsic mechanism for gauging the longitudinal growth. This is consistent with the observations made here and reported previously that retarded leaf growth via repression of expansin (*EXPA10*), which is normally expressed in the midrib (Cho and Cosgrove, 2000), is largely due to alteration in extension along the longitudinal axis. This suggests that lamina growth may be coordinated with midrib growth, either directly through cell adhesion (tissue mechanics) or indirectly via molecular coordination of midrib elongation (Scanlon, 2000). The complexity of leaf blade development is further indicated by the fact that growth repression is less apparent in the lamina than petiole in response to the manipulation of expansin expression, as reported here.

The apparent complexity of the control of blade growth may be due to the presence of feedback mechanism(s) which act as a growth rheostat, also known as the elusive compensatory mechanism(s) (Tsukaya, 2003). It seems that a robust failsafe mechanism is present in leaves, so that in the case of missing elements or disrupted signalling pathways, a compensatory mechanism ensures a basic morphogenic pattern is maintained for essential leaf function (Fleming, 2002). Studies of mutants and transgenic lines have revealed that cell division and cell expansion are coordinated by multiple mechanisms, so that inhibition of one is compensated by increased activity of the other and vice-versa (Ferjani *et al.*, 2007). This could partly explain the counter-intuitive observations in this study. At the cellular level, the mesophyll cell size was not decreased when expansin expression was down-regulated, but showed a tendency to increase, especially across the cell width (Table 4.2). Similarly, the palisade mesophyll cell size in the petiole was significantly increased in the expansin overexpressor line (pOpON::CsEXPA1) despite repressed leaf growth (Figure 4.11). The increase in the palisade mesophyll cell size may reflect a feedback response against reduced epidermal cell length and reduced number of cell files with. This also supports the overriding role of the epidermal layer in controlling growth. At the whole-organ level, the growth of lamina appeared to be enhanced in width when the petiole growth was repressed in staged-transfer experiments (Figure 4.17-18). This may indicate an organ-wide regulation such that a reduced petiole length is compensated by increased lamina area.

The situation is further complicated by the fact that a cellular response to perturbation may depend on the developmental state of the cell. This window of

sensitivity to manipulation is a consequence of the gradient of development. For example, the epinastic sensitivity to auxin appears transiently during the development of tobacco leaves and moves as a wave from the distal end of the blade to the base. Interestingly, the highest sensitivity coincides with the profound slowing, if not complete cessation, of growth in the intact leaf (Keller and Van Volkenburgh, 1997). This was also shown by Sloan *et al.* (2009) and the current study (first leaf-pair experiments, Figure 4.21 - Chapter 4) in the case of expansin manipulation during leaf development, such that the leaf response to the up- or down-regulation of expansin gene expression is most sensitive during the mid-phase of leaf development when absolute expansion rate is at a maximum.

Additionally, the growth of the leaf blade and petiole can be regulated independently (Tsukaya, 2002; Keller *et al.*, 2011). During the shade-avoidance response, the growth of the leaf blade is inhibited whereas the petiole elongation is strongly stimulated (Kozuka *et al.*, 2005). This enhanced petiole elongation is largely driven by vacuolar-linked cell expansion (and sometimes cell proliferation) without changes in the DNA content, in contrast to the normal cell expansion of blade tissue which is often accompanied by increasing ploidy level (Kozuka *et al.*, 2005). It is noteworthy that under normal growth condition the average cellular ploidy level is much greater in the petiole than leaf blade (Kozuka *et al.*, 2005), presumably allowing the plasticity of petiole elongation under environmental stimuli. However, the relationship between ploidy level and growth is still unclear (Sugimoto-Shirasu and Roberts, 2003). There is as yet no evidence to support the involvement of expansins in the shade avoidance syndrome, whereas other cell wall modifying proteins such as xyloglucan endotransglucosylase/ hydrolases (XTHs) have been implicated (Sasidharan *et al.*, 2010; Keuskamp *et al.*, 2011). However, the observed restricted rosette expansion and the absence of a hyponasty response when petiole development is severely impaired by the suppression or overexpression of expansins (Figure 4.8) suggests that expansins do play a role in the developmental programme of petiole elongation.

The shade avoidance syndrome (SAS) of the leaf has attracted intense studies into its mechanism, which is now known to involve a complex and integrated coordination of different photoreceptors and hormone-mediated pathways (Pierik *et al.*, 2009; Kozuka *et al.*, 2010; Keller *et al.*, 2011; Keuskamp *et al.*, 2011). Despite the fact that

large numbers of the expansins are responsive to hormonal treatments (Figure 3.11), there is no supporting evidence for expansin up-regulation during petiole elongation under light stimuli (Sasidharan *et al.*, 2010). However, expansin gene expression in the petiole of flood-tolerant *Rumex palustris* was induced under ethylene regulation during submergence (Vriezen *et al.*, 2000; Vreeburg *et al.*, 2005). The overall expression pattern of *EXPA*s which correlates to the progression of different leaf developmental stages (Figure 3.7) suggests a role for expansin in the default state of leaf developmental programme. This is supported by other studies which showed that certain expansin gene expression patterns are not affected by the hormonal and environmental stimuli (Cho and Cosgrove 2002; Muller *et al.* 2007). Furthermore, none of the expansin members turned up in genome-wide screening for touch-regulated genes (Lee *et al.*, 2005). This indicates a more stable regulation of expansin expression rather than there being a transient response to mechano stimuli or light responses as observed for other cell wall modifying proteins, such as the XTH gene family (Lee *et al.*, 2005; Sasidharan *et al.*, 2010).

These observations suggest the regulation of expansin activity can be much more complex *in planta* than its *in vitro* function on cell wall loosening (McQueen-Mason *et al.*, 1992). It has been proposed that expansin activity in leaf growth might involve an additional factor which determines the susceptibility of the cell wall to expansin action (Sloan *et al.*, 2009), which fits the concept of a sensitivity window of development (McQueen-Mason, 1995). In a normal non-growing leaf, expansin may be present at baseline level and serves a spacer between cellulose and hemicellulose to facilitate the accessibility of other modifying proteins such as XTHs. Therefore, expansin may play an indirect but fundamental role during environmental-stimulated growth which depends on the activities of other cell wall-modifying agents.

A detailed discussion on the hormonal regulations of expansin activity in relation to leaf morphogenesis is beyond the scope of this thesis. However, there are a few interesting observations to point out with relevance to expansin activity amidst the complex interdependent networks of hormone responses in plants (Nemhauser *et al.*, 2004; Nemhauser *et al.*, 2006). This is in relation to the anisotropic leaf expansion observed after manipulation of *EXPA5* and *EXPA10*. Brassinosteroids (BRs) have been implicated in the control of leaf longitudinal growth due to the rounded leaf phenotype observed in all mutant plants deficient in or insensitive to BRs (Kim *et al.*,

1998; Guo *et al.*, 2010; Koyama *et al.*, 2010). This phenotype resembles that observed in plants with altered expansin expression (Figure 4.8). The expression pattern of a BR biosynthetic gene, *CYP90D1*, specifically expressed in vascular tissue of the petiole and partially, the midrib (Kim *et al.*, 2005) is similar to that of *EXPA10*. Furthermore, *CYP90D1* shows upregulated expression during elongation in darkness. *EXPA5* has been shown to be upregulated by brassinolide and downregulated by ethylene (Park *et al.*, 2010). Thus, *EXPA5* could be promoting early cell expansion around the leaf margin and petiole under the control of BR. This may also involve another BR biosynthesis gene which is expressed in the leaf blade (*ROT3/CYP90C1*) which has an established function in elongation of the leaf blade (Kim *et al.*, 1998; Kim *et al.*, 2005). This inference requires further experimental study for verification, but it raises the interesting prospect of BR having a role in the differential regulation of expansins, which is consistent with an independent control of leaf blade and petiole development.

6.4 Future work

There is a gap in our knowledge of the signalling and regulatory pathways governing the expression of expansin and the ultimate function of the protein. Expansins were originally discovered as mediators of acid growth, which refers to the widespread characteristic of growing plant cell walls to expand faster at lower (acidic) pH than at neutral pH (McQueen-Mason *et al.*, 1992). Since cell wall acidification has long been linked with auxin activity, expansins have been linked to auxin action, which is involved in almost every aspect of plant development. Expansins are also linked to cell enlargement and cell wall changes induced by plant hormones other than auxin and brassinosteroids (Sanchez *et al.*, 2004), such as gibberellin (Cho and Kende, 1997c), cytokinin (Downes and Crowell, 1998), and ethylene (Cho and Cosgrove, 2002). The experimental exploration of *cis*-regulatory elements in the upstream regions of expansin genes might indicate potential routes of hormonal or tissue-specific regulation, linking the roles of expansin and hormones in leaf morphogenesis (Cho and Cosgrove, 2002). However, a caveat to bear in mind, is that although expansins such as *EXPA5* and *EXPA8* in Arabidopsis have been described as brassinosteroid (BR)-inducible genes from DNA microarray analysis (Goda *et al.*,

2002; Müssig *et al.*, 2002), there have been few reports on the induction of *EXPA* gene transcripts by BR in relation to organ elongation.

There is a complicated relationship between genes, the plant cell wall and growth (Wojtaszek, 2000). Bridging the gaps to establish a causal relationship for an observed phenotype as a consequence of altered cell wall mechanics following the manipulation of a cell wall gene requires a direct approach to study tissue mechanics. I have demonstrated that AFM is a promising approach for *in vivo* studies of plant tissue mechanics. The next step would be to combine this approach with molecular genetics. For instance, the pOpON::amiREXP transgenic lines that I have generated with the flexibility of localised down-regulation of expansin gene expression could be used for further study of the mechanics of guard cells, for example to test the reported results on the role of EXPA1 in regulating guard cell volumetric modulus *in planta* (Zhang *et al.*, 2011b). Such studies would also serve as a proof of functionality for the AFM technique at a single-cell level. Furthermore, such investigations might shed light on the reported role of expansins in abiotic stress response (Gao *et al.*, 2010), which might actually be an indirect affect of altered guard cell physiology. In addition, the pOpON::amiREXP lines (which target the clade I expansins) could be utilised in the study of resistance to nematode infection, since the downregulation of *LeEXPA5* (clade I homolog) in tomato has shown to reduce the parasitism of root-knot nematode egg mass per gall (Gal *et al.*, 2006; Wieczorek *et al.*, 2006) .

There are many unresolved questions remaining on the regulation of expansin activity, the mechanistic role of expansin in leaf growth and the ultimate quest for a deeper understanding of the mechanism of leaf morphogenesis. Some of these issues have been extensively discussed in this thesis. Hopefully this has contributed to a better understanding of the relationship between expansins, cell wall mechanics and leaf growth, as well as opening up new opportunities for the study of plant tissue mechanics. The use of new techniques for the direct quantification of tissue mechanics will allow the testing of various hypotheses/ models of the mechanism underpinning the wondrous variety of leaf forms. Meanwhile, one cannot help but feel apprehensive about the mammoth task of unravelling the secrets behind the robust but plastic nature of growth and development manifested by a ubiquitous and essential biological entity, the leaf.

References

Alonso JL, Goldmann WH (2003) Feeling the forces: Atomic force microscopy in cell biology. Life Sciences **72:** 2553-2560

Altmann T (1998) Recent advances in brassinosteroid molecular genetics. Current Opinion in Plant Biology **1:** 378-383

Alvarez JP, Pekker I, Goldshmidt A, Blum E, Amsellem Z, Eshed Y (2006) Endogenous and synthetic microRNAs stimulate simultaneous, efficient, and localized regulation of multiple targets in diverse species. Plant Cell **18:** 1134-1151

Amirsadeghi S, McDonald A, Vanlerberghe G (2007) A glucocorticoid-inducible gene expression system can cause growth defects in tobacco. Planta **226:** 453-463

Anastasiou E, Lenhard M (2007) Growing up to one's standard. Current Opinion in Plant Biology **10:** 63-69

Aoyama T, Chua NH (1997) A glucocorticoid-mediated transcriptional induction system in transgenic plants. Plant Journal **11:** 605-612

Backhaus A, Kuwabara A, Bauch M, Monk N, Sanguinetti G, Fleming A (2010) Leafprocessor: A new leaf phenotyping tool using contour bending energy and shape cluster analysis. New Phytologist **187:** 251-261

Baker-Brosh KF, Peet RK (1997) The ecological significance of lobed and toothed leaves in temperate forest trees. Ecology **78:** 1250-1255

Barkoulas M, Galinha C, Grigg SP, Tsiantis M (2007) From genes to shape: regulatory interactions in leaf development. Current Opinion in Plant Biology **10:** 660-666

Baselt DR, Baldeschwieler JD (1994) Imaging spectroscopy with the atomic force microscope. Journal of Applied Physics **76:** 33-38

Baskin TI (2005) Anisotropic expansion of the plant cell wall. Annual Review of Cell and Developmental Biology **21:** 203-222

Beemster GTS, De Veylder L, Vercruysse S, West G, Rombaut D, Van Hummelen P, Galichet A, Vuylsteke M (2005) Genome-wide analysis of gene expression profiles associated with cell cycle transitions in growing organs of Arabidopsis. Plant Physiology **138:** 734-743

Beemster GTS, Vercruysse S, De Veylder L, Kuiper M, Inze D (2006) The Arabidopsis leaf as a model system for investigating the role of cell cycle regulation in organ growth. Journal of Plant Research **119:** 43-50

Beerling DJ, Fleming AJ (2007) Zimmermann's telome theory of megaphyll leaf evolution: a molecular and cellular critique. Current Opinion in Plant Biology **10:** 4-12

Bell AD (1991) Plant form: An illustrated guide to flowering plant morphology. Oxford University Press, New York, NY.

Benkova E, Michniewicz M, Sauer M, Teichmann T, Seifertova D, Jurgens G, Friml J (2003) Local, efflux-dependent auxin gradients as a common module for plant organ formation. Cell **115:** 591-602

Benziman M, Haigler CH, Brown RM, White AR, Cooper KM (1980) Cellulose biogenesis: Polymerization and crystallization are coupled processes in *Acetobacter xylinum*. Proceedings of the National Academy of Sciences of the United States of America **77:** 6678-6682

Berleth T, Scarpella E, Prusinkiewicz P (2007) Towards the systems biology of auxin-transport-mediated patterning. Trends in Plant Science **12:** 151-159

Berna G, Robles P, Micol JL (1999) A mutational analysis of leaf morphogenesis in Arabidopsis thaliana. Genetics **152:** 729-742

Bilsborough GD, Runions A, Barkoulas M, Jenkins HW, Hasson A, Galinha C, Laufs P, Hay A, Prusinkiewicz P, Tsiantis M (2011) Model for the regulation of Arabidopsis thaliana leaf margin development. Proceedings of the National Academy of Sciences of the United States of America **108:** 3424-3429

Binnig G, Quate CF, Gerber C (1986) Atomic force microscope. Physical Review Letters **56:** 930-933

Blanvillain R, Young B, Cai YM, Hecht V, Varoquaux F, Delorme V, Lancelin JM, Delseny M, Gallois P (2011) The Arabidopsis peptide kiss of death is an inducer of programmed cell death. EMBO Journal **30:** 1173-1183

Blewett J, Burrows K, Thomas C (2000) A micromanipulation method to measure the mechanical properties of single tomato suspension cells. Biotechnology Letters **22:** 1877-1883

Boudaoud A (2010) An introduction to the mechanics of morphogenesis for plant biologists. Trends in Plant Science **15:** 353-360

Bougourd S, Marrison J, Hasseloff J (2000) An aniline blue staining procedure for confocal microscope and 3D imaging of normal and perturbed cellular phenotypes in mature Arabidopsis embryos. Plant Journal **24:** 543-550

Bowman JL, Eshed Y, Baum SF (2002) Establishment of polarity in angiosperm lateral organs. Trends in Genetics **18:** 134-141

Brummell DA, Harpster MH, Civello PM, Palys JM, Bennett AB, Dunsmuir P (1999a) Modification of expansin protein abundance in tomato fruit alters softening and cell wall polymer metabolism during ripening. Plant Cell **11:** 2203-2216

Brummell DA, Harpster MH, Dunsmuir AP (1999b) Differential expression of expansin gene family members during growth and ripening of tomato fruit. Plant Molecular Biology **39:** 161-169

Burgert I (2006) Exploring the micromechanical design of plant cell walls. American Journal of Botany **93:** 1391-1401

Burnham NA, Colton RJ (1989) Measuring the nanomechanical properties and surface forces of materials using an atomic force microscope. Journal of Vacuum Science and Technology A **7:** 2906-2913

Burnham RJ, Johnson KR (2004) South American palaeobotany and the origins of neotropical rainforests. Philosophical Transactions of the Royal Society B: Biological Sciences **359:** 1595-1610

Byrne ME (2005) Networks in leaf development. Current Opinion in Plant Biology **8:** 59-66

Caderas D, Muster M, Vogler H, Mandel T, Rose JKC, McQueen-Mason S, Kuhlemeier C (2000) Limited correlation between expansin gene expression and elongation growth rate. Plant Physiology **123:** 1399-1413

Candela H, Martínez-Laborda A, Micol JL (1999) Venation pattern formation in Arabidopsis thaliana vegetative leaves. Developmental Biology **205:** 205-216

Carey RE, Cosgrove DJ (2007) Portrait of the expansin superfamily in *Physcomitrella patens*: Comparisons with angiosperm expansins. Annals of Botany **99:** 1131-1141

Carpita NC (1996) Structure and biogenesis of the cell walls of grasses. Annual Review of Plant Physiology and Plant Molecular Biology **47:** 445-476

Carpita NC, Gibeaut DM (1993) Structural models of primary cell walls in flowering plants: Consistency of molecular structure with the physical properties of the walls during growth. Plant Journal **3:** 1-30

Chanliaud E, De Silva J, Strongitharm B, Jeronimidis G, Gidley MJ (2004) Mechanical effects of plant cell wall enzymes on cellulose/xyloglucan composites. Plant Journal **38:** 27-37

Chen F, Dahal P, Bradford KJ (2001) Two tomato expansin genes show divergent expression and localization in embryos during seed development and germination. Plant Physiology **127:** 928-936

Cho HT, Cosgrove DJ (2000) Altered expression of expansin modulates leaf growth and pedicel abscission in Arabidopsis thaliana. Proceedings of the National Academy of Sciences of the United States of America **97:** 9783-9788

Cho HT, Cosgrove DJ (2002) Regulation of root hair initiation and expansin gene expression in Arabidopsis. Plant Cell **14:** 3237-3253

Cho HT, Kende H (1997a) Expansins and internodal growth of deepwater rice. Plant Physiology **113:** 1145-1151

Cho HT, Kende H (1997b) Expansins in deepwater rice internodes. Plant Physiology **113:** 1137-1143

Cho HT, Kende H (1997c) Expression of expansin genes is correlated with growth in deepwater rice. Plant Cell **9:** 1661-1671

Cho HT, Kende H (1998) Tissue localization of expansins in deepwater rice. Plant Journal **15:** 805-812

Choi D, Cho HT, Lee Y (2006) Expansins: Expanding importance in plant growth and development. Physiologia Plantarum **126:** 511-518

Choi D, Lee Y, Cho HT, Kende H (2003) Regulation of expansin gene expression affects growth and development in transgenic rice plants. Plant Cell **15:** 1386-1398

Chomczynski P, Sacchi N (1987) Single-step method of RNA isolation by acid guanidinium thiocyanate-phenol-chloroform extraction. Analytical Biochemistry **162:** 156-159

Cleland RE (1971) Cell wall extension. Annu. Rev. Plant Physiol. **22:** 197-222

Cleveland JP, Manne S, Bocek D, Hansma PK (1993) A nondestructive method for determining the spring constant of cantilevers for scanning force microscopy. Review of Scientific Instruments **64:** 403-405

Clough SJ, Bent AF (1998) Floral dip: A simplified method for Agrobacterium-mediated transformation of Arabidopsis thaliana. Plant Journal **16:** 735-743

Cnops G, Neyt P, Raes J, Petrarulo M, Nelissen H, Malenica N, Luschnig C, Tietz O, Ditengou F, Palme K, Azmi A, Prinsen E, Van Lijsebettens M (2006) The TORNADO1 and TORNADO2 genes function in several patterning processes during early leaf development in Arabidopsis thaliana. Plant Cell **18:** 852-866

Coen E, Rolland-Lagan AG, Matthews M, Bangham JA, Prusinkiewicz P (2004) The genetics of geometry. Proceedings of the National Academy of Sciences of the United States of America **101:** 4728-4735

Cookson SJ, Chenu K, Granier C (2007) Day length affects the dynamics of leaf expansion and cellular development in Arabidopsis thaliana partially through floral transition timing. Annals of Botany **99:** 703-711

Cookson SJ, Granier C (2006) A dynamic analysis of the shade-induced plasticity in Arabidopsis thaliana rosette leaf development reveals new components of the shade-adaptative response. Annals of Botany **97:** 443-452

Cookson SJ, Radziejwoski A, Granier C (2006) Cell and leaf size plasticity in Arabidopsis: What is the role of endoreduplication? Plant, Cell and Environment **29:** 1273-1283

Cookson SJ, Van Lijsebettens M, Granier C (2005) Correlation between leaf growth variables suggest intrinsic and early controls of leaf size in Arabidopsis thaliana. Plant, Cell and Environment **28:** 1355-1366

Cosgrove DJ (1987) Wall relaxation in growing stems: comparison of four species and assessment of measurement techniques. Planta **171:** 266-278

Cosgrove DJ (1993) Wall extensibility: its nature, measurement and relationship to plant cell growth. New Phytologist **124:** 1-23

Cosgrove DJ (1997) Relaxation in a high-stress environment: The molecular bases of extensible cell walls and cell enlargement. Plant Cell **9:** 1031-1041

Cosgrove DJ (1998) Cell Wall loosening by expansins. Plant Physiology **118:** 333-339

Cosgrove DJ (1999) Enzymes and other agents that enhance cell wall extensibility. Annual Review of Plant Biology **50:** 391-417

Cosgrove DJ (2000a) Expansive growth of plant cell walls. Plant Physiology and Biochemistry **38:** 109-124

Cosgrove DJ (2000b) Loosening of plant cell walls by expansins. Nature **407:** 321-326

Cosgrove DJ (2005) Growth of the plant cell wall. Nature Reviews Molecular Cell Biology **6:** 850-861

Cosgrove DJ, Bedinger P, Durachko DM (1997) Group I allergens of grass pollen as cell wall-loosening agents. Proceedings of the National Academy of Sciences of the United States of America **94:** 6559-6564

Cosgrove DJ, Li LC, Cho HT, Hoffmann-Benning S, Moore RC, Blecker D (2002) The growing world of expansins. Plant and Cell Physiology **43:** 1436-1444

Coutand C, Martin L, Leblanc-Fournier N, Decourteix M, Julien JL, Moulia B (2009) Strain mechanosensing quantitatively controls diameter growth and PtaZFP2 gene expression in poplar. Plant Physiology **151:** 223-232

Cox MCH, Benschop JJ, Vreeburg RAM, Wagemaker CAM, Moritz T, Peeters AJM, Voesenek LACJ (2004) The roles of ethylene, auxin, abscisic acid, and gibberellin in the hyponastic growth of submerged *Rumex palustris* petioles. Plant Physiology **136:** 2948-2960

Craft J, Samalova M, Baroux C, Townley H, Martinez A, Jepson I, Tsiantis M, Moore I (2005) New pOp/LhG4 vectors for stringent glucocorticoid-dependent transgene expression in Arabidopsis. Plant Journal **41:** 899-918

Czechowski T, Stitt M, Altmann T, Udvardi MK, Scheible WR (2005) Genome-wide identification and testing of superior reference genes for transcript normalization in *Arabidopsis*. Plant Physiology **139:** 5-17

D'Costa NP, Hoh JH (1995) Calibration of optical lever sensitivity for atomic force microscopy. Review of Scientific Instruments **66:** 5096-5097

Dale JE (1988) The control of leaf expansion. Annual Review of Plant Physiology and Plant Molecular Biology **39:** 267-295

Darley CP, Forrester AM, Mcqueen-Mason SJ (2001) The molecular basis of plant cell wall extension. Plant Molecular Biology **47:** 179-195

De Veylder L, Beeckman T, Beemster GTS, Krols L, Terras F, Landrieu I, Van Der Schueren E, Maes S, Naudts M, Inze D (2001) Functional analysis of cyclin-dependent kinase inhibitors of Arabidopsis. Plant Cell **13:** 1653-1667

De Veylder L, Van Montagu M, Inzé D (1997) Herbicide safener-inducible gene expression in *Arabidopsis thaliana*. Plant and Cell Physiology **38:** 568-577

Dengler NG, Tsukaya H (2001) Leaf morphogenesis in dicotyledons: Current issues. International Journal of Plant Sciences **162:** 459-464

Derbyshire P, Findlay K, McCann MC, Roberts K (2007) Cell elongation in Arabidopsis hypocotyls involves dynamic changes in cell wall thickness. Journal of Experimental Botany **58:** 2079-2089

Dewitte W, Riou-Khamlichi C, Scofield S, Healy JMS, Jacqmard A, Kilby NJ, Murray JAH (2003) Altered cell cycle distribution, hyperplasia, and inhibited differentiation in Arabidopsis caused by the D-type cyclin CYCD3. Plant Cell **15:** 79-92

Dintwa E, Tijskens E, Ramon H (2008) On the accuracy of the Hertz model to describe the normal contact of soft elastic spheres. Granular Matter **10:** 209-221

Donnelly PM, Bonetta D, Tsukaya H, Dengler RE, Dengler NG (1999) Cell cycling and cell enlargement in developing leaves of Arabidopsis. Developmental Biology **215:** 407-419

Downes BP, Crowell DN (1998) Cytokinin regulates the expression of a soybean β-expansin gene by a post-transcriptional mechanism. Plant Molecular Biology **37:** 437-444

Dumais J (2007) Can mechanics control pattern formation in plants? Current Opinion in Plant Biology **10:** 58-62

Dumais J (2009) Plant morphogenesis: A role for mechanical signals. Current Biology **19:** R207-R208

Efroni I, Blum E, Goldshmidt A, Eshed Y (2008) A protracted and dynamic maturation schedule underlies Arabidopsis leaf development. Plant Cell **20:** 2293-2306

Eshed Y, Baum SF, Perea JV, Bowman JL (2001) Establishment of polarity in lateral organs of plants. Current Biology **11:** 1251-1260

Ferjani A, Horiguchi G, Yano S, Tsukaya H (2007) Analysis of leaf development in *fugu* mutants of *Arabidopsis* reveals three compensation modes that modulate cell expansion in determinate organs. Plant Physiology **144:** 988-999

Fleming AJ (2002) The mechanism of leaf morphogenesis. Planta **216:** 17-22

Fleming AJ (2006) Leaf initiation: The integration of growth and cell division. Plant Molecular Biology **60:** 905-914

Fleming AJ, Caderas D, Wehrli E, McQueen-Mason S, Kuhlemeier C (1999) Analysis of expansin-induced morphogenesis on the apical meristem of tomato. Planta **208:** 166-174

Fleming AJ, McQueen-Mason S, Mandel T, Kuhlemeier C (1997) Induction of leaf primordia by the cell wall protein expansin. Science **276:** 1415-1418

Gal TZ, Aussenberg ER, Burdman S, Kapulnik Y, Koltai H (2006) Expression of a plant expansin is involved in the establishment of root knot nematode parasitism in tomato. Planta **224:** 155-162

Gao X, Liu K, Lu YT (2010) Specific roles of AtEXPA1 in plant growth and stress adaptation. Russian Journal of Plant Physiology **57:** 241-246

Gatz C, Frohberg C, Wendenburg R (1992) Stringent repression and homogeneous de-repression by tetracycline of a modified CaMV 35S promoter in intact transgenic tobacco plants. Plant Journal **2:** 397-404

Gazzarrini S, McCourt P (2003) Cross-talk in plant hormone signalling: What Arabidopsis mutants are telling us. Annals of Botany **91:** 605-612

Geitmann A (2010) Mechanical modeling and structural analysis of the primary plant cell wall. Current Opinion in Plant Biology **13:** 693-699

Geitmann A, Ortega JKE (2009) Mechanics and modeling of plant cell growth. Trends in Plant Science **14:** 467-478

Gendreau E, Traas J, Desnos T, Grandjean O, Caboche M, Hofte H (1997) Cellular basis of hypocotyl growth in Arabidopsis thaliana. Plant Physiology **114:** 295-305

Gindl W, Gupta HS, Schöberl T, Lichtenegger HC, Fratzl P (2004) Mechanical properties of spruce wood cell walls by nanoindentation. Applied Physics A: Materials Science and Processing **79:** 2069-2073

Goda H, Shimada Y, Asami T, Fujioka S, Yoshida S (2002) Microarray analysis of brassinosteroid-regulated genes in arabidopsis. Plant Physiology **130:** 1319-1334

Granier C, Massonnet C, Turc O, Muller B, Chenu K, Tardieu F (2002) Individual leaf development in *Arabidopsis thaliana*: a stable thermal-time-based programme. Annals of Botany **89:** 595-604

Granier C, Tardieu F (2009) Multi-scale phenotyping of leaf expansion in response to environmental changes: The whole is more than the sum of parts. Plant, Cell and Environment **32:** 1175-1184

Granier C, Turc O, Tardieu F (2000) Co-ordination of cell division and tissue expansion in sunflower, tobacco, and pea leaves: Dependence or independence of both processes? J. Plant Growth Regul. **19:** 45-54

Gray-Mitsumune M, Mellerowicz EJ, Abe H, Schrader J, Winzéll A, Sterky F, Blomqvist K, McQueen-Mason S, Teeri TT, Sundberg B (2004) Expansins abundant in secondary xylem belong to subgroup A of the α-expansin gene family. Plant Physiology **135:** 1552-1564

Green AA, Kennaway JR, Hanna AI, Andrew Bangham J, Coen E (2010) Genetic control of organ shape and tissue polarity. PLoS Biology **8:** e1000537

Green PB (1997) Expansin and morphology: A role for biophysics. Trends in Plant Science **2:** 365-366

Green PB (1999) Expression of pattern in plants: Combining molecular and calculus-based biophysical paradigms. American Journal of Botany **86:** 1059-1076

Greenwood MS, Xu F, Hutchison KW (2006) The role of auxin-induced peaks of α-expansin expression during lateral root primordium formation in *Pinus taeda*. Physiologia Plantarum **126:** 279-288

Grieneisen VA, Scheres B (2009) Back to the future: evolution of computational models in plant morphogenesis. Current Opinion in Plant Biology **12:** 606-614

Guo Z, Fujioka S, Blancaflor EB, Miao S, Gou X, Li J (2010) TCP1 modulates brassinosteroid biosynthesis by regulating the expression of the key biosynthetic gene DWARF4 in arabidopsis thaliana. Plant Cell **22:** 1161-1173

Haigler CH (1991) Relationship between polymerization and crystallization in microfibril biogenesis. *In* CH Haigler, PJ Weimer, eds, Biosynthesis and Biodegradation of Cellulose. Marcel Dekker, New York, pp 99–124

Hamant O, Traas J (2010) The mechanics behind plant development. New Phytologist **185:** 369-385

Harris D, Bulone V, Ding SY, DeBolt S (2010) Tools for cellulose analysis in plant cell walls. Plant Physiology **153:** 420-426

Harrison EP, McQueen-Mason SJ, Manning K (2001) Expression of six expansin genes in relation to extension activity in developing strawberry fruit. Journal of Experimental Botany **52:** 1437-1446

Haswell ES, Peyronnet R, Barbier-Brygoo H, Meyerowitz EM, Frachisse JM (2008) Two MscS homologs provide mechanosensitive channel activities in the Arabidopsis root. Current Biology **18:** 730-734

Heinz WF, Hoh JH (1999) Spatially resolved force spectroscopy of biological surfaces using the atomic force microscope. Trends in Biotechnology **17:** 143-150

Heisler MG, Hamant O, Krupinski P, Uyttewaal M, Ohno C, Jönsson H, Traas J, Meyerowitz EM (2010) Alignment between PIN1 polarity and microtubule orientation in the shoot apical meristem reveals a tight coupling between morphogenesis and auxin transport. PLoS Biology **8:** e1000516

Hemerly A, De Almeida Engler J, Bergounioux C, Van Montagu M, Engler G, Inze D, Ferreira P (1995) Dominant negative mutants of the Cdc2 kinase uncouple cell division from iterative plant development. EMBO Journal **14:** 3925-3936

Hertz H (1882) On the contact of elastic solids. Journal für die Reine und Angewandte Mathematik **92:** 156-171

Heyn ANJ (1933) Further investigations on the mechanism of cell elongation and the properties of the cell wall in connection with elongation. Protoplasma **19:** 78-96

Hiller S, Bruce DM, Jeronimidis G (1996) A micro-penetration technique for mechanical testing of plant cell walls. Journal of Texture Studies **27:** 559-587

Hiwasa K, Rose JKC, Nakano R, Inaba A, Kubo Y (2003) Differential expression of seven α-expansin genes during growth and ripening of pear fruit. Physiologia Plantarum **117:** 564-572

Hofmeister W (1867) Die lehre von der pflanzenzelle. *In* Handbuch der Pflanzenphysiologie, Vol 1. Abt. Engelmann, Leipzig

Hoson T, Nevins DJ (1989) β-d-Glucan antibodies inhibit auxin-induced cell elongation and changes in the cell wall of Zea coleoptile segments. Plant Physiology **90:** 1353-1358

Hu L, Cui D, Neill S, Cai W (2007) OsEXPA4 and OsRWC3 are involved in asymmetric growth during gravitropic bending of rice leaf sheath bases. Physiologia Plantarum **130:** 560-571

Hu Y, Bao F, Li J (2000) Promotive effect of brassinosteroids on cell division involves a distinct CycD3-induction pathway in Arabidopsis. Plant Journal **24:** 693-701

Hunt R (1982) Plant Growth Curves: The Functional Approach to Plant Growth Analysis. University Park Press, Baltimore, Md.

Im KH, Cosgrove DJ, Jones AM (2000) Subcellular localization of expansin mRNA in xylem cells. Plant Physiology **123:** 463-470

Ingber DE (2003a) Mechanosensation through integrins: Cells act locally but think globally. Proceedings of the National Academy of Sciences of the United States of America **100:** 1472-1474

Ingber DE (2003b) Tensegrity II. How structural networks influence cellular information processing networks. Journal of Cell Science **116:** 1397-1408

Inouhe M, Nevins DJ (1991) Inhibition of auxin-induced cell elongation of maize coleoptiles by antibodies specific for cell wall glucanases. Plant Physiology **96:** 426-431

Inzé D, De Veylder L (2006) Cell cycle regulation in plant development. *In* Campell, Anderson, Jones, eds, Annual Review of Genetics, Vol 40, pp 77-105

Iwakawa H, Ueno Y, Semiarti E, Onouchi H, Kojima S, Tsukaya H, Hasebe M, Soma T, Ikezaki M, Machida C, Machida Y (2002) The ASYMMETRIC LEAVES2 gene of Arabidopsis thaliana, required for formation of a symmetric flat leaf lamina, encodes a member of a novel family of proteins characterized by cysteine repeats and a leucine zipper. Plant and Cell Physiology **43:** 467-478

Jakoby MJ, Falkenhan D, Mader MT, Brininstool G, Wischnitzki E, Platz N, Hudson A, Hülskamp M, Larkin J, Schnittger A (2008) Transcriptional profiling of mature Arabidopsis trichomes reveals that NOECK encodes the MIXTA-like transcriptional regulator MYB106. Plant Physiology **148:** 1583-1602

Jamet E, Roujol D, San-Clemente H, Irshad M, Soubigou-Taconnat L, Renou JP, Pont-Lezica R (2009) Cell wall biogenesis of Arabidopsis thaliana elongating cells: Transcriptomics complements proteomics. BMC Genomics **10:** 505

Jarvis MC, Briggs SPH, Knox JP (2003) Intercellular adhesion and cell separation in plants. Plant, Cell and Environment **26:** 977-989

Jarvis MC, McCann MC (2000) Macromolecular biophysics of the plant cell wall: Concepts and methodology. Plant Physiology and Biochemistry **38:** 1-13

Jefferson RA, Kavanagh TA, Bevan MW (1987) GUS fusions: beta-glucuronidase as a sensitive and versatile gene fusion marker in higher plants. EMBO Journal **6:** 3901-3907

Johnson K, Lenhard M (2011) Genetic control of plant organ growth. New Phytologist **191:** 319-333

Johnson KL, Kendall K, Roberts AD (1971) Surface energy and the contact of elastic solids. Proceedings of the Royal Society of London. A. Mathematical and Physical Sciences **324:** 301-313

Jönsson H, Krupinski P (2010) Modeling plant growth and pattern formation. Current Opinion in Plant Biology **13:** 5-11

Juenger T, Perez-Perez JM, Bernal S, Micol JL (2005) Quantitative trait loci mapping of floral and leaf morphology traits in Arabidopsis thaliana: Evidence for modular genetic architecture. Evolution and Development **7:** 259-271

Kakimoto T, Shibaoka H (1992) Synthesis of polysaccharides in phragmoplasts isolated from tobacco BY-2 cells. Plant and Cell Physiology **33:** 353-361

Kam MJ, Hye SY, Kaufman PB, Chang SC, Kim SK (2005) Two expansins, EXP1 and EXPB2, are correlated with the growth and development of maize roots. Journal of Plant Biology **48:** 304-310

Kang HG, Fang Y, Singh KB (1999) A glucocorticoid-inducible transcription system causes severe growth defects in Arabidopsis and induces defense-related genes. Plant Journal **20:** 127-133

Kaplan D, Hagemann W (1991) The relationship of cell and organism in vascular plants. BioScience **41:** 693-703

Kaplan DR (1992) The relationship of cells to organisms in plants: Problem and implications of an organismal perspective. International Journal of Plant Sciences **153:** S28-S37

Karimi M, Depicker A, Hilson P (2007) Recombinational cloning with plant gateway vectors. Plant Physiology **145:** 1144-1154

Keller CP, Van Volkenburgh E (1997) Auxin-induced epinasty of tobacco leaf tissues: A nonethylene-mediated response. Plant Physiology **113:** 603-610

Keller E, Cosgrove DJ (1995) Expansins in growing tomato leaves. Plant Journal **8:** 795-802

Keller MM, Jaillais Y, Pedmale UV, Moreno JE, Chory J, Ballaré CL (2011) Cryptochrome 1 and phytochrome B control shade-avoidance responses in Arabidopsis via partially independent hormonal cascades. Plant Journal **67:** 195-207

Kepinski S (2006) Integrating hormone signaling and patterning mechanisms in plant development. Current Opinion in Plant Biology **9:** 28-34

Kerstetter RA, Bollman K, Taylor RA, Bomblies K, Poethig RS (2001) KANADI regulates organ polarity in Arabidopsis. Nature **411:** 706-709

Keuskamp DH, Sasidharan R, Vos I, Peeters AJM, Voesenek LACJ, Pierik R (2011) Blue-light-mediated shade avoidance requires combined auxin and brassinosteroid action in Arabidopsis seedlings. Plant Journal **67:** 208-217

Kha H, Tuble SC, Kalyanasundaram S, Williamson RE (2010) WallGen, software to construct layered cellulose-hemicellulose networks and predict their small deformation mechanics. Plant Physiology **152:** 774-786

Kheibarshekan L, Dhondt S, Boudolf V, Beemster GTS, Beeckman T, Govaerts W, Inzé D, De Veylder L (2011) Model-based analysis of Arabidopsis leaf epidermal cells reveals distinct division and expansion patterns for pavement and guard cells. Plant Physiology**:** In press

Kidner CA, Timmermans MC (2007) Mixing and matching pathways in leaf polarity. Current Opinion in Plant Biology **10:** 13-20

Kim GT, Cho KH (2006) Recent advances in the genetic regulation of the shape of simple leaves. Physiologia Plantarum **126:** 494-502

Kim GT, Fujioka S, Kozuka T, Tax FE, Takatsuto S, Yoshida S (2005) CYP90C1 and CYP90D1 are involved in different steps in the brassinosteroid biosynthesis pathway in *Arabidopsis thaliana*. Plant Journal **4:** 710-721

Kim GT, Tsukaya H, Uchimiya H (1998) The ROTUNDIFOLIA3 gene of Arabidopsis thaliana encodes a new member of the cytochrome P-450 family that is required for the regulated polar elongation of leaf cells. Genes and Development **12:** 2381-2391

Klein EA, Yin L, Kothapalli D, Castagnino P, Byfield FJ, Xu T, Levental I, Hawthorne E, Janmey PA, Assoian RK (2009) Cell-cycle control by physiological matrix elasticity and *in vivo* tissue stiffening. Current Biology **19:** 1511-1518

Köhler L, Speck T, Spatz HC (2000) Micromechanics and anatomical changes during early ontogeny of two lianescent Aristolochia species. Planta **210:** 691-700

Kotzer AM, Wasteneys GO (2006) Mechanisms behind the puzzle: microtubule–microfilament cross-talk in pavement cell formation. Canadian Journal of Botany **84:** 594-603

Koyama T, Sato F, Ohme-Takagi M (2010) A role of TCP1 in the longitudinal elongation of leaves in *Arabidopsis*. Bioscience, Biotechnology and Biochemistry **74:** 2145-2147

Kozuka T, Horiguchi G, Kim GT, Ohgishi M, Sakai T, Tsukaya H (2005) The different growth responses of the Arabidopsis thaliana leaf blade and the petiole during shade avoidance are regulated by photoreceptors and sugar. Plant and Cell Physiology **46:** 213-223

Kozuka T, Kobayashi J, Horiguchi G, Demura T, Sakakibara H, Tsukaya H, Nagatani A (2010) Involvement of auxin and brassinosteroid in the regulation of petiole elongation under the shade. Plant Physiology **153:** 1608-1618

Krizek BA (2008) Making bigger plants: key regulators of final organ size. Current Opinion in Plant Biology **12:** 1-6

Kuwabara A, Backhaus A, Malinowski R, Bauch M, Hunt L, Nagata T, Monk N, Sanguinetti G, Fleming A (2011) A shift towards smaller cell size via manipulation of cell cycle gene expression acts to smoothen Arabidopsis leaf shape. Plant Physiology**:** In press

Kuwabara A, Nagata T (2006) Cellular basis of developmental plasticity observed in heterophyllous leaf formation of *Ludwigia arcuata* (Onagraceae). Planta **224:** 761-770

Laguna MF, Bohn S, Jagla EA (2008) The role of elastic stresses on leaf venation morphogenesis. PLoS Computational Biology **4:** e1000055

Langlade NB, Feng X, Dransfield T, Copsey L, Hanna AI, Thebaud C, Bangham A, Hudson A, Coen E (2005) Evolution through genetically controlled allometry space. Proceedings of the National Academy of Sciences of the United States of America **102:** 10221-10226

Lee D, Polisensky DH, Braam J (2005) Genome-wide identification of touch- and darkness-regulated Arabidopsis genes: A focus on calmodulin-like and XTH genes. New Phytologist **165:** 429-444

Lee DK, Ahn JH, Song SK, Choi YD, Lee JS (2003) Expression of an expansin gene is correlated with root elongation in soybean. Plant Physiology **131:** 985-997

Lee Y, Choi D, Kende H (2001) Expansins: Ever-expanding numbers and functions. Current Opinion in Plant Biology **4:** 527-532

Lee Y, Kende H (2002) Expression of α-expansin and expansin-like genes in deepwater rice. Plant Physiology **130:** 1396-1405

Leyser O (2001) Auxin signalling: The beginning, the middle and the end. Current Opinion in Plant Biology **4:** 382-386

Li LC, Kang DM, Chen ZL, Qu LJ (2007) Hormonal regulation of leaf morphogenesis in *Arabidopsis*. Journal of Integrative Plant Biology **49:** 75-80

Li Y, Darley CP, Ongaro V, Fleming A, Schipper O, Baldauf SL, McQueen-Mason SJ (2002) Plant expansins are a complex multigene family with an ancient evolutionary origin. Plant Physiology **128:** 854-864

Lin Z, Ni Z, Zhang Y, Yao Y, Wu H, Sun Q (2005) Isolation and characterization of 18 genes encoding α- and β-expansins in wheat (Triticum aestivum L.). Molecular Genetics and Genomics **274:** 548-556

Lippincott BB, Lippincott JA (1971) Auxin-induced hyponasty of the leaf blade of *Phaseolus vulgaris*. American Journal of Botany **58:** 817-826

Malinowski R, Kasprzewska A, Fleming AJ (2011) Targeted manipulation of leaf form via local growth repression. Plant Journal **66:** 941-952

Marcotrigiano M (2001) Genetic mosaics and the analysis of leaf development. International Journal of Plant Sciences **162:** 513-525

Marga F, Grandbois M, Cosgrove DJ, Baskin TI (2005) Cell wall extension results in the coordinate separation of parallel microfibrils: Evidence from scanning electron microscopy and atomic force microscopy. Plant Journal **43:** 181-190

Massonnet C, Vile D, Fabre J, Hannah MA, Caldana C, Lisec J, Beemster GTS, Meyer RC, Messerli G, Gronlund JT, Perkovic J, Wigmore E, May S, Bevan MW, Meyer C, Rubio-Díaz S, Weigel D, Micol JL, Buchanan-Wollaston V, Fiorani F, Walsh S, Rinn B, Gruissem W, Hilson P, Hennig L, Willmitzer L, Granier C (2010) Probing the reproducibility of leaf growth and molecular phenotypes: A comparison of three Arabidopsis accessions cultivated in ten laboratories. Plant Physiology **152:** 2142-2157

McHale NA, Koning RE (2004) Phantastica regulates development of the adaxial mesophyll in Nicotiana leaves. Plant Cell **16:** 1251-1262

McHale NA, Marcotrigiano M (1998) LAM1 is required for dorsoventrality and lateral growth of the leaf blade in Nicotiana. Development **125:** 4235-4243

McQueen-Mason S, Cosgrove DJ (1994) Disruption of hydrogen bonding between plant cell wall polymers by proteins that induce wall extension. Proceedings of the National Academy of Sciences of the United States of America **91:** 6574-6578

McQueen-Mason S, Durachko DM, Cosgrove DJ (1992) Two endogenous proteins that induce cell wall extension in plants. Plant Cell **4:** 1425-1433

McQueen-Mason SJ (1995) Expansins and cell wall expansion. Journal of Experimental Botany **46:** 1639-1650

McQueen-Mason SJ, Cosgrove DJ (1995) Expansin mode of action on cell walls. Analysis of wall hydrolysis, stress relaxation, and binding. Plant Physiology **107:** 87-100

Merks RMH, Guravage M, Inzé D, Beemster GTS (2011) Virtualleaf: An open-source framework for cell-based modeling of plant tissue growth and development. Plant Physiology **155:** 656-666

Milani P, Gholamirad M, Traas J, Arnéodo A, Boudaoud A, Argoul F, Hamant O (2011) In vivo analysis of local wall stiffness at the shoot apical meristem in *Arabidopsis* using atomic force microscopy. Plant Journal**:** In press

Millenaar FF, Van Zanten M, Cox MCH, Pierik R, Voesenek LACJ, Peeters AJM (2009) Differential petiole growth in Arabidopsis thaliana: Photocontrol and hormonal regulation. New Phytologist **184:** 141-152

Mirabet V, Das P, Boudaoud A, Hamant O (2011) The role of mechanical forces in plant morphogenesis. Annual Review of Plant Biology **62:** 365-385

Mitchison GJ (1981) The polar transport of auxin and vein patterns in plants. Philosophical Transactions of the Royal Society B: Biological Sciences **295:** 461-471

Mizukami Y, Fischer RL (2000) Plant organ size control: AINTEGUMENTA regulates growth and cell numbers during organogenesis. Proceedings of the National Academy of Sciences of the United States of America **97:** 942-947

Moore I, Samalova M, Kurup S (2006) Transactivated and chemically inducible gene expression in plants. Plant Journal **45:** 651-683

Morris VJ, Gunning AP, Kirby AR, Round A, Waldron K, Ng A (1997) Atomic force microscopy of plant cell walls, plant cell wall polysaccharides and gels. International Journal of Biological Macromolecules **21:** 61-66

Muller B, Bourdais G, Reidy B, Bencivenni C, Massonneau A, Condamine P, Rolland G, Conejero G, Rogowsky P, Tardieu F (2007) Association of specific expansins with growth in maize leaves is maintained under environmental, genetic, and developmental sources of variation. Plant Physiology **143:** 278-290

Müssig C, Fischer S, Altmann T (2002) Brassinosteroid-regulated gene expression. Plant Physiology **129:** 1241-1251

Nakaya M, Tsukaya H, Murakami N, Kato M (2002) Brassinosteroids control the proliferation of leaf cells of Arabidopsis thaliana. Plant and Cell Physiology **43:** 239-244

Nemhauser JL, Hong F, Chory J (2006) Different plant hormones regulate similar processes through largely nonoverlapping transcriptional responses. Cell **126:** 467-475

Nemhauser JL, Mockler TC, Chory J (2004) Interdependency of brassinosteroid and auxin signaling in *Arabidopsis*. PLoS Biology **2:** e258

Nilsson SB, Hertz CH, Falk S (1958) On the Relation between Turgor Pressure and Tissue Rigidity. II. Physiologia Plantarum **11:** 818-837

Niu QW, Lin SS, Reyes JL, Chen KC, Wu HW, Yeh SD, Chua NH (2006) Expression of artificial microRNAs in transgenic Arabidopsis thaliana confers virus resistance. Nature Biotechnology **24:** 1420-1428

Öpik H, Rolfe S (2005) Plant growth hormones. *In* The Physiology of Flowering Plants. Cambridge University Press, Cambridge, pp 177-204

Ossowski S, Schwab R, Weigel D (2008) Gene silencing in plants using artificial microRNAs and other small RNAs. Plant Journal **53:** 674-690

Palatnik JF, Allen E, Wu X, Schommer C, Schwab R, Carrington JC, Weigel D (2003) Control of leaf morphogenesis by microRNAs. Nature **425:** 257-263

Palevitz BA, Hepler PK (1985) Changes in dye coupling of stomatal cells of Allium and Commelina demonstrated by microinjection of Lucifer yellow. Planta **164:** 473-479

Panteris E, Galatis B (2005) The morphogenesis of lobed plant cells in the mesophyll and epidermis: Organization and distinct roles of cortical microtubules and actin filaments. New Phytologist **167:** 721-732

Pantin F, Simonneau T, Rolland G, Dauzat M, Muller B (2011) Control of leaf expansion: A developmental switch from metabolics to hydraulics. Plant Physiology **156:** 803-815

Park CH, Kim T-W, Son S-H, Hwang J-Y, Lee SC, Chang SC, Kim S-H, Kim SW, Kim S-K (2010) Brassinosteroids control AtEXPA5 gene expression in Arabidopsis thaliana. Phytochemistry **71:** 380-387

Park YW, Baba K, Furuta Y, Iida I, Sameshima K, Arai M, Hayashi T (2004) Enhancement of growth and cellulose accumulation by overexpression of xyloglucanase in poplar. FEBS Letters **564:** 183-187

Peaucelle A, Louvet R, Johansen JN, Höfte H, Laufs P, Pelloux J, Mouille G (2008) Arabidopsis phyllotaxis is controlled by the methyl-esterification status of cell-wall pectins. Current Biology **18:** 1943-1948

Pekker I, Alvarez JP, Eshed Y (2005) Auxin response factors mediate Arabidopsis organ asymmetry via modulation of KANADI activity. Plant Cell **17:** 2899-2910

Peppe DJ, Royer DL, Cariglino B, Oliver SY, Newman S, Leight E, Enikolopov G, Fernandez-Burgos M, Herrera F, Adams JM, Correa E, Currano ED, Erickson JM, Hinojosa LF, Hoganson JW, Iglesias A, Jaramillo CA, Johnson KR, Jordan GJ, Kraft NJB, Lovelock EC, Lusk CH, Niinemets U, Peñuelas J, Rapson G, Wing SL, Wright IJ (2011) Sensitivity of leaf size and shape to climate: Global patterns and paleoclimatic applications. New Phytologist **190:** 724-739

Peters WS, Tomos AD (1996) The history of tissue tension. Annals of Botany **77:** 657-665

Pien S, Wyrzykowska J, McQueen-Mason S, Smart C, Fleming A (2001) Local expression of expansin induces the entire process of leaf development and modifies leaf shape. Proceedings of the National Academy of Sciences of the United States of America **98:** 11812-11817

Pierik R, Djakovic-Petrovic T, Keuskamp DH, de Wit M, Voesenek LACJ (2009) Auxin and ethylene regulate elongation responses to neighbor proximity signals independent of gibberellin and DELLA proteins in Arabidopsis. Plant Physiology **149:** 1701-1712

Piétrement O, Troyon M (2000) Quantitative elastic modulus measurement by magnetic force modulation microscopy. Tribology Letters **9:** 77-87

Poethig RS, Sussex IM (1985) The developmental morphology and growth dynamics of the tobacco leaf. Planta **165:** 158-169

Price CA, Enquist BJ (2007) Scaling mass and morphology in leaves: An extension of the wbe model. Ecology **88:** 1132-1141

Pyke KA, Marrison JL, Leech AM (1991) Temporal and spatial development of the cells of the expanding first leaf of *Arabidopsis thaliana* (L.) Heynh. Journal of Experimental Biology **42:** 1407-1416

Qin G, Gu H, Zhao Y, Ma Z, Shi G, Yang Y (2005) An indole-3-acetic acid carboxyl methyltransferase regulates Arabidopsis leaf development. Plant Cell **17:** 2693-2704

Radmacher M (2002) Measuring the elastic properties of living cells by the atomic force microscope. *In* BP Jena, JK Horber, eds, Atomic Force Microscopy in Cell Biology, Vol 68, pp 67-90

Radmacher M, Fritz M, Kacher CM, Cleveland JP, Hansma PK (1996) Measuring the viscoelastic properties of human platelets with the atomic force microscope. Biophysical Journal **70:** 556-567

Refrégier G, Pelletier S, Jaillard D, Höfte H (2004) Interaction between wall deposition and cell elongation in dark-grown hypocotyl cells in Arabidopsis. Plant Physiology **135:** 959-968

Reidy B, McQueen-Mason S, Nosberger J, Fleming A (2001a) Differential expression of alpha and beta expansin genes in the elongating leaf of *Festuca pratensis*. Plant Molecular Biology **46:** 491-504

Reidy B, Nosberger J, Fleming A (2001b) Differential expression of XET-related genes in the leaf elongation zone of *F. pratensis*. Journal of Experimental Botany **52:** 1847-1856

Reinhardt B, Hanggi E, Muller S, Bauch M, Wyrzykowska J, Kerstetter R, Poethig S, Fleming AJ (2007) Restoration of DWF4 expression to the leaf margin of a dwf4 mutant is sufficient to restore leaf shape but not size: The role of the margin in leaf development. Plant Journal **52:** 1094-1104

Reinhardt D, Pesce ER, Stieger P, Mandel T, Baltensperger K, Bennett M, Traas J, Friml J, Kuhlemeier C (2003) Regulation of phyllotaxis by polar auxin transport. Nature **426:** 255-260

Reinhardt D, Wittwer F, Mandel T, Kuhlemeier C (1998) Localized upregulation of a new expansin gene predicts the site of leaf formation in the tomato meristem. Plant Cell **10:** 1427-1437

Rochange SF, McQueen-Mason SJ (2000) Expression of a heterologous expansin in transgenic tomato plants. Planta **211:** 583-586

Rochange SF, Wenzel CL, McQueen-Mason SJ (2001) Impaired growth in transgenic plants over-expressing an expansin isoform. Plant Molecular Biology **46:** 581-589

Rose JKC, Braam J, Fry SC, Nishitani K (2002) The XTH family of enzymes involved in xyloglucan endotransglucosylation and endohydrolysis: Current perspectives and a new unifying nomenclature. Plant and Cell Physiology **43:** 1421-1435

Rose JKC, Cosgrove DJ, Albersheim P, Darvill AG, Bennett AB (2000) Detection of expansin proteins and activity during tomato fruit ontogeny. Plant Physiology **123:** 1583-1592

Rose JKC, Lee HH, Bennett AB (1997) Expression of a divergent expansin gene is fruit-specific and ripening-regulated. Proceedings of the National Academy of Sciences of the United States of America **94:** 5955-5960

Runions A, Fuhrer M, Lane B, Federl P, Rolland-Lagan AG, Prusinkiewicz P (2005) Modeling and visualization of leaf venation patterns. *In* ACM Transactions on Graphics, Ed 3 Vol 24, Los Angeles, CA, pp 702-711

Ryden P, Sugimoto-Shirasu K, Smith AC, Findlay K, Reiter WD, McCann MC (2003) Tensile properties of Arabidopsis cell walls depend on both a xyloglucan cross-linked microfibrillar network and rhamnogalacturonan II-borate complexes. Plant Physiology **132:** 1033-1040

Sabirzhanova IB, Sabirzhanov BE, Chemeris AV, Veselov DS, Kudoyarova GR (2005) Fast changes in expression of expansin gene and leaf extensibility in osmotically stressed maize plants. Plant Physiology and Biochemistry **43:** 419-422

Sampedro J, Carey RE, Cosgrove DJ (2006) Genome histories clarify evolution of the expansin superfamily: New insights from the poplar genome and pine ESTs. Journal of Plant Research **119:** 11-21

Sampedro J, Cosgrove DJ (2005) The expansin superfamily. Genome Biology **6:** 242

Sampedro J, Lee Y, Carey RE, DePamphilis C, Cosgrove DJ (2005) Use of genomic history to improve phylogeny and understanding of births and deaths in a gene family. Plant Journal **44:** 409-419

Sánchez-Rodríguez C, Rubio-Somoza I, Sibout R, Persson S (2010) Phytohormones and the cell wall in Arabidopsis during seedling growth. Trends in Plant Science **15:** 291-301

Sanchez MA, Mateos I, Labrador E, Dopico B (2004) Brassinolides and IAA induce the transcription of four α-expansin genes related to development in *Cicer arietinum*. Plant Physiology and Biochemistry **42:** 709-716

Sane VA, Chourasia A, Nath P (2005) Softening in mango (*Mangifera indica* cv. Dashehari) is correlated with the expression of an early ethylene responsive, ripening related expansin gene, MiExpA1. Postharvest Biology and Technology **38:** 223-230

Sasidharan R, Chinnappa CC, Staal M, Elzenga JTM, Yokoyama R, Nishitani K, Voesenek LACJ, Pierik R (2010) Light quality-mediated petiole elongation in arabidopsis during shade avoidance involves cell wall modification by xyloglucan endotransglucosylase/hydrolases. Plant Physiology **154:** 978-990

Savaldi-Goldstein S, Chory J (2008) Growth coordination and the shoot epidermis. Current Opinion in Plant Biology **11:** 42-48

Savaldi-Goldstein S, Peto C, Chory J (2007) The epidermis both drives and restricts plant shoot growth. Nature **446:** 199-202

Scanlon MJ (2000) Developmental complexities of simple leaves. Current Opinion in Plant Biology **3:** 31-36

Scheres B (2007) Stem-cell niches: Nursery rhymes across kingdoms. Nature Reviews Molecular Cell Biology **8:** 345-354

Scheuring S, Dufrêne YF (2010) Atomic force microscopy: probing the spatial organization, interactions and elasticity of microbial cell envelopes at molecular resolution. Molecular Microbiology **75:** 1327-1336

Schipper O, Schaefer D, Reski R, Fleming A (2002) Expansins in the bryophyte *Physcomitrella patens*. Plant Molecular Biology **50:** 789-802

Schmid M, Davison TS, Henz SR, Pape UJ, Demar M, Vingron M, Schokopf B, Weigel D, Lohmann JU (2005) A gene expression map of Arabidopsis thaliana development. Nature Genetics **37:** 501-506

Schopfer P, Lapierre C, Nolte T (2001) Light-controlled growth of the maize seedling mesocotyl: Mechanical cell-wall changes in the elongation zone and related changes in lignification. Physiologia Plantarum **111:** 83-92

Schwab R, Ossowski S, Riester M, Warthmann N, Weigel D (2006) Highly specific gene silencing by artificial microRNAs in Arabidopsis. Plant Cell **18:** 1121-1133

Sellen DB (1980) The mechanical properties of plant cell walls. Symposia of the Society for Experimental Biology **34:** 315-329

Sharova EI (2007) Expansins: Proteins involved in cell wall softening during plant growth and morphogenesis. Russian Journal of Plant Physiology **54:** 713-727

Shcherban TY, Shi J, Durachko DM, Guiltinan MJ, McQueen-Mason SJ, Shieh M, Cosgrove DJ (1995) Molecular cloning and sequence analysis of expansins - A highly conserved, multigene family of proteins that mediate cell wall extension in plants. Proceedings of the National Academy of Sciences of the United States of America **92:** 9245-9249

Shipley B, Lechowicz MJ, Wright I, Reich PB (2006) Fundamental trade-offs generating the worldwide leaf economics spectrum. Ecology **87:** 535-541

Shkolnik-Inbar D, Bar-Zvi D (2010) ABI4 mediates abscisic acid and cytokinin inhibition of lateral root formation by reducing polar auxin transport in arabidopsis. Plant Cell **22:** 3560-3573

Shoseyov O, Shani Z, Levy I (2006) Carbohydrate binding modules: Biochemical properties and novel applications. Microbiology and Molecular Biology Reviews **70:** 283-295

Shpigel E, Roiz L, Goren R, Shoseyov O (1998) Bacterial cellulose-binding domain modulates in vitro elongation of different plant cells. Plant Physiology **117:** 1185-1194

Siegfried KR, Eshed Y, Baum SF, Otsuga D, Drews GN, Bowman JL (1999) Members of the YABBY gene family specify abaxial cell fate in Arabidopsis. Development **126:** 4117-4128

Sinha N (1999) Leaf development in angiosperms. Annual Review of Plant Physiology and Plant Molecular Biology **50:** 419-446

Siobhan B, Laurent LG, Emeric B, Cris K, Herman H, Alexis P (2011) The application of atomic force microscopy as a micro-force sensor: Probing the mechanics of living plant cell walls during development. *In* 22nd International Conference on Arabidopsis Research, Madison, Wisconsin, USA

Sloan J, Backhaus A, Malinowski R, McQueen-Mason S, Fleming AJ (2009) Phased control of expansin activity during leaf development identifies a sensitivity window for expansin-mediated induction of leaf growth. Plant Physiology**:** 1844-1854

Smith LG, Hake S, Sylvester AW (1996) The tangled-1 mutation alters cell division orientations throughout maize leaf development without altering leaf shape. Development **122:** 481-489

Sneddon IN (1965) The relation between load and penetration in the axisymmetric boussinesq problem for a punch of arbitrary profile. International Journal of Engineering Science **3:** 47-57

Somerville C, Bauer S, Brininstool G, Facette M, Hamann T, Milne J, Osborne E, Paredez A, Persson S, Raab T, Vorwerk S, Youngs H (2004) Toward a systems approach to understanding plant cell walls. Science **306:** 2206-2211

Son S-H, Jeong S-Y, Kim S-K (2010) Ethylene regulates *AtEXPA5* expression in *Arabidopsis thaliana*. *In* 21st International Conference on Arabidopsis Research, Yokohama, Japan

Sugimoto-Shirasu K, Roberts K (2003) "Big it up": Endoreduplication and cell-size control in plants. Current Opinion in Plant Biology **6:** 544-553

Swarup K, Benková E, Swarup R, Casimiro I, Péret B, Yang Y, Parry G, Nielsen E, De Smet I, Vanneste S, Levesque MP, Carrier D, James N, Calvo V, Ljung K, Kramer E, Roberts R, Graham N, Marillonnet S, Patel K, Jones JDG, Taylor CG, Schachtman DP, May S, Sandberg G, Benfey P, Friml J, Kerr I, Beeckman T, Laplaze L, Bennett MJ (2008) The auxin influx carrier LAX3 promotes lateral root emergence. Nature Cell Biology **10:** 946-954

Szymanski DB, Cosgrove DJ (2009) Dynamic coordination of cytoskeletal and cell wall systems during plant cell morphogenesis. Current Biology **19:** R800-R811

Taiz L (1984) Plant cell expansion: Regulation of cell wall mechanical properties. Annu. Rev. Plant Physiol. **35:** 585-657

Teale WD, Ditengou FA, Dovzhenko AD, Li X, Molendijk AM, Ruperti B, Paponov I, Palme K (2008) Auxin as a model for the integration of hormonal signal processing and transduction. Molecular Plant **1:** 229-237

Thompson DS (2005) How do cell walls regulate plant growth? Journal of Experimental Botany **56:** 2275-2285

Thompson DS (2008) Space and time in the plant cell wall: Relationships between cell type, cell wall rheology and cell function. Annals of Botany **101:** 203-211

Tisne S, Reymond M, Vile D, Fabre J, Dauzat M, Koornneef M, Granier C (2008) Combined genetic and modeling approaches reveal that epidermal cell area and number in leaves are controlled by leaf and plant developmental processes in Arabidopsis. Plant Physiology **148:** 1117-1127

Tomos AD, Leigh RA (1999) The pressure probe: A versatile tool in plant cell physiology. Annual Review of Plant Physiology and Plant Molecular Biology **50:** 447-472

Touhami A, Nysten B, Dufrêne YF (2003) Nanoscale mapping of the elasticity of microbial cells by atomic force microscopy. Langmuir **19:** 4539-4543

Tsuge T, Tsukaya H, Uchimiya H (1996) Two independent and polarized processes of cell elongation regulate leaf blade expansion in Arabidopsis thaliana (L.) Heynh. Development **22:** 1589-1600

Tsukaya H (2002) Leaf development. The Arabidopsis Book **1:** e0072

Tsukaya H (2003) Organ shape and size: A lesson from studies of leaf morphogenesis. Current Opinion in Plant Biology **6:** 57-62

Turner RD, Ratcliffe EC, Wheeler R, Golestanian R, Hobbs JK, Foster SJ (2010) Peptidoglycan architecture can specify division planes in *Staphylococcus aureus*. Nature Communications **1:** 1-9

Uyttewaal M, Traas J, Hamant O (2010) Integrating physical stress, growth, and development. Current Opinion in Plant Biology **13:** 46-52

Van Der Wel NN, Putman CAJ, Van Noort SJT, De Grooth BG, Emons AMC (1996) Atomic force microscopy of pollen grains, cellulose microfibrils, and protoplasts. Protoplasma **194:** 29-39

Van Volkenburgh E (1999) Leaf expansion - An integrating plant behaviour. Plant, Cell and Environment **22:** 1463-1473

Vreeburg RAM, Benschop JJ, Peeters AJM, Colmer TD, Ammerlaan AHM, Staal M, Elzenga TM, Staals RHJ, Darley CP, McQueen-Mason SJ, Voesenek LACJ (2005) Ethylene regulates fast apoplastic acidification and expansin A transcription during submergence-induced petiole elongation in *Rumex palustris*. Plant Journal **43:** 597-610

Vriezen WH, De Graaf B, Mariani C, Voesenek LACJ (2000) Submergence induces expansin gene expression in flooding-tolerant Rumex palustris and not in flooding-intolerant R. acetosa. Planta **210:** 956-963

Waites R, Selvadurai HRN, Oliver IR, Hudson A (1998) The PHANTASTICA gene encodes a MYB transcription factor involved in growth and dorsoventrality of lateral organs in Antirrhinum. Cell **93:** 779-789

Walter A, Schurr U (2005) Dynamics of leaf and root growth: Endogenous control versus environmental impact. Annals of Botany **95:** 891-900

Walther D, Brunnemann R, Selbig J (2007) The regulatory code for transcriptional response diversity and its relation to genome structural properties in *A. thaliana*. PLoS genetics **3:** e11

Wang CX, Wang L, McQueen-Mason SJ, Pritchard J, Thomas CR (2008) pH and expansin action on single suspension-cultured tomato (*Lycopersicon esculentum*) cells. Journal of Plant Research **121:** 527-534

Wang G, Gao Y, Wang J, Yang L, Song R, Li X, Shi J (2011) Overexpression of two cambium-abundant Chinese fir (*Cunninghamia lanceolata*) α-expansin genes ClEXPA1 and ClEXPA2 affect growth and development in transgenic tobacco and increase the amount of cellulose in stem cell walls. Plant Biotechnology Journal **9:** 486-502

Wang IR, Wan JWL, Baranoski GVG (2004) Physically-based simulation of plant leaf growth. Computer Animation and Virtual Worlds **15:** 237-244

Wang L, Hukin D, Pritchard J, Thomas C (2006) Comparison of plant cell turgor pressure measurement by pressure probe and micromanipulation. Biotechnology Letters **28:** 1147-1150

Warthmann N, Chen H, Ossowski S, Weigel D, Herve P (2008) Highly specific gene silencing by artificial miRNAs in rice. PLoS One **3:** e1829

Weigel D, Glazebrook J (2002) How to grow Arabidopsis. Arabidopsis: A Laboratory Manual**:** 1-18

Whitney SEC, Gidley MJ, McQueen-Mason SJ (2000) Probing expansin action using cellulose/hemicellulose composites. Plant Journal **22:** 327-334

Wieczorek K, Golecki B, Gerdes L, Heinen P, Szakasits D, Durachko DM, Cosgrove DJ, Kreil DP, Puzio PS, Bohlmann H, Grundler FMW (2006) Expansins are involved in the formation of nematode-induced syncytia in roots of Arabidopsis thaliana. Plant Journal **48:** 98-112

Wielopolska A, Townley H, Moore I, Waterhouse P, Helliwell C (2005) A high-throughput inducible RNAi vectors for plants. Plant Biotechnology Journal **3:** 583-590

Wiśniewska SK, Nalaskowski J, Witka-Jezewska E, Hupka J, Miller JD (2003) Surface properties of barley straw. Colloids and Surfaces B: Biointerfaces **29:** 131-142

Wojtaszek P (2000) Genes and plant cell walls: A difficult relationship. Biological Reviews of the Cambridge Philosophical Society **75:** 437-475

Wu H-I, Sharpe PJH (1979) Stomatal mechanics II*: material properties of guard cell walls. Plant, Cell & Environment **2:** 235-244

Wu Y, Meeley RB, Cosgrove DJ (2001) Analysis and expression of the a-expansin and b-expansin gene families in maize. Plant Physiology **126:** 222-232

Wu Y, Wang S, Zhou D, Xing C, Zhang Y, Cai Z (2010) Evaluation of elastic modulus and hardness of crop stalks cell walls by nano-indentation. Bioresource Technology **101:** 2867-2871

Wyrzykowska J, Pien S, Shen WH, Fleming AJ (2002) Manipulation of leaf shape by modulation of cell division. Development **129:** 957-964

Yoo SD, Gao Z, Cantini C, Loescher WH, Van Nocker S (2003) Fruit ripening in sour cherry: Changes in expression of genes encoding expansins and other cell-wall-modifying enzymes. Journal of the American Society for Horticultural Science **128:** 16-22

Yu Z, Kang B, He X, Lv S, Bai Y, Ding W, Chen M, Cho H-T, Wu P (2011) Root hair-specific expansins modulate root hair elongation in rice. Plant Journal **66:** 725-734

Zajac AL, Discher DE (2008) Cell differentiation through tissue elasticity-coupled, myosin-driven remodeling. Current Opinion in Cell Biology **20:** 609–615

Zenoni S, Reale L, Tornielli GB, Lanfaloni L, Porceddu A, Ferrarini A, Moretti C, Zamboni A, Speghini A, Ferranti F, Pezzotti M (2004) Downregulation of the *Petunia hybrida* α-expansin gene *PhEXP1* reduces the amount of crystalline cellulose in cell walls and leads to phenotypic changes in petal limbs. Plant Cell **16:** 295-308

Zerzour R, Kroeger J, Geitmann A (2009) Polar growth in pollen tubes is associated with spatially confined dynamic changes in cell mechanical properties. Developmental Biology **334:** 437-446

Zgurski JM, Sharma R, Bolokoski DA, Schultz EA (2005) Asymmetric auxin response precedes asymmetric growth and differentiation of asymmetric leaf1 and asymmetric leaf2 Arabidopsis leaves. Plant Cell **17:** 77-91

Zhang C, Halsey LE, Szymanski DB (2011a) The development and geometry of shape change in Arabidopsis thaliana cotyledon pavement cells. BMC Plant Biology **11:** 27

Zhang N, Hasenstein KH (2000) Distribution of expansins in graviresponding maize roots. Plant and Cell Physiology **41:** 1305-1312

Zhang XQ, Wei PC, Xiong YM, Yang Y, Chen J, Wang XC (2011b) Overexpression of the Arabidopsis α-expansin gene AtEXPA1 accelerates stomatal opening by decreasing the volumetric elastic modulus. Plant Cell Reports **30:** 27-36

Zhao P, Chen S, Wang XC (2006) Arabidopsis expansin AtEXP1 involved in the regulation of stomatal movement. Acta Agronomica Sinica **32:** 562-567